Spring 1997

Membrane-based reactors for ozonolysis of organic pollutants in aqueous and gaseous streams

Purushottam V. Shanbhag
New Jersey Institute of Technology

Copyright Warning & Restrictions

The copyright law of the United States (Title 17, United States Code) governs the making of photocopies or other reproductions of copyrighted material.

Under certain conditions specified in the law, libraries and archives are authorized to furnish a photocopy or other reproduction. One of these specified conditions is that the photocopy or reproduction is not to be "used for any purpose other than private study, scholarship, or research." If a, user makes a request for, or later uses, a photocopy or reproduction for purposes in excess of "fair use" that user may be liable for copyright infringement,

This institution reserves the right to refuse to accept a copying order if, in its judgment, fulfillment of the order would involve violation of copyright law.

Please Note: The author retains the copyright while the New Jersey Institute of Technology reserves the right to distribute this thesis or dissertation

Printing note: If you do not wish to print this page, then select "Pages from: first page # to: last page #" on the print dialog screen

ABSTRACT

MEMBRANE-BASED REACTORS FOR OZONOLYSIS OF ORGANIC POLLUTANTS IN AQUEOUS AND GASEOUS STREAMS

by

Purushottam V. Shanbhag

Many gaseous and aqueous waste streams contain multiple organic pollutants at low concentration levels. It is not economical to recover and reuse these compounds; it would be advantageous to destroy them efficiently within the waste stream. This work employed ozone, a powerful oxidizing agent, in concert with a compact membrane-based phase-contacting device. Three types of membrane devices were studied: two of them (the single-phase membrane ozonator and the two-phase membrane ozonator) treated organic pollutants in wastewater, while the third (the integrated absorption-oxidation membrane ozonator) removed volatile organic compounds (VOCs) from a gaseous waste stream.

In the single-phase membrane ozonator, the polluted wastewater stream was exposed to O_3/O_2 by means of a nonporous silicone capillary membrane. Experiments conducted to ascertain the effect of long-term exposure of O_3 on the membranes measured the permeability of O_2/N_2 across the membrane before and after exposure to O_3; the permeability of O_3 across the nonporous membrane was also experimentally measured and found to be four times that of oxygen. The removal of organic pollutants (phenol, acrylonitrile and nitrobenzene, feed concentrations ~ 100ppm) from wastewater was studied experimentally. A mathematical model was proposed; numerical simulations of the model successfully predicted the performance of this membrane reactor.

The two-phase membrane ozonator and the integrated absorption-oxidation membrane ozonator used an inert fluorocarbon (FC) medium as a liquid membrane and a reaction medium. Ozone has a very high solubility in this FC phase compared to that in water. The performance of the two-phase membrane ozonator was studied experimentally for the following compounds: phenol, nitrobenzene, acrylonitrile, toluene and trichloroethylene (TCE). A mathematical model was developed; the model predictions were close to the experimentally observed reactor performance. The two-phase membrane reactor showed higher rates of pollutant degradation than the single-phase membrane ozonator for nitrobenzene as a model pollutant (feed concentration ~ 120 ppm). Experimentally observed ozone utilization in the two-phase membrane ozonator for nitrobenzene as a model pollutant showed an ozone utilization rate > 15 for a feed concentration of ~ 120 ppm; and 0.1 for a feed concentration of 1400 ppm.

The performance of the integrated absorption-oxidation membrane ozonator was studied for trichloroethylene (TCE) and toluene as representative VOCs. This reactor demonstrated that the two-phase ozonation concept can be successfully extended (with little modification to the membrane reactor) to treat gaseous waste streams with VOCs.

MEMBRANE-BASED REACTORS FOR OZONOLYSIS OF ORGANIC POLLUTANTS IN AQUEOUS AND GASEOUS STREAMS

by
Purushottam V. Shanbhag

A Dissertation
Submitted to the Faculty of
New Jersey Institute of Technology
in Partial Fulfillment of the Requirements for the Degree of
Doctor of Philosophy

Department of Chemical Engineering, Chemistry and Environmental Science

May 1997

APPROVAL PAGE

MEMBRANE-BASED REACTORS FOR OZONOLYSIS OF ORGANIC POLLUTANTS IN AQUEOUS AND GASEOUS STREAMS

Purushottam V. Shanbhag

Dr. Kamalesh K. Sirkar, Dissertation Advisor — Date
Distinguished Professor of Chemical Engineering,
Chemistry and Environmental Science, NJIT

Dr. Gordon A. Lewandowski, Committee Member — Date
Distinguished Professor of Chemical Engineering,
Chemistry and Environmental Science, NJIT

Dr. Basil C. Baltzis, Committee Member — Date
Professor of Chemical Engineering,
Chemistry and Environmental Science, NJIT

Dr. Dana E. Knox, Committee Member — Date
Associate Professor of Chemical Engineering,
Chemistry and Environmental Science, NJIT

Dr. Robert J. Farrauto, Committee Member — Date
Research Fellow, Corporate Research, Engelhard Corporation, Iselin, NJ

BIOGRAPHICAL SKETCH

Author: Purushottam V. Shanbhag

Degree: Doctor of Philosophy

Date: May 1997

Undergraduate and Graduate Education:

- Doctor of Philosophy in Chemical Engineering,
  New Jersey Institute of Technology, Newark, NJ, 1997
- Master of Engineering in Chemical Engineering,
  Stevens Institute of Technology, Hoboken, NJ, 1992
- Bachelor of Engineering in Chemical Engineering,
  Manipal Institute of Technology, Manipal, Karnataka, India, 1990

Major: Chemical Engineering

Presentations and Publications:

P. V. Shanbhag, A. K. Guha and K. K. Sirkar, "Membrane-Based Integrated Absorption-Oxidation Reactor for Destroying VOCs in Air", *Environ. Sci. Tech.*, **1996**, *30*, 3435-3440.

A. K. Guha, P. V. Shanbhag, K. K. Sirkar, D. A. Vaccari, D. H. Trivedi, "Multiphase Ozonolysis of Organics in Wastewater by a Novel Membrane Reactor", *AIChE J.*, **1995**, *41*, 1998-2012.

P. V. Shanbhag, A. K. Guha and K. K. Sirkar, "Single-phase Membrane Ozonation of Hazardous Organic Compounds in Aqueous Streams", *J. of Haz. Mat.*, **1995**, *41*, 95-104.

A. K. Guha, C. H. Yun, P. V. Shanbhag, D. Trivedi, D. Vaccari and K. K. Sirkar, "Novel Membrane-Based Separation and Oxidation Technologies", *Waste Management*, 1993, *13*, 395-401.

BIOGRAPHICAL SKETCH
(Continued)

P. V. Shanbhag, A. K. Guha, and K. K. Sirkar, "Membrane Based Ozonation Processes", 8th Annual Meeting of the North American Membrane Society, Ottawa, Ontario, Canada, May 1996.

P. V. Shanbhag, A. K. Guha and K. K. Sirkar, "Oxidative Destruction of Organic Pollutants in Novel Membrane Reactors", AIChE Annual Meeting, Miami Beach, FL, November 1995.

P. V. Shanbhag, A. K. Guha and K. K. Sirkar, "Membrane Reactors for Single-Phase and Two-Phase Ozonation of Hazardous Organics", AIChE Annual Meeting, St. Louis, MO, November 1993.

A. K. Guha, C. H. Yun, P. V. Shanbhag, D. Trivedi, D. Vaccari and K. K. Sirkar, "Novel Membrane-Based Separation and Oxidation Technologies", 5th Annual Symposium on Emerging Technologies: Metals, Oxidation and Separation, Gulf Coast Hazardous Substance Research Center, Lamar University, Beaumont, TX, February 1993.

P. V. Shanbhag, A. K. Guha, D. Vaccari and K. K. Sirkar, "A Novel Membrane Reactor for Degradation of Hazardous Organics", 5th Annual Meeting of the North American Membrane Society, Lexington, KY, May 1992.

This thesis is dedicated to

Kusum P. (Tai) Shanbhag
Durgabai V. (Abai) and Vishwanath M. (Aba) Telang
Indira Y. (Pam) and Y. Bhandarkar
Urmila V. (Ai) and Vishnu P. (Baba) Shanbhag
Vinita B. (Nini) Jambotkar and Balkrishna G. (Fulagi-baba) Jambotkar
Aparna D. (Manju Mami) and Deepak Y. (Deepu Mama) Bhandarkar
Urbano D'souza
Shirley Lobo
Dilip Kumar Sen
Dr. P. G. Krishnamoorthy

ACKNOWLEDGEMENTS

I would like to thank God, without whom I would have foundered and lost my way a long ago. I would like to express my deepest gratitude and appreciation to Prof. Kamalesh K. Sirkar. He gave me an opportunity and the room, to learn, grow and finally realize my potential. His drive and desire were a constant source of inspiration. I was extremely fortunate at having Profs. Basil Baltzis, Gordon Lewandowski, Dana Knox and Dr. Robert Farrauto on my committee; their support, encouragement and recommendations proved invaluable to the rendition of this dissertation.

I was extremely fortunate in having supportive parents, who let me do my thing and advised me well when I arrived at various cross-roads. I hope I have made them proud, despite my various peccadillos and periods of thoroughly unmitigated stupidity. During this work I lost my paternal grandmother and maternal grandfather, each in their own way showed me what I was capable of, and what I should refrain from, doing. This work would not have been possible without the stewardship of Dr. Asim K. Guha and Dr. Sudipto Majumdar. Their patience and sagacity was very influential in my decision to pursue this work. I have to thank Sarma Kovvali, my cohort-in-arms for manning the compass in the choppy seas of indecipherable and often "weird" results. I hope someday, soon, I am able to return the favor, but without as many cigarettes! I must thank Dilip and Aparna Mandal for their help and the dinners on some very bleak Sundays. I have to thank Gordana and Xiao-Ping for bringing laughter into the labs and bringing a smile to one and all. I have to thank Sukla, Stephanie and Jun-Seok Cha for their support and encouragement. Ashish, his food, his gossip and above all his cheer

were a welcome addition to the lab. I must thank Dr. Zhi-Fa Yang, for his ongoing encouragement and his interest in my development as a "career" graduate student. I thank Drs. Abou-Nemeh and Bhaumik for patiently putting up with my tantrums and pressing on with their points. Of the newer additions to the group, I thank you all, Ram Prakash, Anirban, Boya, Jose and Chaiya for making life cheerful and interesting.

My stay here was made more rewarding and less problematic by Judy, who plied me with chocolates, gave me superb advice and above all smacked me upside the head like my mother, thank you! To Peggy and Nina, Dr. Perna and the rest of the Chemical Engineering department, I will always have the utmost of respect and affection, thank you for everything.

I must thank my friends, Raju Matta, Ulfat and Hassan Baxi, Srini, Dilip, Kunal, Sunil, Muneer, Raju, Purnendu and Sahir for tolerating my perpetual gripes and my coming of age. My friends from Manipal Inst. of Tech., who as part of the MIT-Net kept cheering me on. To my friend Sharda, I have to thank for the pithy advice, it helped; and to Vipuli, I hope I am able to give back some of the support and understanding that she has shown over the past five years, when she begins her travails with her PhD. My brother Uday and his fiancee/wife Aparna, my brother Narayan and my sister Deepali and her husband Sameer I thank for keeping me grounded. Without the support and love of my uncles, Balkrishna G. Jambotkar and Deepak Y. Bhandarkar and aunts, Vinita Jambotkar and Aparna Bhandarkar I would never have been an engineer. I have to thank my girlfriend and now wife Sofia, for the cheer, the smile, the love and the reality check. Finally to Bubba, Gizmo, Chancho and Wolvie, Miaouw!

TABLE OF CONTENTS

TABLE OF CONTENTS
(Continued)

TABLE OF CONTENTS
(Continued)

TABLE OF CONTENTS
(Continued)

TABLE OF CONTENTS
(Continued)

LIST OF FIGURES

LIST OF FIGURES
(Continued)

LIST OF FIGURES
(Continued)

LIST OF FIGURES
(Continued)

LIST OF TABLES

LIST OF TABLES
(Continued)

NOMENCLATURE

a = specific surface area per unit volume of reactor, m^2/m^3.

a, b = stoichiometric coefficient in the aqueous phase.

A = species A, pollutant.

A_1, A_2 = constants of integration, Equation 3.3.12.

A1, A2, A3, A4 = parameters defined in Equations 2.3.29, 2.3.31 and 2.3.32.

Ar_{sil} = logarithmic permeation area defined in Equation 3.3.22, m^2.

B = species B, ozone.

B1, B2, B3, B4 = parameters defined in Equations 2.3.30, 2.3.33 and 2.3.34.

C_A, C_B = concentration of species A and B respectively, $kgmol/m^3$.

Coeff = parameter defined in Equation 2.3.23.

d_i = inner diameter of aqueous feed fiber, m.

d_o = outer diameter of aqueous feed fiber, m.

d_{lm} = logarithmic mean diameter of aqueous feed fiber, m.

d_p = packing size, Equation 2.4.8, m.

D_A, D_B = diffusion coefficient of species A and B, respectively, m^2/s.

g = acceleration due to gravity, 9.81 m/s^2.

J_{O_2} = molar flux of O_2 across membrane, Equation 2.4.2, $kgmol/(m^2.\ s)$.

k_1^F = pseudo first order reaction rate constant, defined by product of k_2^F and $\bar{C}_B|_{inlet}$, Equation 3.3.29, s^{-1}.

k_{11}^F = pseudo first order reaction rate constant, defined by product of k_2^F and $\bar{C}_B|_{inlet}$, Equation 3.3.11, s^{-1}.

k_{12}^F = pseudo first order reaction rate constant, defined by product of k_2^F and $\bar{C}_A|_{inlet}$, Equation 3.3.14, s^{-1}.

k_2^F = second order reaction rate constant for reaction in fluorocarbon phase, $(kgmol/m^3)^{-1}\ s^{-1}$.

k_2^W = second order reaction rate constant for reaction in aqueous phase, $(kgmol/m^3)^{-1}\ s^{-1}$.

k_g = mass transfer coefficient based on gas phase, Equation 2.4.7, m/s.

k_l = mass transfer coefficient based on liquid phase, Equation 2.4.7, m/s.

k_w = mass transfer coefficient in aqueous phase, Equation 3.3.34, m/s.

$\bar{k}$ = mass transfer coefficient in the organic phase, defined by Equation 3.3.31, m/s.

kons = parameter defined in Equation 2.3.21.

l = wall thickness of membrane, Equation 2.4.2, m.

L = effective length of the module, m.

m_A = distribution coefficient of species A between fluorocarbon and aqueous phase, Equation 3.3.1.

M_1, M_2 = constants of integration, Equation 3.3.30.

N_{Fibs} = no. of silicone capillaries in the SILCAP module, Equation 2.3.2.

N_{sil} = no. of silicone capillaries in the SILTEF module, Equation 3.3.22.

N_{Tef} = number of Teflon tubules in the module, Equation 3.3.23.

N_{Ay} = radial pollutant flux defined in Equation 3.3.33, $kgmol/m^2\ s$.

p_A = partial pressure of species A in gas phase, kPa.

P_z^l = pressure along the length in the liquid phase, Equation 2.3.4, kPa.

Q_B^m = permeability of ozone through silicone membrane, kgmol-m/(m²-s-kPa).

Q_{Sil}^m = permeability of ozone through silicone membrane, defined in Equation A.3.1, kgmol-m/(m²-s-kPa).

$Q_{O_2}^m$ = permeability of oxygen through silicone membrane, kgmol-m/(m²-s-kPa).

$Q_{N_2}^m$ = permeability of nitrogen through silicone membrane, kgmol-m/(m²-s-kPa).

Q_w = volumetric flow rate of the aqueous phase, m³/s (ml/min).

Q_G = volumetric flow rate of the gas phase, m³/s, (ml/min)

r_i = inside radius of tubule/capillary, m.

r_o = outside radius of tubule/capillary, m.

r_f = radius of free surface from Happel's model, Equation 2.3.1, m.

R = universal gas constant, (kPa-m³)/ (kgmol-K).

R_T = estimate of number of moles diffusing per unit time across silicone capillary wall for a module of length L, kgmol/s.

S_i = solubility of species i in silicone rubber, Equation 2.4.5, kgmol/ (m³-membrane-kPa).

U = nondimensional aqueous pollutant concentration defined in Equation 2.3.17.

U = nondimensional pollutant concentration in fluorocarbon phase defined in Equation 3.3.5.

U_i = nondimensional pollutant concentration at aqueous-fluorocarbon interface defined in Equation 3.3.5.

U_{sl} = superficial liquid velocity, Equation 2.4.8, m/s.

v = velocity, m/s.

V = nondimensional aqueous ozone concentration defined in Equation 2.3.17.

V = nondimensional ozone concentration in fluorocarbon phase defined in Equation 3.3.5.

V_i = nondimensional ozone concentration at silicone membrane-fluorocarbon interface defined in Equation 3.3.5.

W = nondimensional gaseous ozone concentration defined in Equation 2.3.17.

X = nondimensional length defined in Equation 2.3.17.

X_A = conversion of species A in reactor, Equations 2.4.8, 3.3.28 and 4.3.1.

y = radial direction

y_L = distance between the o.d. of the aqueous fiber and the o.d. of the gas fiber in shell side of the membrane reactor, m

z = axial direction

overbar = organic phase (for membrane reactor model)

Greek

α, β = nondimensional parameters defined in Equations 2.3.19 and 2.3.20.

$\alpha_{O_2-N_2}$ = separation factor between O_2 and N_2 for membrane, Equation 2.4.4.

δ = thickness of the free surface layer, Equation 2.4.11.

δ_m = diffusion path from Teflon tubule o.d. to silicone capillary, o.d., m.

ϵ = void fraction in shell of module, Equation A.1.3.

NOMENCLATURE
(Continued)

ϵ	=	porosity of microporous membrane, Equation A.3.6.
γ	=	Hatta Number defined in Equation 3.3.30.
γ_1	=	parameter defined in Equation 3.3.8.
γ_2	=	parameter defined in Equation 3.3.10.
Γ_1	=	parameter defined in Equation 3.3.11.
Γ_2	=	parameter defined in Equation 3.3.14.
ϕ	=	Hatta number, defined in Equation 2.4.11.
τ_s	=	tortuosity of membrane pore in a microporous membrane, Equation A.3.6.
η	=	nondimensional radius, Equation 2.3.17.
λ	=	nondimensional outer radius of the silicone capillary, Equation 2.3.18.
η	=	nondimensional distance between aqueous-FC interface and O.D. of silicone capillary, Equation 3.3.5.

Superscripts

f	=	feed gas phase, Equation 2.4.2.
F	=	FC phase.
g	=	gas (ozone) phase.
l	=	liquid (aqueous) phase.
p	=	permeate gas phase, Equation 2.4.2.
sil	=	silicone capillary, Equations, 2.4.1, A.3.1.
Tef	=	Teflon tubule, Equation 3.3.6a.
W	=	aqueous phase.

NOMENCLATURE
(Continued)

Subscripts

A	=	pollutant.
Ai	=	pollutant at y=0, Equation 3.3.32.
Ab	=	bulk aqueous phase, Equation 3.3.34.
B	=	ozone.
f	=	refers to free surface.
fibs	=	refers to number of fibers.
i	=	refers to inside diameter of capillary/Tubule.
i	=	radial coordinate, section 2.3.3.
j	=	axial coordinate, section 2.3.3.
lm	=	refers to liquid membrane, Equations, 3.4.4., A.3.4.
LM	=	log mean average
o	=	refers to outer diameter of capillary/Tubule.

CHAPTER 1

INTRODUCTION

The ubiquity of use of organic compounds as solvents and reactants in the chemical process industries has led to problems associated with the perils of these compounds in the effluent from these industries, viz. toxicity and mutagenicity. The removal of these compounds from aqueous and gaseous streams in a cost effective and efficient manner is therefore the subject of continuing research. Government regulations, e.g. RCRA (Resource Conservation and Recovery Act) and the CAAA (Clean Air Act Amendments, 1990) have reduced the discharge of such compounds into the environment, but they still pose a problem due to their recalcitrant and persistent nature (Mukhopadhyay and Moretti, 1993).

There are a number of physical, chemical and biological processes (depending upon the mode of treatment) that seek to effectively rid gaseous and aqueous effluent streams of organic compounds. Each process has its inherent limitations in terms of applicability, effectiveness and cost. Physical processes such as adsorption, absorption, steam stripping, air stripping, etc. transfer the pollutant from the effluent phase to a second phase either to recover the pollutant for reuse or for subsequent disposal. Recovery processes are typically feasible if the concentration of the species in the effluent stream is large and the recovery and reuse of the species has definite commercial viability. However processes like adsorption are typically used for more dilute streams and seek to concentrate the organic compounds for subsequently disposal or reuse

depending upon the type of species that have been concentrated, e.g. presently chlorofluorocarbon (CFC) compounds are recovered and reused or stored for subsequent destruction.

Chemical and biological treatment processes aim to degrade the organic compounds into harmless products economically and efficiently. Chemical processes become efficient and cost effective when they are used to treat toxic, recalcitrant mixtures of compounds present in concentrations lower than those where physical processes would be applicable. Typically chemical oxidation processes are selective but slow to moderate in rate or nonselective and rapid resulting in appreciable oxidant or reactor costs. For wastewater applications, chemical processes include incineration, supercritical water oxidation (SCWO) (Modell et al., 1982), wet air oxidation (WAO) (Zimmerman, 1958), the use of H_2O_2, O_3, UV, ultrasound either singly or in combination to take advantage of any synergy that may occur (Glaze and Kang, 1989a), etc. and in the case of effluent gas streams incineration, catalytic oxidation (Heck and Farrauto, 1995), etc. At times the use of chemical oxidation processes may yield by-products which are toxic as a result of inadequate oxidation. Aerobic biological processes are common for the treatment of wastewater and are now coming into vogue for gaseous streams containing volatile organic compounds (VOCs) in the form of biofilters (Bohn, 1992). The applicability of biological processes is limited when the organic compounds to be treated is either recalcitrant to biodegradation or inhibitory or toxic to the bioculture. Presently researchers are studying whether integration of chemical and biological processes for the wastewater treatment is more efficient for recalcitrant and biogenic compounds (Scott and Ollis, 1995).

The use of membranes to effect removal of organic species from effluent waste streams has only recently begun to be realized as commercially viable. Membrane-based devices offer flexibility in terms of modes of operation, ease of use and scale up. To remove organic pollutants from effluent streams, membrane-based devices are typically used as "end-of-pipe" devices. Membrane-based separation processes currently being studied include membrane-assisted air stripping, pervaporation and membrane-based solvent extraction. Membrane-assisted air stripping removes the organic species from a wastewater stream to an air stream; the two streams remain separated by a microporous membrane. The microporous membrane provides the physical contact between the air and water phases, while allowing independent control of gas and liquid flow rates unlike that in packed beds and tray towers. The membrane offers a small resistance to mass transfer from the gas-liquid interface on one side of the membrane to the bulk gas phase on the opposite side of the membrane phase. Earlier the air stream was discharged to the atmosphere; presently it is subjected to pollution control processes like catalytic oxidation or UV oxidation as in the closed loop air stripping process (CLASP) (Bhowmick and Semmens, 1994) or recovery of the organic species using a membrane vapor permeation system (Baker et al, 1996).

Pervaporation is in a sense a true membrane process, viz. the nonporous membrane selectively picks up the more volatile organic species from a liquid feed phase and then desorbs into a vapor phase on the permeate side of the membrane. The efficacy of separation is determined by the physicochemical nature of the membrane. Whereas with air stripping, the separation is effected by virtue of vapor-liquid equilibrium of the

organic species between the wastewater and gas phases, pervaporation uses the membrane to effect separation of volatile organic compounds; as a result a substance present at low concentration in the feed stream can be highly enriched in the permeate (Fleming and Slater, 1992).

The use of solvents to extract and recover minute quantities of organic compounds dissolved in an effluent aqueous phase is an old and established process. The process utilizes an organic phase immiscible with water but having a substantial affinity for the organic species dissolved in water. The dispersion to create a large interfacial area between the two liquid phases and subsequent separation of the two immiscible liquid phases was traditionally effected by means of mixer-settlers. More recently microporous membranes have been used to achieve intimate contact between the two phases without the formation of a dispersion to yield a large interfacial area (Prasad and Sirkar, 1992 and references quoted therein; Yun et al., 1992; Reed et al., 1994; Hutter et al., 1994). The second organic solvent loaded with the organic pollutant has to be regenerated for reuse in the extraction process.

For gaseous effluent streams containing organic vapors, membrane-based processes have been utilized to recover the vapors from such streams (Baker et al., 1987; Baker et al., 1996). Alternately the physical absorption of volatile organic compounds (VOCs) into inert nonvolatile oils having a high solubility for such compounds and subsequent stripping of the VOCs from the oils using membranes is also being explored (Poddar et al., 1996a, 1996b).

The membrane processes described so far enable the physical recovery of organic species from effluent streams. The use of chemical oxidation processes in conjunction with membrane-based contacting devices to remove hazardous organic chemicals from waste effluent streams is an area that has yet to see much development.

Chemical oxidation processes are principally used to oxidize organic compounds to terminal end products which range from CO_2 and H_2O and mineral acids for halogenated compounds or nitrogen bearing compounds or intermediate compounds that are more readily biodegradable or less toxic. To treat organic compounds in wastewater, ozone, hydrogen peroxide, chlorine, chlorine dioxide and potassium permanganate are commonly used as oxidants. The use, however, of chlorine and chlorine dioxide is being reduced because of concerns regarding the formation of trihalomethanes and other halogenated reaction products due to the reaction of chlorine with natural humic substances present in raw waters (Rook, 1977). These compounds are shown to have toxic and carcinogenic properties. Ozone is the strongest oxidant of the five previously mentioned compounds having a reduction potential of 2.07 V for the half cell

$$O_3 + 2H^+ + 2e^- \rightarrow O_2 + H_2O \qquad (1.1.1)$$

reaction shown above (Wojtowicz, 1991). This makes it the third most powerful oxidizing agent after F_2 and the hydroxyl radical (OH•). Ozone has a water solubility of 0.14 - 0.17 mg/l of water for a gas phase composition of 1 mg/l at 25°C. The corresponding Henry's constant is 128,600 atm l/(gmol) at 25°C (Langlais et al., 1991).

The use of ozone in the treatment of drinking water was started in Europe in 1903. Presently there exist about 2000 such installations primarily in Europe. In addition,

ozone is used to provide high quality water for semiconductor applications, odor control in industrial waste control and treatment of municipal secondary effluents. To resolve the problem of effluent streams containing recalcitrant organic compounds the interest in ozone as an oxidizing agent has soared. Current research trends are exploring the potential of ozone as an oxidant to treat waste aqueous streams containing pesticides, surfactants, chlorinated hydrocarbons, BTEX, etc. (Masten and Davies, 1994).

The mechanism with which ozone reacts with an organic compound dissolved in a medium depends upon both the organic compound reacting with ozone and the solvent within which the reaction is occurring. Solvents like water participate during the ozonation of organic compounds, by consuming some of the dissolved ozone and generating hydroxyl radicals, which also participate in the destruction of the dissolved organic compounds. Solvents like CCl_4, allow reaction between ozone and dissolved organic species but do not participate in the generation of secondary oxidizing species like OH radicals (Masten and Davies, 1994).

The direct reaction of ozone with organic species depends upon the type of organic species. Alkanes exhibit little or no reaction with ozone while dissolved in solvents like CCl_4; studies of the reaction of alkanes while dissolved in water are limited owing to the low solubility of alkanes in water. The majority of the initial research done on ozonation dealt with the elucidation of the reaction between ozone and alkenes. Ozone is an electrophile and the reaction of alkenes with ozone involves the addition of ozone to the double bond via the Criegee mechanism, forming an unstable ozonide. This reaction in water ultimately leads to the cleavage of the double bond and formation of

a carboxylic acid and an aldehyde or ketone depending upon the parent alkene. Aldehydes in general react with ozone faster than alcohols; carboxylic acids are essentially unreactive to ozone. Also the more chlorinated an organic compound the less easily it is oxidized by ozone (Hoigne and Bader, 1983a).

Reactions with aromatic compounds occur at much slower rates than those with alkenes. Aromatic compounds with electron-donating groups (-OH, $-NH_2$) are attacked electrophilicly at the ortho and para positions while those with electron-withdrawing groups (-COOH, $-NO_2$) are attacked nucleophilicly at the meta position. Also aromatic compounds with electron-donating groups react faster than aromatic compounds with electron-withdrawing groups. For the common recalcitrant aromatic compounds, like phenol, toluene, benzene, chlorobenzene, nitrobenzene, the reaction rate with ozone in aqueous solutions shows the following trend: phenol > toluene > benzene > chlorobenzene > nitrobenzene (Hoigne and Bader, 1983a). Typical degradation products are polyhydroxy aromatic compounds, unsaturated aliphatic compounds (alcohols, dicarboxylic acids and esters), saturated aliphatic compounds, quinoids and ultimately CO_2 and H_2O. For a majority of organic compounds, ozonation in water does not lead to total mineralization, i.e. CO_2 and water. Partial oxidation is achieved because of the low reactivity of the intermediates formed during the reaction, e.g. oxalic and acetic acids.

Although the destruction of organic compounds in water by means of ozone is hindered by the low solubility of ozone in water, the slow kinetics with some of the targeted compounds, e.g. carboxylic acids and the presence of non-targeted contaminants

like HCO_3^- ions which consume O_3 rapidly, it is found that ozonation at neutral and alkaline pH is inevitably aided by the presence of hydroxyl radicals. The hydroxyl radical is an extremely powerful oxidant and the rate constants of its reactions with typical organic pollutants are in the range of 10^8 - 10^{10} $(gmol/l)^{-1}$ s^{-1}; it is generated during the reaction of ozone in water with UV, H_2O_2, or OH^- and H^+ ions in complex chain mechanisms during a series of single-electron and atom-transfer processes (Glaze et al., 1987). Therefore the use of ozone as an oxidant in conjunction with UV, H_2O_2 or under high pH conditions to generate OH radicals as a method of treating recalcitrant organic species is termed an Advanced Oxidation Process (AOP). A simple diagram showing the reaction of organic compounds with ozone and hydroxyl radicals generated in situ is shown in Figure 1.1.1. Although the steady state OH radical concentration is of the order 10^{-10} - 10^{-12} gmol/l during such processes, the nonspecific nature of the reactions and extremely high reaction rates makes these processes highly attractive; most research related to AOP is therefore aimed at generating and maximizing the concentration of hydroxyl radicals.

Despite the strides made in understanding the mechanism of ozonation of organic compounds in water, one of the most obvious drawbacks of any aqueous phase ozonation process, is simply the low solubility of ozone in water. This results in low volumetric mass transfer coefficients "k_la" for the ozonators being presently used to treat wastewater. The "k_l" is controlled by the hydrodynamics of the phase controlling mass transfer, which in this case would be the aqueous phase boundary layer. Conventional methods of gas-liquid contacting for ozonation of wastewaters include bubble columns

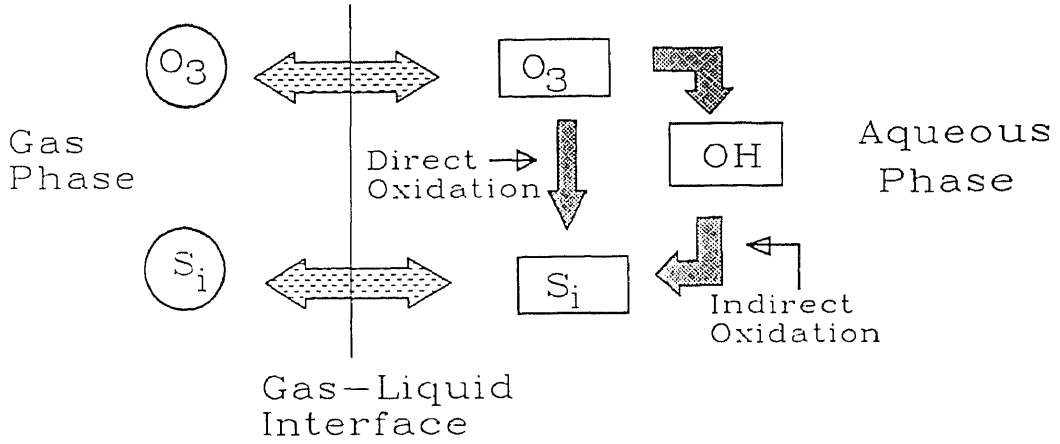

Figure 1.1.1. Schematic of the major reaction steps during ozonation of an organic pollutant dissolved in water.

and packed beds. The use of inline ozone injectors in conjunction with static mixers is also being explored as a method of improving the hydrodynamic aspects of the mass transfer coefficient (Langlais et al., 1991).

The aspect of improving "a", the interfacial area per unit volume of contactor, available between the gas and liquid phases has not been extensively addressed for the purpose of ozonation. The use of structured packings in packed beds does indeed mitigate some the problems of low "a" which is not possible with conventional packings like berl saddles and raschig rings. The use of membrane-based devices as a method of contacting the gas and liquid phases nondispersively is given impetus by the fact that these devices are able to provide much higher interfacial area "a" than conventional contacting devices. Membrane-based contactors also allow independent control of the two flowing phases, without the concomitant problems of flooding, loading and weeping associated with packed and tray towers. Past studies have demonstrated that membrane-based contacting devices are able to provide a sizeable increase in "a" over conventional gas absorption towers (30 cm^{-1} for membrane devices as opposed to 0.1 - 4 cm^{-1} for plate columns) (Qi and Cussler, 1985; Karoor and Sirkar, 1993). The use of a membrane to aid the process of ozonation by allowing higher "a" interfacial area per unit volume of the reactor is undertaken as part of this study and will be referred to as **single-phase membrane ozonation** as opposed to **two-phase membrane ozonation** described next. Single-phase membrane ozonation will be described in detail in Chapter 2.

The equilibrium value of solubility of ozone in water $\sim$14 mg/l for a gas phase composition of 100 mg/l in gas phase is typical for situations where corona discharge

ozone generators are used to generate ozone. This value is reduced further under actual ozonation conditions where ozone may be scavenged by reaction products, OH radicals, nontargeted inorganic species like the HCO_3^-, etc. This leads to the consideration of whether a second solvent having an inherently high solubility for ozone, immiscible in water yet in intimate contact with the aqueous phase would aid in the ozonation process. The use of such solvents to aid the mass transfer of a solute gas species has been suggested by Sharma (1983) and has been studied as a viable method of improving oxygen absorption into an aqueous phase in presence of fine organic droplets (Bruining et al., 1986). The use of a perfluorocarbon as a dispersed organic medium to improve the oxygen transfer rates to a fermentation medium has also been explored (Junker et al., 1990).

In the case of ozonation of organic pollutants in wastewater, the second medium has to have a high solubility for ozone and very little solubility in water, be immiscible in water, and inert towards ozone and any reactive intermediates formed during the course of the reaction. Studies using a perfluorocarbon solvent in an oxidative environment were carried out using oxygen at elevated temperatures and pressures in presence of catalysts to destroy phenol, β-naphthol and carboxylic acids, viz. acetic, propionic and butyric acids demonstrating the concept that indeed such solvents could be used to oxidize organic compounds dissolved in an aqueous phase (Hamrin et al., 1984; Bhattacharyya et al., 1986). A similar perfluorocarbon solvent was used to study the ozonation of β-naphthol and phenol in water (Stich and Bhattacharyya, 1986) and the ozonation of chlorinated organic compounds dissolved in water e.g. 2-4 dichlorophenol,

(Chang and Chen, 1994), pentachlorophenol, 1,3 dichlorobenzene, trichlorophenol and trichloroethylene (Bhattacharyya et al., 1995). The ozonation studies utilized a presaturator where the ozone was brought into contact with the perfluorocarbon solvent and then the solvent loaded with ozone was brought into contact with the aqueous phase containing the pollutants (Stich and Bhattacharyya, 1986), (Chang and Chen, 1994). This involves physical transfer of the fluorocarbon fluid and the resultant and inevitable handling losses in the dispersive two-phase process. Further, reduction of solvent loss by volatilization into the O_3-containing gas phase requires higher viscosity of the perfluorocarbon fluid; this makes the two-phase dispersive reactor operation very inefficient. This raised a question: can a membrane device used in concert with this perfluorocarbon liquid allow intimate contact between the ozone containing gas phase and aqueous phase containing pollutants in a manner that does not require physical handling or transfer of the solvent. It would certainly result in a drastic lowering of the solvent volume used in the process leading to significant cost reduction.

A thin layer of the perfluorocarbon liquid between the ozone-bearing gas phase and the organic pollutant containing aqueous phase can serve as a reaction medium as well as a form of a liquid membrane. The liquid layer, an interphase between the two flowing phases, allows selectively the contact between the organic species in the liquid phase and the ozone, and satisfies the definition of a membrane. There are three types of liquid membranes based upon the configuration in which they are used: emulsion liquid membranes (ELM), supported or immobilized liquid membrane (SLM or ILM) and contained liquid membrane (CLM). ELM was developed for use in liquid-liquid

extraction studies (Ho and Li, 1992) and are inapplicable within the present scope of study. SLM is formed by immobilizing a thin volume of liquid within a porous substrate. The liquid is held in place by capillary forces. The porous substrates that have been used are polymeric, e.g. polypropylene or Teflon or ceramic, and are in the form of flat disks, sheets, porous tubes or capillaries. The two phases which are the subject of the separation process flow on either side of the substrate and the SLM is in intimate contact with both phases allowing the selective transport of species from one phase into the other through the liquid membrane. It becomes apparent that the SLM has certain disadvantages, viz. that the liquid membrane is held in a place by capillary forces and therefore it is as stable as the strength of those forces. If there is a large pressure differential between the two sides of the membrane, then it is extremely likely that the phase at the higher pressure can push the liquid membrane out and break through to the opposite side of the substrate. Also if the liquid membrane is volatile and/or has a significant solubility, then a loss of liquid membrane by stripping into one or both of the flowing phases may be incurred and in the case of loss by stripping, there is no way to replace the depleted liquid membrane during the process.

An improvement to the SLM process was suggested by Majumdar et al., (1988) and is termed contained liquid membrane (CLM). The process as applied to substrates in the form of hollow fibers, which are essentially long slender tubes with either semipermeable or porous walls, is termed as hollow fiber contained liquid membrane (HFCLM) (Majumdar et al.; 1988, Majumdar et al., 1992). Essentially, the process involves two sets of these hollow fibers setup in a shell or housing, such that the two

flow paths are isolated from each other and the void space within the shell. The porous nature of the walls of these capillaries allows free transport of species across the wall by diffusion. Each flowing phase (the aqueous phase containing the pollutant and the ozone bearing gas phase) passes through one set of hollow fiber and the void space in the shell is filled with this perfluorocarbon fluid, Figure 1.1.2. The immediate and obvious advantage is the stability of the membrane and along with the fact that the concomitant loss of the membrane liquid by stripping into the flowing phases is no longer an issue. An earlier study demonstrated the viability of such a process to treat organic pollutants dissolved in wastewater, but the study was rather abruptly terminated because the polypropylene hollow fiber microporous membranes were not durable in the harsh oxidizing environment (Trivedi, 1992). The study of such a membrane reactor using membranes which are more resistant to oxidation is undertaken here to investigate the utility of such a device to treat organic pollutants dissolved in wastewater. This reactor referred to as a **two-phase membrane reactor** will be discussed in Chapter 3 of this study.

Ozonation is presently limited to the destruction of organic compounds in water. The present range of technologies to treat the problem of VOCs either recover them or oxidize them at elevated temperatures, with or without catalysts. VOCs are recovered and reused if economics permit such a practice. More often, especially if the VOCs are mixtures, which are difficult to separate, the entire gaseous stream is subjected to a catalytic oxidation at an elevated temperature or if the calorific value of the stream is high, incineration. Catalytic oxidation of VOCs is a process under development and the

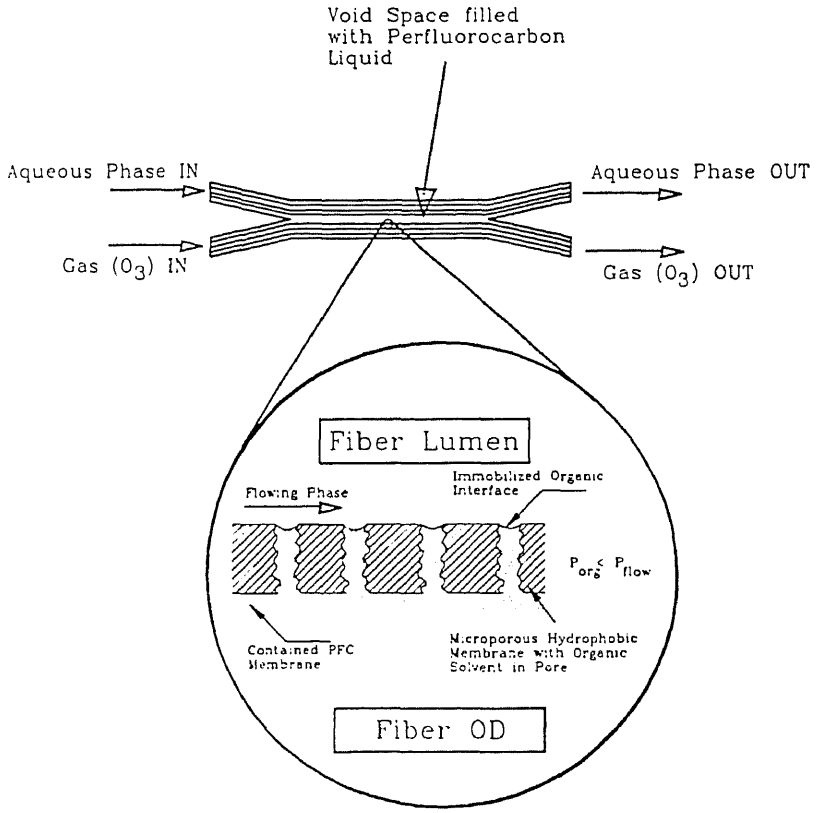

Figure 1.1.2. Schematic of the hollow fiber contained liquid membrane reactor (HFCLMR).

quest for a catalyst or a mixture of catalysts that can handle different VOCs (halogenated, aromatic, etc.) as well as different concentration ranges is being actively pursued (Heck and Farrauto, 1995).

The two-phase membrane reactor described above uses a perfluorocarbon fluid as a membrane and a reaction medium. Such a fluid should therefore show a strong affinity for compounds hydrophobic in nature; many volatile organic compounds (VOCs), e.g. toluene and trichloroethylene (TCE) are of this type. This is demonstrated by the large partition coefficients that these compounds (toluene and trichloroethylene) have into the fluorocarbon phase versus hydrophilic compounds like phenol and nitrobenzene (Shanbhag, 1992). This suggests that a membrane reactor almost identical to the one described above may be used to remove VOCs from a gas stream surrounded by the perfluorocarbon fluid with ozone as an oxidant. The use of ozone as an oxidant to treat VOCs in a gas phase is novel in practice. The reactor, termed as an **absorption-oxidation membrane ozonator**, is discussed in Chapter 4.

The compounds used in this study as organic pollutants in aqueous waste streams are phenol, nitrobenzene, acrylonitrile, toluene and trichloroethylene (TCE); they represent the gamut of organic compounds found in the effluent streams of chemical process industries. Phenol, nitrobenzene and acrylonitrile are extensively used as intermediates, in the production of adhesives, resins, (e.g. phenol is used to make Bisphenol-A, which is extensively used in the production of polycarbonate and epoxy resins, styrene acrylonitrile resins (SAN), etc.), caprolactam (which is subsequently used to make nylon), rubber (e.g. acrylonitrile butadiene styrene (ABS)), aniline (almost all

of the nitrobenzene is used to make aniline which is used as a dye intermediate, manufacture of polyurethane foams, etc.) and to a smaller extent pharmaceutical products (nitrobenzene is used to make acetaminophen) (Kent, 1992). Toluene and trichloroethylene (TCE) represent some of the chemicals that are termed as volatile organic compounds, VOCs (Mukhopadhyay and Moretti, 1993) and account for the formation of ground level ozone and smog. Some halogenated VOCs by virtue of free radical reactions are also responsible for the depletion of the tropospheric ozone layer. Toluene is used as the feedstock for the manufacture of benzene, in automotive fuel (particularly in unleaded premium gasolines) and as a solvent (in the paint, adhesive and pharmaceutical industries). TCE is primarily used in the vapor degreasing of manufactured metal parts, and to lesser extents as a component in paint-strippers and adhesives (Kent, 1992).

The following Chapters (2, 3 and 4) will examine in detail the performance of each reactor to remove organic pollutants from synthetic wastewater streams (single-phase membrane ozonator, Chapter 2; two-phase membrane ozonator, Chapter 3) and waste gas streams (integrated absorption-oxidation membrane ozonator, Chapter 4). The introduction to each chapter will outline briefly the salient features of the reactor, followed by a description of the construction of the individual reactors and the experimental protocols followed in establishing the performance of reactor. Modeling of the degradation of organic pollutants has been undertaken for the single-phase membrane ozonator and the two-phase membrane ozonator and are presented in Chapters 2 and 3 respectively. A rational basis for comparison between the single-phase membrane

ozonator and the two-phase membrane ozonator (since both treat organic compounds in wastewater) will be the amount of pollutant destroyed per unit time per unit aqueous interfacial area. The significance of the above value for each of the reactors will be discussed in greater detail, when discussing the experimental performances of the reactors in Chapters 2 and 3. The experimentally observed amount of ozone utilized per pollutant molecule in the two-phase membrane ozonator as well as its relevance towards improving the design of the membrane module will also be discussed in Chapter 3, for different feed compositions of a particular pollutant. The experimental performance of the integrated absorption-oxidation membrane ozonator for toluene and trichlorethylene as model VOCs will be presented and discussed in Chapter 4.

CHAPTER 2

SINGLE-PHASE MEMBRANE OZONATOR

2.1. Introduction

The contacting of gas and liquid phases to effect the transfer of species between the two phases has been conventionally done using staged towers, packed towers, spray towers, venturi scrubbers, etc. The use of membranes, porous or nonporous, as phase contacting devices offers numerous advantages over conventional contacting equipment. Firstly, membrane devices are not subject to flooding or loading problems as the flow of gas and liquid phases can be independently controlled. Membrane-based contacting devices offer a solution to the problem of liquid entrainment and carryover which limits the contacting efficiency of conventional tower contactors. Much of the phase contacting research, development and commercialization has been carried out using microporous membranes, since these offer less membrane resistance to the transfer of solute species than nonporous membranes (Sirkar, 1992).

The use of nonporous or microporous membranes in ozonation is limited by membrane durability under the extreme oxidizing environment typical of any ozonation reaction. During ozonation the formation of hydroxyl radicals and reactive intermediates which aid in the destruction of the pollutants also increase the attack on the membrane materials. If the membrane material is prone to oxidative attack then the membranes and consequently the membrane ozonator is compromised (Trivedi, 1992; Castro and Zander, 1995). Therefore the selection of the membrane material is critical to the function and

use of the membrane material. Of the materials available, there are only two materials, that are known to be resistant to oxidative degradation and available as tubular membranes, Teflon and silicone rubber.

The large diameters (2 mm OD) of the currently available Teflon tubules do not allow enough tubules to be packed into an ozonator shell to warrant a sufficient increase in "a", the surface area available per unit ozonator volume. The surface area of contact available per unit volume of ozonator, "a", increases considerably as the diameter of the tubule is decreased and consequently limits the use of Teflon tubules in the single phase membrane ozonator.

The other material, silicone, is available in tubular form in dimensions (0.635 mm OD) much smaller than those for the Teflon tubules. Silicone rubber (PDMS - polydimethylsiloxane) has an illustrious history as a material of choice for the study of the separation of O_2 and N_2, especially since it possesses a large permeability for oxygen (933 barrers) compared with most membrane materials (Zolandz and Fleming, 1992) and a moderate permselectivity for O_2 over N_2. The literature is replete with examples of the eclectic uses of silicone rubber (PDMS) as a membrane. Silicone rubber in a tubular membrane form (either as a thin film coated on a porous substrate or as a homogeneous capillary) has been used to oxygenate water (Tang and Hwang, 1976), to obtain oxygen enriched air (Majumdar et al., 1987, and all references quoted therein), to remove organic vapors (VOCs) from air (Baker et al. 1987; Baker et al., 1996), to remove organic compounds from water by pervaporation (Slater and Fleming, 1992), etc.

The durability of such a material under the oxidative conditions at the outset is

unknown. Since silicone rubber is used in a variety of applications, where it is exposed to various solvents without serious compromise of the integrity of the material, it seems likely that such a material could be used to study, at least for a short duration of time, the performance of a single phase membrane ozonator device. A schematic of the way silicone rubber in the form of a nonporous membrane could be used to ozonate a compound "A" dissolved in water is shown in Figure 2.1.1.

This chapter details the study of the single-phase membrane ozonator to degrade pollutants dissolved in wastewater. The experimental section outlines the construction of the membrane ozonator, the measurement of the permeability coefficients of O_2 and O_3 across the silicone capillaries prior to and after exposure to ozone and the experimental performance of the reactor. A theoretical model based upon the diffusion of ozone and a model pollutant and the second order reaction between ozone and a model pollutant in water is proposed to study the behavior of this ozonator. This model is supposed to clarify the resistances to mass transfer for ozone and the pollutant and the concomitant effects on the performance of the reactor to treat a stream of the pollutant. By understanding the effects of either reaction or mass transfer, the design of reactor may be improved resulting in a more efficient ozonation process.

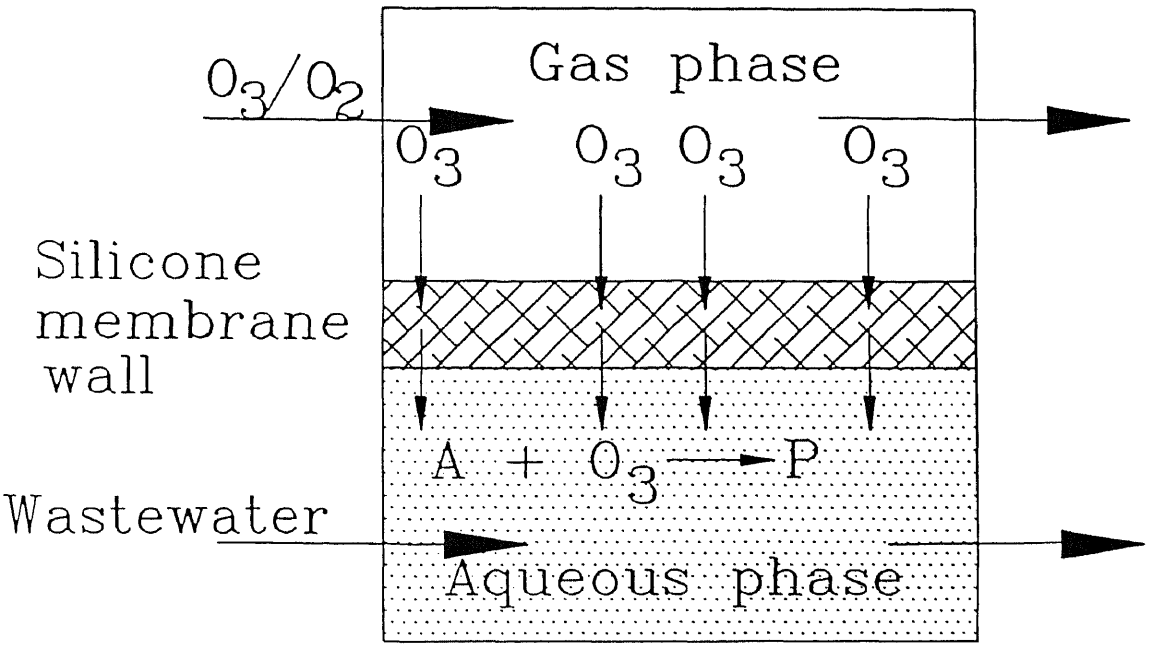

Figure 2.1.1. Schematic of a single-phase membrane-based ozonation process.

2.2. Experimental Procedure

2.2.1. Materials, Chemicals and Equipment

The following materials, chemicals and equipment were used in the experiments.

Ozone generator (Model T-408, Polymetrics, Colorado Springs, CO).

Ozone monitor (Model HC 400, PCI Technologies, West Caldwell, NJ).

High Performance Liquid Chromatograph, HPLC (Model 1090A, Hewlett Packard, Paramus, NJ) with a UV filter photometric detector.

HPLC integrator (Model 3390, Hewlett Packard, Paramus, NJ).

HPLC autosampler (Micromeritics, Alcott Chromatography, Norcross, GA).

HPLC column (type Hypersil ODS, length 10 cm, dia. 3 mm, Chrompack, Bridgewater, NJ).

Gas Chromatograph, GC (Model 5890, Hewlett Packard, Paramus, NJ) with a thermal conductivity detector (TCD) and a 6 port gas sampling valve.

GC integrator (Model 3393A, Hewlett Packard, Paramus, NJ).

GC column (type Molecular Sieve, 13X, Mesh 80/100, 0.085" ID, 1/8" OD, 10 feet length, Alltech Associates, Waukegan, IL).

Silicone capillaries (Silastic, medical-grade, (by Dow Corning, Midland, MI) Baxter Diagnostics, Edison, NJ).

FEP tubing and polypropylene Y and T-barbed fittings (Cole Parmer, Chicago, IL).

Rotameter (Cole Parmer, Chicago, IL).

Four Way Valve (cross-over), 1/8" NPT (Swagelock, R. S. Crum, Mountainside, NJ).

Mass flow controller transducer (Model 8272, Matheson, East Rutherford, NJ).

Multichannel dyna-blender (Model 8284, Matheson, East Rutherford, NJ).

Oxygen Extra Dry, Helium High Purity, Nitrogen Extra Dry, Air Zero (Matheson, East Rutherford, NJ).

Phenol, acrylonitrile, nitrobenzene, sulfuric acid, sodium thiosulfate, potassium iodide and potassium dichromate (ACS grade, Fisher Scientific, Springfield, NJ).

Acetonitrile (HPLC grade, Fisher Scientific, Springfield, NJ).

2.2.2. Preparation of Membrane Reactors

The fabrication of the single phase membrane ozonator employed nonporous silicone capillaries of the following dimensions, 1.6 mm ID, 2.4 mm OD for module 1 and 0.3 mm ID, 0.63 mm OD for all subsequent single phase membrane ozonator modules (Table 2.2.1).

Table **2.2.1.** Details of silicone capillary (SILCAP) membrane-based ozonators

Module no.	Capillary dimensions I.D./O.D.(mm)	Active length (cm)	No. of capill.	Shell volume (cm^3)	a[a] (cm^2/cm^3)
SILCAP 1	1.58/2.41	28.0	4	39.77	2.39
SILCAP 2-6	0.305/0.610	21.59	97	20.6	15.28

[a] Specific surface area per unit volume of ozonator based on OD of the capillary.

These silicone capillaries (silastic medical grade) were counted, cut to length and laid out in the form of a mat. The ends of the capillaries were bunched and tied; then the capillaries were inserted in a transparent FEP shell of dimensions 0.61 cm ID, 1.03 cm OD (Cole Parmer, Chicago Il) fitted with barbed polypropylene Y-fittings at the two ends (Cole Parmer, Chicago Il). The two fiber ends were potted using two sets of epoxies (Beacon Chemical Co., Mount Vernon, NY). The external tube sheet was formed using the A2 epoxy with activator "A", using the proportion of 8 drops of activator to 5 grams of epoxy. The A2-A epoxy, a viscous paste, was liberally applied by means of a spatula to seal the void space between the silicone capillaries and the barbed Y-connector. The internal tube sheet was formed using the C4 epoxy with activator "D", using the proportions of 1 part activator to 4 parts epoxy by weight. The C4-D epoxy mixture was degassed in a desiccator by a vacuum pump and then poured in place via a small hole drilled into the side of the barbed Y-fitting. The hole itself was sealed up with the epoxy. The epoxies were allowed to cure for seven days and then the module was filled with water on the shell side; the water pressure in the shell was raised to 10 psig to check for leaks. Table 2.2.1 provides the geometrical specifications of the membrane modules henceforth identified as the SILCAP modules. Figure 2.2.1(a) shows the arrangement of the epoxy layers in the capillary end of the module, while 2.2.1(b) is a photograph of the module.

2.2.3. Analytical Techniques to Measure Organic Pollutants in Water

The aqueous feed was analyzed for pollutants using a High Performance Liquid Chromatograph (HPLC) equipped with a Hypersil ODS analytical glass column and a

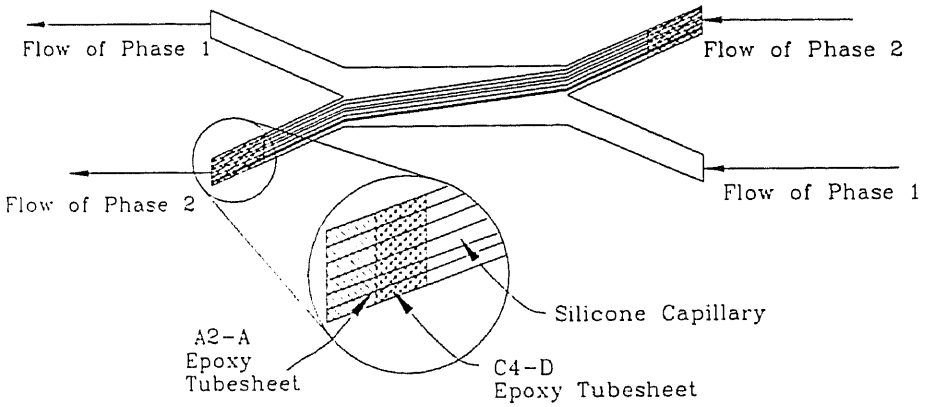

Figure 2.2.1(a). Schematic of single-phase membrane ozonator module showing the fiber ends embedded in an epoxy layer.

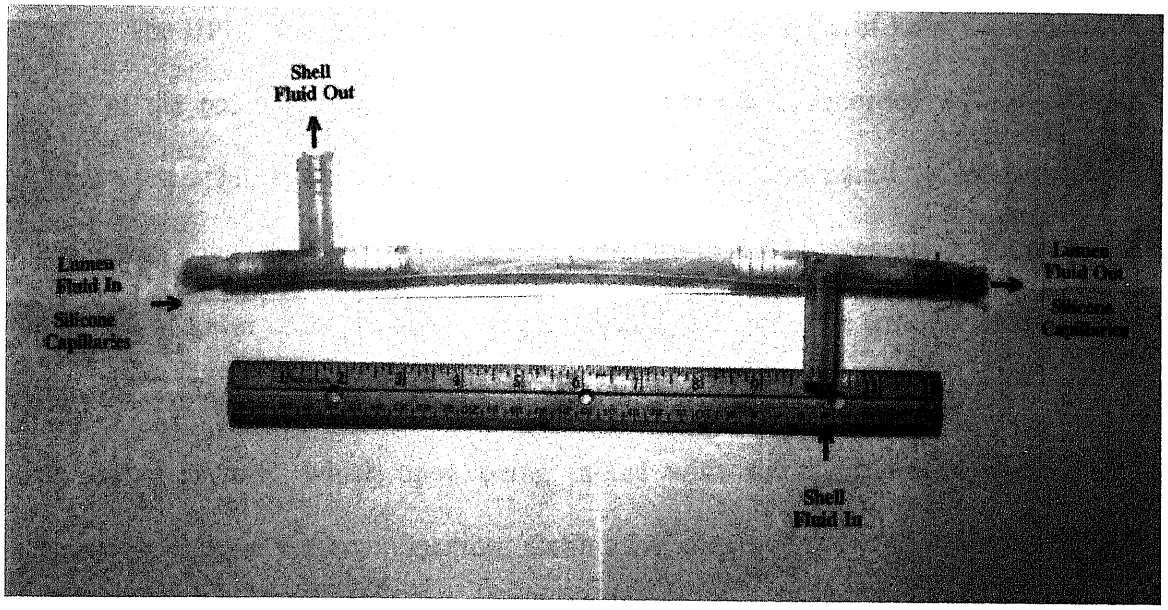

Figure 2.2.1(b). Photograph of the single-phase membrane ozonator.

filter photometric UV detector. Table 2.2.2 indicates the HPLC conditions employed to detect and determine the concentration of pollutants in the aqueous phase.

Table 2.2.2. HPLC conditions for the organic compounds studied

Compound	Wavelength (nm)	Composition[a] (%)	Flow rate (cc/min)
Acrylonitrile	210	40 AC/60 H_2O	0.4
Phenol	254	40 AC/60 H_2O	0.4
Nitrobenzene	254	40 AC/60 H_2O	0.4

[a] Acetonitrile (AC) and water were used as the mobile phase.
A sample loop of 10 μl was used.

The HPLC was initially calibrated by injecting samples of known composition of each of the pollutants and noting the area of the peaks recorded by the integrator. Aqueous samples of nitrobenzene and acrylonitrile were prepared by spiking deionized water with a pure liquid sample of the pollutant to give the necessary feed composition. Samples of lower concentrations were obtained by diluting the original feed samples to the required extent. For phenol, the aqueous feed was prepared by weighing out a sample of phenol crystals, which upon being mixed with deionized water would give the necessary aqueous feed composition. Calibration curves displaying the concentration of the aqueous pollutant versus the recorded peak area were plotted for acrylonitrile, phenol and nitrobenzene. These are shown as Figures 2.2.2, 2.2.3 and 2.2.4 respectively.

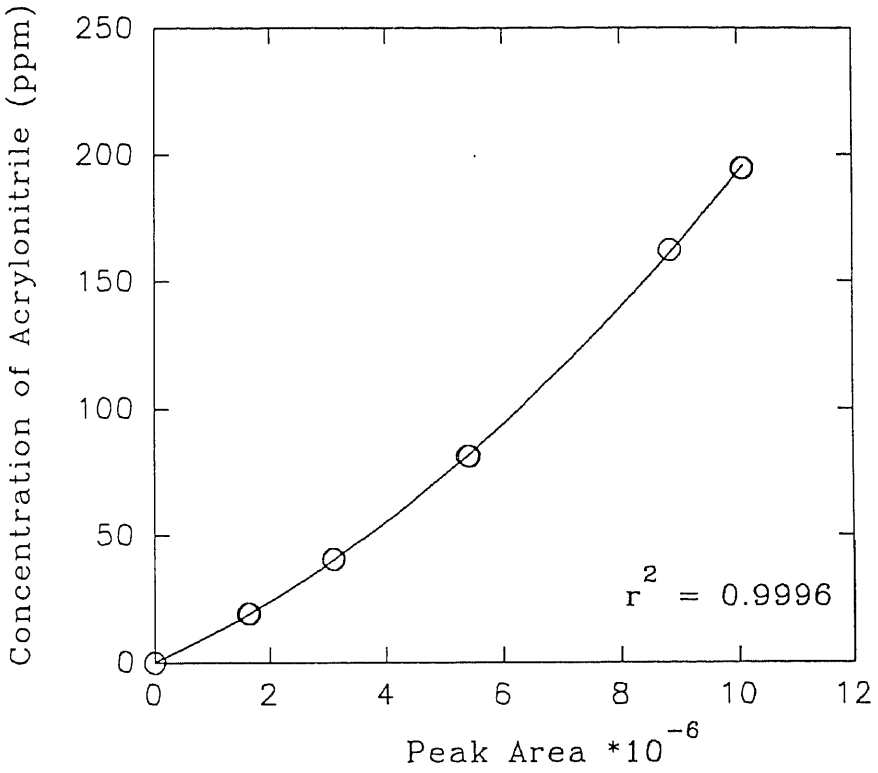

$$\text{Conc.} = 6e{-}2 + (1e{-}5 * \text{Peak Area}) + (9.15e{-}13 * \text{Peak Area}^2)$$

Figure 2.2.2. HPLC calibration curve for acrylonitrile.

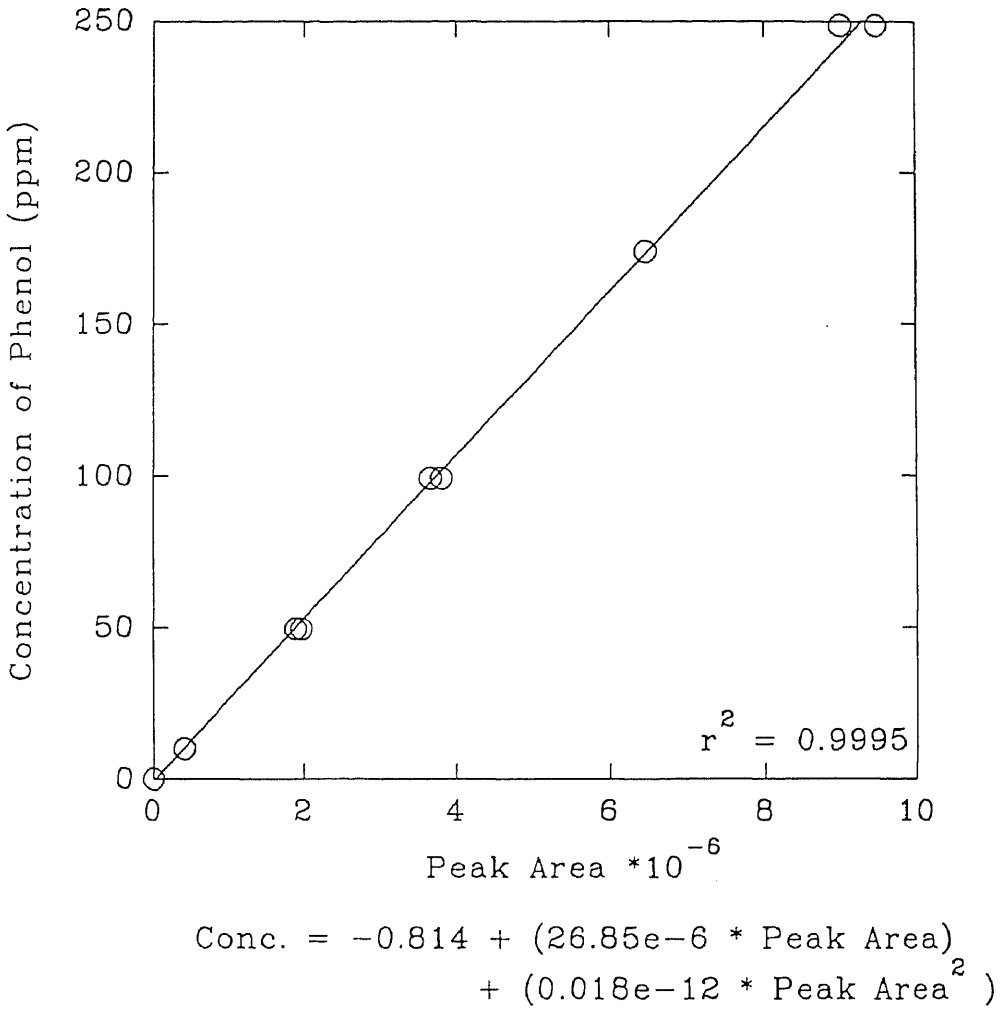

Figure 2.2.3. HPLC calibration curve for phenol.

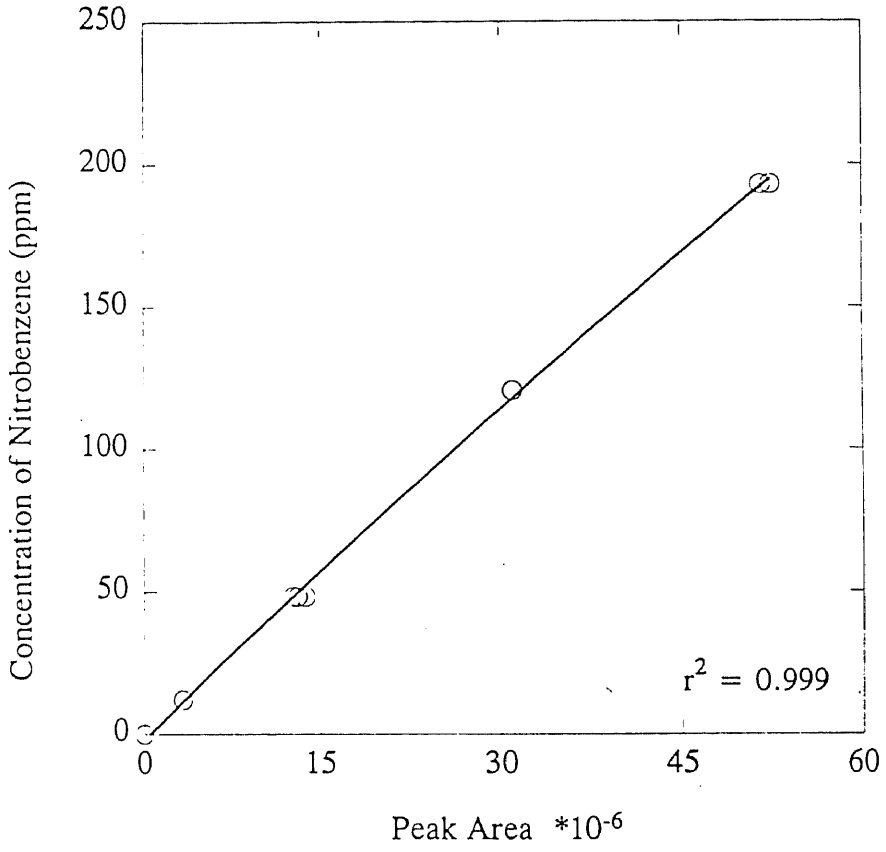

Conc. = -2.0 + (4.0 e-6 * Peak Area)
+ (-4.5 e-16 * Peak Area^2)

Figure 2.2.4. HPLC calibration curve for nitrobenzene.

2.2.4. Source of Ozone

Ozone was generated by feeding a pure oxygen gas stream from a gas cylinder to the ozone generator. The ozone generator was operated at a voltage setting of 90 volts; the pressure within the ozone generator was held at 9 psig (163.4 kPa) by a back pressure regulator. The flow rate of oxygen through the ozone generator was maintained at 0.6 standard liters per minute (SLPM). A small portion of the ozone/oxygen mixture (O_3/O_2) was diverted for experimental purposes. The major portion was vented after passing through two KI (2% concentration by weight) wash bottles linked in series to break down any ozone and a sodium thiosulfate bottle to trap any entrained iodine.

2.2.5. Measurement of the Permeability Coefficient and Separation Factor of Oxygen and Nitrogen Across the Silicone Membrane

Permeability coefficients of nitrogen (N_2) and oxygen (O_2) across the silicone capillary membranes were measured before and after exposure to ozone. The permeability values of O_2 and N_2 were compared with those available in literature to ascertain the viability of the experimental technique. Gas phase mixtures of different compositions were generated by means of air and helium cylinders connected to mass flow controller transducers. The mass flow controllers allowed precise flow control of each of the gas phases. The gas chromatograph (GC) was calibrated for O_2 and N_2 by sampling gas phase mixtures of known proportions of air and helium and noting the peak areas obtained from the GC. The gas was sampled by a gas sampling valve through which the flow was maintained between 10 and 30 ml/min. The GC operating conditions are listed in Table 2.2.3. A sample calibration is shown in Figure 2.2.5.

Table 2.2.3. Operating conditions of the gas chromatograph to measure the permeability of O_2 and N_2 across the silicone membrane.

Gas Chromatograph	Hewlett Packard Model 5890
Detector	Thermal Conductivity Detector (TCD)
Sampling Method	6 port gas sampling valve
Data Acquisition	Hewlett Packard integrator 3393A.

Column : Molecular Sieve 13X, Mesh 80/100, 0.085" ID, 0.125" OD, 10 feet length.

Property	Condition
Column Temperature	50 °C
Injector Temperature	100 °C
Detector Temperature	300 °C
Attenuation	6
Threshold	3.0

The schematic to measure the permeability coefficients of O_2 and N_2 is shown in Figure 2.2.6. Experiments were conducted by passing the air stream through the tube side and the helium stream cocurrently through the shell side of the module, and then changing the streams so that air was fed into the shell and helium fed into the tube side. The conditions of pressure and flow rates were kept as identical as possible when air was in the tube and vice versa. This precluded any possible variations of permeability

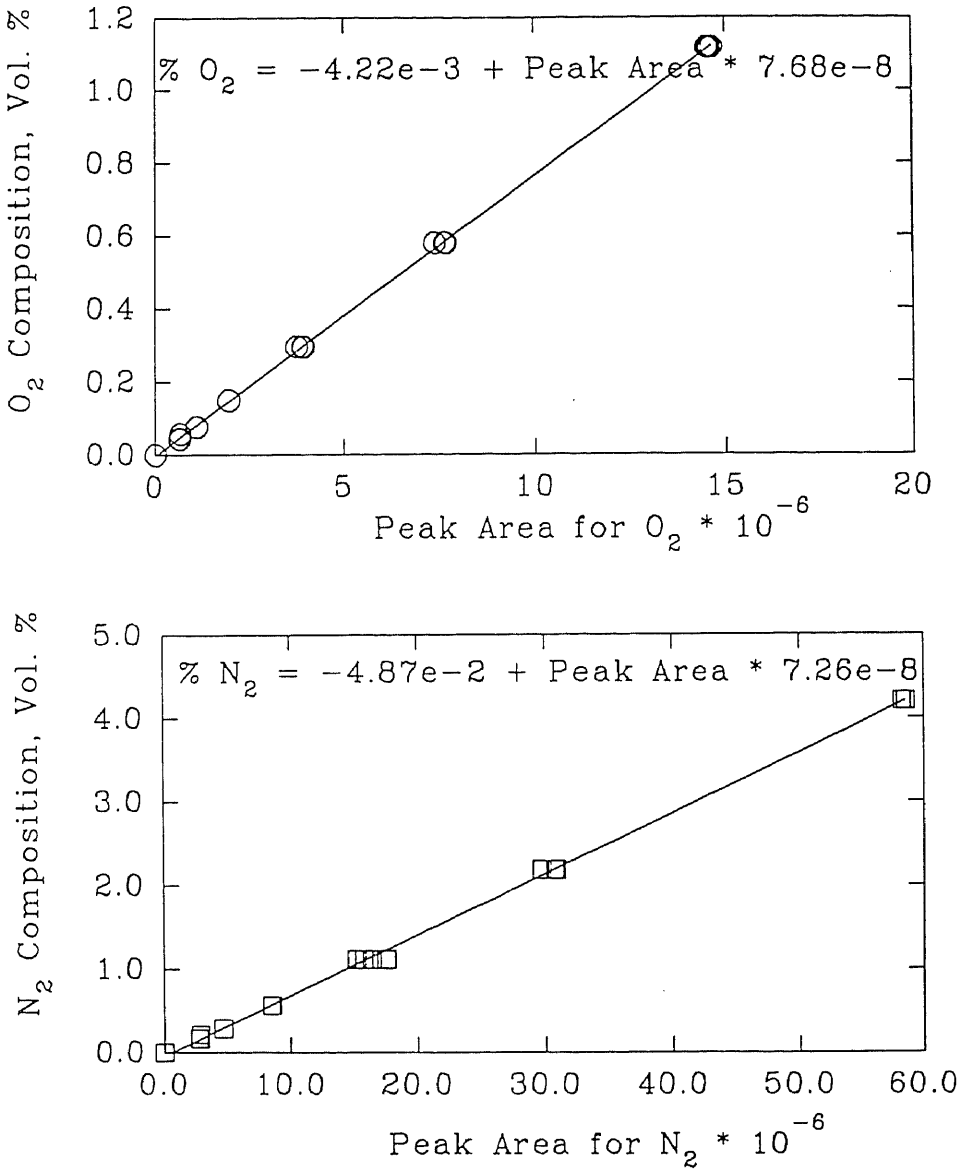

Figure 2.2.5. GC calibration curves for N_2 and O_2.

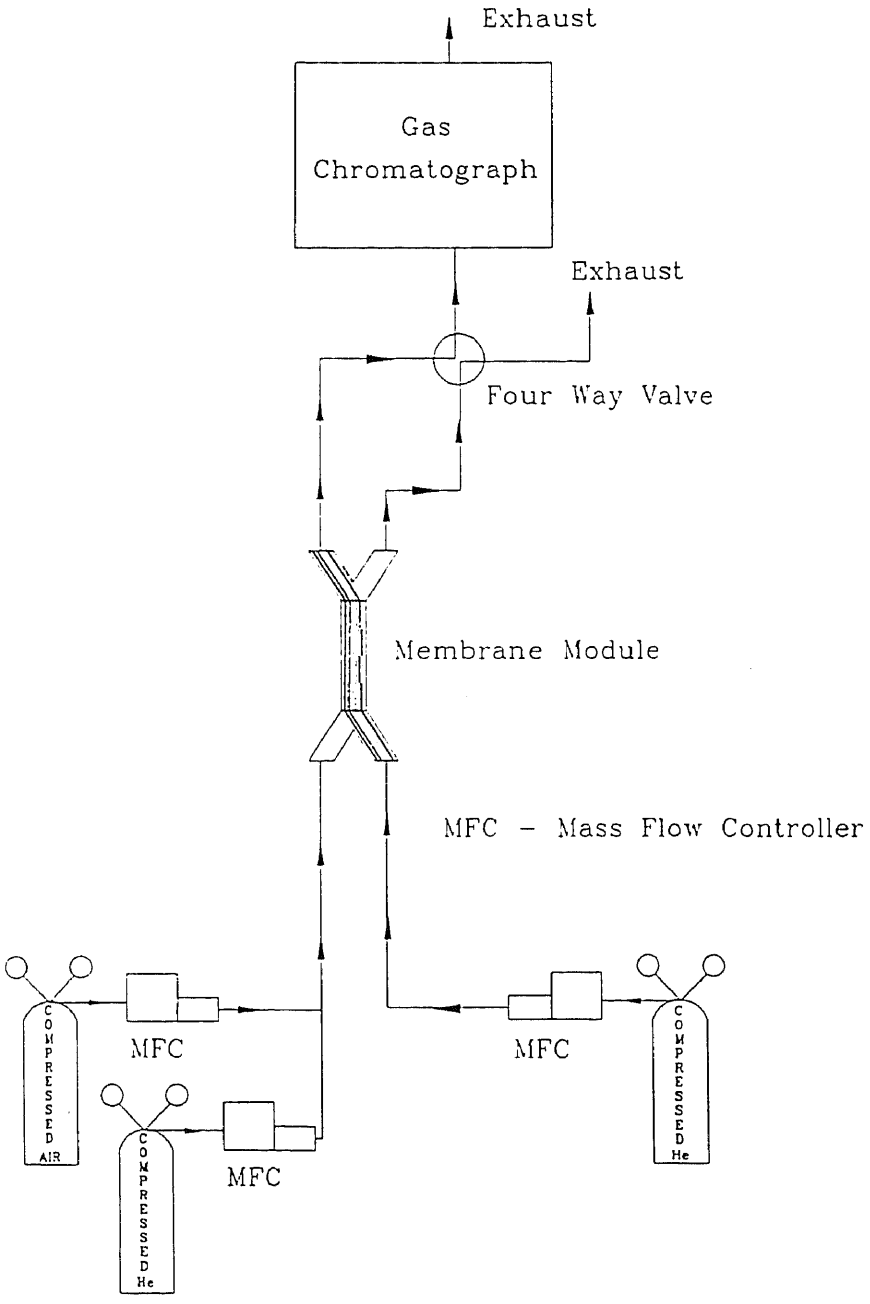

Figure 2.2.6. Schematic of the setup to measure the permeability of O_2 and N_2 through silicone capillaries.

coefficient due to the geometry and elasticity of the silicone capillaries. The pressures of both streams were kept as close to atmospheric as possible to preclude any pressure drop effects across the length of the capillaries. The sweep gas, He, was sampled via the gas sampling valve of the GC periodically. The steady state was rapidly reached; it was ascertained by the constant peak areas obtained for N_2 and O_2. At this point the feed outlet was also sampled to measure the change in the feed concentration. Since the feed flow rate and concentrations were fairly high, the variation between inlet and outlet feed concentrations were found to be negligible. This was established by checking the feed outlet concentration after steady state had been reached. Since the objective was to determine the effect, if any, of exposure to ozone and ozonation reactions upon the permeabilities of oxygen and nitrogen, three modules were selected for the study. The characteristics of modules, SILCAP #1 and #5 are tabulated in Table 2.2.1, while that of the module NEWCON #1 is tabulated later in Table 4.2.1 of Chapter 4.

2.2.6. Measurement of Permeability Coefficient of Ozone across the Silicone Membrane

The measurement of permeability coefficient of ozone in silicone rubber (PDMS) was conducted with the three modules, SILCAP 1 and 5 and NEWCON 1. The flow rate of ozone through any of three modules had to be measured accurately. Ozone displays a propensity to attack most materials and this precluded the use of a gas flow controller in line with the O_3/O_2 gas stream. Therefore a rotameter had to be used to determine the flow rate of ozone through the module. The experimental setup was completed as shown in Figure 2.2.7.

The ozone monitor used in this study was a Model HC 400; it had a range of 0 - 15 wt% (0 - 99,000 ppm by volume). It was equipped with inlet needle valves for the sample and zero gas, a flow meter (of rotameter type), a solenoid valve and a sample chamber. The unit measured ozone by comparing the UV absorption of the sample with that of the zero gas, which for this study, was oxygen. Depending upon whether the sample or zero gas was present in the sample chamber, the intensity of the UV light traversing across the sample chamber was attenuated as described by the Beer-Lambert Law. The ratio of the intensities was determined and the result was processed by a microcomputer built into the device to determine the ozone concentration and display it on a digital readout. The switching of the flow between the zero and the sample gas was initiated by a solenoid valve built into the ozone monitor with a cycle time of 20 seconds. During the period when the zero gas was being sampled via the solenoid valve, the sample gas flow was stopped.

For the measurement of the permeability coefficient of ozone in the silicone rubber capillaries in the set up (Figure 2.2.7), each module, SILCAP 1 and 5 and NEWCON 1 was taken in turn and connected to the setup. The measurement of permeability coefficient of ozone through the silicone capillaries for the module NEWCON 1 was carried on one set of silicone capillaries after most of the experiments had been performed, as will be described in Chapter 4. It was found that extensive experimentation had severely compromised the integrity of the second set. The four other ports comprising of the damaged silicone capillary set and Teflon tubule set were capped

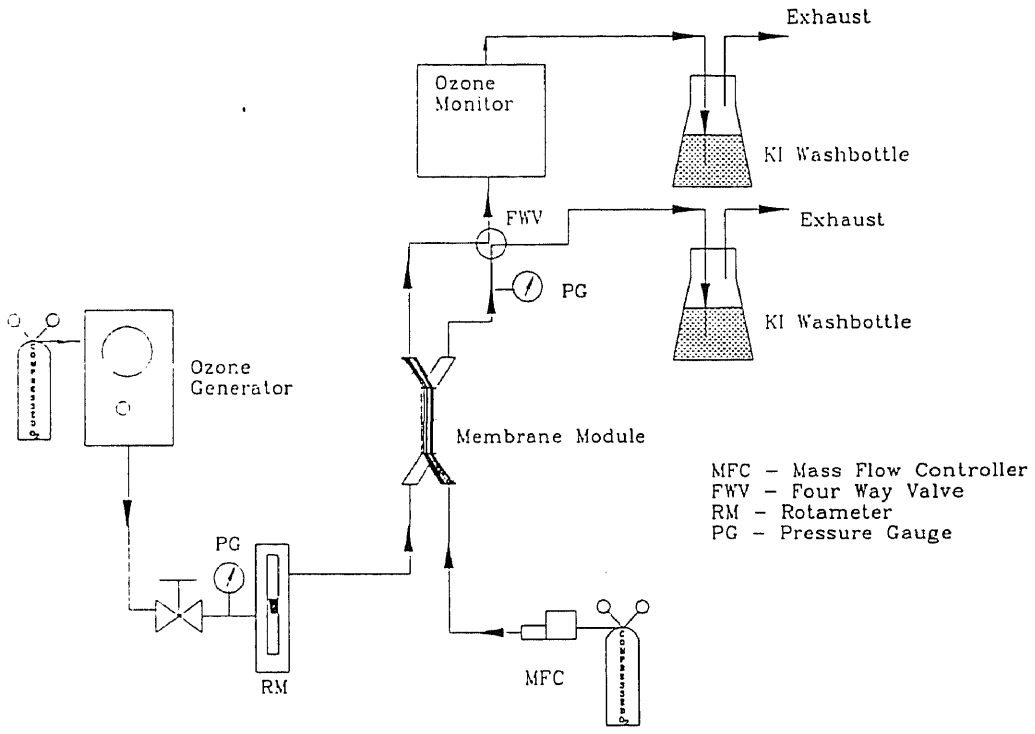

Figure 2.2.7. Schematic of the setup to measure the permeability of ozone through silicone capillaries.

for the duration of the experiment. Prior to the commencement of experiments, the rotameter was calibrated with oxygen. Since the mass flow controller allowed a precise gas flow measurement this flow rate was used to calibrate the reading on the rotameter. Concurrently the gauge pressures recorded by gauges 1 and 2 were recorded. The setup, a modification of that shown in Figure 2.2.7, is shown in Figure 2.2.8 and the calibration is shown in Figure 2.2.9. Oxygen was used as a sweep gas since it was also used as a blank in the ozone monitor and was the diluent phase of the ozone stream. The four way valve allowed cross-over of the two streams, so that the ozone concentration in each of the streams could be monitored. For the majority of the experiments, the sweep stream comprising of oxygen and any ozone that has permeated across the silicone membrane phase was sampled. After steady state was achieved, the outlet of the feed gas stream was sampled. Experiments were carried out by admitting the feed of O_3/O_2 in the shell side of the module as well in the tube side of the module.

2.2.7. Measurement of Reactor Performance to Degrade Organic Pollutants in Water

The SILCAP reactor was positioned in the reactor loop as shown in Figure 2.2.10. The aqueous feed was prepared by spiking deionized water with a pure liquid sample of the pollutant to give the necessary feed composition in the case of nitrobenzene and acrylonitrile. For phenol, the aqueous feed was prepared by weighing out a sample of phenol crystals, and dissolving in a given volume of deionized water to achieve the necessary aqueous feed composition. The aqueous feed was poured into a stainless vessel,

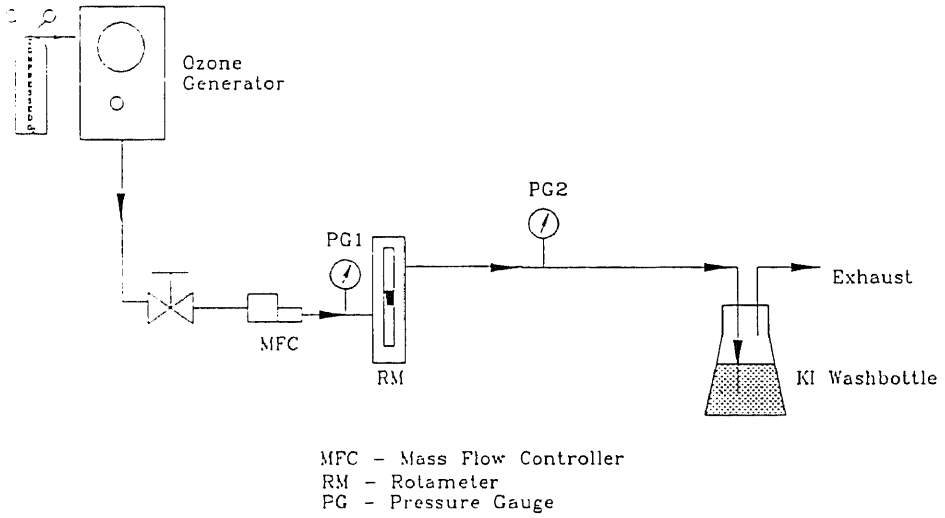

Figure 2.2.8. Schematic of the setup to calibrate the rotameter for O_2.

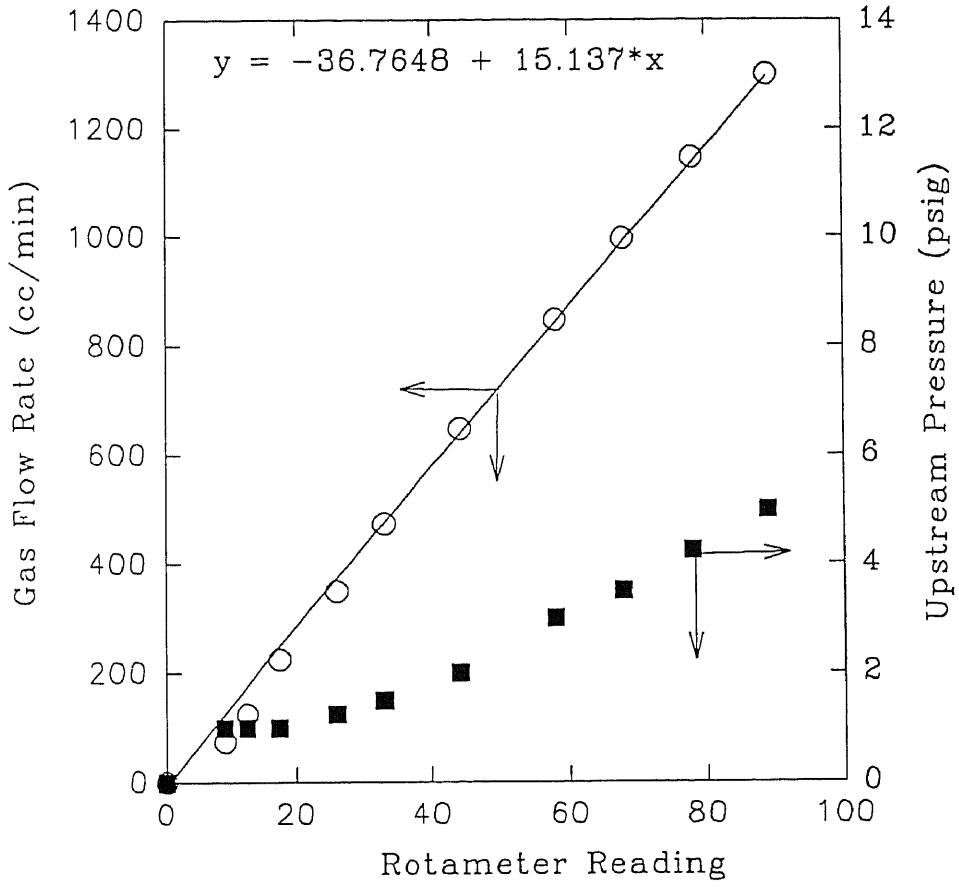

Figure 2.2.9. Calibration curve of rotameter for O_2.

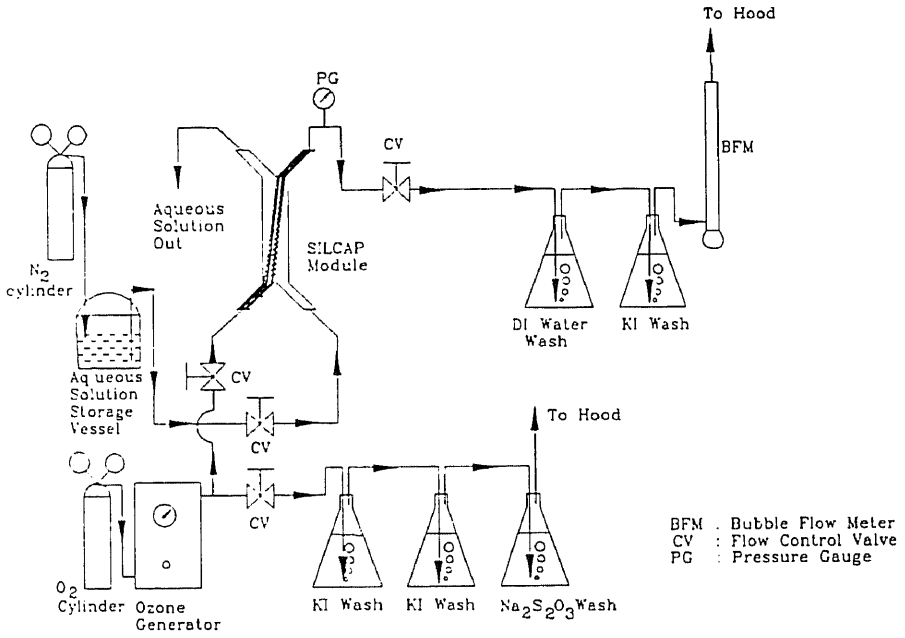

Figure 2.2.10. Schematic of the experimental setup to study the degradation of organic pollutants in wastewater by the single-phase membrane ozonator.

which was subsequently pressurized with N_2 to deliver the aqueous phase. Experiments were carried out by passing the aqueous stream in the shell side of the module, while on the tube side of the module, an O_3/O_2 mixture was passed. The aqueous phase flow rate was controlled by a needle valve. The pressure of the aqueous phase was kept slightly higher than that of the gas phase. This eliminated the formation of bubbles of oxygen, which would cause the buildup of gas slugs. The aqueous phase was sampled periodically and a sample was injected into the HPLC to determine the pollutant concentration.

Two types of experimental startup procedures were adopted. The first procedure had both the aqueous phase and the oxygen phase admitted simultaneously into the module (the ozone generator was not switched on) and the flow rates of each phase were adjusted. The ozone generator was switched on and the experiment proceeded as outlined in the paragraph above. The second startup procedure was carried out to study the uptake of the pollutant by the silicone capillaries. This study was carried out with nitrobenzene as a model pollutant. During this startup, both phases were admitted into the ozonator. The ozone generator was kept switched off and the outlet pollutant concentration was monitored by injecting aqueous samples into the HPLC periodically. As soon as the exit concentration rose to the feed concentration, the ozone generator was switched on and the experiment was allowed to proceed as outlined earlier.

2.2.8. Measurement of the Mass-Transfer Coefficient of Ozone

To determine the liquid phase mass-transfer coefficient of ozone, the setup was completed as shown in Figure 2.2.11. Prior to the start of the experiment, a solution of

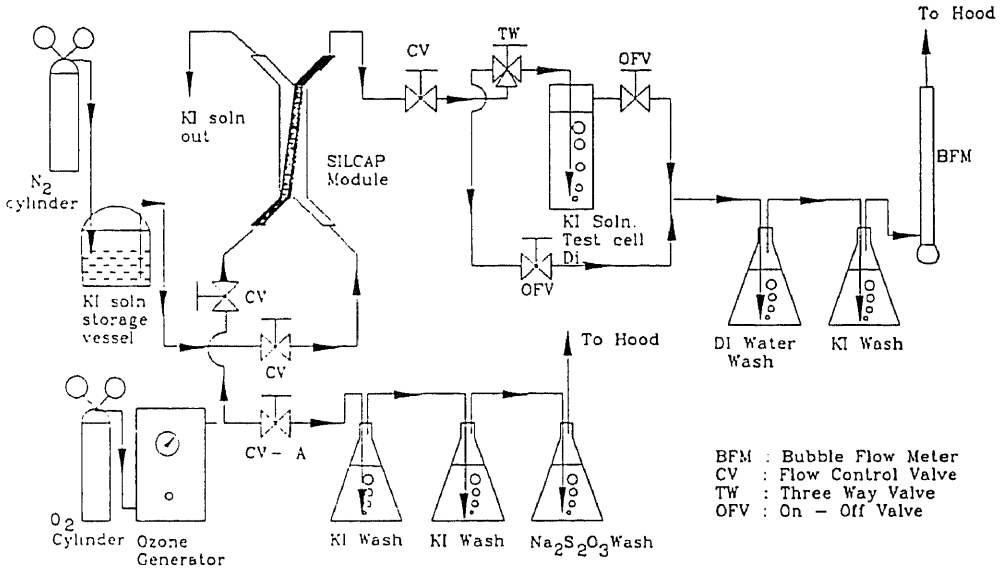

Figure 2.2.11. Schematic of the experimental setup to measure the mass transfer coefficient of ozone in the single-phase membrane ozonator.

potassium dichromate ($K_2Cr_2O_7$) was carefully prepared. A small sample of powdered $K_2Cr_2O_7$ was weighed out and transferred to a 1 liter standard flask and made upto the mark with distilled water. A solution of sodium thiosulfate ($Na_2S_2O_3$) was prepared by weighing out a sample of $Na_2S_2O_3$ into a 2 liter standard flask and made upto the mark with distilled water. This solution of $Na_2S_2O_3$ was standardized with the $K_2Cr_2O_7$ solution as follows. A portion of this solution was transferred to a 50 ml burette. A 10 ml sample of the $K_2Cr_2O_7$ was pipetted into a 50 ml conical flask. It was acidified with a few drops of sulfuric acid (H_2SO_4) and then titrated against the $Na_2S_2O_3$ solution, with a starch solution as an indicator, close to the onset of the endpoint. A 2% solution of potassium iodide (KI) was prepared by adding 120 grams of KI crystals to 6 liters of distilled water and transferred to a stainless steel pressure vessel. The KI solution thus prepared was passed on the shell side of the single phase membrane reactor module, at a measured flow rate by pressurizing the storage vessel with N_2, while a measured flow rate of O_3/O_2 was admitted through the lumen of the silicone capillaries. The pressure of the aqueous phase was kept slightly above atmospheric pressure to alleviate the extensive formation of O_2 bubbles on the wall of the silicone capillary on the aqueous side of the membrane.

A measured volume of KI solution was collected at the outlet of the module, acidified with a few drops of H_2SO_4, buffered with a few drops of $NaHCO_3$ and titrated against $Na_2S_2O_3$ with starch as an indicator towards the final stages of titration. During the major portion of the experiment, the O_3/O_2 gas stream was passed out to a bubble flow meter via a deionized water wash and a KI wash to remove ozone. To determine the concentration of ozone in the gas stream leaving the reactor, the O_3/O_2 stream was

bypassed to an Erlenmeyer flask filled with 150 ml of KI solution for a measured duration of time. During this period the gas flow rate through the flask was measured and noted. At the end of the time duration, the flow was reverted back, so that it bypassed the Erlenmeyer flask. A 20 ml sample of the KI solution from the Erlenmeyer flask was pipette into a conical flask, acidified with a few drops of H_2SO_4, buffered with a few drops of $NaHCO_3$ and titrated against a standardized $Na_2S_2O_3$ solution with a starch solution used as an indicator close to the onset of endpoint. The concentration of ozone in the feed O_3/O_2 stream was measured by passing the gas stream through the Erlenmeyer flask filled with 150 ml of KI solution for a measured amount of time. The pressure over the duration of this experiment as in all experiments was kept very close to atmospheric pressure and this was observed by means of a pressure gauge plumbed inline with the gas streams.

2.3. Development of Mathematical Model

2.3.1. Mathematical Description of the System

The modeling of the degradation of an aqueous pollutant by ozone in a single phase membrane ozonator is undertaken subject to a few assumptions. The liquid phase flows on the shell side of the module: the rationale for this has been outlined in the preceding section. The flow of liquid on the shell side is akin to that of liquid flowing on the shell side of a shell-and-tube heat exchanger in the absence of shell-side baffles. The difference here is that the fiber bundle is randomly arranged unlike the regularly arranged tubes of a heat exchanger tube bundle. The flow of liquid around a bank of tubes in the context of heat transfer has been examined by a number of investigators. The work of Happel (1959) in describing the flow of liquid around a bank of tubes outlined the "free surface model". This model tacitly assumes that each tube is surrounded by an envelope of liquid; the boundary of this envelope is termed as a "free surface". A schematic of the tubular membrane surrounded by the free surface envelope is shown in Figure 2.3.1. There is no momentum, heat or mass transferred across this surface, which physically means that there is no tube-to-tube (in the case of tubular membranes or heat transfer tube banks) interaction. The fractional volume of liquid in the envelope bounded by the free surface is equivalent to the ratio of fluid volume to the total volume in the shell. The model is inapplicable above a tube packing fraction of 0.5 (or conversely if the void fraction in the shell is below 0.5) and assumes a regular pitch (e.g. equilateral triangular spacing). This model has been used to analyze the performance of

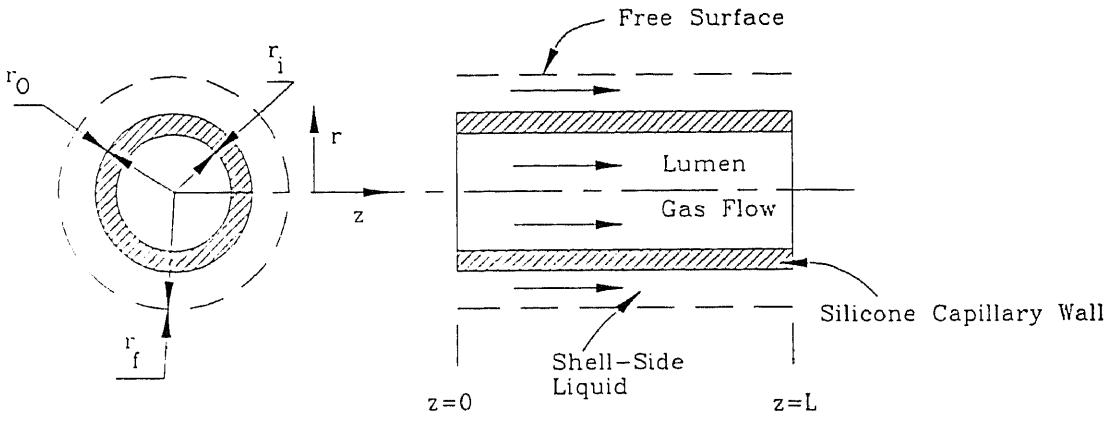

Figure 2.3.1. Schematic of the free surface surrounding a silicone capillary.

hollow fiber based reverse osmosis (Gill and Bansal, 1973), the absorption of CO_2 and SO_2 in water (Karoor and Sirkar, 1993) and the study of hollow fiber membrane-based rapid pressure swing absorption (Bhaumik et al., 1996).

The outside radius of the free surface from Happel's model (1959) as shown in Figure 2.3.1 is given by the following equation

$$r_f = \left[\frac{1}{1-\epsilon}\right]^{\frac{1}{2}} r_o \tag{2.3.1}$$

where r_f and r_o are the free surface radius and outside radius of the silicone capillary respectively, and ϵ is the shell-side void volume fraction. The shell-side void volume fraction ϵ is defined by

$$\frac{1}{1-\epsilon} = \frac{r_s^2}{N_{fibs}\, r_o^2} \tag{2.3.2}$$

where N_{fibs} is the total number of silicone capillaries and r_s is the shell radius. The above two relations lead to r_f being expressed as

$$r_f^2 = \frac{r_s^2}{N_{fibs}} \tag{2.3.3}$$

The derivation of the above equations based upon Happel's "free surface model" is discussed in Appendix 1. Based upon this theory, the liquid velocity $v_z^l(r)$ in the shell side of the module is derived from the momentum balance equation:

$$\frac{1}{r}\frac{d}{dr}\left[r\,\frac{dv_z^l(r)}{dr}\right] = \frac{1}{\mu_l}\frac{dP_z^l}{dz} \tag{2.3.4}$$

The boundary conditions are as follows.

$$\text{At} \quad r = r_f , \; \frac{d v_z^l}{dr} = 0 .$$

$$\text{At} \quad r = r_o , \; v_z^l = 0 .$$

Solving the equation 2.3.4 with the boundary conditions shown above for flow in the positive z direction yields the following velocity profile in the liquid envelope:

$$v_z^l(r) = - \frac{dP_z^l}{dz} \frac{1}{4 \mu_l} \left[- r^2 + r_o^2 + 2 r_f^2 \ln \left[\frac{r}{r_o} \right] \right] \tag{2.3.5}$$

The average liquid velocity on the shell side can be derived by integrating the above equation over the shell radius as

$$v_z^l(av) = \frac{\pi \int_{r_o}^{r_f} v_z^l(r) \, r \, dr}{\pi (r_f^2 - r_o^2)} \tag{2.3.6}$$

which gives an equation for the average liquid velocity as follows

$$v_z^l(av) = - \frac{dP_z^l}{dz} \frac{r_f^2}{8 \mu_l (r_f^2 - r_o^2)} \left[- 3 r_f^2 - \frac{r_o^4}{r_f^2} + 4 r_o^2 + 4 r_f^2 \ln \frac{r_f}{r_o} \right] \tag{2.3.7}$$

The above equation together with equation (2.3.5) can be rearranged to give the velocity profile in terms of the average liquid velocity in the free surface envelope:

$$v_z^l(r) = 2\, v_z^l(av) \left[1 - \frac{r_o^2}{r_f^2}\right] \frac{\left[\frac{r^2}{r_f^2} - \frac{r_o^2}{r_f^2} + 2\ln\frac{r_o}{r}\right]}{\left[3 - 4\frac{r_o^2}{r_f^2} + \frac{r_o^4}{r_f^4} + 4\ln\frac{r_o}{r_f}\right]} \qquad (2.3.8)$$

Where $v_z^l(av)$ is the average velocity of the aqueous phase in the shell side of the module and is defined by equation (2.3.6).

For the present analysis, the flow of gas in the lumen of the silicone capillaries and liquid in the shell space of the module are cocurrent; a schematic of flow of the liquid and gas phases is shown in Figure 2.3.2. The reaction between the pollutant (species A) and ozone (species B) occurs in the aqueous phase. It is assumed for simplicity, that a single reaction of the type shown below occurs in the aqueous phase,

$$a\,A + b\,B \rightarrow \text{products} \qquad (2.3.9)$$

where a, b are the stoichiometric coefficients.

The mass balance equation for each species within the liquid layer enveloped by the free surface may be written as follows. For species A, the pollutant, the equation is

$$v_z^l(r)\frac{\partial C_A^l}{\partial z} = D_A^l \left[\frac{1}{r}\frac{\partial}{\partial r}\left[r\frac{\partial C_A^l}{\partial r}\right]\right] + R_A \qquad (2.3.10)$$

while for species B, ozone,

$$v_z^l(r)\frac{\partial C_B^l}{\partial z} = D_B^l \left[\frac{1}{r}\frac{\partial}{\partial r}\left[r\frac{\partial C_B^l}{\partial r}\right]\right] + R_B \qquad (2.3.11)$$

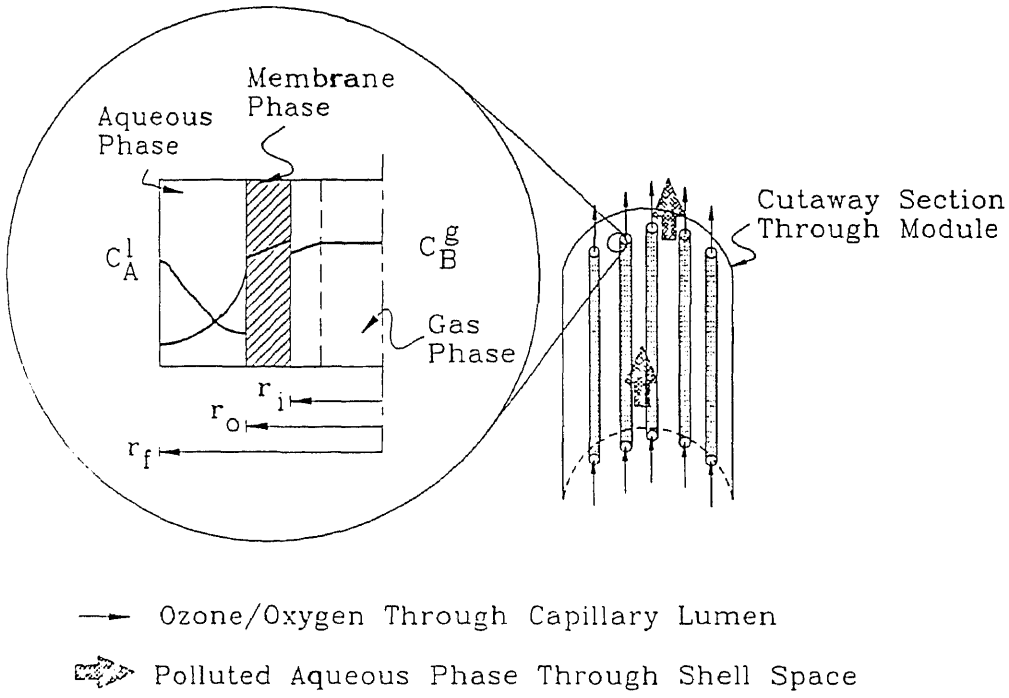

Figure 2.3.2. Schematic of the diffusion and reaction of pollutant (A) and ozone (B) in the single-phase membrane ozonator.

The molar rates of reaction, R_A and R_B, are defined as follows:

$$R_A = - k_2 C_A^l C_B^l \tag{2.3.12}$$

$$R_B = \frac{b}{a} R_A = - \frac{b}{a} k_2 C_A^l C_B^l \tag{2.3.13}$$

Here k_2 is the second order reaction rate constant in the aqueous phase.

Two boundary conditions and an initial condition exist for each mass balance equation shown above within the liquid envelope.

For species A, the pollutant, they are:

$$\text{At } z = 0 \quad , \quad r_f > r > r_o \quad , \quad C_A^l = C_{Ai}^l \ .$$

$$\text{At } r = r_o \quad , \quad \frac{\partial C_A^l}{\partial r} = 0 \ .$$

$$\text{At } r = r_f \quad , \quad \frac{\partial C_A^l}{\partial r} = 0 \ .$$

For species B, ozone in the aqueous phase, the boundary conditions are:

$$\text{At } z = 0 \quad , \quad r_f > r > r_o \quad , \quad C_B^l = 0 \ .$$

$$\text{At } r = r_o \ , \quad -D_B^l \frac{\partial C_B^l}{\partial r} = N_B \Big|_{r = r_o} \ .$$

$$\text{At } r = r_f \ , \quad \frac{\partial C_B^l}{\partial r} = 0 \ .$$

The material balance for species B, ozone, in the lumen of the silicone capillaries can be described as follows:

$$- \frac{Q_G}{2 \pi r_o N_{fibs} R T} \frac{\partial C_B^g}{\partial z} = N_B \Big|_{r_o} \tag{2.3.14}$$

where Q_G is the total flow rate of gas in the lumen of the N_{fibs} number of silicone capillaries, C_B^g is the bulk concentration of ozone in the lumen of the silicone capillaries

and $N_B|_{r_o}$ is the flux of ozone at the outer diameter of the silicone capillary. $N_B|_{r_o}$ can be described as follows:

$$N_B\big|_{r_o} = \frac{C_B^g - H\,C_B^l\big|_{r_o}}{\left[\frac{r_o/r_i}{k_g} + \frac{r_o \ln(r_o/r_i)}{Q_B^m}\right]} \qquad (2.3.15)$$

where H is the Henry's Law constant for ozone in water and is given by C_B^g / C_B^l, Q_B^m is the permeability of ozone in silicone rubber and k_g is the mass-transfer coefficient of ozone in the gas phase in the lumen of silicone capillaries.

The mass balance in the lumen of the silicone capillaries is given by equating Equations 2.3.14 and 2.3.15 as follows :

$$-\frac{Q_G}{2\pi r_o N_{fibs} R T}\frac{\partial C_B^g}{\partial z} = \frac{C_B^g - H\,C_B^l\big|_{r_o}}{\left[\frac{r_o/r_i}{k_g} + \frac{r_o \ln(r_o/r_i)}{Q_B^m}\right]} \qquad (2.3.16)$$

2.3.2. Nondimensional Forms of the Equations

To solve differential equations 2.3.10 and 2.3.11 using appropriate boundary conditions, a finite difference method was adopted. However, prior to expressing the equations in the finite difference forms, the variables in the equations were made dimensionless by the introduction of the following normalized variables:

$$\eta = \frac{r}{r_f} \quad , X = \frac{z}{L} \quad , U = \frac{C_A^l}{C_{Ai}^l} \quad , V = \frac{C_B^l}{\left(C_{Bi}^g / H \right)} \quad , W = \frac{C_B^g}{C_{Bi}^g} \tag{2.3.17}$$

Equation 2.3.8 may be written as follows:

$$v_z^l(\eta) = v_z^l(av)\, f(\eta)$$

$$f(\eta) = 2\left(1 - \lambda^2\right) \frac{\left[\eta^2 - \lambda^2 + 2 \ln \frac{\lambda}{\eta} \right]}{\left(3 - 4\lambda^2 + \lambda^4 + 4 \ln\lambda\right)} \tag{2.3.18}$$

where $\lambda = \frac{r_o}{r_f}$.

Equation 2.3.10 may be rewritten as

$$f(\eta)\, \beta \frac{\partial U}{\partial X} = \left[\frac{1}{\eta} \frac{\partial}{\partial \eta} \left[\eta \frac{\partial U}{\partial \eta} \right] \right] - \alpha \left[\frac{C_{Bi}^l}{C_{Ai}^l} \right] U V \tag{2.3.19}$$

and equation 2.3.11 as

$$f(\eta)\, \beta \left[\frac{D_A^l}{D_B^l} \right] \frac{\partial V}{\partial X} = \left[\frac{1}{\eta} \frac{\partial}{\partial \eta} \left[\eta \frac{\partial V}{\partial \eta} \right] \right] - \alpha \left[\frac{b}{a} \frac{D_A^l}{D_B^l} \right] U V \tag{2.3.20}$$

where

$$\alpha = \frac{k_2\, C_{Ai}^l\, r_f^2}{D_A^l} \quad , \quad \beta = \frac{r_f^2\, v_z^l(av)}{D_A^l L} \, .$$

The boundary conditions for species A may be written in dimensionless form as follows

$$\text{At } X = 0 \quad , \quad U = 1.0 \quad , \quad 1 > \eta > \lambda \, .$$

$$\text{At } \eta = \lambda \quad , \quad \frac{\partial U}{\partial \eta} = 0 \quad , \quad X > 0 \, .$$

$$\text{At } \eta = 1.0 \quad , \quad \frac{\partial U}{\partial \eta} = 0 \quad , \quad X > 0 \, .$$

Similarly, for species B:

$$\text{At } X = 0 \;, \quad V = 1.0 \;, \quad 1 > \eta > \lambda \;.$$

$$\text{At } \eta = \lambda \;, \quad -\frac{\partial V}{\partial \eta} = \frac{(W - V|_{\eta=\lambda})}{kons} \;, \quad X > 0 \;.$$

$$\text{At } \eta = 1.0 \;, \quad \frac{\partial V}{\partial \eta} = 0 \;, \quad X > 0 \;.$$

Here

$$kons = \frac{\lambda D_B^l}{H}\left[\frac{1}{r_i k_g} + \frac{1}{Q_B^m}\ln\left[\frac{r_o}{r_i}\right]\right]$$

In the above equation, the resistance to permeation is far higher than the resistance to mass transfer in the gas phase. Therefore the equation for kons is rewritten as

$$kons = \frac{\lambda D_B^l}{H}\left[\frac{1}{Q_B^m}\ln\left[\frac{r_o}{r_i}\right]\right] \tag{2.3.21}$$

Equation 2.3.16 maybe rewritten in the dimensionless form as

$$-\frac{\partial W}{\partial X} = \frac{W - V|_{r_o}}{Coeff} \tag{2.3.22}$$

where

$$Coeff = \frac{Q_G}{2\pi N_{fibs} R T}\left[\frac{1}{r_i k_g} + \frac{\ln(r_o/r_i)}{Q_B^m}\right]$$

If the gas phase mass resistance is disregarded then the equation can be rewritten as follows :

$$Coeff = \frac{Q_G}{2\pi N_{fibs} R T}\cdot\left[\frac{\ln(r_o/r_i)}{Q_B^m}\right] \tag{2.3.23}$$

2.3.3. Method of Solution

The set of dimensionless equations shown above are solved by finite difference techniques, where the axial term for each species is discretized as shown below using a one point backward upwind difference scheme to ensure the stability of the solution:

$$\frac{\partial U}{\partial X} = \frac{U_{ij} - U_{ij-1}}{\Delta X} \quad ; \quad \frac{\partial V}{\partial X} = \frac{V_{ij} - V_{ij-1}}{\Delta X} \quad , \quad \frac{\partial W}{\partial X} = \frac{W_j - W_{j-1}}{\Delta X}$$

where i is the radial coordinate and j is the axial coordinate.

For the radial terms, a centered difference scheme is adopted for each of the species as shown:

$$\frac{\partial U}{\partial \eta} = \frac{U_{i+1\,j} - U_{i-1\,j}}{2\,\Delta\eta} \quad ; \quad \frac{\partial V}{\partial \eta} = \frac{V_{i+1\,j} - V_{i-1\,j}}{2\,\Delta\eta} \quad ;$$

$$\frac{\partial^2 U}{\partial \eta^2} = \frac{U_{i+1\,j} - 2\,U_{ij} + U_{i-1\,j}}{\Delta\eta^2} \quad ; \quad \frac{\partial^2 V}{\partial \eta^2} = \frac{V_{i+1\,j} - 2\,V_{ij} + V_{i-1\,j}}{\Delta\eta^2}$$

Based upon the finite difference scheme, equation 2.3.19 is rewritten as follows:

$$f(\eta)\,\beta\,\frac{(U_{ij} - U_{ij-1})}{\Delta X} = \frac{(U_{i+1\,j} - U_{i-1\,j})}{2\,\Delta\eta\,\eta_i} + \frac{(U_{i+1\,j} - 2\,U_{ij} + U_{i-1\,j})}{\Delta\eta^2} - \alpha\left[\frac{C_{Bi}^l}{C_{Ai}^l}\right] U_{ij}\,V_{ij} \qquad (2.3.25)$$

while equation 2.3.20 can be written as :

$$f(\eta)\,\beta\left[\frac{D_A^l}{D_B^l}\right]\frac{(V_{ij} - V_{ij-1})}{\Delta X} = \frac{(V_{i+1\,j} - V_{i-1\,j})}{2\,\Delta\eta\,\eta_i} + \frac{(V_{i+1\,j} - 2\,V_{ij} + V_{i-1\,j})}{\Delta\eta^2} - \alpha\,\frac{b}{a}\left[\frac{D_A^l}{D_B^l}\right] U_{ij}\,V_{ij} \qquad (2.3.26)$$

The term $U_{ij}\ V_{ij}$ is nonlinear since neither U_{ij} or V_{ij} is known a priori; therefore a linearization strategy is adopted (Stephanopoulos, 1981). This linearization is carried out by doing a Taylor's series expansion of the term $U_{ij}\ V_{ij}$ around a point, where the values of U and V are known, which in this case is (i, j-1), as follows

$$U_{ij}\,V_{ij} = U_{ij-1}\,V_{ij-1} + \left[\frac{\partial(U_{ij}\,V_{ij})}{\partial U_{ij}}\right]_{ij-1}(U_{ij} - U_{ij-1}) + \left[\frac{\partial(U_{ij}\,V_{ij})}{\partial V_{ij}}\right]_{ij-1}(V_{ij} - V_{ij-1}) \tag{2.3.27}$$

This upon simplification gives

$$U_{ij}\,V_{ij} = U_{ij-1}\,V_{ij} + U_{ij}\,V_{ij-1} - U_{ij-1}\,V_{ij-1} \tag{2.3.28}$$

The substitution of (2.3.28) into (2.3.26) and (2.3.25) and the subsequent collection of all the radial terms on one side of the equation leads to the following equations for species A

$$A1_{ij}\,U_{i-1\,j} + A2_{ij}\,U_{ij} + A3_{ij}\,U_{i+1\,j} = A4_{ij} \tag{2.3.29}$$

where

$$A1_{ij} = \left[\frac{\Delta X\,\Delta\eta}{2\,\eta_i} - \Delta X\right]$$

$$A2_{ij} = \left[f(\eta_i)\,\beta\,(\Delta\eta)^2 + 2\,\Delta X + \Delta X\,(\Delta\eta)^2\,\alpha\left[\frac{C^l_{Bi}}{C^l_{Ai}}\right] V_{ij-1}\right]$$

$$A3_{ij} = -\left[\frac{\Delta X\,\Delta\eta}{2\,\eta_i} + \Delta X\right]$$

$$A4_{ij} = U_{ij-1}\left[f(\eta_i)\,\beta\,(\Delta\eta)^2 - \Delta X(\Delta\eta)^2\,\alpha\left[\frac{C_{Bi}^{l}}{C_{Ai}^{l}}\right](V_{ij} - V_{ij-1})\right]$$

while for species B

$$B1_{ij}\,V_{i-1\,j} + B2_{ij}\,V_{ij} + B3_{ij}\,V_{i+1\,j} = B4_{ij} \qquad (2.3.30)$$

where

$$B1_{ij} = \left[\frac{\Delta X\,\Delta\eta}{2\,\eta_i} - \Delta X\right]$$

$$B2_{ij} = \left[f(\eta_i)\,\beta\,(\Delta\eta)^2\left[\frac{D_A^l}{D_B^l}\right] + 2\,\Delta X + \Delta X(\Delta\eta)^2\,\alpha\left[\frac{b}{a}\right]\left[\frac{D_A^l}{D_B^l}\right]U_{ij-1}\right]$$

$$B3_{ij} = -\left[\frac{\Delta X\,\Delta\eta}{2\,\eta_i} + \Delta X\right]$$

$$B4_{ij} = V_{ij-1}\left[f(\eta_i)\,\beta\,(\Delta\eta)^2\left[\frac{D_A^l}{D_B^l}\right] - \Delta X(\Delta\eta)^2\left[\frac{b}{a}\right]\alpha\left[\frac{D_A^l}{D_B^l}\right](U_{ij} - U_{ij-1})\right]$$

The boundary conditions for equation 2.3.29 are derived as follows

$$\text{At } \eta = \lambda\ ,\quad \frac{\partial U}{\partial \eta} = 0$$

Applying the centered radial difference yields at $\eta=\lambda$, i=1

$$\left[\frac{\partial U}{\partial \eta}\right]_{\eta=\lambda} = \frac{U_{2j} - U_{0j}}{2\,\Delta\eta} = 0$$

$$\therefore\ U_{2j} = U_{0j}$$

which substituted into equation 2.3.29 yields

$$A2_{1j}\,U_{1j} + A3_{1j}\,U_{2j} = A4_{1j} \qquad (2.3.31)$$

where

where

$$A2_{1j} = f(\eta_i)\,\beta\,(\Delta\eta)^2 + 2\Delta X + \Delta X(\Delta\eta)^2\alpha\left[\frac{C^l_{Bi}}{C^l_{Ai}}\right] V_{ij-1}$$

$$A3_{1j} = -2\Delta X$$

$$A4_{1j} = U_{1j-1}\left[f(\eta_i)\,\beta\,(\Delta\eta)^2 - \Delta X(\Delta\eta)^2\alpha\left[\frac{C^l_{Bi}}{C^l_{Ai}}\right](V_{1j} - V_{1j-1})\right]$$

At the free surface where $\eta = 1$ and i = NR, the use of the centered difference scheme yields $U_{NR-1\,j} = U_{NR+1\,j}$, which gives at the free surface

$$A1_{NRj}\,U_{NR-1\,j} + A2_{NRj}\,U_{NRj} = A4_{NRj} \qquad (2.3.32)$$

where

$$A1_{NRj} = -2\Delta X$$

$$A2_{NRj} = f(\eta_i)\,\beta\,(\Delta\eta)^2 + 2\Delta X + \Delta X(\Delta\eta)^2\alpha\left[\frac{C^l_{Bi}}{C^l_{Ai}}\right] V_{NRj-1}$$

$$A4_{NRj} = U_{NRj-1}\left[f(\eta_i)\,\beta\,(\Delta\eta)^2 - \Delta X(\Delta\eta)^2\alpha\left[\frac{C^l_{Bi}}{C^l_{Ai}}\right](V_{NRj} - V_{NRj-1})\right]$$

At j=1 which is the inlet of the module, $U_{i1} = 1.0$.

The boundary conditions for equation 2.3.30 are derived as follows

$$\text{At } \eta = \lambda \quad , \quad -\frac{\partial V}{\partial \eta} = \frac{W - V\big|_{\eta=\lambda}}{kons}$$

Applying the centered radial difference yields at $\eta = \lambda$, i=1

which substituted into equation 2.3.30 yields

$$B2_{1j}\,V_{1j} + B3_{1j}\,V_{2j} = B4_{1j} \qquad (2.3.33)$$

$$B2_{1j} = \left[f(\eta_i)\,\beta\,(\Delta\eta)^2 \left[\frac{D_A^l}{D_B^l}\right] + 2\,\Delta X + \Delta X\,(\Delta\eta)^2\,\alpha \left[\frac{b}{a}\right] \left[\frac{D_A^l}{D_B^l}\right] U_{1j-1} \right] - \frac{\Delta X\,(\Delta\eta)^2}{\eta_i\, kons} + \frac{2\,\Delta X\,\Delta\eta}{kons}$$

$$B3_{1j} = -2\,\Delta X$$

$$B4_{1j} = V_{1j-1} \left[f(\eta_i)\,\beta\,(\Delta\eta)^2 \left[\frac{D_A^l}{D_B^l}\right] - \Delta X\,(\Delta\eta)^2 \left[\frac{b}{a}\right] \alpha \left[\frac{D_A^l}{D_B^l}\right] (U_{1j} - U_{1j-1}) \right] - W \left[\frac{\Delta X\,(\Delta\eta)^2}{\eta_i\, kons} + \frac{2\,\Delta X\,\Delta\eta}{kons} \right]$$

At the free surface where $\eta = 1$ and i = NR, the use of the centered difference scheme yields $V_{NR-1\,j} = V_{NR+1\,j}$, which gives at the free surface

$$B1_{NR\,j}\,V_{NR-1\,j} + B2_{NR\,j}\,V_{NR\,j} = B4_{NR\,j} \qquad (2.3.34)$$

where

$$B1_{NR\,j} = -2\,\Delta X$$

$$B2_{NR\,j} = \left[f(\eta_i)\,\beta\,(\Delta\eta)^2 \left[\frac{D_A^l}{D_B^l}\right] + 2\,\Delta X + \Delta X\,(\Delta\eta)^2\,\alpha \left[\frac{b}{a}\right] \left[\frac{D_A^l}{D_B^l}\right] U_{NRj-1} \right]$$

$$B4_{NR\,j} = V_{NR\,j-1} \left[f(\eta_i)\,\beta\,(\Delta\eta)^2 \left[\frac{D_A^l}{D_B^l}\right] - \Delta X\,(\Delta\eta)^2 \left[\frac{b}{a}\right] \alpha \left[\frac{D_A^l}{D_B^l}\right] (U_{NR\,j} - U_{NR\,j-1}) \right]$$

At j=1 which is the inlet of the module, $V_{i\,1} = 0.0$.

Equation 2.3.22 can be rewritten as

$$-\frac{(W_j - W_{j-1})}{\Delta X} = \frac{W_j - V_{1j}}{Coeff} \qquad (2.3.35)$$

This can be rearranged to give

$$W_j = \frac{\left[W_{j-1} + V_{1j} \frac{\Delta X}{Coeff} \right]}{\left[1 + \frac{\Delta X}{Coeff} \right]} \qquad (2.3.36)$$

At j=1, the inlet of the module, $W_1 = 1$.

The above equations 2.3.29, 2.3.30 and 2.3.36 together with the boundary conditions, 2.3.31 - 2.3.34 comprise a sparse tridiagonal matrix, where all of the coefficients are zero except those on the leading diagonal and on each adjacent diagonal. Such a matrix is subject to solution by a process of elimination and back-substitution known as Thomas Algorithm (de Vahl Davis, 1986) and is outlined in Appendix 2. The computer program used to simulate the single-phase membrane ozonator is provided in Appendix 3.

2.4. Results and Discussion

2.4.1. Introduction

The physical characteristics of the single-phase membrane reactors that were constructed are summarized in Table 2.2.1. The experimental results are presented and discussed in the following order: 1) experimental determination of the permeabilities and separation factor of O_2-N_2; 2) experimental determination of the permeability of O_3 in a silicone capillary membrane; 3) determination of module k_la and comparison with conventional ozonation devices; 4) degradation of phenol, acrylonitrile and nitrobenzene in the single-phase membrane ozonator and comparison of the reactor performance with that of the model. Reactor SILCAP #1 was used in the preliminary study to degrade phenol; for all subsequent studies to gain understanding of the performance of single phase membrane ozonator, reactors SILCAP #2-5 were used.

2.4.2. Measurement of the Permeability Coefficients and the Separation Factors of Oxygen and Nitrogen Across the Silicone Membrane

The measurement of the permeabilities of oxygen and nitrogen across silicone rubber was carried out in three modules, SILCAP #5 and #1 and NEWCON #1. SILCAP #5 was a freshly prepared module which had not been exposed to ozone prior to the measurement of O_2 and N_2 permeabilities. SILCAP #1 had been exposed to ozone as part of the ongoing study to degrade organic pollutants in wastewater, while the silicone membranes in the module NEWCON #1 had been exposed to both ozone and the fluorocarbon phase (FC) as part of the study to remove VOCs from air. The three modules represent the gamut of situations that were possible during the membrane-based ozonation of organic

compounds in waste streams. It allowed consideration of any possible change in permeability or O_2/N_2 separation factor of silicone rubber due to the exposure to ozone in the absence or presence of the fluorocarbon phase.

The physical characteristics of modules SILCAP #1 and #5 and NEWCON #1 not explicitly summarized in Tables 2.2.1, 3.2.1 and 4.2.1, viz. log mean permeation area and the wall thickness are given Table 2.4.1.

Table 2.4.1. Details of modules used to measure permeabilities of O_3, O_2 and N_2

Module	Capillary ID/OD, (cm)	No. of Caps.	Module Length, (m)	Mem .Wall Thickness, (m)	LMP. Area†, (m^2)
SILCAP #5	0.03/0.06	98	0.22	1.65 e-4	2.99 e-2
SILCAP #1	0.16/0.24	4	0.28	4.19 e-4	6.90 e-3
NEWCON #1	0.03/0.06	25	0.38	1.65 e-4	1.32 e-2

† Log Mean Permeation Area.

The log mean area available for permeation is defined as follows

$$\text{Log Mean Permeation Area} = \pi \frac{d_o^{sil} - d_i^{sil}}{\ln (d_o^{sil} / d_i^{sil})} N_{fibs} L \qquad (2.4.1)$$

For modules SILCAP #1 and #5 and NEWCON #1, the experimental values of the permeability coefficient of oxygen through silicone rubber and the separation factor for O_2/N_2, are listed below in Tables 2.4.2 - 2.4.4 respectively. It is assumed that the feed and permeate gas phases obey ideal gas law and Fick's Law is applicable for the permeation of O_2 and N_2 through the polymer. Therefore

$$J_{O_2} = \frac{Q^m_{O_2}}{l} \left(p^f_{O_2} - p^p_{O_2} \right)_{LM} \qquad (2.4.2)$$

where J_{O_2} is the molar flux of O_2 across the silicone capillary membrane, $Q^m_{O_2}$ is the permeability coefficient of oxygen through silicone rubber, l is the wall thickness of the silicone capillary membrane given in Table 2.4.1 above. The log mean partial pressure driving force is defined as follows:

$$\left(p^f_{O_2} - p^p_{O_2} \right)_{LM} = \frac{\left(p^f_{O_2} - p^p_{O_2}\right)\Big|_{inlet} - \left(p^f_{O_2} - p^p_{O_2}\right)\Big|_{outlet}}{\ln \left[\frac{\left(p^f_{O_2} - p^p_{O_2}\right)\Big|_{inlet}}{\left(p^f_{O_2} - p^p_{O_2}\right)\Big|_{outlet}} \right]} \qquad (2.4.3)$$

For all experiments, the permeate side partial pressure of oxygen (and nitrogen) was negligible compared to the feed side partial pressure; this observation gave the separation factor for O_2-N_2 as the ratio of the two permeability coefficients, which is as follows:

$$\alpha_{O_2 - N_2} = \frac{p^p_{O_2} / p^f_{O_2}}{p^p_{N_2} / p^f_{N_2}} \cong \frac{Q^m_{O_2}}{Q^m_{N_2}} \qquad (2.4.4)$$

Based upon the above definitions, the separation factor for O_2-N_2 can be calculated knowing the feed and permeate concentrations for nitrogen and oxygen. For the sake of brevity, the permeability coefficient of oxygen will be shown in Tables 2.4.2 - 2.4.4; the corresponding permeability coefficient for nitrogen can be calculated from the above equation.

Table 2.4.2. O_2 and N_2 permeability coefficients through silicone rubber for SILCAP #5*

Feed Flow Conf.	Perm O_2 (Vol %)	Perm N_2 (Vol %)	$p^p_{O_2}$ (kPa)	LMPD† (kPa)	J_{O_2} (kgmol/ m^2.s)	$Q^{m\ *}_{O_2}$	α O_2/N_2
Feed	1.05	1.89	1.06	20.54	2.78 e-08	2.23 e-13	2.11
In	1.05	1.90	1.07	20.54	2.79 e-08	2.24 e-13	2.11
Tube	1.05	1.90	1.07	20.54	2.78 e-08	2.24 e-13	2.11
Feed	1.05	1.90	1.07	20.54	2.79 e-08	2.24 e-13	2.11
In	1.05	1.90	1.07	20.54	2.79 e-08	2.25 e-13	2.11
Shell	1.05	1.90	1.07	20.54	2.79 e-08	2.24 e-13	2.11

* Freshly prepared module.
† Log Mean Partial Pressure Difference between the feed and permeate channels (Equation 2.4.3). O_2 feed partial pressure: 21.8 kPa.
* Units of Permeability Coefficient (kgmol.m) / (m^2.s.kPa).
Feed flow rate : 90.9 ml/min. Helium flow rate on permeate side : 112.2 ml/min.

Table 2.4.3. O_2 and N_2 permeability coefficients through silicone rubber for SILCAP #1*

Perm O_2 (Vol %)	Perm N_2 (Vol %)	$p^p_{O_2}$ (kPa)	LMPD† (kPa)	J_{O_2} (kgmol/ m^2.s)	$Q^{m\ *}_{O_2}$	α O_2/N_2
0.13	0.22	1.32 e-1	21.01	1.45 e-08	2.9 e-13	2.25
0.13	0.21	1.26 e-1	21.01	1.39 e-08	2.79 e-13	2.31
0.12	0.21	1.26 e-1	21.01	1.39 e-08	2.77 e-13	2.31
0.12	0.20	1.25 e-1	21.01	1.39 e-08	2.76 e-13	2.31

* Module exposed to aqueous phase ozonation. Feed on tube-side of module.
† Log Mean Partial Pressure Difference between the feed and permeate channels (Equation 2.4.3). O_2 feed partial pressure: 21.8 kPa.
* Units of Permeability Coefficient (kgmol.m) / (m^2.s.kPa).
Feed flow rate : 90.9 ml/min. Helium flow rate on permeate side : 112.2 ml/min.

Table 2.4.4. O_2 and N_2 permeability coefficients through silicone rubber for NEWCON #1■

Feed Flow Conf.	Perm O_2 (Vol %)	Perm N_2 (Vol %)	$p^{p}_{O_2}$ (kPa)	LMPD† (kPa)	J_{O_2} (kgmol/ m^2.s)	$Q^{m}_{O_2}$ *	α O_2/N_2
Feed	0.44	0.78	0.45	20.85	2.60 e-08	2.05 e-13	2.15
In	0.44	0.78	0.45	20.85	2.60 e-08	2.05 e-13	2.15
Tube	0.44	0.79	0.45	20.85	2.60 e-08	2.06 e-13	2.15
Feed	0.43	0.78	0.44	20.86	2.55 e-08	2.01 e-13	2.13
In	0.43	0.77	0.44	20.86	2.54 e-08	2.01 e-13	2.13
Shell	0.43	0.77	0.44	20.86	2.54 e-08	2.01 e-13	2.13

■ Module exposed to O_3 and FC phase prior to measurement of permeability coefficient.
† Log Mean Partial Pressure Difference between the feed and permeate channels (Equation 2.4.3). O_2 feed partial pressure: 21.8 kPa.
* Units of Permeability Coefficient (kgmol.m) / (m^2.s.kPa)
Feed flow rate : 90.9 ml/min. Helium flow rate on permeate side : 112.2 ml/min.

The above tables give the results for the permeability coefficient of O_2 and the separation factor of O_2 and N_2 through the silicone capillary membranes. At first glance it can be seen that regardless of whether the feed is in the shell or in the fiber lumen, the measured permeability coefficient of O_2 is almost unchanged. The capillaries used in SILCAP #1 had a wall thickness about 4 times that for modules SILCAP #5 and NEWCON #1. This is the reason why even though the observed flux of oxygen through the capillaries of SILCAP #1 is lower, the permeability coefficient calculated for oxygen is higher. The permeability coefficient of O_2 and the separation factor, α between O_2 and N_2 increase with an exposure to ozone (Table 2.4.2 and Table 2.4.3) but these values

diminish, the permeability coefficient by about 30% of the value for the virgin polymer, when the polymer is exposed to ozone in the presence of the FC phase.

The permeability coefficient for a species through a polymer is generally described by the following equation:

$$Q_i^m = D_i S_i \tag{2.4.5}$$

where Q_i^m is the permeability coefficient of a species i, while D_i and S_i are the diffusivity and the solubility of species i in the polymer respectively (Zolandz and Fleming, 1992). The solubility S_i of species i in a polymer matrix is thermodynamic in nature and is related to the condensibility of the species and any interaction between the polymer matrix and the permeating species. A species that is easily condensable (a high T_C and a high T_b) will have a high solubility in the polymer. In literature, it is seen that for O_2 and N_2, the diffusivities, D_{N_2} and D_{O_2}, in silicone rubber are essentially identical, 21 e-10 m^2/s but the solubility, S_{N_2} in silicone rubber is less than S_{O_2}, 4.35 e-5 kgmoles/(m^3-membrane-kPa) for N_2 versus 8.37 e-5 kgmoles/(m^3-membrane-kPa) for O_2 (La Pack et al., 1994). This is attributed to the lower T_C of N_2 (decreased condensibility), leading to a higher value of permeability coefficient of O_2.

When the silicone elastomer is exposed to ozone, in the absence of any solvents, it is likely that ozone will participate in reactions that will lead to greater crosslinking densities; such behavior has been observed for structural silicone materials (Keshavaraj and Tock, 1994). Crosslinking with ozone as a crosslinking agent in such a polymeric material can lead to several possibilities. The polymer becomes increasingly rigid reducing the dimensions of the openings between the polymer chains in the polymeric

matrix, through which O_2 and N_2 can traverse. O_2 has a slightly smaller kinetic sieving diameter than N_2 (3.46 Å for O_2 vs 3.64 Å for N_2); this would lead to greater selectivity for O_2 than for N_2, although the magnitude of the diffusivity for the individual species would be somewhat reduced (Zolandz and Fleming, 1992). Since ozone works as a crosslinking agent, an alternate hypothesis can be postulated that the increased concentration of oxygen atoms within the polymer matrix cause an increase in solubility of O_2 in the polymer matrix leading to an overall higher permeability coefficient. This explains both the increase in permeability of O_2 and the increase in $\alpha_{O_2-N_2}$ between the modules SILCAP #5 and #1 shown in Tables 2.4.2 and 2.4.3 respectively. Which of these mechanisms plays a more critical role in the increase in $\alpha_{O_2-N_2}$ and the permeability of O_2 is presently unknown.

The reduction in the permeability for silicone capillaries, when the capillaries are exposed to ozone in presence of the FC medium in Table 2.4.4, could be explained by the higher ozone concentrations seen by the silicone capillaries, since ozone is highly soluble in the FC phase. This can lead to the polymer chains becoming extremely rigid in their lateral motions (lateral to the axis of permeation of the solute species) and lead to the observed drop in permeability coefficients due to the drop in diffusivities of the species, since the diffusion coefficients of permanent gases through glassy polymers are roughly two orders of magnitude smaller than those for rubbery polymers. Also the attack of free radicals present during the reaction of ozone with organic species dissolved in the FC medium could contribute to further modification of the polymer resulting in the concomitant reduction in O_2 permeability coefficient and the corresponding N_2 permeability coefficient.

Table 2.4.5 compares the experimental data shown above with those found in literature. The silicone capillaries used in all the experiments reported here are of the "Silastic Grade", with about 31 wt% fumed silica particles (0.011 μm) (La Pack et al., 1994). The experiments shown above were conducted at an ambient temperature of 27 ± 2 °C. When compared with the results of Majumdar et al. (1987) and Robb (1965), etc., the results for the virgin polymer in module SILCAP #5 appear to be in fair agreement to those found in literature. Majumdar et al. (1987) conducted their experiments at 22 °C while Robb conducted his experiments at 25 °C. The value shown by Zolandz and Fleming (1992), appears to be for the PDMS polymer in the absence of any inert fillers and therefore represents the intrinsic value of the permeability. The separation factors for N_2 and O_2 observed experimentally seem to correspond well with those found in literature.

Table 2.4.5. Comparison between experimental values and literature values for the permeability coefficient of O_2 and α of O_2-N_2

Reference	$Q_{O_2}^{m}$ *	α O_2-N_2	Remarks
SILCAP #5	2.24 e-13	2.11	Fresh Silicone Capillaries
SILCAP #1	2.81 e-13	2.30	Exposed to O_3 and H_2O
NEWCON #1	2.03 e-13	2.14	Exposed to O_3 and FC
Robb (1965)	2.00 e-13	2.14	-
Majumdar et al. (1987)	1.69 e-13	2.06	-
Zolandz and Fleming (1992)	3.12 e-13	2.12	No inert fillers
LaPack et al. (1994)	1.77 e-13	1.89	-

* Units of Permeability Coefficient (kgmol.m) / (m^2.s.kPa)

2.4.3. Measurement of the Permeability Coefficient of Ozone across the Silicone Membrane

The measurement of the permeability coefficient of O_3 across the silicone capillaries was carried out in a manner similar to that described for O_2 and N_2. The physical details of the modules necessary to calculate the permeability coefficient of O_3 through silicone capillaries are shown in Table 2.4.1. The results in the order shown in Tables 2.4.6 - 2.4.8 are as follows : SILCAP #5, which was not exposed to any ozone prior to the measurement of its permeability through silicone rubber; SILCAP #1, which was exposed to O_3 and water prior to the permeability experiments; NEWCON #1 which was exposed to O_3 and the FC phase.

Table 2.4.6. Permeability coefficient of O_3 through silicone rubber for SILCAP #5

Permeate O_2 Flow (ml/min)	$p^f_{O_3}$ (kPa)		$p^p_{O_3}$ (kPa)	LMPD† (kPa)	J_{O_3} (kgmol/ m^2. s)	$Q^{m*}_{O_3}$
	In	Out				
60.7	3.62	3.55	1.15	2.97	1.55 e-8	8.61 e-13
112.1	3.62	3.51	0.705	3.19	1.75 e-8	9.05 e-13

† Log Mean Partial Pressure Difference between the feed and permeate channels.
* Units of Permeability Coefficient (kgmol.m) / (m^2.s.kPa)
Feed in fiber lumen of silicone capillaries.
O_3/O_2 flow rate = 463 ml/min at 0 psig (atmospheric pressure).

Table 2.4.7. Permeability coefficient of O_3 through silicone rubber for SILCAP #1

Flow Conf.	Permeate Flow O_2 (ml /min)	$p^f_{O_3}$ (kPa)	$p^p_{O_3}$ (kPa)	LMPD† (kPa)	J_{O_3} (kgmol/ m^2 .s)	$Q^{m*}_{O_3}$
Feed	93.2	3.61	1.02 e-1	3.56	9.09 e-9	1.07 e-12
In	134.5	3.61	6.77 e-2	3.57	8.73 e-9	1.02 e-12
Shell	59.8	3.61	1.59 e-1	3.53	9.12 e-9	1.08 e-12
Feed	98.6	3.74	9.53 e-2	3.69	9.00 e-9	1.04 e-12
In	134.5	3.74	7.12 e-2	3.70	9.16 e-9	1.03 e-12
Tube	59.8	3.74	1.61 e-1	3.66	9.25 e-9	1.06 e-12

† Log Mean Partial Pressure Difference between the feed and permeate channels.
* Units of Permeability (kgmol.m) / (m^2.s.kPa)
O_3/O_2 flow rate = 463 ml/min at 0 psig (atmospheric pressure).

Table 2.4.8. Permeability coefficient of O_3 through silicone rubber for NEWCON #1

Flow Conf.	Permeate Flow O_2 (ml/min)	$p^{f}_{O_3}$ (kPa)	$p^{p}_{O_3}$ (kPa)	LMPD† (kPa)	J_{O_3} (kgmol/ m^2.s)	$Q^{m*}_{O_3}$
Feed In Shell	59.8	3.53	5.10 e-1	3.27	1.53 e-8	7.70 e-13
	112.1	3.53	3.07 e-1	3.37	1.73 e-8	8.42 e-13
	149.1	3.53	2.33 e-1	3.41	1.74 e-8	8.41 e-13

† Log Mean Partial Pressure Difference between the feed and permeate channels.
* Units of Permeability Coefficient (kgmol.m) / (m^2.s.kPa)
O_3/O_2 flow rate = 463 ml/min at 0 psig (amospheric pressure).

The SILCAP #5 module had the highest permeation area of the three modules and the observed change in the feed side O_3 composition between inlet and outlet was less than 2 % of the inlet O_3 composition. Therefore for the subsequent calculation of permeability coefficient of O_3 for modules SILCAP #1 and NEWCON #1, the inlet O_3 was assumed to be essentially the feed O_3 composition.

From the results shown in Tables 2.4.6 - 2.4.8 and those shown prior in Tables 2.4.2 - 2.4.4, it is clear that O_3 has a much higher permeability than O_2 through the silicone capillary membranes. This can be explained by the higher solubility that O_3 has in silicone rubber since it has a much higher T_C and T_B than O_2 (T_B of O_2 is -183 °C and T_C is -118.6 °C while for O_3, T_B is -112 °C and T_C is -12.15°C) and therefore is more easily condensable than O_2. It is also immediately apparent that when the three modules are considered in turn, the permeability coefficient of O_3 follows the same trend shown by O_2 in Tables 2.4.2 - 2.4.4. The silicone capillary membranes show a slight increase in O_3 permeability coefficient, when exposed to ozone and water and a decrease in

permeability when exposed to ozone and the FC phase. The increase can be attributed to an increase in solubility of O_3 in the membrane that had been previously exposed to O_3. The subsequent decrease in permeability shown in Table 2.4.8 for the module NEWCON #1 can be attributed to the rigidity of the silicone polymer matrix as a result of extensive cross-linking in the presence of higher concentrations of O_3 and results in a decreased diffusivity of ozone across the silicone polymer matrix. Figure 2.4.1 is a comparison between the values of permeability of O_3 and O_2 for each of three modules studied.

2.4.4. Determination of the Module Average Volumetric Mass Transfer Coefficient of Ozone

The volume percent of ozone in the feed gas phase under the experimental conditions was determined to be 2.9% (Trivedi, 1992). The reaction between ozone and KI can be written as follows:

$$O_3 + 2I^- + H_2O \rightarrow I_2 + O_2 + 2OH^- \qquad (2.4.6)$$

The iodine released provides an estimate of the amount of ozone permeating across the silicone capillaries. The rate of oxidation for the iodide ion is $\sim 10^{-4}$ s^{-1}, a fast irreversible first order oxidation reaction that occurs at the membrane-liquid interface and no ozone is transferred into the bulk liquid phase (Langlais et al., 1991). The $k_l a$ was determined from the experimental data in the following manner:

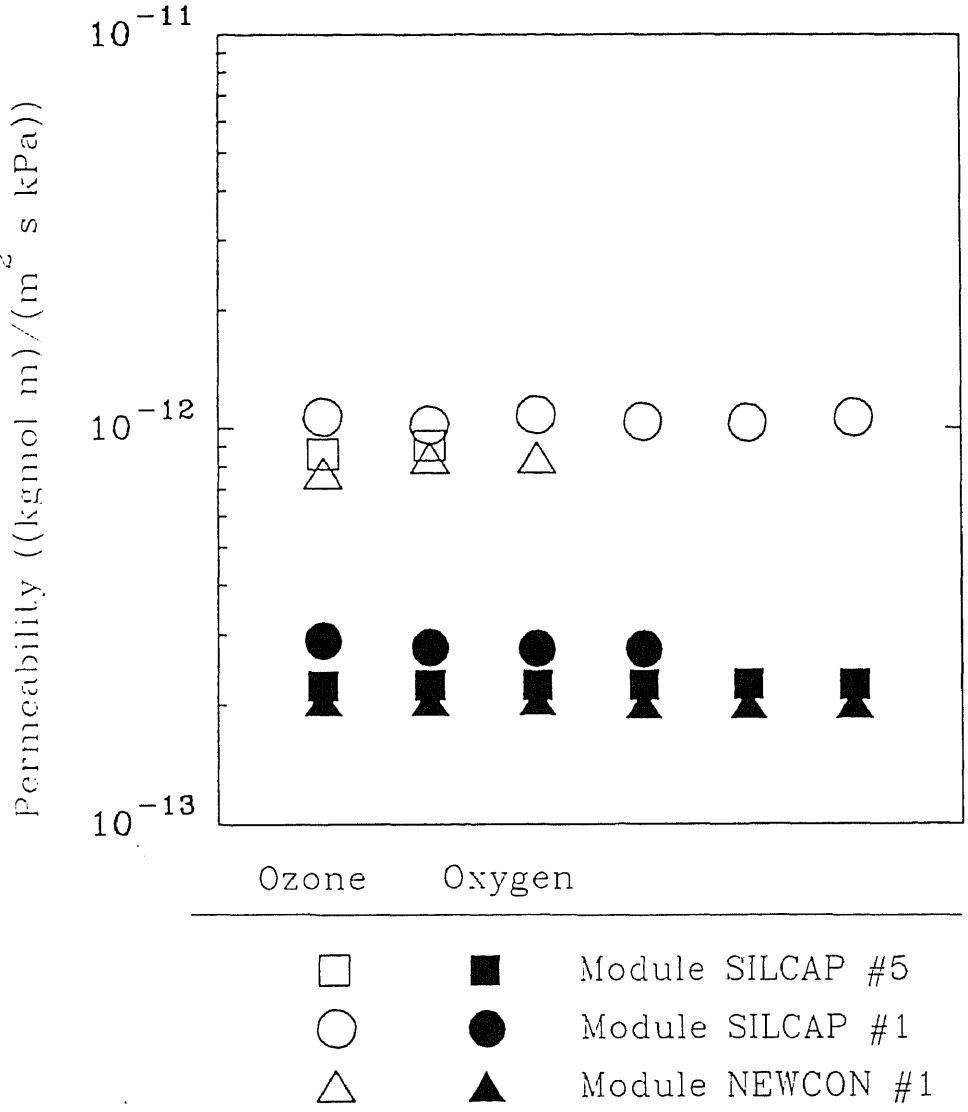

Figure 2.4.1. Comparison between the experimentally observed permeability values for O_2 and O_3.

$$k_l a = H k_g a = H \frac{\text{permeation rate of } O_3}{\left[\frac{p_{O_3}^{in} - p_{O_3}^{out}}{\ln (p_{O_3}^{in} / p_{O_3}^{out})} \right]} \qquad (2.4.7)$$

where H is the Henry's law constant for ozone , p_{O_3} is the partial pressure of ozone; k_l and k_g are the mass transfer coefficients based on liquid and gas phases, respectively, and a is the interfacial area per unit volume of reactor. The relevant data and other information pertaining to the calculation of $k_l a$ are shown in Table 2.4.9.

Table 2.4.9. Results of mass transfer experiments for module SILCAP #2

No.	Aq. Flow Rate (ml/min)	Gas Flow Rate (ml/min)	O_3 Exit Concentration[a]		Perm. Rate[b] (mg/cm^2.s)	k_g^* [c] (mg/s. cm^2.atm)	$k_l a^*$ [d] (s^{-1})
			(mg/l)	(atm)			
1	11.4	13.7	35.4	19.7 e-3	3.85 e-6	1.55 e-4	5.82 e-3
2	9.6	17.5	36.3	19.3 e-3	3.84 e-6	1.56 e-4	5.84 e-3

[a] Exit concentration was corrected to 0°C and 14.7 psia from 29°C and 16.7 psia.
[b] Average permeation area considered = 417.8 cm^2
[c] Feed gas concentration was 58.4 mg/l (partial pressure of O_3 in feed = $31*10^{-3}$ atm).
[d] a = 15.3 cm^2/cm^3
Henry's law constant = $1.18 *10^5$ atm.ml/gmol (25°C, Langlais et al., 1991).

The k_g and $k_l a$ for the module (SILCAP #2) in the presence of the ozone - KI reaction were designated k_g^* and $k_l a^*$. $k_l a^*$ was found to be 5.8×10^{-3} s^{-1} (a = 15.28 cm^{-1}) at a superficial liquid velocity of 0.2 cm/s and a superficial gas velocity of 4 cm/s.

It was also observed that the SILCAP #2 module could not be used with KI over long durations of time, because the iodine released by the reaction was being adsorbed on the silicone capillaries. Subsequent washing of the silicone capillaries with deionized water in the presence of ozone did remove the pinkish tinge by the adsorbed iodine to a certain extent. However the information derived from the two runs shown above was valuable in that it allowed comparison of the membrane device with conventional mass transfer equipment.

At a comparable superficial liquid velocity of 0.2 cm/s in a packed column containing Raschig ring packings of nominal size "d_p" 1.3 cm and "a" of 3.64 cm^{-1} (Treybal, 1981), Onda's correlation shown below for gas-liquid mass transfer in a packed bed (Langlais et al., 1991) predicted a $k_l a$ of 4.6×10^{-4} s^{-1} without any chemical reaction.

$$\frac{k_l}{a D_{O_3}} = 5.1 * 10^{-3} (a d_p)^{0.4} \left[\frac{U_{sl} \rho_l}{a \mu_l}\right]^{\frac{4}{3}} \left[\frac{U_{sl} a}{g}\right]^{-\frac{1}{3}} \left[\frac{\mu_l}{\rho_l D_{O_3}}\right]^{\frac{1}{2}} \quad (2.4.8)$$

where a and d_p are the surface area per unit volume of packing and packing size respectively (Langlais et al., 1991). U_{sl} is the liquid superficial velocity through the packed bed. The iodometric reaction occurs very close to the aqueous-gas interface and is assumed to be practically instantaneous. This yields an enhancement of mass transfer due to the iodometric reaction of about 2.3 (Langlais et al., 1991). The $k_l a$ obtained from the above equation is multiplied by the enhancement factor 2.3; to yield the mass transfer coefficient under reaction conditions, 1.058 e-3 s^{-1}. The value of $k_l a^*$ from a correlation for bubble columns at similar superficial gas velocities of 4.13 e-2 m/s was similarly calculated to be 3.22 e-4 s^{-1} (Langlais et al., 1991).

Table **2.4.10.** Comparison of mass transfer coefficient of SILCAP #2 with packed bed and bubble column contactor under iodometric reaction conditions

Contactor	Gas Vel. (m/s)	Liq. Vel. (m/s)	$k_l a$ (s^{-1})
Packed Bed	-	2 e-3	1.058 e-3
Bubble Column	4.13 e-2	-	3.22 e-4
SILCAP #2	4.13 e-2	2 e-3	5.8 e-3

The packed bed type contactor and the bubble column were compared for similar superficial gas and liquid velocities using mass transfer correlations available in the literature (Langlais et al., 1991) under similar iodometric conditions. It must also be emphasized that the two commercial contactors mentioned above do not have the flexibility of independent control of liquid and gas flow rates and operate within a narrow window to prevent flooding by the liquid phase or slugging by the gas phase in the contacting device.

The $k_l a$ value for the silicone capillary-based membrane ozonator under conditions of ozonation was found to be considerably larger than that obtained in conventional ozonation equipment for similar superficial liquid and gas velocities. Although the k_l (mass transfer coefficient in the absence of reaction) obtained in the silicone capillary membrane ozonator is of the same order as that obtained in packed beds and bubble columns, the "a" obtained in the single-phase membrane ozonator is considerably higher than either of the aforementioned contactors, 1530 m^{-1} for the single-phase membrane ozonator, ~400-600 m^{-1} for bubble columns and ~800-1400 m^{-1} for packed beds (depending

upon the packing used). It must also be noted that the specific contact area for conventional contactors is directly proportional to the amount of power that must be spent in creating the extra area (Westerterp et al., 1984). In the case of the single-phase membrane reactor, the specific contact area is proportional to size of the capillary membranes and the number of capillary membranes packed into the contactor. This indicates that the ozonation of wastewater can be carried out more efficiently in the single-phase membrane reactor than in conventional contacting equipment.

2.4.5. Degradation of Organic Pollutants in the Silicone Capillary Membrane Ozonator

This section deals with the experimentally determined removal of organic pollutants from wastewater and comparison of the results with the model described in section 2.3. The experiments were carried out using SILCAP #1 and SILCAP #2, #5 and #6 with phenol, nitrobenzene and acrylonitrile as model pollutants. A literature search provided estimates of aqueous diffusivities and reaction rate parameters for the direct ozonation reactions with compounds listed above; these values are summarized in Table 2.4.11. These values were used in the model for the single phase membrane ozonator discussed in section 2.3. For most of the runs, as mentioned in section 2.2, the aqueous phase was run on the shell side of the module. A few runs were made using SILCAP #1 by passing wastewater containing phenol on the lumen side of the silicone capillaries. Although these runs are reported, these experiments were not extensively pursued because of the formation of gas slugs which would periodically build up and reduce the gas-liquid contacting efficiency. These gas slugs became more difficult to control, and remove, at lower liquid flow rates

and therefore for all subsequent experiments with the three compounds, the aqueous phase was passed on the shell side of the module. The values of the diffusivity of the pollutants and ozone in water were calculated from the Wilke-Chang correlation (Perry and Green, 1984). Some of the values of the reaction rate coefficients shown below were obtained by monitoring the disappearance of ozone during the ozonation of the pollutant (Hoigne and Bader, 1983a; Pryor et al., 1984). The ozonation reaction rate coefficient for the pollutant was calculated by dividing the value reported in the literature by the reported stoichiometric ratio. The values shown in Table 2.4.11 are for ozonation reactions typically carried out in buffered aqueous solutions at pH 7.

The conversion X_A for a pollutant "A" is calculated as shown below

$$\text{Conversion}, \; X_A = \frac{C_A^{in} - C_A^{out}}{C_A^{in}} \qquad (2.4.9)$$

where C_A^{in}, C_A^{out} are the module entrance and exit concentrations of the pollutant at steady state, which is ascertained by a constant pollutant exit composition. Most experiments reached steady state in about 3-4 hours of continuous reactor operation at constant aqueous and gas flow rates.

Table 2.4.11. Estimates of diffusion coefficients and reaction rate parameters from literature

Compound	D_A^W # (m^2/s)	k_2^W §	b/a‡	k_2^W §	Ref.
Phenol	0.91 e-9	90-140	~4	~ 115	Joshi & Shambaugh (1982)
Nitrobenzene	0.84 e-9	0.09±0.02*	2.5	~ 0.04†	Hoigne & Bader (1983a)
Acrylonitrile	1.16 e-9	870±115*	1	~ 870†	Pryor et al. (1984)

Estimated from the Wilke-Chang equation (Perry and Green, 1984).
§ units $(kgmol/m^3)^{-1}\ s^{-1}$.
* k_2 = Reaction rate coefficient determined on the basis of the disappearance of ozone.
‡ Stoichiometric ratio : No. of moles of ozone required per mole of pollutant (Equation 2.3.9).
† $k_2^W = (k_2) / (b/a)$.

a) Phenol as a model pollutant

Figure 2.4.2 shows the results for the module SILCAP #1, where the degradation of phenol was used to demonstrate the performance of the single-phase membrane ozonator. The symbol ◯ represents experiments where the aqueous phase was run in the shell side of the module. It is seen that for flow rates of about 0.1 ml/min and a feed concentration of 107 ppm, phenol conversion of about 0.9 is observed. As the aqueous flow rate is increased it is seen that the conversion falls to about 0.2 at a flow rate of 0.7 ml/min. When the aqueous phase is run on the tube side indicated by the symbols ▽ and □, a 20% conversion is obtained at an aqueous flow rate of 2 ml/min. The solid line shown is the simulation for aqueous phase flowing through the shell side of the module, for a k_2^W of 115 $((kgmol/m^3)^{-1}\ s^{-1})$. The simulation overpredicts the experimental

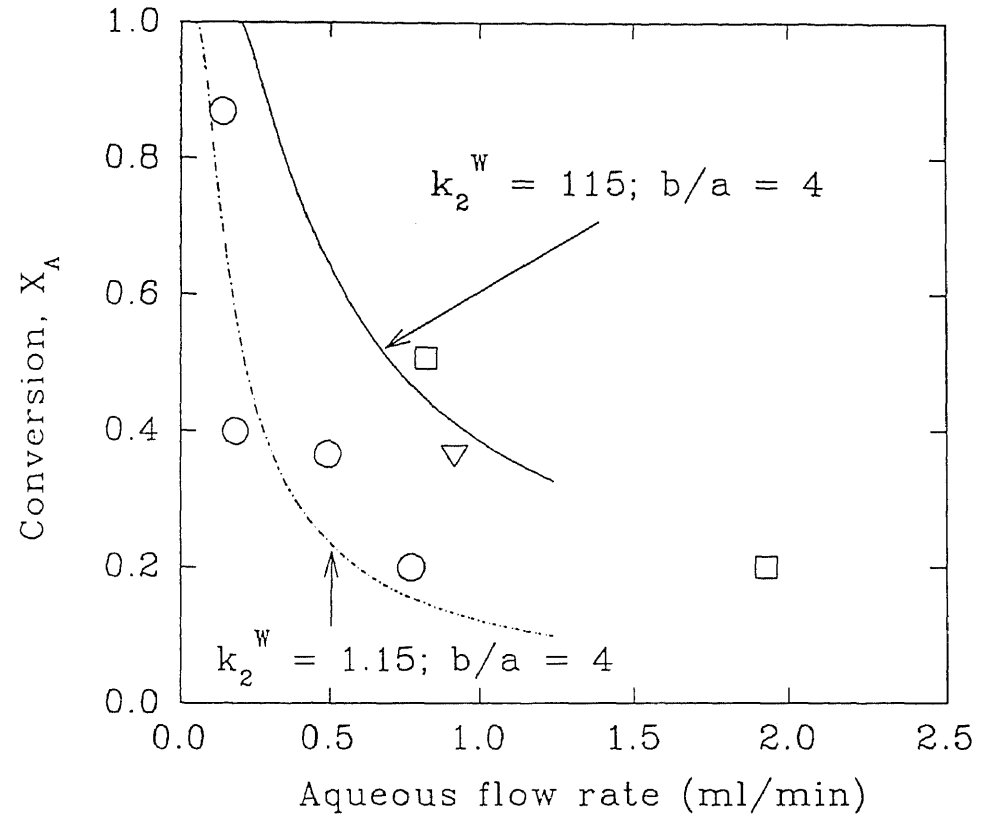

□ Tube-side Aq. Flow; Av. Feed = 89 ppm, Gas Flow = 57 ml/min

▽ Tube-side Aq. Flow; Av. Feed = 102 ppm, Gas Flow = 47 ml/min

○ Shell-side Aq. Flow; Av. Feed = 107 ppm, Gas Flow = 39 ml/min

- - - —— Simulations for Aq. Flow on Shell Side of Module

Figure 2.4.2. Degradation of phenol in a single-phase membrane ozonator (SILCAP #1).

conversion by a factor of 3. It should be mentioned again, that the simulation assumes that there is no shell side bypassing and that the tubes (silicone capillaries in this study) are rigid and conform to a triangular pitch. SILCAP #1, is a module with 4 silicone capillaries, each having an outer diameter of 0.24 cm. The silicone capillaries are not rigid structures, a problem that is exacerbated at higher aqueous flow rates, when the likelihood of the flexible tubular membranes bunching together is greater than it would be at lower aqueous flow rates. The prospect of increased channeling and bypassing at higher aqueous flow rates would lead to lower aqueous phase conversions. This problem is quite clearly seen when flow of liquid through the tube is contrasted with flow of liquid in the shell. At an aqueous phase flow rate of 0.75 ml/min, flow through the shell had a liquid residence time of 53.3 min (shell void volume = 40 ml) with an observed phenol conversion of ~ 0.2, while aqueous flow through the tube side had a residence time of 3 min (tube lumen volume = 2.2 ml), yet exhibited a markedly higher conversion of phenol of ~ 0.5. This clearly demonstrates that the bypassing of the aqueous phase in the shell side of the module leads to lower observed experimental conversions of aqueous pollutants. Since the majority of the resistance to the mass transfer of ozone in a gas-liquid contacting process lies in the aqueous phase boundary layer, aqueous phase run on the shell side of the module results in a markedly lower overall mass transfer coefficient due to aqueous phase bypassing and channeling, than when it is run on the tube side, leading to lower pollutant removal as evinced from Figure 2.4.2. The products of ozonation of phenol range from structures with an intact aromatic ring, viz. catechol and ortho-quinone, which upon ring rupture result in, muconaldehyde, nuconic acid, glyoxal,

glyoxalic, oxalic and formic acids. The phenolate ion has been shown to react very rapidly with ozone at pH values above the pKa of phenol, which is 9.9. The ozonation rate constant at basic pH is shown to be anywhere from two to six orders of magnitude higher than that for ozonation at neutral and acidic pH depending upon the reference (Joshi and Shambaugh, 1982; Hoigne and Bader - I, 1983; Hoigne and Bader - II, 1983) indicating that the precise mechanism of ozonation of phenol is still not understood well and the kinetic parameters still need further refinement.

b) Nitrobenzene as a model pollutant

Figure 2.4.3 shows the performance of the single phase membrane ozonator when nitrobenzene is used as a model pollutant, with the aqueous phase flowing on the shell side of the module. The experiments were conducted using three different reactors, SILCAP #2, 5, 6. These modules had a higher surface area per reactor volume than SILCAP #1 and a smaller shell void volume than SILCAP #1 (40 ml for SILCAP #1, 20 ml for SILCAP #2-#6). Even though these reactors were identical in all aspects, i.e module length, number of silicone capillaries used, the disparity observed in the reactor performances cannot solely be explained by differences in channeling and bypassing that would be unique to each reactor. The amount of prior exposure of the polymer to ozone is seen to affect the reactor performance and is discussed in the following paragraphs. For the convenience of understanding the results, the experiments have been summarized in Table 2.4.12.

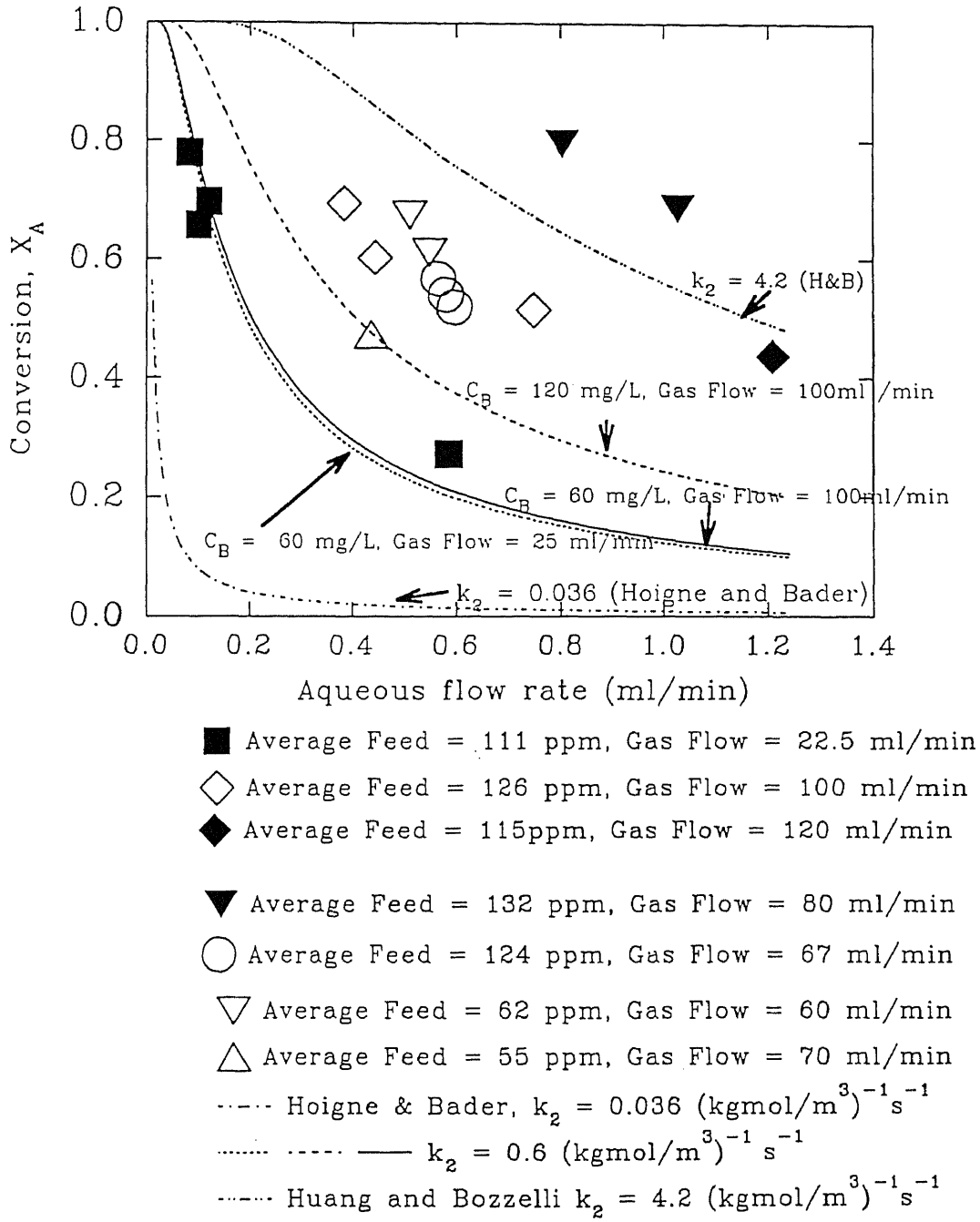

Figure 2.4.3. Degradation of nitrobenzene in the single-phase membrane ozonator (SILCAP #2-6).

Table 2.4.12. Summary of the experimental results for nitrobenzene as a pollutant in the single-phase membrane ozonator (SILCAP #2-6)

Symbol	Module	Feed Conc. (ppm)	Prior Ozone Exposure	Remark
■ [a]	SILCAP #2	111	~32 hours	Exposed to KI soln. and O_3[†]
◯ [b]	SILCAP #5	124	~ 4 hours	Exposed to O_3[§]
△ [b]	SILCAP #5	55	subsequent to above run	Exposed to O_3[‡]
▽ [b]	SILCAP #5	62	subsequent to above run	Exposed to O_3[‡]
▼ [a]	SILCAP #6	132	virgin polymer	-
◇ [b]	SILCAP #6	126	subsequent to above run	Exposed to O_3[‡]
◆ [b]	SILCAP #6	115	subsequent to above run	Exposed to O_3[‡]

[a] Membrane saturated with pollutant prior to experiment.
[b] Membrane not saturated with pollutant prior to experiment.
[§] Module exposed to KI solution and ozone prior to pollutant degradation experiments.
[†] Module exposed to dry ozone prior to pollutant degradation experiments.
[‡] Module exposed to ozone and polluted aqueous phase prior to experiment.

The results shown with the symbols ■ are for the module SILCAP #2. This module had been exposed to ozone during prior experiments used to measure the mass transfer of ozone into the aqueous stream. The results marked with △, ▽, ◯ are for the module SILCAP #5. This module had been exposed to ozone during the measurement of ozone permeability, for a much shorter time (~4 hours) than SILCAP #2 (~32 hours). During these experiments with SILCAP #5, the membrane was saturated with the nitrobenzene solution, prior to the start of the ozone gas flow. The inverted solid

triangles, ▼ represent runs for the module SILCAP #6 where the virgin polymer was also saturated with the nitrobenzene solution prior to experimentation. Finally the results shown by ◇, ◆ are for the module SILCAP #6 without any prior saturation of polymer with nitrobenzene. These experiments were performed after the runs marked ▼.

The module that was used in these ozonation studies with the most prior exposure to ozone was SILCAP #2 (about 32 hours of total ozone exposure prior to the runs with nitrobenzene), while module SILCAP #6 had the least exposure to ozone. Since the exposure of ozone in presence of the aqueous phase is seen to increase the permeability of ozone, the drop in reactor performance can in no way be directly ascribed to change in ozone permeability. However the probability that the reaction of ozone with KI in proximity of the membrane had severely reduced the ozone permeability far more than the reduction observed for NEWCON #1 is unknown. This would indicate that the history of exposure of the polymer to ozone has an effect in the overall reactor performance. This could be attributed to the increased crosslinking of the polymer by ozone. How this crosslinking affects the reaction and subsequently the performance of the reactor is not altogether clear at this point, but a simple hypothesis could be postulated that the reaction is somehow enhanced as a result of partitioning into the silicone phase, this partitioning effect is reduced as the polymer becomes increasingly cross-linked. The results marked as ■, for SILCAP #2 most probably represent the long term behavior of the reactor. Also from the data shown, the pre-saturation of the polymer by nitrobenzene does not affect the steady state behavior of the reactor. The overall trend also shows that at low aqueous flowrates (i.e. high liquid residence times) conversions

of ~80% are observed, while at higher flow rates these conversions drop to ~50%. The experimental results also indicate that the reactor performance is not directly influenced by the inlet pollutant composition. This is indicated by the similar conversions observed for feeds ~ 60 ppm (△, ▽) and ~ 120 ppm (◇, ◆).

The lines shown in Figure 2.4.3 represent simulations carried out using the single phase membrane ozonator model, discussed in Chapter 2.3. A value of 8.0 e-13 (kgmol .m)/(m^2.s.kPa) was used for Q_B^m, the permeability of ozone through silicone capillaries, in all the simulations. The line marked k_2 = 0.036 represents a simulation where the second order reaction constant in the model is equal to 0.036 $(kgmol/m^3)^{-1}$ s^{-1} and represents a simulation using the kinetic data presented in Table 2.4.11. The line marked k_2 = 4.2 represents a simulation where k_2 = 4.17 $(kgmol/m^3)^{-1}$ s^{-1} (Huang and Bozzelli, 1986). The value reported in this publication is much higher than that reported in literature, shown in Table 2.4.11. This value was obtained by fitting the nitrobenzene ozonation time decay profile with a complex rate expression. This seems to be rather system specific, i.e. it is strongly dependent upon the choice of the chemical rate model that is used to fit the decay profile. A value of k_2 = 0.6 $(kgmol/m^3)^{-1}$ s^{-1} is used to simulate and obtain the three middle lines; the upper most is for a gas flow rate of 100 ml/min and feed gas concentration of 120 mg/L, the one lower than that for a feed gas concentration of 60 mg/L, while the third line is for a gas flow rate of 25 ml/min and a feed concentration of 60 mg/L. From these three lines, it is apparent that the performance of the single phase membrane ozonator depends more upon the feed ozone concentration, which translates to a higher ozone concentration in the aqueous phase and

higher reaction rates. Since the model did not account for any pollutant-membrane interactions, the results shown by ◇, ◆, △, ▽, ◯, and ▼ could not be successfully simulated. However the value of k_2 = 0.6 $(kgmol/m^3)^{-1}$ s^{-1} did fairly well in simulating the data for SILCAP #2 as a membrane reactor with nitrobenzene as a model pollutant shown by the points ■. The products of ozonation of nitrobenzene that are formed include nitric acid, formic acid, glyoxal, glyoxalic acid, oxalic acid and carbon dioxide (Caprio et al., 1984). The initial attack results in an elimination of nitric acid, breaking the ring structure and ozonation of the unsaturated products result in the formation of aforementioned organic species. Compared to the parent compound the product species are more recalcitrant towards ozonation, but readily biodegradable unlike the parent compound (Bhattacharyya et al., 1995).

c) Acrylonitrile as a model pollutant

Figure 2.4.4 shows the results for the module SILCAP #2, where degradation of acrylonitrile was used to demonstrate the performance of the single-phase membrane ozonator. For a feed concentration of 206 ppm, the conversion of acrylonitrile was observed to be about 0.6 for an aqueous flow rate of about 0.05 ml/min and dropped to 0.2 at an aqueous flow rate of 0.4 ml/min. Prior to this set of experiments, this module had been exposed to ozone for a total overall period of about 60 hours. Further experiments to measure the permeability of ozone could not be carried out with SILCAP#2, because it was found that the integrity of the silicone capillaries had been compromised leading to breakage of a large number of the capillaries.

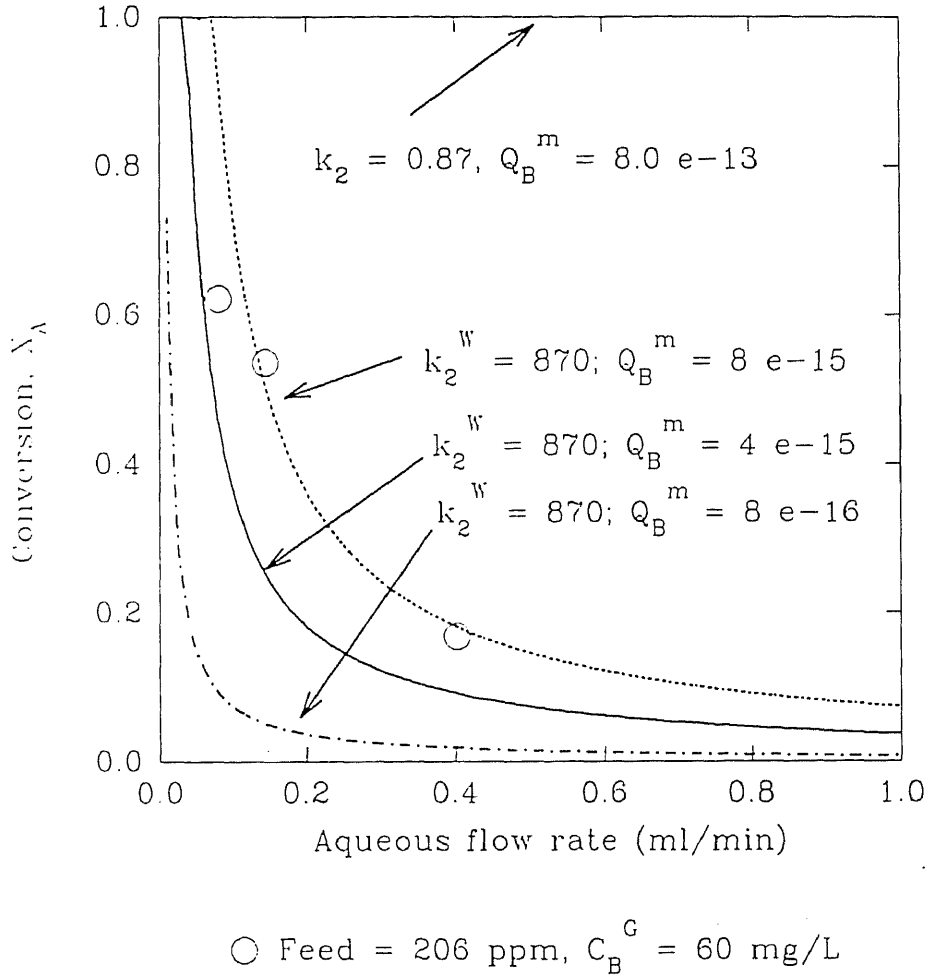

Figure **2.4.4.** Degradation of acrylonitrile in the single-phase membrane ozonator (SILCAP #2).

The simulation for acrylonitrile as a model pollutant is shown by the various lines that are drawn in Figure 2.4.4. At the value listed in Table 2.4.11, k_2^W = 870 $(kgmol/m^3)^{-1}\ s^{-1}$, for Q_B^m = 8.0 e-13 (kgmol.m)/(m^2.s.kPa), it is seen that the simulation gives nearly 100% conversion and the simulation line merges with the top axis. The reason for the discrepancy between observed and simulated pollutant conversions is not altogether clear at this moment. The present kinetic data allows a starting guess as to what would be a good estimate for the reaction rate constant for simulation of the experimental data.

The reaction of ozone with KI solution in the proximity of the silicone capillaries coupled with the extended exposure to ozone during the degradation of nitrobenzene would probably lead to considerable crosslinking within the silicone polymer matrix. Crosslinking of the polymer would make the substance more rigid and therefore glassy-like in properties. In literature O_2 has a permeability in silicone rubber (a rubbery polymer) of 933 barrer and a permeability in polycarbonate (bisphenol-A-polycarbonate, a glassy polymer) of 1.48 barrer, a difference of 2 orders of magnitude. The simulation that best describes the data is for a Q_B^m = 8.0 e-15 (kgmol.m)/(m^2.s.kPa) with k_2^W = 870 $(kgmol/m^3)^{-1}\ s^{-1}$ and a gas feed concentration of $C_B^G \mid_{inlet}$ = 60 mg/l. This value of Q_B^m is two orders of magnitude lower than the experimentally determined Q_B^m found for ozone in section 2.4.3.

During the experiments with acrylonitrile the gradual hardening (increased cross-linking) of the capillaries which led to much lower ozone permeabilites would have also led to the inevitable breakage of capillaries that has been mentioned above.

d) Mass transfer characteristics of the single-phase membrane ozonator

Conventional ozonation of organic compounds in water is known to be limited by the mass transfer of ozone into the aqueous phase. Whether this is also true for the single-phase silicone membrane ozonator has to be ascertained.

Based upon the stagnant film model for the reaction shown below (Equation

$$a\,A + b\,O_3 \rightarrow \text{products} \qquad (2.4.10)$$

2.4.10), the Hatta number gives an idea of the predominant resistance, reaction or mass transfer, to the transfer of ozone from the gas to the liquid phase. For a second order reaction between species A and O_3, with O_3 partitioning from a gas phase and dissolving in the aqueous phase while reacting with species A dissolved in the liquid phase, it is defined as:

$$\text{Hatta Number},\ \phi = \delta \sqrt{\frac{k_2^W C_A^l}{D_{O_3}^l}} = \left[\frac{(k_2^W C_A^l C_{O_3,i}^l \delta)}{\frac{D_{O_3}^l C_{O_3,i}^l}{\delta}} \right]^{1/2} \qquad (2.4.11)$$

where δ is the thickness of the film within which diffusion occurs. For the single-phase membrane ozonator, δ can be assumed to be equal to $(r_f - r_o)$, the thickness of the liquid layer bounded by the free surface (3.27 e-4 m). C_A^l is the aqueous phase concentration of the pollutant, which for the sake of comparison between the three pollutants is assumed to be ~100 ppm and $D_{O_3}^l$ is the diffusivity of ozone in the aqueous phase (2.01 e-9 m^2/s) and $C_{O_3,i}^l$ is the concentration of ozone in the aqueous phase at the aqueous-

silicone interface. The square of the Hatta number defined above, ϕ^2 is equal to the ratio of the maximum conversion rate of ozone in the film per unit area of the interface and the maximum diffusional transport rate of ozone in the film in the absence of reaction. Therefore for $\phi < 0.3$, hardly any reaction takes place in the film while for $\phi > 2$ all of the ozone is consumed in the film. The result of the calculation for each of the pollutant in turn is shown in Table 2.4.13.

Table 2.4.13. Calculation of Hatta numbers for the three pollutants in the single-phase membrane ozonator

Compound (MW)	C_A^l (kgmol/m^3) / (ppm)	$k_2^{W\,\dagger}$ (kgmol /m^3)$^{-1}$ s^{-1}	$\phi^\dagger$	$k_2^{W\,\S}$ (kgmol /m^3)$^{-1}$ s^{-1}	$\phi^\S$
Phenol (94)	1.06 e-3 / 100	115	2.55	11.5	0.81
Acrylonitrile (53)	1.89 e-3 / 100	870	9.4	870	9.4
Nitrobenzene (123)	8.12 e-4 / 100	0.04	0.042	0.6	0.16

† Second order reaction rate constant from Table 2.4.11.
§ Second order reaction rate constant which best fit the experimental data.

From the table above, the Hatta number, ϕ, calculated using the reaction rate coefficients that best fitted the data shown in Figures 2.4.2-2.4.4, gave values >2 for acrylonitrile, and <0.3 for nitrobenzene as model pollutants. Phenol appears to be in a reaction regime in between those for the aforementioned pollutants. If the values listed in Table 2.4.11 are used to calculate ϕ, then for both phenol and acrylonitrile the

situation appears to be in a regime where ozone is consumed in the liquid film bounded by the free surface, indicated by $\phi > 2$. The actual situation within the reactor is also very much different than what is simulated, since the free surface model does not account for the bypassing and channeling of the aqueous phase in the shell side of the module.

Consumption of ozone within the liquid film, for $\phi > 2$ could lead to situation where ozone becomes the limiting reactant and the membrane reactor is inefficiently utilized to remove the pollutant from the aqueous phase. The ozonator capacity to treat a given concentration of the aqueous pollutant is determined by the interfacial area between the gas and liquid phases; this in turn is determined by the membrane area available per unit volume of the device. There is however an upper limit to this area with the presently available silicone capillaries and the aspect of increased aqueous phase bypassing as the packing coefficient in the shell side of the module is increased has to be considered too.

For a situation in the single-phase membrane ozonator where the Hatta number is less than 0.3, the reaction is considered slow and taking place in the bulk and the rate of mass transfer of ozone into the bulk aqueous phase controls the overall process. The maximization of the transfer of ozone into the aqueous phase can be achieved in a number of different ways; 1) increasing the residence time of the aqueous phase within the reactor. This allows more time for ozone to permeate into the aqueous phase and come into contact with the aqueous pollutant. This however results in a lower mass transfer coefficient leading to larger equipment in order to treat a waste aqueous stream. 2) Since the process is limited by the mass transfer of ozone, increasing the aqueous

phase concentration of ozone by raising its gas phase concentration will increase the amount of ozone transferred to the liquid in a given amount of time. Increasing the aqueous concentration of ozone will also allow the treatment of a greater amount of pollutant per unit volume of aqueous phase within the reactor. 3) The overall volumetric mass transfer coefficient, $k_l a$ of ozone into the aqueous phase can be maximized as will be described below.

The two major resistances to mass transfer of ozone from the gas phase to the aqueous phase are those due to the membrane phase and the aqueous side boundary layer. The absence of a stable substrate which would lend to the fabrication of fine microporous capillaries to pack sufficient membrane area into a membrane device leads to the conclusion that the liquid side boundary layer resistance is the only resistance that lends to any optimization. There are a number of ways that this resistance may be reduced in a membrane device. a) The increase in the amount of membrane area available per unit volume of the device leads to higher volumetric mass transfer coefficient $k_l a$ as is shown in Section 2.4.4. This means that more ozone is available in the aqueous phase to destroy the pollutant and leads to a better ozone utilization per unit volume of the device. b) Increasing the aqueous flow rate reduces the mass transfer resistance for the diffusion of ozone, but also reduces the residence time of a liquid element exposed to ozone in the membrane device. This requires the use of a pump and a temporary storage vessel in order to have high liquid recirculation flow rates through the module. The increase in mass transfer coefficient is however at the expense of a higher aqueous pressure drop along the module. c) The introduction of cross-flow of the aqueous phase across the

membrane surface would allow for a much higher mass-transfer coefficient. This due to the fact that having the liquid phase flow transversely across a tubular membrane rather than parallel to the tubular membrane means that the aqueous boundary layer at the aqueous-membrane interface is subject to shearing forces. This reduces the thickness of the boundary layer leading to a higher mass transfer coefficient.

e) Cumulative duration of the ozonation modules

As seen in the experimental sections pertaining to the permeability of ozone and the degradation of nitrobenzene and acrylonitrile as model pollutants, the stability and durability of the silicone membrane is an issue that dictates the utility of the device. The module SILCAP #1, the physical dimensions of which are listed in Table 2.2.1 was exposed to ozone for a total period of 54 hours without any observable change in physical properties. An increase in the permeability of ozone and oxygen was observed as compared to a module with virgin silicone capillaries as has been indicated in Table 2.4.7. Module SILCAP #2 which was exposed to ozone for a comparable amount of time and was exposed to KI solution failed. The presence of free iodine in the proximity of the silicone capillaries during the ozonation of KI solution seems to be detrimental to the integrity of the silicone capillaries and results in the hardening of the silicone capillaries leading to their failure. An additional consideration is the integrity of the epoxies used to fabricate the module. They tend to adopt a yellow tinge with long term exposure to ozone and display small cracks with long term exposure to ozone.

The durability of such devices is therefore contingent not only upon the membrane materials used but also on the materials used to fabricate the module, like the shell casing, epoxies, etc.

CHAPTER 3

TWO-PHASE MEMBRANE OZONATOR

3.1. Introduction

The use of a "thin layer" of liquid as a membrane to remove species from a bulk phase to another bulk phase, selectively and efficiently, has received considerable attention, since it allows separation of species that would otherwise not be efficient with the use of conventional polymeric membranes. There are three types of liquid membranes, depending upon the way this "thin layer" is interspersed between the two bulk phases. For the case where the species are transferred between two liquid phases, e.g. the removal of mercury from wastewater, it is possible to use a "thin layer" of liquid to remove mercury from wastewater and enrich it in a "receiving" aqueous phase. This is possible by a technique known as Emulsion Liquid Membrane (ELM) : a double emulsion is created wherein the two bulk liquid phases are kept apart by a thin organic liquid layer which constitutes the liquid membrane. Since ELMs are generally used for the transfer of species between two liquid phases, further discussion of this technique will not be pursued.

Conventionally liquid membranes are utilized by immobilizing the liquid in a microporous matrix; this matrix is spontaneously wetted by the liquid and is held in place by means of capillary forces. This is termed as an Immobilized Liquid Membrane (ILM) or a Supported Liquid Membrane (SLM); it can be used to bring two gases or two liquids into contact with the two sides of the ILM (or a liquid and a gas into contact) to

selectively transfer species from one bulk phase to another bulk phase. The use of ILMs however has not had very many commercial applications, since they have a number of serious drawbacks. The membrane is as stable as the amount of liquid present, which is small, and renewal or replacement of the liquid membrane is required. An imbalance of transmembrane pressure due to either of the bulk phases can lead to loss of liquid membrane, with the fluid at the higher pressure expelling the liquid membrane out of the porous support. Also whenever gases are used in conjunction with SLMs, the gases have to be humidified to reduce the depletion of the liquid membrane by evaporation.

To overcome some of the shortcomings of SLMs mentioned above, the contained liquid membrane technique was developed first to study the separation of gases (Majumdar et al., 1988) and subsequently to study the selective removal of dissolved species from an aqueous phase (Sengupta et al., 1988). Since this method uses tubular microporous membranes, in the form of hollow fibers, to convey the flowing bulk phases, it is termed a Hollow Fiber Contained Liquid Membrane (HFLCM) technique. The microporous hollow fibers are sheathed in a shell, much like a shell-and-tube heat exchanger with two sets of tubes with independent manifolds to transport the two flowing bulk phases. The liquid membrane is "contained" in the void space in the shell amidst the hollow fibers as shown in Figure 3.1.1.

The term "membrane reactor" is used to describe a membrane device where the membrane acts either to separate the feed or product of a reaction or as a reaction medium or contains a catalyst (enzymatic or inorganic) which enhances the reaction between species permeating through the membrane. Therefore the use of a liquid

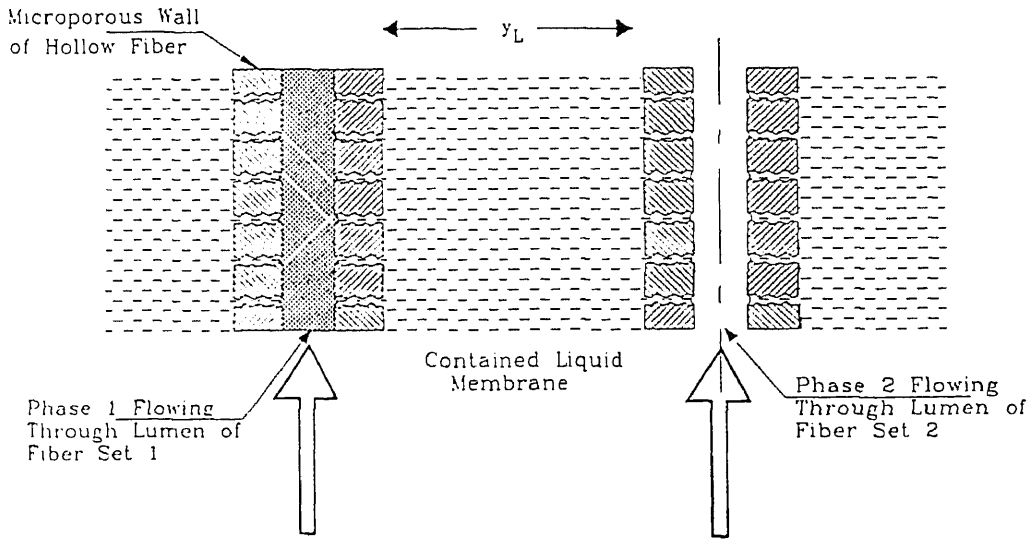

Figure 3.1.1. Schematic of a hollow fiber contained liquid membrane (HFCLM)

membrane which has a higher solubility for the reacting species and functions as a reaction medium in a device would constitute a membrane reactor. The use of liquid membranes in integrated separation and reaction devices was introduced during the study of the heterogenous catalytic oxidation of ethylene to actelaldehyde using $PdCl_2$ and $CuCl_2$ as catalysts (Ollis et al., 1972); liquid membranes were also studied to selectively remove CO_2 from an O_2-CO_2 feed mixture by facilitated transport through a bicarbonate solution supported on a highly porous cellulose acetate film (Ward and Robb, 1967). This concept has been readily used to study the ethylene hydroformylation, where the homogeneous catalyst is "supported" in a porous support sandwiched between two membranes (Kim and Datta, 1991). The membranes prevent the loss of the catalyst into the bulk streams and to prevent the passage of the product into the feed stream. Tubular membranes were used to study the oxidation of ethylene to acetaldehyde using an aqueous solution of $PdCl_2$ and $CuCl_2$ as a catalyst (Chen et al., 1992). The study emphasized the merits of keeping the two gaseous reactant streams apart in two sets of tubular membranes in order to maximize the conversion of ethylene to acetaldehyde. The aqueous solution was "contained" in the shell side void space of the module.

As mentioned in Chapter 1, the solubility of ozone in water is low. This becomes an issue when there are species present in the aqueous stream which are capable of scavenging ozone; this limits the efficiency of ozonation. The utility of a second perfluorocarbon (FC) phase which has a high solubility for ozone and is capable of behaving as a reaction medium has been demonstrated in a number of studies (Stich and Bhattacharyya, 1987; Chang and Chen, 1994; Bhattacharyya et al., 1995; Freshour et al.,

1996). The gas-liquid contacting processes as detailed in Figure 3.1.2 that these studies have used, involve a saturator where the perfluorocarbon (FC) phase is contacted with the ozone stream. The ozone- bearing FC stream is then brought into contact with the wastewater stream to destroy the pollutant in the aqueous phase. Such a system leads to inevitable handling losses of the FC phase. The liquid holdup volume of the FC phase in such a contacting system is typically 3-4 times the reactor volume. The contacting efficiency in such a setup depends upon the efficiency of mixing of the aqueous and FC phases in the reactor. The FC phase chosen is therefore subject to a number a constraints : it has to have low volatility, since the saturator will allow some FC losses by physical bubbling of ozone into the FC phase. The FC phase cannot be viscous since this will hinder mixing of the FC and aqueous phases and make the pumping of the FC phase harder. It will also reduce the diffusion coefficients of ozone and the organic pollutants requiring either greater FC liquid holdup or longer reaction times.

Based upon the drawbacks of the prior studies described, the use of the HFCLM device is therefore warranted a harder look. If the membranes used in such a device were resistant to oxidative degradation by ozone, then the use of a fluorocarbon medium in the shell space of such a device would allow higher ozonation efficiencies. The FC medium would be used as a liquid membrane as well as a reaction medium classifying this device as a membrane reactor. In the case of hydrophobic pollutants, the FC medium behaves like an organic extractant, allows higher rates of reaction by concentrating the organic species prior to ozonation in the same phase.

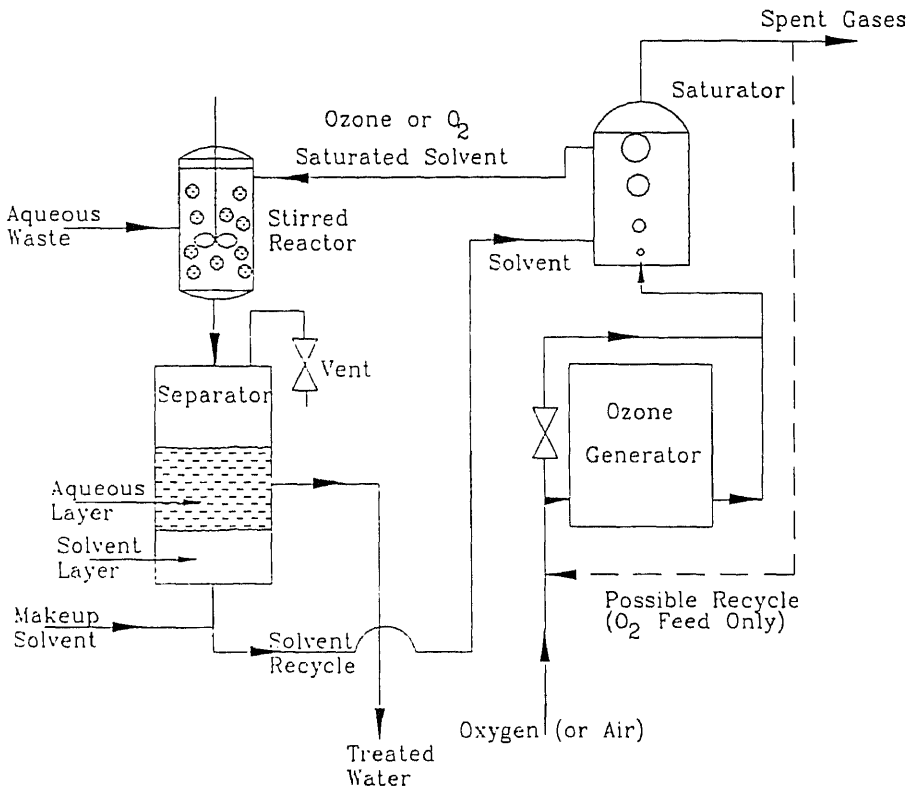

Figure 3.1.2. Schematic of a conventional two-phase ozonation scheme for the degradation of organic pollutants in wastwater (Stich and Bhattachayya, 1987).

The performance of the two-phase membrane ozonator with regards to its capability to degrade a number of model pollutants is the subject of study here. This chapter begins by detailing the construction of the membrane reactor, the estimation of the liquid membrane thickness in this membrane reactor and the use of the ozonator to treat a model wastewater stream. A simple mathematical model is derived to explain the performance of the reactor based on a second order reaction rate model. The kinetic parameters used for this model are calculated from batch experiments (Shanbhag, 1992; Sirkar et al., 1994). The performance of the reactor is evaluated based upon the capability of the reactor to degrade model pollutants, the levels of pollutant loading, the order of the resistances of mass transfer as opposed to the rates of reaction for individual pollutants. Finally some results concerning the utilization of ozone are presented and the relevance of an estimate of ozone utilization towards understanding of the reactor performance is discussed. Using nitrobenzene as a model pollutant, the utilization of ozone per mole of pollutant destroyed is also experimentally studied.

3.2. Experimental Procedure

3.2.1. Materials, Chemicals and Equipment

The following materials, chemicals and equipment were used in the experiments.

Ozone generator (Model T-408, Polymetrics, Colorado Springs, CO).

Ozone monitor (Model HC 400, PCI Technologies, West Caldwell, NJ).

High Performance Liquid Chromatograph, HPLC (Model 1090A, Hewlett Packard, Paramus, NJ) with a UV filter photometric detector.

HPLC integrator (Model 3390, Hewlett Packard, Paramus NJ).

HPLC autosampler (Micromeritics, Alcott Chromatography, Norcross, GA).

HPLC column (type Hypersil ODS, length 10 cm, dia. 3 mm, Chrompack, Bridgewater, NJ).

Teflon tubules (Impra/IPE Inc., Tempe, AZ).

Silicone capillaries (Silastic, medical-grade, (by Dow Corning, Midland, MI) Baxter Diagnostics, Edison, NJ).

FEP tubing and polypropylene barbed crosses (Cole Parmer, Chicago, IL).

Rotameter, (Cole Parmer, Chicago, IL).

Four Way Valve (cross-over), 1/8" NPT (Swagelock, R. S. Crum, Mountainside, NJ).

Mass flow controller transducer (Model 8272, Matheson, East Rutherford, NJ).

Multichannel dyna-blender (Model 8284, Matheson, East Rutherford, NJ).

Oxygen extra dry, helium high purity, nitrogen extra dry, air zero, carbon dioxide extra dry (Matheson, East Rutherford, NJ).

Phenol, acrylonitrile, nitrobenzene, toluene and trichloroethylene (ACS grade, Fisher Scientific, Springfield, NJ).

Fluorinert FC 43, perfluorobutylamine, (3M, St. Paul, MN).

Acetonitrile (HPLC grade, Fisher Scientific, Springfield, NJ).

Sodium thiosulfate, potassium iodide, potassium dichromate, sulfuric acid (ACS grade, Fisher Scientific, Springfield, NJ).

3.2.2. Preparation of Membrane Reactors

The fabrication of the two-phase membrane ozonator employed nonporous silicone capillaries (0.3 mm ID, 0.63 mm OD) and microporous Teflon tubules (0.99 mm ID and 2.0 mm OD). The silicone capillaries were of silastic medical grade. The porous Teflon tubules had a porosity of 50% and a pore size range of 12-19 μm. The silicone capillaries and Teflon tubules were counted, cut to length and laid out in the form of a mat. The ends of the silicone capillaries and Teflon tubules were bunched together and tied, keeping the bunched silicone ends separate from the bunched Teflon ends. The capillaries and tubules were simultaneously inserted in a transparent FEP shell (0.61 cm ID, 1.03 cm OD (Cole Parmer, Chicago, IL)). This was achieved by tying the bunched ends together by means of a string, covering the bunched tubule and capillary ends by a piece of Teflon tape and pulling the ends through the shell by means of the string tied around them. The disparate bunched ends were separated from one another and inserted into the appropriate ends of the barbed crosses, before the barbed crosses were gently pushed into the FEP shell to complete the structure of the module.

The four fiber ends were potted using two sets of epoxies (Beacon Chemical Co., Mount Vernon, NY). The external tube sheet was formed using the A2 epoxy with activator "A", using the proportion of 8 drops of activator to 5 gms of epoxy. The A2-A epoxy, a viscous paste, was liberally applied by a spatula to seal the void space between the silicone capillaries and the barbed cross-connector. The same procedure was repeated for the Teflon tubules. The internal tube sheet was formed using the C4 epoxy with activator "D", using 1 part activator to 4 parts epoxy by weight. The C4-D epoxy mixture was degassed in a desiccator by a vacuum pump and then poured in place via small holes predrilled into the each fiber end side of the barbed cross-fitting taking each of the ends in turn. The hole itself was sealed up with the epoxy. The epoxies were allowed to cure for seven days. The module was then filled with water on the shell side and the pressure in the shell was raised to 10 psig to check for leaks. Table 3.2.1 provides the geometrical specifications of the membrane modules identified henceforth as the SILTEF reactors. Figure 3.2.1(a) shows the arrangement of the epoxy layers in the capillary ends of the module, while Figure 3.2.1(b) shows a photograph of the module. Figure 3.2.2 shows a schematic of the completed module.

Table 3.2.1. Details of the two-phase (SILTEF) membrane-based ozonators

SILTEF Reactor Nos.	Active Length cm	First Fiber Set		Second Fiber Set		Effective Thickness* μm
		Total Number	ID/OD μm	Total Number	ID/OD μm	
1, 2	20.8	48[a]	305/635	6[b]	990/2280	-

[a] Nonporous silicone capillaries. [b] Microporous Teflon tubules.
* Actual FC-phase thickness will incorporate porosity and tortuosity of the fiber walls, (Majumdar et al., 1992).
Void space in shell : 68.7%. Surface area per unit vol. available : 5.1 cm^{-1}.

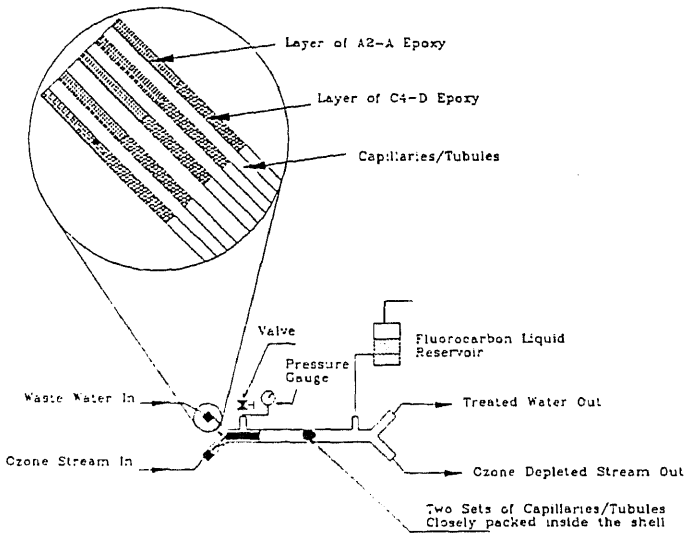

Figure 3.2.1(a). Schematic of novel membrane ozonator for multiphase oxidative degradation showing fiber ends embedded in epoxy layers.

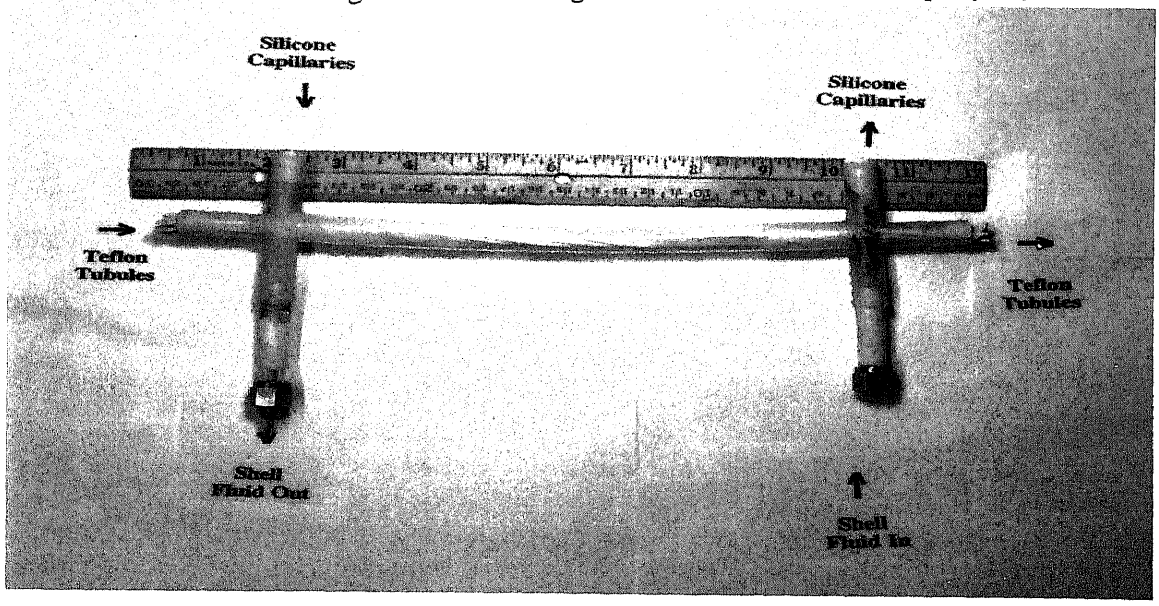

Figure 3.2.1(b). Photograph of the two-phase membrane ozonator.

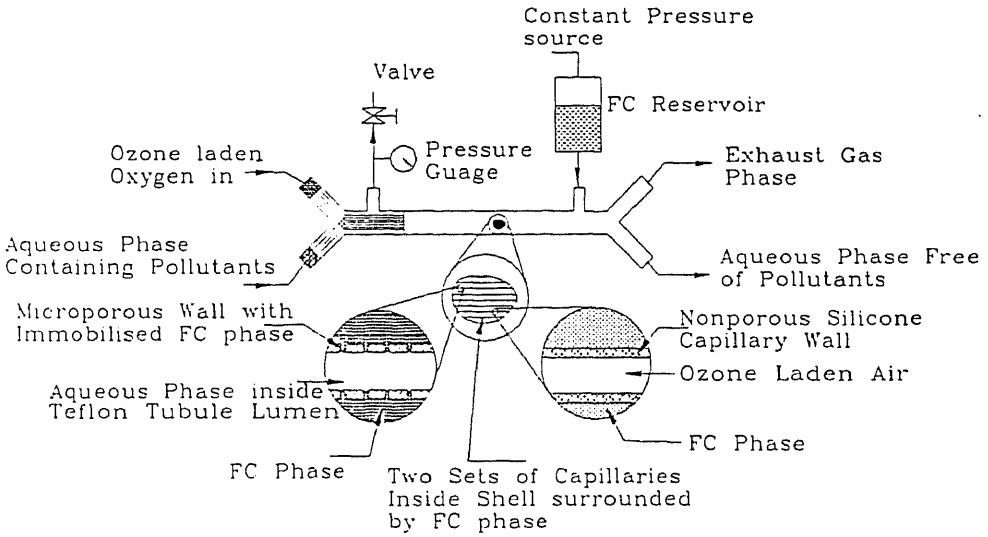

Figure 3.2.2. Schematic of two-phase membrane ozonator.

3.2.3. Analytical Techniques to Measure Organic Pollutants in Water

The aqueous feed was analyzed for pollutants using a HPLC equipped with a Hypersil ODS analytical glass column and a filter photometric UV detector. Table 3.2.2 indicates the HPLC conditions to detect and determine the concentration of pollutants in the aqueous phase.

Table 3.2.2. HPLC conditions for the organic compounds studied

Compound	Wavelength (nm)	Composition[a] (%)	Flow rate (cc/min)
Acrylonitrile	210	40 AC/60 H_2O	0.4
Phenol	254	40 AC/60 H_2O	0.4
Nitrobenzene	254	40 AC/60 H_2O	0.4
Trichloroethylene (TCE)	210	60 AC/40 H_2O	0.4
Toluene	210	60 AC/40 H_2O	0.4

[a] Acetonitrile (AC) and water were used as the mobile phase.
A sample loop of 10 μl was used.

The HPLC was initially calibrated by injecting samples of known composition of each of the pollutants and noting the area of the peaks recorded by the integrator. Aqueous samples of toluene, trichloroethylene, nitrobenzene and acrylonitrile were prepared by spiking deionized water with a pure liquid sample of the pollutant to give the necessary feed composition. Samples of lower concentrations of nitrobenzene and acrylonitrile were obtained by diluting the original feed samples by the requisite amount, while those of toluene and trichloroethylene were obtained by spiking deionized water

with pure samples of the two compounds by a Hamilton microliter syringe. For phenol, the aqueous feed was prepared by weighing out a sample of phenol crystals, which when mixed with deionized water would give the necessary aqueous feed composition. Sample calibration curves for phenol and nitrobenzene are shown in Figures 2.2.3 and 2.2.4 respectively, while those for toluene and trichloroethylene are provided in Figures 3.2.3 and 3.2.4 respectively.

3.2.4. Source of Ozone

Ozone was generated by feeding a pure oxygen gas stream to the ozone generator. The ozone generator was operated at a voltage setting of 90 volts; the pressure within the ozone generator was held at 9 psig (163.4 KPa) by a back pressure regulator. The flow rate of oxygen through the ozone generator was maintained at 0.6 standard liters per minute (SLPM). A small portion of the ozone/oxygen mixture (O_3/O_2) was diverted for experimental purposes. The major portion of this gas was vented after passing through two KI (2% concentration by weight) wash bottles linked in series to break down any ozone and a sodium thiosulfate bottle to trap any entrained iodine.

3.2.5. Measurement of Membrane Thickness of the Two-Phase Membrane Ozonator

The thickness of the contained liquid membrane in the two-phase membrane ozonator module was determined in the setup shown in Figure 3.2.5. One end of the Teflon tubules was connected to a cylinder of CO_2 while the other end was connected to a pressure gauge and a back pressure regulator. The two ends of the silicone capillaries

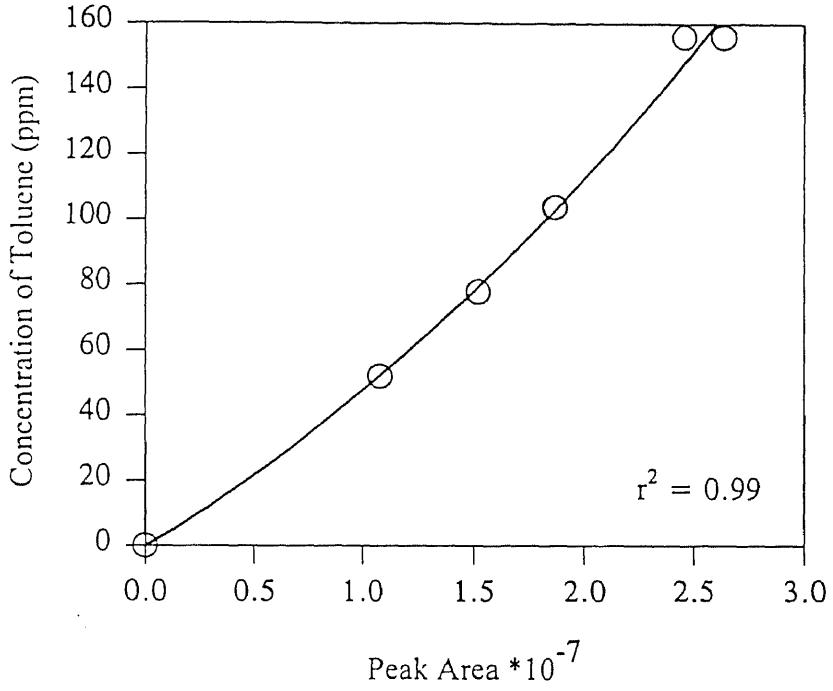

Conc. = (3.928e-6 * Peak Area) + (8.51e-12 * Peak Area^2)

Figure 3.2.3. HPLC calibration curve for toluene.

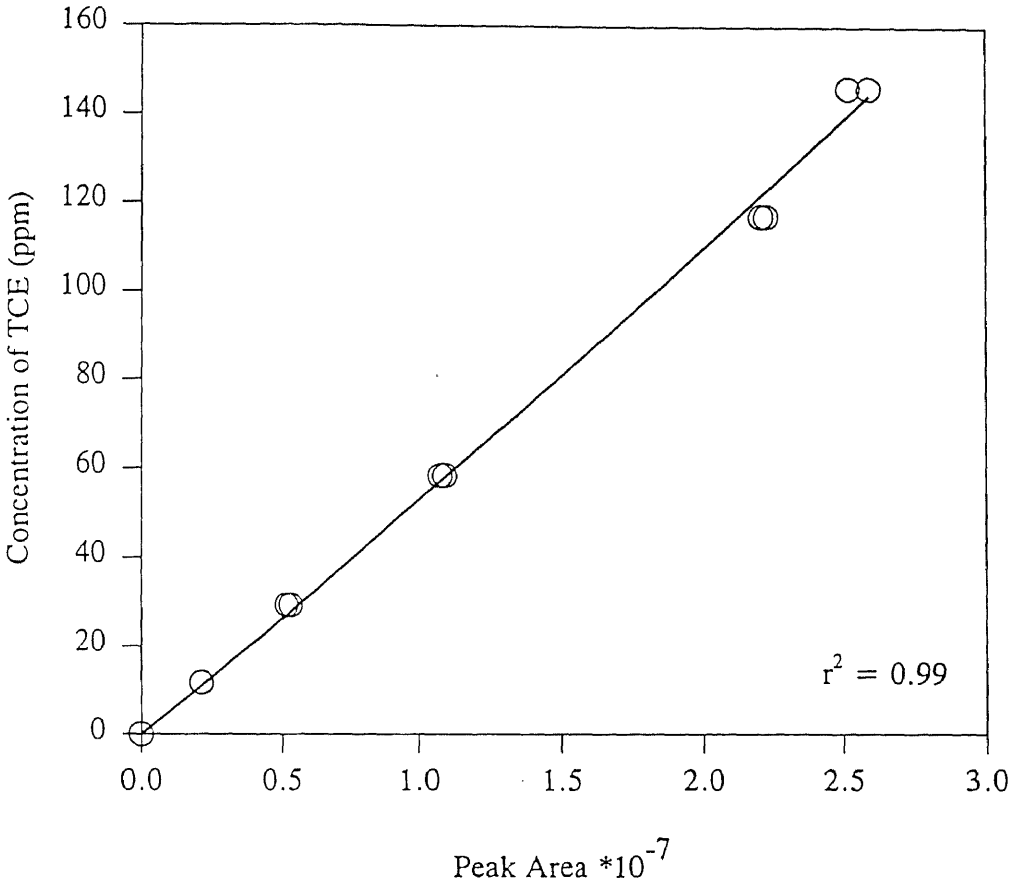

Conc. = (5.15e-6 * Peak Area) +
(1.68e-14 * Peak Area^2)

Figure 3.2.4. HPLC calibration curve for TCE.

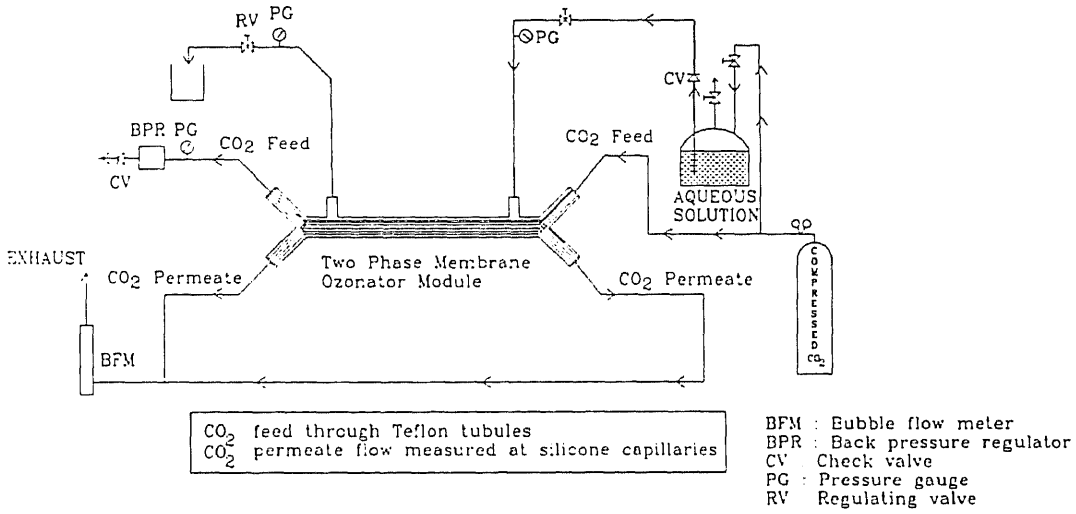

Figure 3.2.5. Schematic of the experimental setup used to measure contained liquid membrane thickness of two-phase membrane ozonator.

were connected together by means of T-fitting and the third end of the T-fitting was connected to a bubble flow meter. The shell side was filled with water from a pressure vessel which in turn was pressurized by the feed CO_2 cylinder. The pressure of the aqueous phase in the shell side of the module was kept slightly higher than that in the Teflon tubules to prevent the bubbling of CO_2 gas into the shell side. If the pressure of the aqueous phase in the shell side of the module was kept higher ($\Delta P_{(transmembrane)} > 2 \sim 3$ psig (115.1 KPa ~ 122.01 KPa)), it was found that water would freely enter the lumen of the Teflon tubules because of the comparatively large pores in the Teflon membrane wall. Therefore a transmembrane pressure of 0.5 ~ 1.25 psig (104.7 KPa ~ 109.9 KPa) between the shell side of the module and the Teflon tubule was maintained. The rate of permeation of CO_2 across the liquid membrane was monitored by means of a bubble flow meter and was used to calculate a module average membrane thickness.

The membrane thickness thus measured provided an estimate of the average effective distance between the external diameter of the Teflon tubules and the internal diameter of the silicone capillaries.

3.2.6. Measurement of Reactor Performance to Degrade Organic Pollutants in Water

The SILTEF reactor was positioned in the reactor loop shown in Figure 3.2.6. When toluene, trichloroethylene (TCE), nitrobenzene and acrylonitrile were studied as representative pollutants, the aqueous feed was obtained by spiking deionized water with a pure liquid sample of the pollutant to give the necessary feed composition. For phenol,

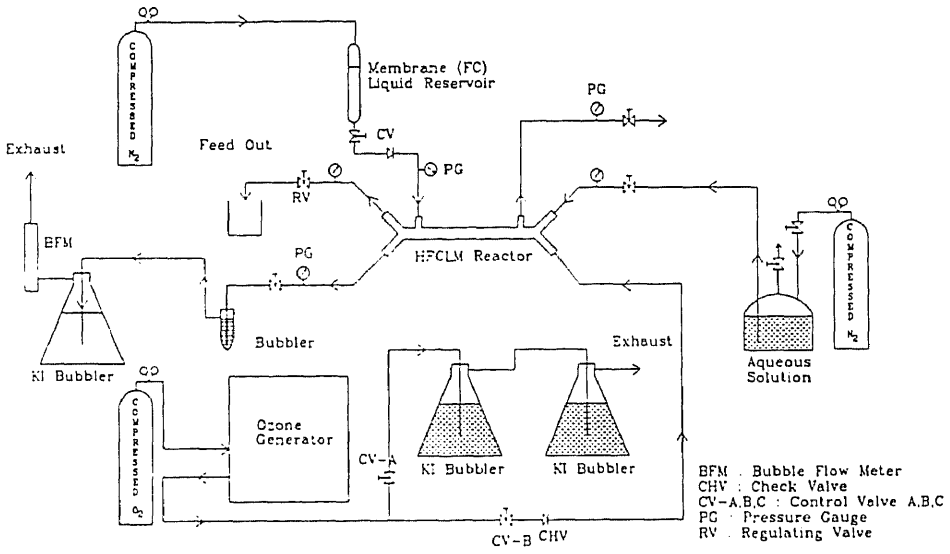

Figure 3.2.6. Schematic of the experimental setup used to study the degradation of organic pollutants in wastewater in the two-phase membrane ozonator.

the aqueous feed was prepared by weighing out a sample of phenol crystals, which upon being mixed with deionized water would give the necessary aqueous feed composition. The feed concentration was verified by injecting a feed sample into the HPLC and comparing the area obtained against a standard calibration. The aqueous feed was poured into a stainless steel pressure vessel, subsequently pressurized with N_2 to deliver the aqueous phase at a measured flow rate to the Teflon tubules of the module. The fluorocarbon phase was stored in a small aluminum storage vessel. Prior to the start of the experiment, this vessel was filled partially with the fluorocarbon phase. The fluorocarbon phase used in all two-phase membrane reactor studies was a fluorocarbon labeled FC 43; its physical properties (from the 3M product manual) are reported in Table 3.2.3.

Table 3.2.3 Properties of fluorocarbon (FC) liquid used[a]

FC	Mol. Weight	Boiling Point (°C)	Vapor[b] Pressure (mmHg)	Density[b] (gm/ml)	Kinematic Viscosity[b] (cs)	Solubility of Water[b] (ppm (wt.))	Solubility of FC in Water (ppm)
FC-43	670	174	1.3	1.88	2.8	7	ins.[c]

[a] Product Manual, 3M Fluorinert™ Electronic Liquids, 1989. [b] Measured at 25°C; [c] ins. = insoluble.

Experiments were conducted by first starting the aqueous phase flow through the Teflon tubules at a pressure of 1 ~ 2 psig (108.2 KPa ~ 115.1 KPa) and a predetermined flow rate. The fluorocarbon phase was then admitted into the shell side of the module. Since the FC reservoir was kept at a higher position than the module, the

fluorocarbon phase would flow into the module by gravity. However, on occasion it was necessary to gently begin the flow of the FC phase by pressurizing the FC reservoir with nitrogen. The O_3/O_2 gas phase was passed through the lumen of the silicone capillaries. The aqueous phase flow rate was controlled by means of a needle valve and the pressure of the aqueous phase was kept slightly higher than that of the fluorocarbon phase maintained at atmospheric pressure. The aqueous phase was sampled periodically; a sample was injected into the HPLC to determine the pollutant concentration. The flow of O_3/O_2 phase was monitored by a bubble flow meter and the flow rate was adjusted by means of valve A shown in Figure 3.2.6.

3.2.7. Measurement of Ozone Utilization during Two-Phase Ozonation

The utilization of ozone during two-phase ozonation was studied in a setup shown in Figure 3.2.7. This setup was nearly identical to that in Figure 3.2.6 used to observe the degradation of pollutants in the SILTEF membrane reactor. There, however, was one exception: at the outlet of the O_3/O_2 gas outlet from the module, a modification was made to accommodate the in-line ozone monitor. A makeup O_2 stream was also provided as shown in Figure 3.2.7 , since the operating gas flow rate for the ozone monitor was of the order of 1 slpm. The ozone monitor was equipped with a built-in solenoid valve; to preclude the possibility of an erroneous readings of ozone concentrations due to the buildup of pressure of gas in the O_3/O_2 flow loop, a bypass for the outlet gas was installed as shown in Figure 3.2.7, when the ozone monitor sampled the reference O_2 gas. A washbottle of KI solution was also installed to accommodate the O_3/O_2 stream

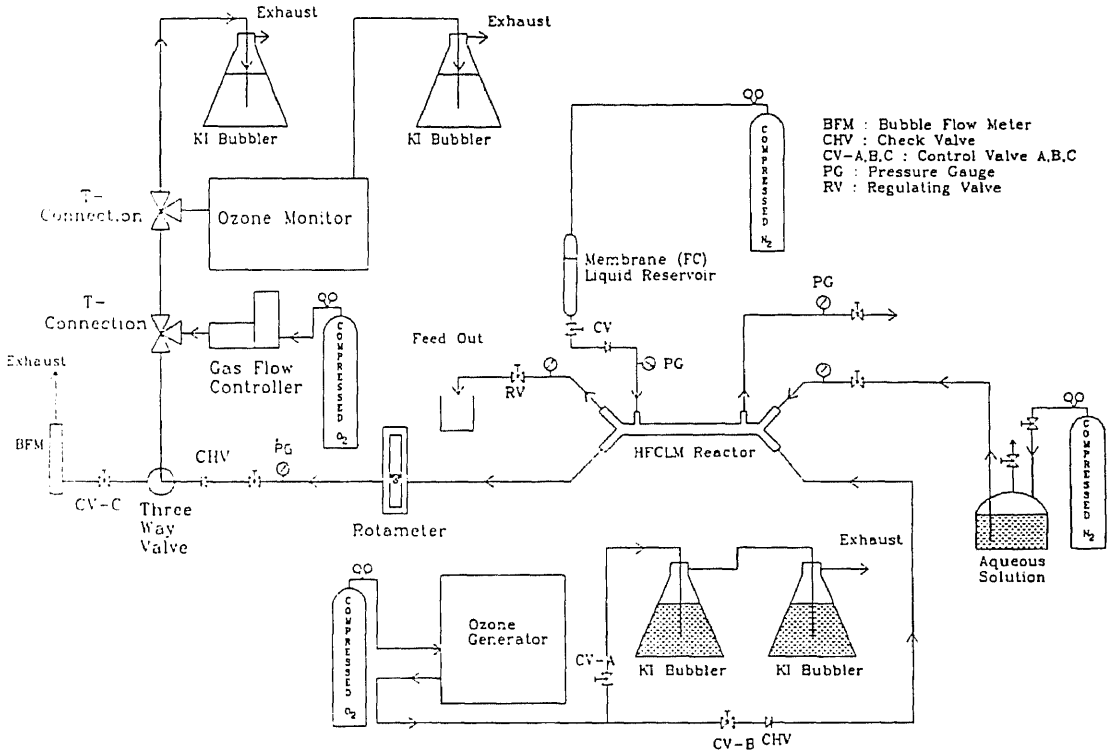

Figure 3.2.7. Schematic of the experimental setup used to study the utilization of ozone during the degradation of organic pollutants in the two-phase membrane ozonator.

which was bypassed when it was not being sampled. This setup obviated the need for a back pressure regulator. To measure the flow rate of O_3/O_2 gas through the module, a three-way valve was installed together with a rotameter before the module, a control valve C and a bubble flow meter at one end of the three-way valve.

Experiments were started with the SILTEF module shunted away from the supply of ozone. The aqueous flow to the module was started and the fluorocarbon phase was admitted into the shell side of the module as described before. While this was being done, the ozone generator was switched on and the rotameter reading was observed. The O_3/O_2 was then bypassed to control valve C and the bubble flow meter by means of the 3-way valve. Control valve C was adjusted so that the rotameter reading was identical prior to switchover and the gas flowrate was measured. The 3-way valve was switched back, so that the gas flow proceeded through the ozone monitor loop and the reading of the ozone monitor was observed and noted. The SILTEF reactor was then inserted into the O_3/O_2 gas loop. The 3 way valve was switched back to the bubble flow meter and the gas flow rate through the module was observed. Any adjustment in the O_3/O_2 gas flow that was necessitated because of the extra pressure drop brought about due to the presence of the module in the O_3/O_2 gas loop was effected by manipulating valve A, shown in Figure 3.2.7. During the experiment the reading of the ozone monitor was monitored and noted at frequent intervals of time, especially when the aqueous phase was being sampled for the pollutant.

At the conclusion of the experiment the SILTEF module was disconnected from the O_3/O_2 gas loop and the O_3/O_2 gas inlet was directly connected to the ozone monitor

loop as shown in Figure 3.2.8. Any adjustment in the gas flow rate due the absence of the SILTEF reactor was effected by means of valve A. The feed O_3/O_2 concentration as measured by the ozone monitor was noted.

3.3. Development of Mathematical Model

3.3.1. Model for a General Case

The mathematical description of the two-phase membrane ozonator is derived to determine the performance of the reactor, i.e. pollutant conversion, ozone utilization, etc. for given aqueous and O_3/O_2 flowrates. Consider any axial location, in the "z" direction (aqueous flow direction), within the membrane reactor as shown in Figure 3.3.1; the aqueous phase flows through the lumen of the Teflon tubules while ozone flows cocurrently through the lumen of the silicone capillaries. The organic pollutant partitions from the aqueous phase into the FC phase at the aqueous-FC interface, while ozone diffuses across the nonporous walls of the silicone capillaries and dissolves in the fluorocarbon phase. The partition coefficient of pollutant A between the FC and aqueous phases, m_A, is defined as

$$m_A = \frac{\bar{C}_A}{C_A} \tag{3.3.1}$$

where $\bar{C}_A$ is the concentration of A in the FC phase and C_A is the corresponding aqueous phase concentration at equilibrium. The two species diffuse along the "y" axis across the FC phase in opposite directions, with the reaction occurring simultaneously within the FC phase. Concentration profiles of the organic pollutant and ozone at any axial location is a function of the partition coefficients (Henry's constant for ozone), diffusion coefficients and reaction rate constants.

The reaction between the pollutant (A) and ozone (B) is described by the following equation:

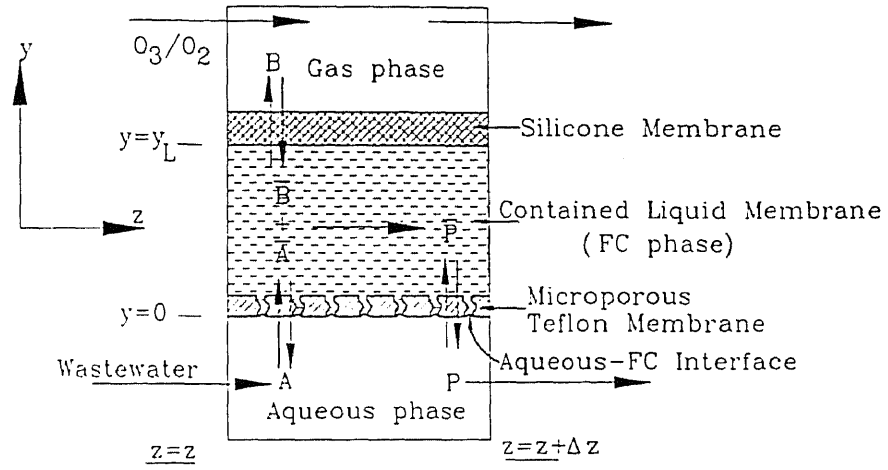

Figure 3.3.1. Schematic of the cross-section of the two-phase membrane ozonator.

$$aA + bB \rightarrow \text{products} \qquad (3.3.2)$$

where a and b are stoichiometric coefficients of the pollutant and ozone respectively. A number of assumptions are made to simplify the derivation of the reactor model. Axial diffusion in the "z" direction of either species in the stationary FC film is neglected. A constant effective FC-membrane thickness is assumed over the length of the reactor. This value was experimentally determined for water as a liquid membrane as outlined in section 3.2.5. The rate of stripping of pollutants into the gas phase is assumed to be negligible. Any O_3 supplied is consumed in the FC phase and none appears in the water phase. The governing diffusion-reaction equations for pollutant A and ozone B at any axial location in the stagnant FC phase are written as follows:

$$\bar{D}_A \frac{d^2 \bar{C}_A}{dy^2} = k_2^F \bar{C}_A \bar{C}_B \qquad (3.3.3)$$

$$\bar{D}_B \frac{d^2 \bar{C}_B}{dy^2} = \left[\frac{b}{a}\right] k_2^F \bar{C}_A \bar{C}_B \qquad (3.3.4)$$

where $\bar{C}_A$ and $\bar{C}_B$ are concentrations of species A and B in the fluorocarbon phase respectively, and k_2^F is the second order reaction rate constant in the FC phase. The boundary conditions follow:

$$\text{At } y = 0 \;,\; \bar{C}_A = \bar{C}_{Ai} \;;\; \frac{d\bar{C}_B}{dy} = 0 \;.$$

$$\text{At } y = y_l \;,\; \frac{d\bar{C}_A}{dy} = 0 \;;\; \bar{C}_B = \bar{C}_{Bi} \;.$$

The values $\bar{C}_{Ai}$ and $\bar{C}_{Bi}$ are determined at each axial point by mass balances in the bulk aqueous and gaseous phases respectively. This is a boundary value problem; the values

of $\bar{C}_{Ai}$ and $\bar{C}_{Bi}$ are not known a priori at each axial point and have to be estimated in order to solve the problem.

The following dimensionless variables are introduced into equations 3.3.3 and 3.3.4:

$$\eta = \frac{y}{y_l} \; , \; U = \frac{\bar{C}_A}{\bar{C}_A\big|_{inlet}} \; , \; V = \frac{\bar{C}_B}{\bar{C}_B\big|_{inlet}} \; , \; U_i = \frac{\bar{C}_{Ai}}{\bar{C}_A\big|_{inlet}} \; , \; V_i = \frac{\bar{C}_{Bi}}{\bar{C}_B\big|_{inlet}} \qquad (3.3.5)$$

where y_l is the effective distance between the aqueous-FC interface and the outer diameter of the silicone membranes. This distance incorporates the thickness of the wall of the Teflon tubule and the effective membrane thickness that was experimentally determined in section 3.2.5. and is given by the following relation:

$$y_l = \frac{d_i^{tef}}{d_{lm}^{tef}} \frac{\tau \, (d_o^{tef} - d_i^{tef})}{2 \, \epsilon} + \frac{d_i^{tef}}{d_o^{tef}} \delta_m \qquad (3.3.6a)$$

where δ_m is the experimentally determined membrane thickness and d_{lm}^{tef} is given by

$$d_{lm}^{tef} = \frac{d_o^{tef} - d_i^{tef}}{\ln \, (d_o^{tef} \, / \, d_i^{tef})} \qquad (3.3.6b)$$

Equation 3.3.3, is written in nondimensional variables as follows:

$$\frac{d^2 U}{d \eta^2} = \gamma_1 \, U \, V \qquad (3.3.7)$$

where

$$\gamma_1 = \frac{k_2^F \, y_l^2 \, \bar{C}_B\big|_{inlet}}{\bar{D}_A} \qquad (3.3.8)$$

Similarly, equation 3.3.4 can be rewritten as

$$\frac{d^2 V}{d \eta^2} = \gamma_2 \, U \, V \qquad (3.3.9)$$

where

$$\gamma_2 = \frac{b}{a} \frac{k_2^F y_1^2 \bar{C}_A \Big|_{inlet}}{\bar{D}_B} \qquad (3.3.10)$$

The boundary conditions become:

$$\eta = 0 \; ; \; U = U_i \; ; \; \frac{dV}{d\eta} = 0 \quad \text{and} \quad \eta = 1 \; ; \; \frac{dU}{d\eta} = 0 \; ; \; V = V_i \; .$$

In order to solve this set of equations, the initial guesses to the boundary conditions shown above, the concentration profiles and the corresponding fluxes of species A and B within the FC phase are required at each axial point. These are then introduced into an IMSL subroutine called B2PFD, to solve a boundary value problem. At each axial point this is run to calculate the fluxes and concentrations of the pollutant and ozone within the FC phase based upon the boundary conditions shown above.

The initial estimates for the concentration profiles were determined by employing pseudo first order approximations of equations 3.3.7 and 3.3.9 respectively and were derived as follows. Consider equation 3.3.7; if the fluorocarbon phase were saturated with ozone, then the concentration of ozone in the FC phase would change very little in the η direction and therefore as a first order estimate, V could be assumed to be constant along the η direction, which would lead to the following equation

$$\frac{d^2 U}{d\eta^2} = \Gamma_1^2 U \qquad (3.3.11)$$

where

$$\Gamma_1 = \sqrt{\frac{k_2^F \bar{C}_B\Big|_{inlet} y_1^2}{\bar{D}_A}} = \sqrt{\frac{k_{11}^F y_1^2}{\bar{D}_A}}$$

where k_{11}^F is a pseudo first order rate constant, derived with the assumption that the ozone concentration in the FC phase is a constant and is calculated by the product of the second order reaction rate coefficient and the ozone concentration at the module inlet in the FC phase. This equation can be analytically solved to yield the solution shown below

$$U = A_1 Cosh\ (\Gamma_1 \eta) + A_2 Sinh\ (\Gamma_1 \eta) \tag{3.3.12}$$

Applying the boundary conditions shown above results in

$$A_1 = U_i \quad ; \quad A_2 = - U_i Tanh\, \Gamma_1$$

This when inserted into equation 3.3.12 and subject to the appropriate trigonometric identity gives an analytical solution for U as follows:

$$U = U_i \frac{Cosh\ (\Gamma_1\ (1 - \eta))}{Cosh\ (\Gamma_1)} \tag{3.3.13}$$

If the same procedure is followed for species B (where it is assumed that the concentration of species A (pollutant) is an invariant across the FC phase), then equation 3.3.9 may be written as

$$\frac{d^2 V}{d \eta^2} = \Gamma_2^2 V \tag{3.3.14}$$

where

$$\Gamma_2 = \sqrt{\frac{b}{a} \frac{k_2^F\ \bar{C}_A\big|_{inlet}\ y_l^2}{\bar{D}_B}} = \sqrt{\frac{k_{12}^F\ y_l^2}{\bar{D}_B}}$$

where k_{12}^F is a pseudo first order rate constant derived with the assumption that pollutant concentration in the FC phase is a constant and is calculated by the product of the second order reaction rate constant and the concentration of the pollutant in the FC phase at the

inlet of the module. A general solution for the concentration of species B in the FC phase is then obtained as follows:

$$V = B_1 \, Cosh \, (\Gamma_2 \, \eta) + B_2 \, Sinh \, (\Gamma_2 \, \eta) \qquad (3.3.15)$$

Applying the boundary conditions shown earlier leads to

$$B_1 = \frac{V_i}{Cosh \, \Gamma_2} \quad ; \quad B_2 = 0$$

The following analytic pseudo-first-order solution for B is obtained

$$V = V_i \, \frac{Cosh \, (\Gamma_2 \, \eta)}{Cosh \, (\Gamma_2)} \qquad (3.3.16)$$

At each axial point the values of U_i and V_i were calculated from a mass balance in the lumen of the Teflon tubule and silicone capillaries as follows.

For the Teflon tubules, differentiating equation 3.3.13 and applying it at y = 0 (η = 0) to give the flux at the aqueous-FC interface :

$$N_A = - \bar{D}_A \left[\frac{d \bar{C}_A}{dy} \right]_{y=0 \, , \, \eta = 0} = \frac{\bar{C}_{Ai} \, \bar{D}_A \, \Gamma_1 \, Tanh \, (\Gamma_1)}{y_l} \qquad (3.3.17)$$

This flux should be balanced by the flux of pollutant from the bulk of the liquid given as follows:

$$N_A = k_l \, (C_{Ab} - C_{Ai}) \qquad (3.3.18)$$

where k_l is the volumetric mass transfer coefficient in the aqueous phase boundary layer and is obtained from the Graetz solution (Prasad and Sirkar, 1992). Using equations 3.3.1, 3.3.17 and 3.3.18, $\bar{C}_{Ai}$ and U_i are calculated as follows:

For the silicone capillaries, an estimate for the concentration of ozone at the silicone-FC

$$U_i = \frac{\bar{C}_{Ai}}{\bar{C}_A|_{inlet}} = \frac{k_l C_{Ab}}{\left[\frac{k_l}{m_A} + \frac{\bar{D}_A \Gamma_1 Tanh\,\Gamma_1}{y_l}\right]} \frac{1}{\bar{C}_A|_{inlet}} \qquad (3.3.19)$$

boundary $\bar{C}_{Bi}$ and V_i derived as follows:

$$V_i = \frac{\bar{C}_{Bi}}{\bar{C}_B|_{inlet}} = \frac{1}{H_B}\left[p_B - \frac{R_T \Delta z}{\frac{Ar_{sil} Q_B^m L}{\delta_l}}\right] \frac{1}{\bar{C}_B|_{inlet}} \qquad (3.3.20)$$

where H_B is the Henry's constant for ozone between the gas and FC phase, Q_B^m is the experimentally determined permeability of ozone across the silicone capillary wall, p_B is the bulk gas partial pressure of ozone in Pascals and δ_l is given as follows:

$$\delta_l = \frac{(d_o^{sil} - d_i^{sil})}{2} \qquad (3.3.21)$$

Here Ar_{sil} is calculated for a differential axial length Δz as follows:

$$Ar_{sil} = \pi \left[\frac{d_o^{sil} - d_i^{sil}}{\ln d_o^{sil} / d_i^{sil}}\right] \Delta z\, N_{sil} \qquad (3.3.22)$$

R_T is an estimate of the number of moles diffusing across the silicone capillary wall per unit time over a length Δz for the SILTEF module. This is calculated on the basis that the bulk gas concentration of ozone is based on p_B and the concentration of ozone at the aqueous-FC interface is zero and the calculation of R_T is shown in detail in Appendix 4.

Once B2PFD has converged to a solution at an axial position, the correponding pollutant and O_3 in the bulk phases can be calculated as follows. Within the Teflon

tubules a mass balance over a differential length Δz on the pollutant is carried out as follows:

$$Q_w C_A^l|_{OUT} = Q_w C_A^l|_{IN} - (\pi d_i^{Tef} N_{Tef} \Delta z) FLUXAq \qquad (3.3.23)$$

FLUXAq is the value of the pollutant flux leaving the aqueous phase as calculated by the IMSL subroutine, B2PFD at that particular axial position.

For the gas phase the following procedure is adopted to calculate the mass balance at each axial position over a differential length Δz :

$$Q_G C_B^G|_{OUT} = Q_G C_B^G|_{IN} - (Ar_{sil}) FLUXO_3 \qquad (3.3.24)$$

This equation can be rearranged to obtain a balance in the form of O_3 partial pressure in the silicone capillary lumen as follows:

$$p_{O_3}|_{OUT} = p_{O_3}|_{IN} - \left[\frac{Ar_{sil} R T}{Q_G}\right] FLUXO_3 \qquad (3.3.25)$$

In this case FLUX O_3 is derived in the following manner

$$FLUX O_3 = \frac{Q_B^m}{\delta}\left[\frac{p_{O_3}|_{OUT} + p_{O_3}|_{IN}}{2} - H_B \bar{C}_{Bi}^{Calc}\right] \qquad (3.3.26)$$

where $\bar{C}_{Bi}^{Calc}$ is obtained from the converged solution of B2PFD at that axial position.

Combining Equations 3.3.25 and 3.3.26, the following result is obtained for the mass balance for ozone in the silicone capillary lumen over an axial length Δz:

$$p_{O_2}|_{OUT} = \frac{\left\{\frac{2}{\epsilon} - 1\right\} p_{O_2}|_{IN} + 2 H_B \bar{C}_{Bi}^{Calc}}{\left\{\frac{2}{\epsilon} + 1\right\}} \qquad (3.3.27)$$

where

$$\epsilon = \frac{Q_B^m}{\delta} \frac{R T A r_{sil}}{Q_G}$$

3.3.2. Solution Algorithm

The above set of equations for a boundary value problem were solved using a Fortran program (provided in Appendix 5), which implemented an IMSL subroutine, B2PFD, at each axial point along the reactor. The schematic of the algorithm is shown in Figure 3.3.2.

At the beginning of the program the model requires specification of the aqueous and gaseous flow rates, the concentrations of each species in the respective phases, the physical properties and kinetic parameters of the reaction shown in equation 3.3.2. At each axial point, from the mass balances of the flowing phases from the previous segment, the initial estimates of the concentration profiles and their respective fluxes in the FC phase are generated based upon the pseudo-first order models discussed in the preceding section. These are used as initial guesses to run the IMSL subroutine B2PFD. The results from the IMSL subroutine (the concentration profiles and the respective fluxes designated with prime) are designated as U_{old}, U'_{old}, V_{old} and V'_{old} are used as guesses to get a more refined solution from the IMSL subroutine B2PFD. The results from B2PFD are designated as U_{new}, U'_{new}, V_{new} and V'_{new} and are compared with the

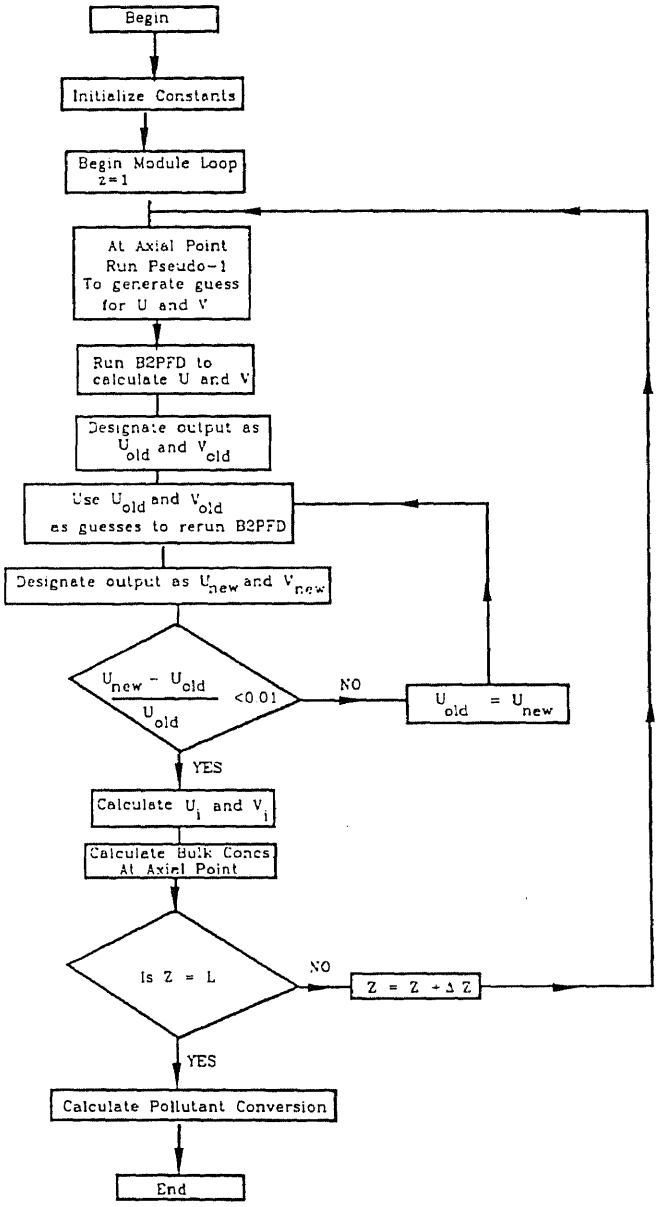

Figure 3.3.2. Solution algorithm to solve the model of the two-phase membrane ozonator.

corresponding U_{old}, U'_{old}, V_{old} and V'_{old}. If the convergence criteria shown in figure 3.3.2 are not met then the values of U_{old}, U'_{old}, V_{old} and V'_{old} are replaced with U_{new}, U'_{new}, V_{new} and V'_{new} and B2PFD is run again. If the convergence criteria are met, then the values of U_{new}, U'_{new}, V_{new} and V'_{new} are used to calculate the mass balances of the pollutant in the aqueous phase and ozone in the bulk gas phase respectively and the program proceeds with the calculations for the next axial segment. When the program reaches the end of the module, the pollutant conversion for the given aqueous and gaseous flow rate is calculated as follows:

$$\text{Conversion, } X_A = \frac{C_A^{in} - C_A^{out}}{C_A^{in}} \tag{3.3.28}$$

3.3.3. Model for Pollutants with Low m_A

Pollutants like phenol have a low m_A into the FC phase. For such compounds it can be assumed that the ozone concentration is uniform and in large excess compared to that of the pollutant. Based upon this simplifying assumption, equation (3.3.3) can be written as:

$$\bar{D}_A \frac{d^2 \bar{C}_A}{dy^2} = k_1^F \bar{C}_A \tag{3.3.29}$$

where the pseudo first order rate constant k_1^F is given by the product of k_2^F and $\bar{C}_B\big|_{inlet}$.

The above equation is integrated analytically to give

$$\bar{C}_A = M_1 \, Cosh\left[\gamma \frac{y}{y_L}\right] + M_2 \, Sinh\left[\gamma \frac{y}{y_L}\right] \tag{3.3.30}$$

$$\text{where } \gamma = \text{Hatta Number} = \frac{\sqrt{k_1^F \bar{D}_A}}{\bar{k}}$$

Here y_L is defined via

$$\frac{y_L}{\bar{D}_A} = \frac{1}{\bar{k}} = \frac{d_i^{tef}}{d_{lm}^{tef}} \frac{\tau (d_o^{tef} - d_i^{tef})}{2 \bar{D}_A \epsilon} + \frac{d_i^{tef}}{d_o^{tef}} \frac{\delta_m}{\bar{D}_A} \qquad (3.3.31)$$

which takes into account the diffusion in the pores in the hollow fiber wall along with that in the stagnant FC liquid of thickness δ_m in the shell side. Boundary conditions for equation 3.3.29 are

$$\text{at } y = 0 \quad \bar{C}_A = \bar{C}_{Ai} \; ; \quad \text{at } y = y_L \quad \bar{C}_A = 0$$

Using the boundary conditions shown above, constants M_1 and M_2 of equation 3.3.30 are evaluated. The concentration profile of A in the FC phase $\bar{C}_A$ is shown below

$$\bar{C}_A = \bar{C}_{Ai} \frac{Sinh\, \gamma \left[1 - \frac{y}{y_L}\right]}{Sinh\, \gamma} \qquad (3.3.32)$$

while the pollutant flux at the aqueous-FC interface can be determined by differentiating the above equation at y = 0 to give the following result:

$$N_{Ay} = -\bar{D}_A \left[\frac{d\bar{C}_A}{dy}\right]_{y=0} = \frac{\gamma \bar{D}_A \bar{C}_{Ai}}{y_L \tanh \gamma} \qquad (3.3.33)$$

Radial pollutant flux across the aqueous boundary layer can also be written in terms of a concentration difference as

$$N_{Ay} = k_w (C_{Ab} - C_{Ai}) = k_w \left(C_{Ab} - \frac{\bar{C}_{Ai}}{m_A}\right) \qquad (3.3.34)$$

The aqueous side mass transfer coefficient k_w can be found from the Graetz solution (Prasad and Sirkar, 1992). From equations 3.3.33 and 3.3.34, one can get the pollutant flux expression as

$$N_{Ay} = \left[\frac{\frac{\gamma \bar{D}_A m_A C_{Ab}}{y_L \tanh\gamma}}{1 + \frac{\gamma \bar{D}_A m_A}{y_L k_w \tanh\gamma}} \right] \tag{3.3.35}$$

For the pollutant concentration change along the module length, one can write

$$-\left[\frac{Q_w}{\pi d_i^{tef} N_{tef}}\right] \frac{dC_{Ab}}{dz} = \left[\frac{\frac{\gamma \bar{D}_A m_A C_{Ab}}{y_L \tanh\gamma}}{1 + \frac{\gamma \bar{D}_A m_A}{y_L k_w \tanh\gamma}} \right] \tag{3.3.36}$$

If k_w does not vary along the reactor length, a simplified result is obtained by integrating equation 3.3.36 using boundary conditions at z=0, $C_{Ab} = C_{Ab}|_{inlet}$ and at z=L, $C_{Ab} = C_{Ab}|_{outlet}$ giving the following equation:

$$C_{Ab}|_{outlet} = C_{Ab}|_{inlet} \quad \exp \left[- \frac{\frac{\gamma \bar{D}_A m_A C_{Ab}}{y_L \tanh\gamma}}{1 + \frac{\gamma \bar{D}_A m_A}{y_L k_w \tanh\gamma}} \left[\frac{\pi d_i^{tef} N_{tef} L}{Q_w} \right] \right] \tag{3.3.37}$$

Conversion in such a reactor is defined by equation 3.3.28.

3.4. Results and Discussion

3.4.1. Introduction

The physical characteristics of the two-phase membrane ozonator are summarized in Table 3.2.1. The physical properties of the FC phase used are summarized in Table 3.2.3. The experimental results are presented in the following order: 1) the experimental determination of the liquid membrane thickness for the two-phase membrane ozonator module; 2) the experimental reactor performance to degrade organic pollutants in wastewater and comparison of the experimental reactor performance with the model described in section 3.3; 3) the experimentally observed utilization of ozone for nitrobenzene as a model pollutant; 4) comparison between single and two-phase ozonation for nitrobenzene as a model pollutant. Nitrobenzene was chosen as a model pollutant to study the utilization of ozone for the following reasons: it had a high boiling point, and therefore a low likelihood of being stripped into the gas phase; and its reaction rate coefficient with ozone in water as a reaction was lowest recorded for the five pollutants studied, phenol, acrylonitrile, nitrobenzene, toluene and trichloroethylene (TCE). Figure 3.4.1 shows the partition coefficients of the five pollutants studied for the FC-water system (Shanbhag, 1992). This figure shows that nitrobenzene has a partition coefficient midway between the lowest value (phenol ~ 0.01) and the highest value (TCE and toluene, ~ 40) measured.

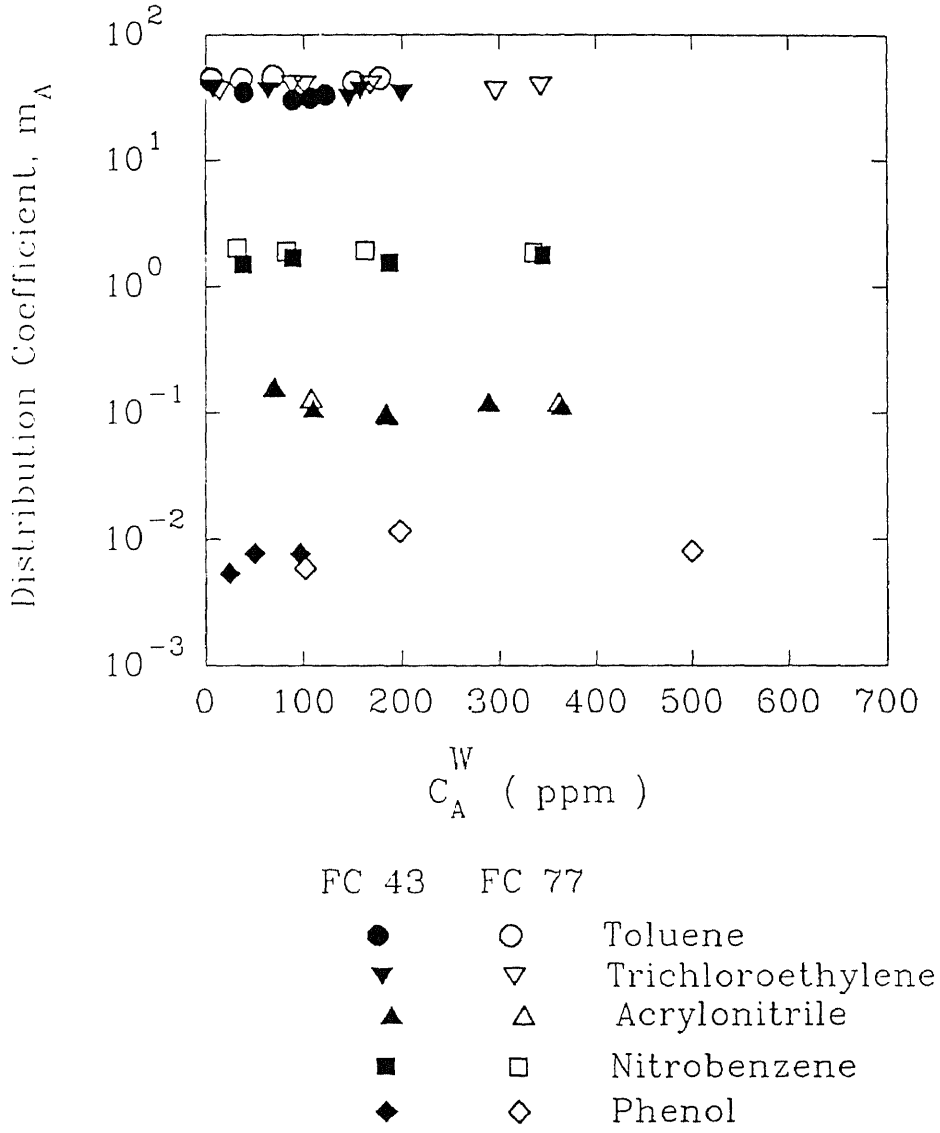

Figure 3.4.1. Distribution coefficients of the various pollutants between FC phase and water.

3.4.2 Measurement of the Membrane Thickness of the Two-Phase Membrane Ozonator

The thickness of the contained liquid membrane was calculated by measuring the amount of CO_2 permeating across an aqueous liquid membrane. The feed CO_2 gas was passed at a pressure of 5.5 psig (139.2 kPa) through the lumen of the Teflon tubules and the permeate CO_2 gas flow rate was collected at the outlet of the silicone capillaries at atmospheric pressure 0 psig (~ 101.325 kPa). Since the Teflon tubules have comparatively large pores, it was observed that if membrane thickness measurment experiment was run overnight, the permeation rate fell due to the progressive wetting of the pores by water. Therefore the permeation rate that was used to calculate the membrane thickness was a value based on an average collected over a period of the first 2 hours.

For a feed gas pressure of 5.5 psig (139.2 kPa) and shell side liquid pressure of 6 psig (142.7 kPa) a permeation rate, R_T, of CO_2 was recorded as 0.112 ml/min and this value was used to calculate the liquid membrane thickness as follows.

The permeation flux of CO_2 across the silicone capillaries can be written as follows:

$$J = \frac{R_T}{A_{sil}} = \frac{Q_{CO_2}^{sil}}{\delta_{sil}} (p_o^{sil} - p_i^{sil}) \qquad (3.4.1)$$

where p_o^{sil} and p_i^{sil} are the partial pressures of CO_2 at the outer and inner radii of the silicone capillaries; $Q_{CO_2}^{sil}$ is the permeability coefficient of CO_2 through the silicone capillary membranes, δ_{sil} is the wall thickness of the silicone capillaries and A_{sil} is the log mean permeation area defined by equation 2.4.1 and shown below:

$$A_{sil} = \pi \frac{(d_o^{sil} - d_i^{sil})}{\ln (d_o^{sil} / d_i^{sil})} N_{sil} L \qquad (3.4.2)$$

The permeation flux of CO_2 across the aqueous liquid membrane can be written as follows:

$$\frac{R_T}{A_{lm}} = k_m (C_o^{Tef} - C_o^{sil}) = k_m H (p_o^{Tef} - p_o^{sil}) \qquad (3.4.3)$$

where H is the Henry's Law constant for CO_2 between water and the gas phase. k_m is the mass transfer coefficient of CO_2 through water and is given by $D_{CO_2}^{Water} / \delta_{lm}$ where δ_{lm} is the contained liquid membrane thickness being calculated. A_{lm} is log mean transfer area and is calculated as follows (Yang et al., 1995):

$$A_{lm} = \pi L \frac{(d_o^{Tef} N_{Tef} - d_o^{sil} N_{sil})}{\ln (d_o^{Tef} N_{Tef} / d_o^{sil} N_{sil})} \qquad (3.4.4)$$

At steady state, the amount of CO_2 permeating per unit time across each of the regions is constant and equal to R_T. Assuming that the Teflon pores are not wetted out by the aqueous phase and $p_o^{Tef} = p_i^{Tef}$, equations 3.4.1 and 3.4.3 can be rearranged and rewritten as follows :

$$R_T \left\{ \frac{1}{\left[\frac{Q_{CO_2}^{sil} A_{sil}}{\delta_{sil}} \right]} + \frac{1}{\left[\frac{D_{CO_2}^{Water} A_{lm} H}{\delta_{lm}} \right]} \right\} = p_i^{Tef} - p_i^{sil} \qquad (3.4.5)$$

From Equations 3.4.2 and 3.4.4, A_{sil} and A_{lm} are calculated to be 1.4115 e-2 m^2 and 1.37 e-2 m^2. $Q_{CO_2}^{sil}$ is found to be 1.012 e-12 (kgmol.m)/(s.m^2.kPa) (La Pack et al., 1994). $D_{CO_2}^{Water}$ (@ 25 °C) is found to be 1.92 e-9 m^2/s and H (@ 25°C) for CO_2 is calculated as 365.76 e-6 (kgmol)/(m^3 kPa) (Majumdar et al., 1988). Based upon these values, δ_{lm} is calculated to be 4800 e-6 m or 4800 μm. This value of δ_{lm} was used in the simulation of the two-phase membrane ozonator outlined in Section 3.3.

3.4.3. Degradation of Organic Pollutants in the Two-Phase Membrane Ozonator

The degradation of the organic pollutants in the two-phase membrane ozonator modules SILTEF #1 and #2 is described in this section. The experiments were carried out with each of the five pollutants listed above taken in turn. The fluorocarbon used in all of these studies was FC43 whose physical properties are listed in Table 3.2.3. The solubility of ozone in FC43 was found to be 78 mg/l at the prevailing ozone concentration in the gas phase of ~60 mg/l at a temperature of ~28°C (Trivedi, 1992). This value gave a Henry's Law Coefficient for ozone in FC43 of 1.905 e3 (kPa)/((kgmol)/(m^3 of FC43)). The solubility of ozone in other inert organic compounds like CCl_4 was found to be 1.96 (gmol/l(L))/(gmol/l(G)) at a temperature of 25°C (Aleksandrov et al., 1983). This gave a Henry's Law constant for ozone in CCl_4 as 1.264 e3 (kPa)/((kgmol)/(m^3 of CCl_4)). This translated to a liquid concentration of 117.6 mg/l ((@ 25 °C) at the same gas concentration of 60 mg/l. In Freon 11 ($CFCl_3$), the solubility of ozone was found to be 3.65 (gmol/l(L))/(gmol/l(G)) at a temperature of 20 °C (Aleksandrov et al., 1983). This

gave a Henry's Law constant for ozone in Freon 11 as 0.667 e3 (kPa)/((kgmol)/(m^3 of Freon 11)). This translated to a liquid concentration of 219 mg/l (@ 20 °C) in Freon 11 for a gas concentration of 60 mg/l.

Table 3.4.1. Parameters used in simulation of pollutant degradation in SILTEF membrane reactor

Pollutant	m_A	k_{11}^{F} † (s^{-1})	k_2^{F} † (m^3/(kgmol s))	(b/a)*	D_A^{W} ++ x 10^9 (m^2/sec)	D_A^{F} ++ x 10^9 (m^2/sec)
Ozone	-	-	-	-	2.01	1.37
Phenol	0.01	1.0-1.2	40.0	2.0	0.9135	0.756
Acrylonitrile	0.12	0.1-0.35	40.0	0.5	1.1621	0.798
Nitrobenzene	1.9	0.003-0.01	3.5	3.0	0.8346	0.556
TCE	40	-	-	-	0.9784	0.705
Toluene	45	-	-	-	0.8618	0.617

† Sirkar et al. (1994).
* Stoichiometric ratio (moles of ozone/mole of pollutant), Sirkar et al.(1994).
++ Diffusivities of solutes in aqueous and FC-phase calculated from the Wilke-Chang correlation (Perry and Green (1984)).

Table 3.4.1 provides a list of the compounds used in the study and some of their physical parameters used to run the simulation of the two-phase membrane reactor. The values of the diffusivities in water and FC43 were calculated from the Wilke-Chang correlation (Perry and Green, 1984). The values of k_{11}^{F} and k_2^{F} were determined from batch and semibatch experiments, where ozone and pollutant were brought together in the two phase FC-water system. The reaction was assumed to occur in the FC phase

(Shanbhag, 1992; Sirkar et al., 1994). Second order kinetics for a reaction of the type shown in Equation 3.3.2 were used to fit the experimentally obtained C_A vs t data to determine k_2^F (Sirkar et al., 1994). For compounds with a very low partition coefficient into the FC phase like phenol, the data were fit to pseudo first order kinetics to determine k_{11}^F. It was assumed that for these compounds the FC phase concentration of ozone was very large compared to that of the compound (e.g. phenol) and essentially constant for the first hundred seconds of the batch experiment (Shanbhag, 1992). This yielded a pseudo first order reaction rate constant of 1 s^{-1}. Stich and Bhattacharyya (1987) saw a 100% removal of 100 ppm feed of phenol in 2 mins but their observations of observations of phenol consisted of two data points, at time t = 0 and t = 2 mins. They reported a pseudo first order reaction rate constant of 0.05 min^{-1} (8.33 e-4 s^{-1}) by observing the Total Organic Carbon (TOC) removal. Ozone is indiscriminate in its attack of organic compounds and would attack both the parent and product compounds and the TOC removal would be a measure of the ozone's reaction with the most recalcitrant of the product compounds giving a low value for the reaction rate constant.

Table 3.4.2. Second order ozonation rate constants obtained from literature

Compounds	k_2^E (m^3/(kgmol s))	(b/a)	Remark	Reference
Acrylonitrile	40 @ 262K 155 @ 300K	1	Rxn in CCl_4	Pryor et al., 1983
Acrylonitrile	60 @ 296K	-	Rxn in Gas Phase	Atkinson et al., 1982
Acrylonitrile	83 @ 298K	-	Rxn in Gas Phase	Munshi et al., 1989
Nitrobenzene	4.2 @ 296K	-	Rxn in Gas Phase	Atkinson et al., 1987
Toluene	0.166 @ 298K	3	Rxn in CCl_4	Nakagawa et al., 1960
Toluene	0.0903 @ 297K	-	Rxn in Gas Phase	Pate et al., 1976
TCE	3.6 @ 298K	1	Rxn in CCl_4	Williamson and Cvetanovic, 1968
TCE	2.06 @ 298K	1	Rxn in CCl_4	Pryor et al., 1983
TCE	30.115 @ 298K	-	Rxn in Gas Phase	Atkinson et al., 1989

The reaction rate constant of 1 s^{-1} used in a pseudo first order model of the polypropylene hollow fiber based two-phase membrane ozonator was found to reproduce the experimental data fairly well for phenol (Trivedi, 1992) and this value was used to simulate the SILTEF reactor. There is a dearth of kinetic parameters in literature for the ozonation of organic compounds in inert non-aqueous media. For pollutants other than phenol, which required the use of a second order reaction rate model, kinetic parameters available in literature are tabulated above in Table 3.4.2. For acrylonitrile, the experimentally obtained reaction rate coefficient shown in Table 3.4.1 is seen to be corroborated by the values shown in Table 3.4.2 for ozonation reactions in CCl_4. Furthermore it is seen for acrylonitrile, that an ozonation reaction carried out in the gas phase had an observed reaction rate constant of comparable magnitude to that for the

ozonation in CCl_4. For nitrobenzene, a k_2^E in CCl_4 was not available in literature, but the value observed for ozonation of nitrobenzene in a gas phase was of a comparable magnitude to the value observed during two phase FC-water ozonation as seen in Table 3.4.1 and 3.4.2. It is also seen from Table 3.4.2, that for reactions carried out in a gas phase and in CCl_4 between ozone and toluene, the estimates of the second order reaction rate coefficients are of comparable magnitudes. The ozonation of TCE seems to be an exception to this observation.

The simulation of the degradation of organic pollutants in the two-phase membrane ozonator requires the knowledge of the physical properties of the tubular membranes in addition to the kinetics and the solubility data listed above. The physical dimensions of both the silicone capillaries and Teflon tubules are listed in Table 3.2.1. The permeability of ozone through the silicone capillaries was taken to be 8 e-13 (kgmol.m)/(m^2.s.kPa) (Section 2.4.3). The porosity of the Teflon tubules was taken to be 0.5 (Green, 1994). The values of tortuosity that have been cited in literature for microporous membranes, range from 2.4 for the X-20 polypropylene hollow fiber membrane (Prasad and Sirkar, 1992) to 1.7 for a Gore-Tex flat membrane (Matson and Quinn, 1992). Since the present tubular, microporous, Teflon membranes have rather large pores, ~ 16 μm (Green, 1994), therefore a tortuosity value of 1.5 was used to simulate the two-phase membrane ozonator. Also a conservative ozone concentration in the gas phase of 60 mg/l was chosen as a basis for the simulation of the degradation of organic pollutants in the aqueous phase. This gave a lower operating limit for the device. The simulated conversions of the pollutant would be higher at higher ozone concentrations in the gas phase.

a) Phenol as a model pollutant

Figure 3.4.2 shows the performance of the two-phase membrane reactor for phenol as a model pollutant at a feed concentration of ~150 ppm. These results were obtained from the reactor at steady state, i.e. the reactor was run for a period of about 2~3 hours (4~6 hours for the lowest aqueous flow rates) at particular aqueous and gas flow rates until the aqueous pollutant concentration sampled at the exit of the reactor was constant. Pollutant conversion in such a reactor was calculated as shown below:

$$\text{Conversion } X_A = \frac{C_A^{in} - C_A^{out}}{C_A^{in}} \qquad (3.4.6)$$

A conversion of 0.6 was observed for an aqueous flow rate of ~0.1 ml/min and this was reduced to 0.1 when the aqueous flow rate was increased to 1.2 ml/min. A liquid element would have a residence time within the reactor of about 10 min at a flow rate of 0.1 ml/min and 0.8 min at a flow rate of 1.2 ml/min. The pseudo first order model of the two-phase membrane ozonator was found to reproduce the experimental data fairly well for phenol for a $k_{11}^F = 1\ s^{-1}$. At low aqueous flow rates however, the assumption of constant wall composition or constant wall flux, that is demanded by the Graetz solution (Prasad and Sirkar, 1992) is probably not obeyed and the model slightly underpredicts the experimental data (see Appendix 6 for pollutant and ozone concentration profiles across the FC phase).

The generation of hydroxyl radicals by the dissolution of ozone in water at the aqueous-FC interface is a well-documented phenomenon (Glaze and Kang, 1989). Since the reaction occurs close to the aqueous-FC interface, it is likely that hydroxyl radicals are generated by the presence of ozone at the interface. These probably also react with

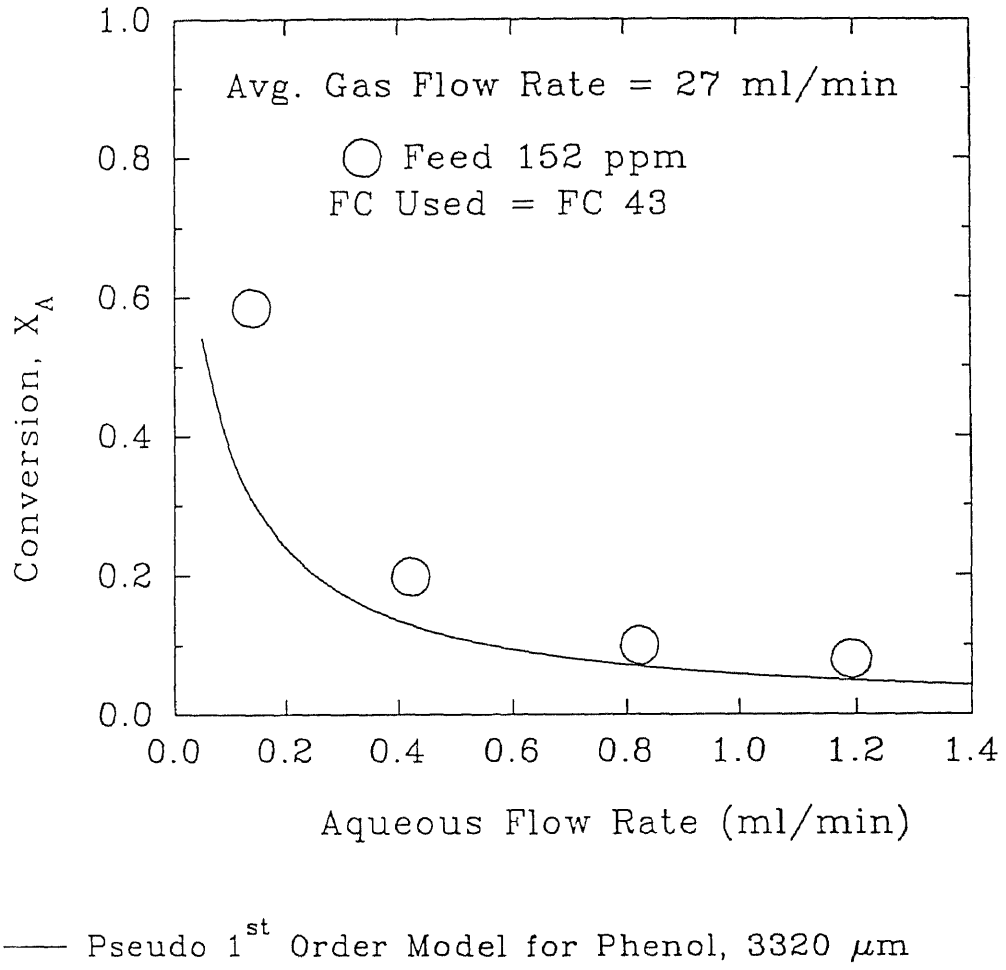

Figure 3.4.2. Degradation of phenol in the two-phase membrane ozonator (SILTEF #1).

phenol leading to the experimentally observed conversions higher than those predicted. The O_3/O_2 gas flow rate through the silicone capillaries was maintained at 30 ml/min and since this model assumed that the FC phase had a much larger and practically constant ozone concentration, therefore any change in the O_3/O_2 gas flow rate would not affect the reactor performance for phenol as a pollutant.

b) Acrylonitrile as a model pollutant

Figure 3.4.3 shows the performance of the reactor for acrylonitrile as a model pollutant in the two-phase membrane reactor. An average feed concentration of 158 ppm was used to simulate the degradation of acrylonitrile in the two-phase membrane ozonator. An average gas flow rate used in the study was ~27.5 ml/min. It is seen that at an aqueous flow rate of 0.1 ml/min, a conversion as defined in Equation 3.4.6 of about 0.85 was observed. When the flow rate was increased to 0.55 ml/min, the conversion fell to 0.2. The solid and dotted lines in the figure show the performance of the second order kinetic model in predicting the degradation of acrylonitrile in the two phase membrane ozonator. The dotted line indicates the model performance for a rate constant of ~90 $m^3/(kgmol\ s)$ while the solid line shows the simulation for ~40 $m^3/(kgmol\ s)$ for a "b/a" ratio of 0.5 as indicated in Table 3.4.1. It is seen that though the reaction rate coefficient was increased by a factor of 2.5, there was very little change in the model performance indicating the system seems to be limited by diffusional transfer limitations within the FC phase rather than being limited by the reaction rate. Hydroxyl radicals generated by the presence of ozone at the aqueous-FC interface also react with acrylonitrile leading to the difference in the observed and model-predicted removal of acrylonitrile as seen in Figure 3.4.3.

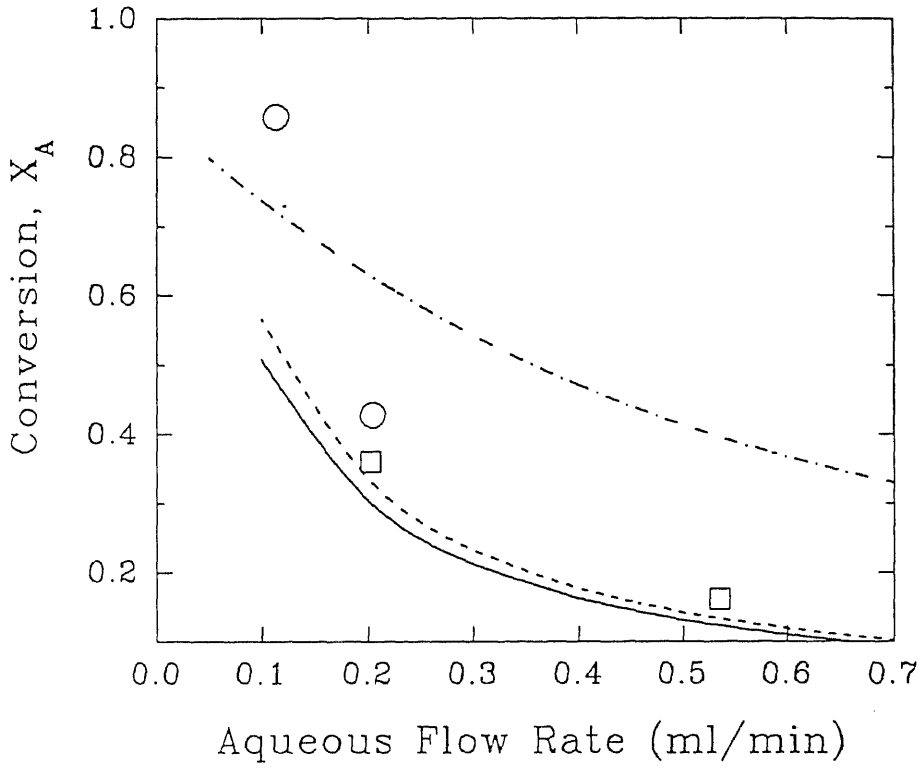

○ C_{A0}^{W} = 160 ppm, Avg. Gas Flow = 28 ml/min

□ C_{A0}^{W} = 156 ppm, Avg. Gas Flow = 27 ml/min

Simulated Feed Conc. = 158 ppm

----- Pseudo 1st Order Model, k_{11}^{F} = 0.26 s^{-1}

—— 2nd Order Model, k_2^{F} = 38.2 $m^3/(kgmol\ s)$

----- 2nd Order Model k_2^{F} = 90 $m^3/(kgmol\ s)$

Figure 3.4.3. Degradation of acrylonitrile in the two-phase membrane ozonator (SILTEF #1).

Acrylonitrile is a compound with an m_A of ~0.1 (Table 3.4.1). At low aqueous flow rates (aqueous residence times > 10 mins), diffusional resistance in the aqueous phase begins to also affect the reactor performance. It is probably likely that the simple Graetz solution used in the aqueous phase mass transfer model cannot properly predict the mass transfer coefficients at low aqueous flow rates (low N_{RE}), leading to the large disparity between the predicted and experimentally observed acrylonitrile conversions. The contact between the aqueous phase and the FC phase occurs at the ID of the two-phase membrane ozonator and this area of contact is equal to 3.9 e-3 m^2. At low aqueous flow rates of 0.1 ml/min for a 160 ppm acrylonitrile feed, the amount of acrylonitrile that is brought into contact with the FC phase is 1.3 e-9 kgmol/m^2.s, while at an aqueous flow rate of 0.55 ml/min, the amount of acrylonitrile brought into conatct with the FC phase is 7.2 e-9 kgmol/m^2.s, i.e. 6 times as much acrylonitrile is brought into contact with the FC phase at higher aqueous flow rates than at lower aqueous flow rates. Therefore it is quite likely that at low aqueous flow rates a pseudo first order model would better predict the removal of acrylonitrile from wastewater. The pseudo first order model for acrylonitrile for a k_{11}^F = 0.26 s^{-1} (Table 3.4.1) (shown by the dash-dot line) shows an improvement in the prediction of the conversion of acrylonitrile in the two-phase membrane ozonator (see Appendix 6 for pollutant and ozone concentration profiles across the FC phase).

At higher aqueous flow rates, acrylonitrile has a lower residence time within the reactor, hence less of an opportunity to come into contact with either ozone or hydroxyl radicals, leading to the lower observed and predicted pollutant conversions.

c) Nitrobenzene as a model pollutant

i) Low feed concentrations

Figure 3.4.4 shows the performance of the two-phase membrane ozonator in treating nitrobenzene as a model pollutant. Nitrobenzene has a partition coefficient into the FC phase of $1 \sim 2$, i.e. an order of magnitude greater than acrylonitrile. The first observation that can be made from the data is that the removal of nitrobenzene is fairly independent for the concentration range studied. It is clear that the model does a better job in predicting the removal of nitrobenzene than the removal of acrylonitrile. This could be attributed to the fact that since nitrobenzene has a much higher partition coefficient into the FC phase, less ozone would be available at the FC-water interface since it would be consumed within the FC phase by direct reaction with nitrobenzene. However at low aqueous flow rates, < 0.1 ml/min, the model slightly underpredicts the removal of nitrobenzene. It would be reasonable to assume a similar phenomenon occuring at the aqueous-FC interface as that for acrylonitrile, though to a lesser extent on account of the higher partition coefficient that nitrobenzene has into the FC phase. Though it is not discernible from Figure 3.4.4, since the two lines of simulation overlap one another, the model does not exhibit any change in performance even if the O_3/O_2 gas flow rate is raised from 30 ml/min to 100 ml/min. Also raising the gas concentration of ozone from 50 mg/l to 60 mg/l had very little discernible change in the pollutant conversion. The model does however reflect changes in the Henry's Law Constant. A Henry's Law Constant equal to 1.818 e4 kPa/(kgmol/m^3) (which was calculated from solubility data for ozone in FC-77, a fluorocarbon with a lower molecular weight (Stich

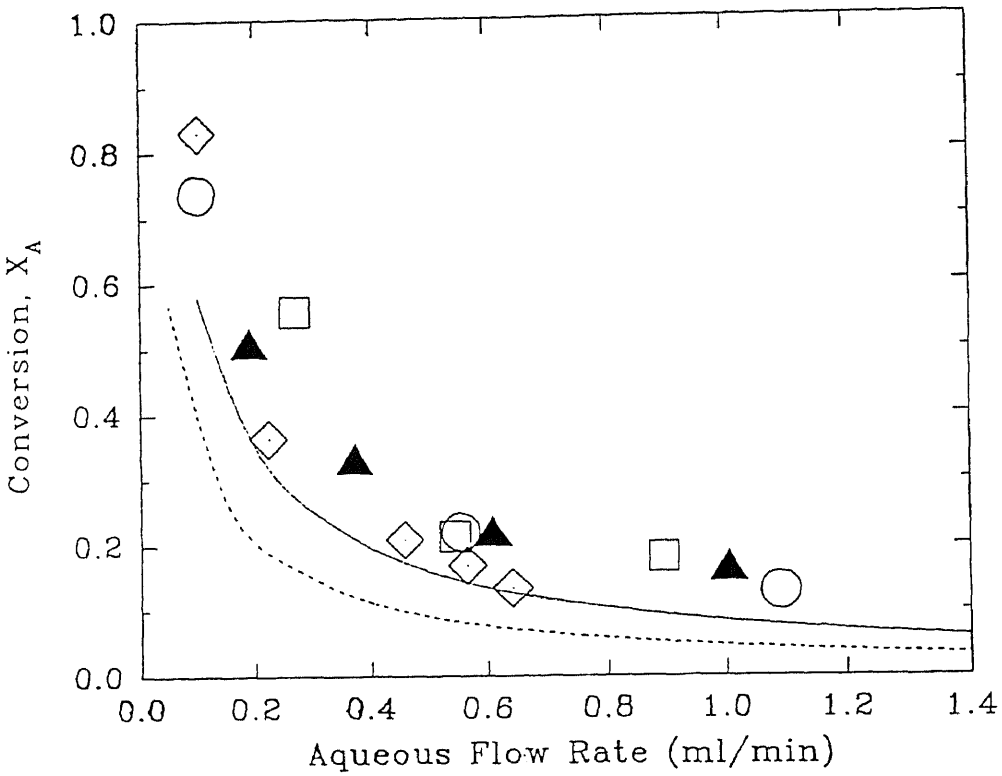

□ Feed Conc. = 165 ppm ◇ Feed Conc. = 105 ppm

▲ Feed Conc. = 107 ppm ○ Feed Conc. = 117 ppm

····· 2^{nd} Order Simul., k_2 = 3.5 m^3/(kgmol s), b/a = 3, Feed ≈ 120 ppm
H_B = 1.818 e4 kPa/(kgmole/m^3)

—— 2^{nd} Order Simul., k_2 = 3.5 m^3/(kgmol s), b/a = 3, Feed ≈ 120 ppm
H_B = 2000 kPa/(kgmole/m^3), V_G = 30 ml/min

- - - 2^{nd} Order Simul., k_2 = 3.5 m^3/(kgmol s), b/a = 3, Feed ≈ 120 ppm
H_B = 2000 kPa/(kgmole/m^3), V_G = 100 ml/min

Figure 3.4.4. Degradation of nitrobenzene in the two-phase membrane ozonator: low concentration runs (SILTEF #1-2).

and Bhattacharyya, 1987)) which meant a lower concentration of ozone in the FC phase resulted in much lower predicted conversions as shown by the dashed line in Figure 3.4.4 (see appendix 6 for ozone and pollutant concentration profiles across the FC phase).

As the aqueous flow rate is increased to ~1 ml/min, the residence time of a liquid element drops to about 1 min and the conversion observed in the two-phase membrane ozonator falls to 0.1 reflecting the lack of surface area available in the module. Trivedi (1992) observed conversions of 0.4 for a polypropylene module for the same aqueous flow rate and a feed concentration of ~ 100 ppm. The polypropylene module had a specific surface area of 20 cm^2/cm^3 module volume as opposed to 5 cm^2/cm^3 module volume for the SILTEF device and allowed much better contacting efficiency.

ii) High feed concentrations

Figure 3.4.5 shows the performance of the reactor for two different feed concentrations of nitrobenzene: ~978 ppm (□) and ~1400 ppm (○). At these concentrations, a conversion of 0.5 is observed at a flow rate of 0.1 ml/min; at a flow rate of around 1 ml/min, this conversion falls to 0.05 due to a lack of surface area available in the reactor. The simulation of conversion for high concentrations of nitrobenzene feed is shown by the lines in Figure 3.4.5. It is seen that the simulations appear to describe the performance of the reactor well over the range of the aqueous flow rate studied. From the two lines it is clear that when the ozone flow rate is increased from 30 ml/min to 100 ml/min, the simulations show a discernible improvement in the reactor performance. Also there were no discernible changes in model prediction for variations in nitrobenzene feed compositions, indicated by the overlap of the lines in Figure 3.4.5 (see appendix 6 for pollutant and ozone concentration profiles across the FC phase).

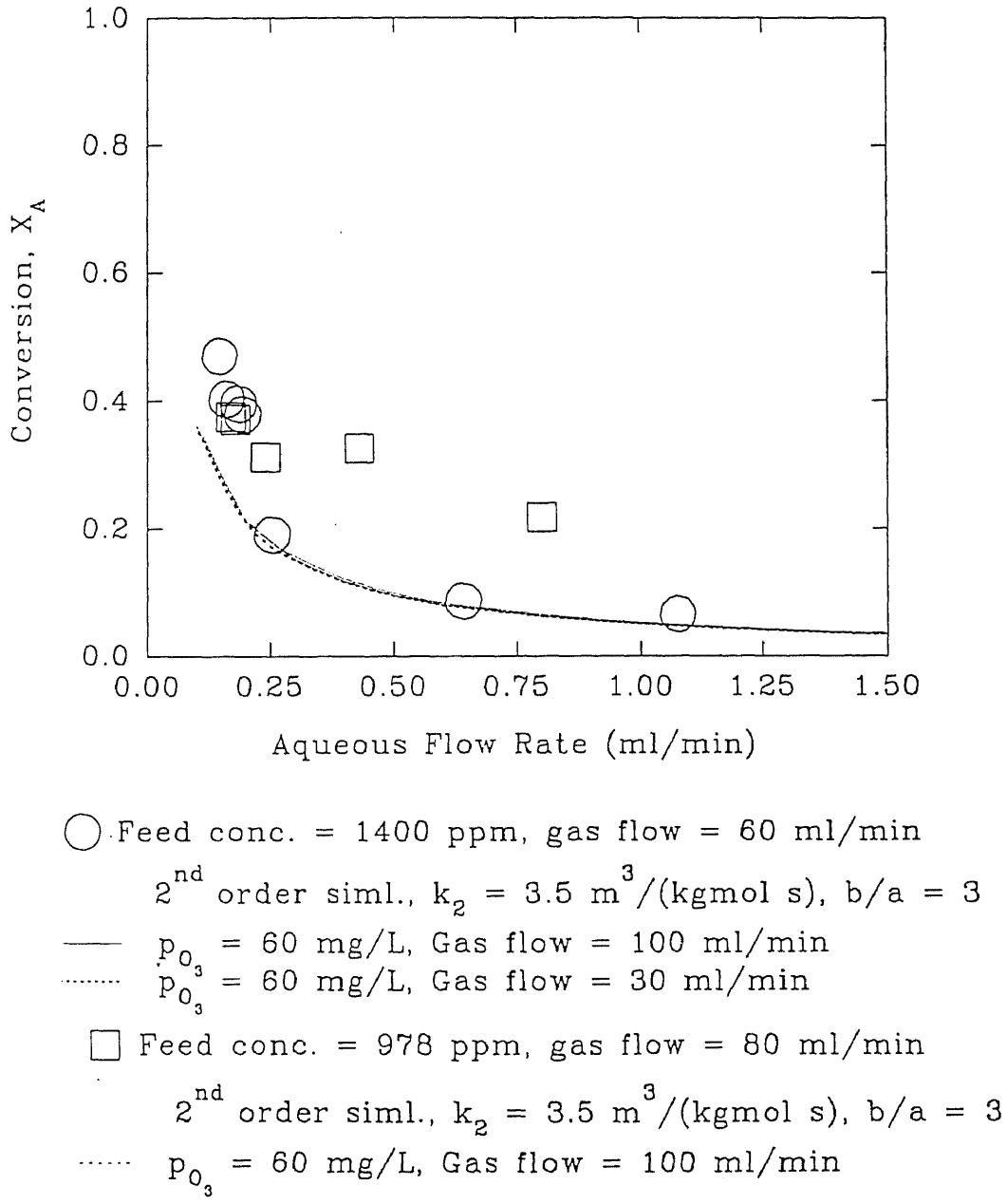

Figure 3.4.5. Degradation of nitrobenzene in the two-phase membrane ozonator: high concentration runs (SILTEF #1-2).

d) Toluene as a model pollutant

Figure 3.4.6 shows the performance of the two-phase membrane reactor, for toluene as a model pollutant. It is seen that even at high aqueous flow rates of 1.2 ml/min, the experimentally observed conversion is 0.5 for an aqueous feed concentration of 121 ppm. The conversion rose to 0.9 when the aqueous flow rate was reduced to 0.1 ml/min. The results obtained in Figure 3.4.6 are steady state values, that were recorded after running the reactor continuously for a period of 3-5 hours, the longer period of time for the lowest aqueous flow rate. Toluene has a much larger partition coefficient, m_A, into the fluorocarbon phase as shown in Figure 3.4.1. At the aqueous-organic interface, toluene is extracted by simple partitioning into the organic medium, where it is destroyed by ozone. The partitioning effect is particularly evident at aqueous flow rates >1 ml/min while comparing the removal of toluene with that of acrylonitrile. Acrylonitrile has a m_A of about 0.1 and the experimentally observed conversion is only about 0.1 at a flow rate of ~ 0.55 ml/min, when compared to the conversion observed for toluene, 0.7, for a similar flow rate, despite the fact that acrylonitrile has a higher reaction rate coefficient as seen in Table 3.4.3. The higher m_A however resulted in causing the second order simulation for toluene to diverge and the results of mathematical simulations for removal of toluene are not presented here.

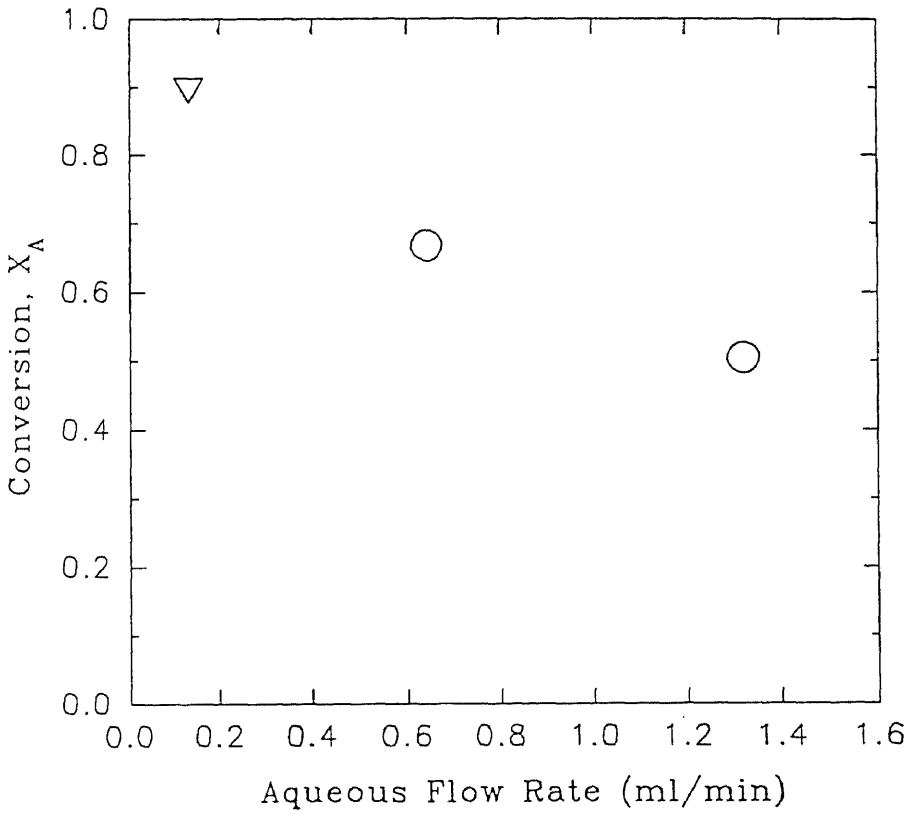

Figure 3.4.6. Degradation of toluene in the two-phase membrane ozonator (SILTEF #1).

e) Trichloroethylene (TCE) as a model pollutant

Figure 3.4.7 shows the reactor performance for trichloroethylene (TCE) as a model pollutant. Conversions between 0.6 for an aqueous flow rate of 0.5 ml/min and 0.4 for an aqueous flow rate of 2.3 ml/min are observed for feed compositions of 65 ~ 80 ppm. It is also seen that the reactor conversion over the concentration range studied is fairly independent of the feed composition. Also trichloroethylene has a high m_A into the FC phase and this results in high removal of TCE even at aqueous flowrates >2.0 ml/min.

Past studies involving the removal of TCE from wastewater involve feed concentrations of 500 μg/l (500ppb) (Glaze and Kang, 1988). They demonstrated in semibatch expermiments that ~70% of the TCE can be removed in 25 minutes. This device shows that it can achieve ~60% conversion for a 80 mg/l (80 ppm) feed with a 2 minute residence time (0.5 ml/min aqueous phase flow rate). Since this device concentrates the organic compound in the FC phase prior to ozonation, it is versatile enough to handle a broader range of feed concentrations than conventional ozonation.

The removal of organic pollutants using the two-phase membrane ozonator can be classified into two types based upon the m_A of the pollutant into the FC phase. If one assumes that each pollutant has the same reaction rate coefficient in the FC phase and that the resistance to mass transfer of ozone is identical in both cases, then the results and further developement of the two-phase membrane reactor can be explained using the basis that has been developed for and applied to membrane solvent extraction (Prasad and Sirkar, 1992). In a manner akin to membrane solvent extraction, there exist three

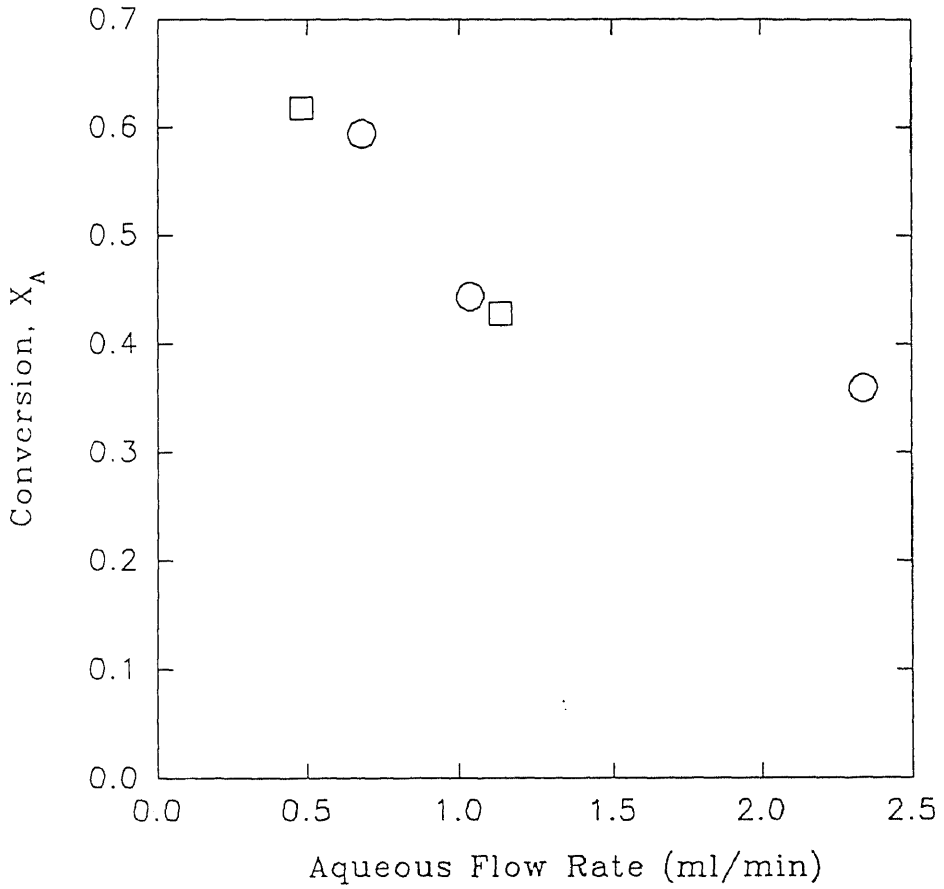

Figure 3.4.7. Degradation of trichloroethylene (TCE) in the two-phase membrane ozonator (SILTEF #1).

resistances to the mass transfer of the pollutant in the two-phase membrane ozonator: 1) the aqueous phase boundary layer, 2) the membrane wetted out by the FC-phase and 3) the FC phase. For compounds with a low m_A, like phenol and acrylonitrile, the resistance to mass transfer is dominated by the membrane resistance and the FC phase resistance. Therefore the removal of phenol and acrylonitrile can be maximized, by a) increasing aqueous-organic interfacial area or b) by raising the residence time of the aqueous phase in the lumen of the Teflon tubules. For compounds with a high m_A like toluene and TCE, the bulk of resistance exists in the aqueous phase boundary layer and the removal of these compounds can be maximized by a) increasing the Reynolds No., i.e. increasing the volumetric flow rate or b) introducing some surface roughening on the inside surface of the membrane to break up the aqueous phase boundary layer and reduce the mass transfer resistance (see Appendix 6 for further discussion).

f) Effect of O_3/O_2 flow rate on the removal of the pollutant

Figure 3.4.8 shows the effect of a variation in O_3/O_2 flow rate on the conversion of phenol and toluene in the two-phase membrane reactor at a constant aqueous flow rate. Phenol has an extremely low partition coefficient into the FC phase and the FC is nearly completely saturated with O_3, and the system is practically pseudo first order with respect to the removal of ozone. This is reflected by the lack of any change in observed phenol conversion despite increasing the ozone flow rate by a factor of 4. Toluene also shows a similar behavior, where the observed conversion remains unaltered inspite of raising the gas flow rate from 20 ml/min to 40 ml/min. Over the aqueous and gas flow range

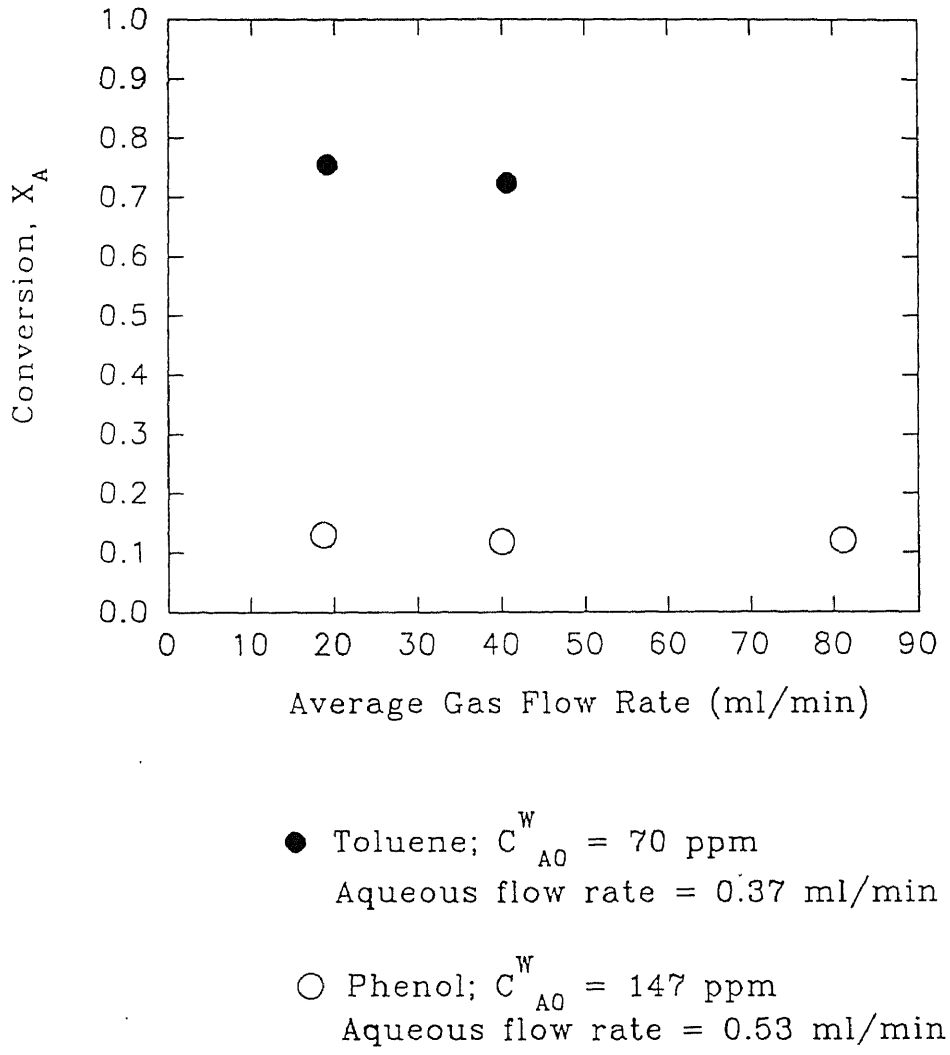

Figure 3.4.8. Effect of variation of gas flow rate on the degradation of organic pollutants in the two-phase membrane ozonator (SILTEF #1).

studied, it is observed that there is no stripping of toluene into the gas phase, since there is no increase in toluene conversion with the concomitant increase in gas flow rate.

g) Experimentally observed ozone utilization

The experimentally observed ozone utilization is calculated by the ratio of the number of moles of ozone consumed per mole of pollutant destroyed. This quantity allows comparison and some insight into the efficiency of the process when compared with single-phase membrane ozonation. In the FC-membrane, ozone is consumed not only by the particular pollutant, but also by the products of the reaction. Studies were carried out using nitrobenzene as a model pollutant since it has an intermediate value of m_A and a low vapor pressure. Therefore at steady state the disappearance of nitrobenzene from the aqueous phase can only be attributed due to its reaction with ozone. For the reaction between ozone and nitrobenzene ($C_6H_5NO_2$), anywhere from 5 moles of ozone to 15 moles of ozone can be used to completely convert the above compound to CO_2, H_2O and HNO_3. 5 moles of ozone would be required, if it were assumed that the ozone molecule was incorporated into the oxidized products. It however seems more likely during the oxidation by ozone, that the ozone molecule would donate an O atom to the organic molecule with the elimination of an O_2 molecule which would require 15 moles of O_3 (Bailey, 1982). Table 3.4.3. shows the results for utilization of ozone for the two-phase membrane ozonator with nitrobenzene as a model pollutant for low aqueous feed concentrations.

Table 3.4.3. Experimental results of ozone utilization : low aqueous feed composition

Aq. Flow Rate (ml/min)	NB. Aq. Conc. (ppm)		NB Cons.[§] (gmol /sec)	O_3 Flow (ml/ min)	Ozo. Gas Conc.* (mg/L)		Ozone Dosed (gmol/ sec)	Ozone Util. (mol O_3/ mol pol)
	Feed	Exit			Feed	Exit		
0.44	68	55	0.82 e-9	122	56.05	53.18	121.9 e-9	149.1
0.18	93	54	0.93 e-9	77	62.57	60.09	66.5 e-9	71.3
0.20	93	60	0.89 e-9	35	77.24	71.21	46.8 e-9	81.9
0.42	94	65	1.61 e-9	60	30.77	18.44	255 e-9	158.2
0.89	93	82	1.29 e-9	29	71.23	66.63	72.5 e-9	36.4
0.10	107	18	1.23 e-9	72	55.49	51.64	96.4 e-9	78.2
0.22	107	68	1.17 e-9	62	55.18	54.48	15.0 e-9	12.8
0.26	103	69	1.21 e-9	134	43.29	42.89	17.6 e-9	14.6
0.45	107	85	1.38 e-9	62	55.18	50.78	94.2 e-9	68.3
0.57	103	85	1.33 e-9	74	54.54	52.65	48.6 e-9	36.7
0.64	103	89	1.19 e-9	74	54.54	53.47	27.1 e-9	22.8

[§] Nitrobenzene Consumption Rate. * Makeup O_2 flowrate 349 ml/min.

Figure 3.4.9 summarizes the above table in the form of a figure plotting the aqueous feed composition versus the experimentally observed ozone utilization with the symbol shown as ◯. The elucidation of the utilization of ozone is done by considering the cross-section of the two-phase membrane ozonator as shown in Figure 3.4.10 (similar to Figure 3.3.1). Nitrobenzene has a m_A (partition coefficient) of about 2.0 (Figure 3.4.1). When low concentrations of nitrobenzene ~100 ppm are fed to the reactor, the

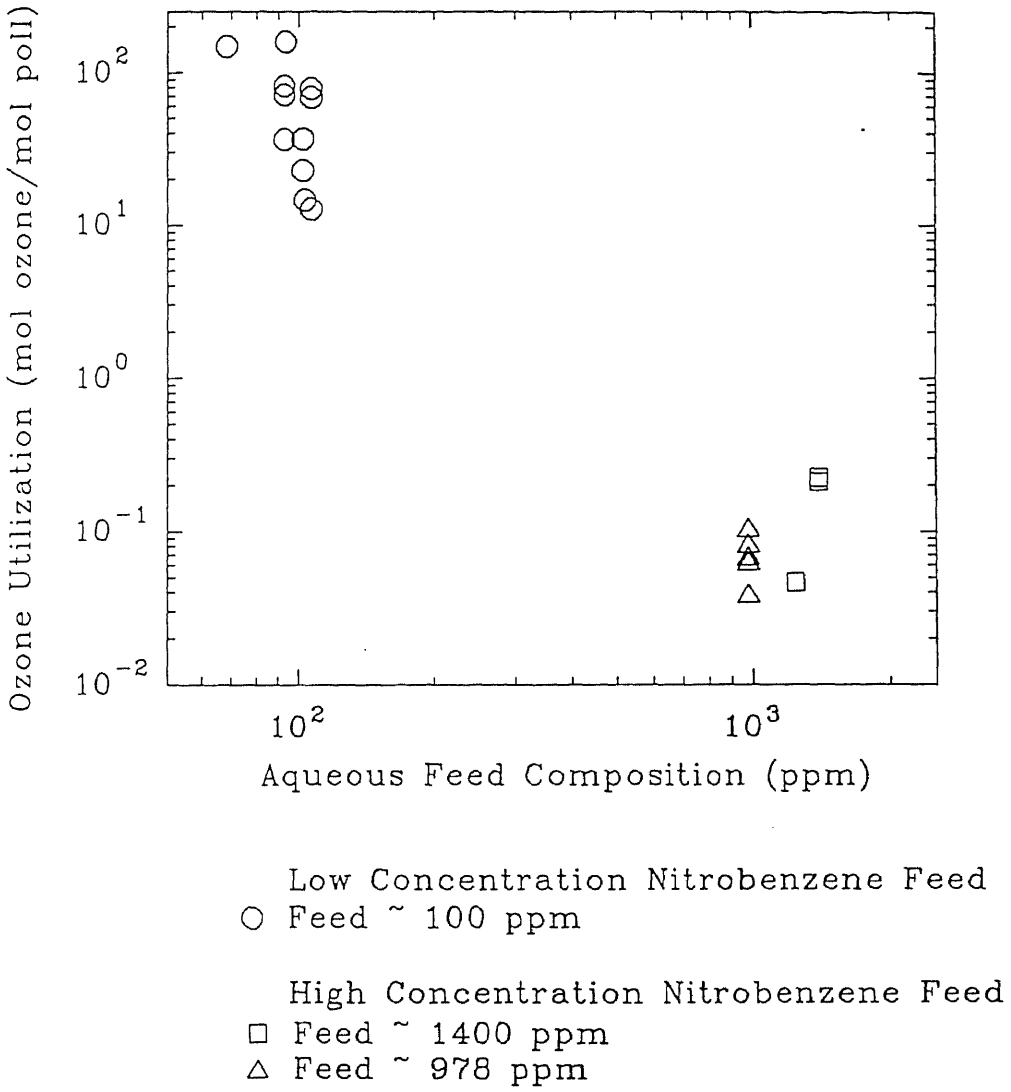

Figure 3.4.9. Experimentally observed utilization of ozone in the two-phase membrane ozonator for nitrobenzene as a pollutant.

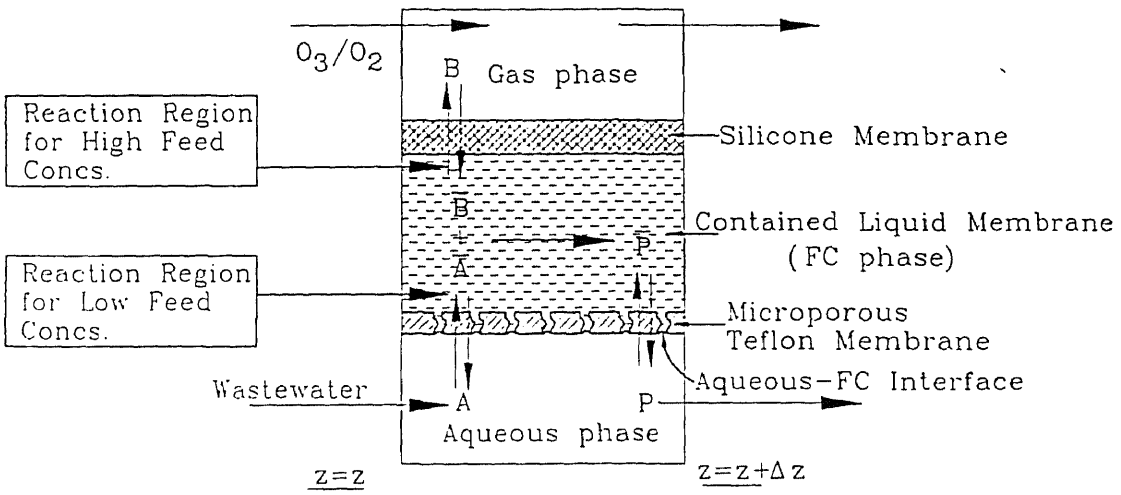

Figure 3.4.10. Schematic of the cross-section of the two-phase membrane ozonator showing the probable regions of reaction for varying feed concentrations of nitrobenzene as a model pollutant.

corresponding concentration in the fluorocarbon phase is ~200 ppm (3.054 e-3 kgmol/m^3), while the corresponding concentration of ozone is about 78 mg/l for 60 mg/l gas feed concentration (1.625 e-3 kgmol/m^3). The likelihood that the ozonation reaction occurs close to the aqueous organic interface is high, since ozone has a diffusion coefficient in the FC phase twice that of nitrobenzene (Table 3.4.1). The proximity of the aqueous phase, allows the formation of acidic reaction products, which partition easily into the aqueous phase. The experimentally observed values of ozone utilization numbers seen are of the order of 15 and higher. The byproducts of simple aqueous ozonation of nitrobenzene are nitric acid, carbon dioxide, formic acid, glyoxal, glyoxalic acid and oxalic acid (Caprio et al., 1984). The acids produced are relatively recalcitrant towards ozonation, though the destruction of oxalic acid has been observed in the two-phase ozonation process, albeit slowly (Freshour et al., 1996). Bhattacharyya et al. (1995) studied batch two-phase ozonation system for the destruction of 2, 4, 6 trichlorophenol (TCP) and pentachlorophenol (PCP). They studied the "feed ozone dosage", M, which was given by the number of moles of ozone fed into the two-phase system per mole of pollutant destroyed. They observed nearly 100 % conversion of TCP for M = 12, with 90% of the chlorine appearing as "free chloride" after 25 mins of contact time. The rapid conversion of TCP and PCP observed by Bhattacharyya and co-workers (Bhattacharyya et al., 1995) is due to the pseudo first order ozonation rates of ~6.5 min^{-1} at neutral to acidic pH; nitrobenzene has a pseudo first order reaction rate coefficient, k_{11}^F in the two-phase system of ~0.18-0.6 min^{-1} (Shanbhag, 1992).

In the case of the two-phase membrane ozonator as seen from Figure 3.4.10, ozone has to diffuse across the silicone membrane, through the fluorocarbon liquid membrane to react with nitrobenzene close to the aqueous-FC interface. Along this diffusion path, ozone can a) react with the silicone capillaries, b) react with nitrobenzene, c) react with the more hydrophobic products of reaction in the FC phase and d) also be scavenged by hydroxyl radicals at the aqueous-FC interface. Silicone capillaries do get attacked by ozone, but the ozone consumed by this process at any given time is a very small fraction of the total ozone consumed. The predominant consumer of ozone in the FC phase, given its concentration, is nitrobenzene followed by the hydrophobic products of reaction. To a very small extent, if any, ozone species do appear at the aqueous-FC interface where they generate hydroxyl radicals. This has been verified by Bhattacharyya and coworkers (Bhattacharyya et al., 1995), where they found that sodium bicarbonate, a hydroxyl radical scavenger, dissolved in the aqueous phase did not affect the conversion of TCP, a compound with a similar m_A, for M = 12. Along with these four possibilities, Bailey (1982) also observed that ozonation of aromatic compounds like benzene in non-participating solvents like CCl_4 led to formation of epoxides. Bailey (1982) also reported on the ozonation of phenol in water by Gould and Weber (referenced in Bailey, 1982), where they mentioned that 4-6 moles of ozone per mole of phenol were sufficient to remove all the aromatic material, but as much as 150 moles of ozone were required to convert all the organic material to CO_2.

Table 3.4.4 and Figure 3.4.9 shown below summarizes the results for the utilization of ozone for high nitrobenzene feed compositions. In Figure 3.4.9, the symbol

□ is for a feed concentration of ~1400 ppm, while the symbol Δ is for a feed concentration of 978 ppm.

Table 3.4.4. Experimental results of ozone utilization : high aqueous feed composition

Aq. Flow Rate (ml/min)	NB. Aq. Conc. (ppm)		NB Cons.§ (gmol /sec)	O_3 Flow (ml /min)	Ozo. Gas Conc.* (mg/L)		Ozone Dosed (gmol/ sec)	Ozone Util. (mol O_3/ mol pol)
	Feed	Exit			Feed	Exit		
0.15	1244	656	1.13 e-8	63	41.72	40.22	5.28 e-10	0.047
0.25	1403	1135	0.92 e-8	58	61.20	56.92	1.48 e-9	0.161
0.64	1403	1283	1.04 e-8	62	61.13	54.83	2.20 e-9	0.210
1.1	1403	1312	1.33 e-8	62	61.13	52.52	2.98 e-9	0.224
0.17	978	611	0.85 e-8	79	36.16	33.56	8.92 e-10	0.106
0.18	978	615	0.87 e-8	116	22.91	21.19	6.0 e-10	0.069
0.24	978	673	1 e-8	82	39.70	37.34	8.31 e-10	0.083
0.43	978	659	1.85 e-8	64	43.84	41.71	7.26 e-10	0.039
0.80	978	765	2.3 e-8	64	43.84	39.58	1.47 e-9	0.064

§ Nitrobenzene Consumption Rate. * Makeup O_2 flowrate = 349 ml/min.

The ozone utilization for high ozone feed compositions are seen to be radically different from than those observed for low feed concentrations of nitrobenzene. In this case for a nitrobenzene feed concentration of ~1000 ppm, the concentration in the FC phase is about 2000 ppm (3.054 e-2 kgmol/m^3) while the corresponding concentration of ozone is ~78 mg/l of FC43 (1.625 e-3 kgmol/m^3). There is 20 times as much nitrobenzene in the FC phase as there is ozone. Such a disparity in the concentration will mean that

the ozonation reaction occurs very close to the FC-silicone interface. Under these circumstances, the observed ozone utilization rates can be explained by the formation of peroxidic products, which in turn show a propensity to polymerize. Bailey (1982) has shown that such a behavior is highly probable for the ozonation of benzene in CCl_4 and in some instances the highly unstable peroxides have been isolated in solid form. The peroxidic products are relatively recalcitrant towards ozone attack which would explain the much lower ozone utilization. In this reactor no buildup of the peroxidic products was observed. This is probably due to the fact that the FC phase has a large solubility for the peroxidic products. Also, these products upon formation would slowly diffuse towards the aqueous-FC interface, where they would be hydrolyzed by water to give carboxylic acids. This effect however tends to defeat the purpose of the two-phase membrane ozonator, since nitrobenzene is not being immediately degraded into simpler and more easily manageable products like carboxylic acids, nitric acid, CO_2 and H_2O. Since this effect seems to be exacerbated by the thickness of the FC membrane phase, it seems possible at least from hindsight that the reduction of the thickness of the membrane phase will possibly reduce this effect and raise the ozone utilization to a point where ozone is being used to degrade the compound. There are two ways, at this point hypothetically, in which the FC membrane phase can be reduced in thickness. Firstly, keeping the number and size of the silicone capillaries the same as SILTEF #1, 2, by using more numbers of finer Teflon tubules, and thereby increasing the amount of area of aqueous phase exposed to the FC phase. This results in a larger quantity of aqueous phase that can be treated in a given reactor volume, but with the penalty that the amount of ozone

available to destroy nitrobenzene may become the limiting factor. If the size and number of Teflon tubules were kept the same as SILTEF #1, 2, and the number of silicone capillaries were increased, the amount of area available for ozone to permeate would be higher; and given the smaller liquid membrane thickness, the likelihood that a molecule of nitrobenzene would meet with a molecule of ozone in the proximity of the aqueous phase would also be higher. This becomes an optimization problem; and given the crude kinetic data available, the solution is not presently possible.

h) Comparison between single and two-phase ozonation processes for nitrobenzene as a model pollutant

Two methods to destroy organic pollutants in wastewater have so far been presented in this work. The single-phase membrane ozonator contacts an organic pollutant bearing wastewater stream with an ozone containing gas stream using a nonporous membrane. The two-phase membrane ozonator uses an inert fluorocarbon medium to extract the organic pollutant from wastewater and absorb O_3 from the gas phase and allow reaction. This section will attempt to compare the ability of each of the reactors to treat an aqueous pollutant, nitrobenzene was chosen as the model pollutant, since it was relatively recalcitrant towards ozonation, as compared to phenol and acrylonitrile and it had an intermediate value of m_A, the partition coefficient into the FC phase.

If experimental data at similar feed concentrations were to be compared, (Figures 2.4.3 and 3.4.4), then it would have to be on the basis of amount of pollutant destroyed per unit time per aqueous interfacial area. The aqueous interfacial area for the single-phase membrane ozonator would be given by the interfacial area calculated using the

outer diameter of the silicone membrane; for the module SILCAP #2, this is given by $\pi d_o^{sil} L N_{sil}$=4.01 e-2 m^2. Since the aqueous phase flows through the lumen of the Teflon tubules and comes into contact with the FC phase at the i.d. of the Teflon tubule, the interfacial area considered for the two-phase membrane ozonator is based on the inner diameter. This is given by $\pi d_i^{Tef} L N_{Tef}$=3.88 e-3 m^2.

Table 3.4.5. Comparison of experimental performance between single-phase and two-phase membrane ozonation for nitrobenzene as a model pollutant

Aq. Fl. Rate (ml/min)	Single-Phase Ozonation §			Two-Phase Ozonation ‡		
	Feed (ppm)	Exit (ppm)	Poll. Des.†	Feed (ppm)	Exit (ppm)	Poll. Des.†
0.1	110	38	2.43 e-11	117	31	3.00 e-10
0.37 ~ 0.38	126	38	1.13 e-10	107	71	4.77 e-10
0.6	124	60	1.29 e-10	117	91	5.44 e-10
1 ~ 1.2	115	65	1.85 e-10	107	89	6.91 e-10

§ Interfacial area = 4.01 e-2 m^2
‡ Interfacial area = 3.88 e-3 m^2
† kgmol/(m^2.s).

From the above table, it is seen that the experimentally observed pollutant consumption rate for the single-phase membrane ozonator is lower by at least a factor of 5 than that for the two-phase membrane ozonator. It is seen also that this pollutant consumption rate increases about 10 times for an aqueous flow rate increase from 0.1 ml/min to 10 ml/min. Increasing the aqueous flow rate decreases the resistance to mass transfer for both species in the aqueous phase resulting in the observed increase in the pollutant consumption rate. In the case of the two-phase membrane ozonator, increasing

the aqueous flow rate allows higher amounts of nitrobenzene to come to the aqueous-FC interface, where it partitions into the FC phase. Since the major resistance to mass transfer exists in the FC phase, increasing the aqueous flowrate increases the pollutant consumption rate by a factor of 5 from the lowest to the highest aqueous flow rates.

Using the mathematical models introduced in sections 2.3 and 3.3 for the single-phase and two-phase ozonators respectively, the predicted pollutant consumption rate is shown in the upper plot in Figure 3.4.11. The predicted pollutant consumption rate for the two-phase ozonator shown by the solid line, is seen to be about 8-10 times that for the single phase pollutant consumption (dashed line) and both models show an increase at low aqueous flow rates, but flatten out at higher aqueous flow rates, when the resistance in the aqueous phase becomes smaller. The discrepancy between the predicted and experimentally observed pollutant consumption rates is probably due to the fact that the pollutant is destroyed not only by direct reaction with ozone but also by other side reactions. In the single-phase membrane ozonator this may be due to the presence of hydroxyl radicals which are generated by the presence of ozone in the aqueous phase. The situation existing in the FC-membrane phase in the two-phase membrane ozonator is however far more complex, and one can only speculate about the nature of reactions that may occur. However, both the models provide a useful guide, i.e. they provide the worst case scenario for the pollutant consumption rates and the experimentally observed rates are always higher.

If the pollutant conversion is compared for both reactors, then it is seen that the two-phase membrane ozonator shows far less conversion than the single-phase membrane

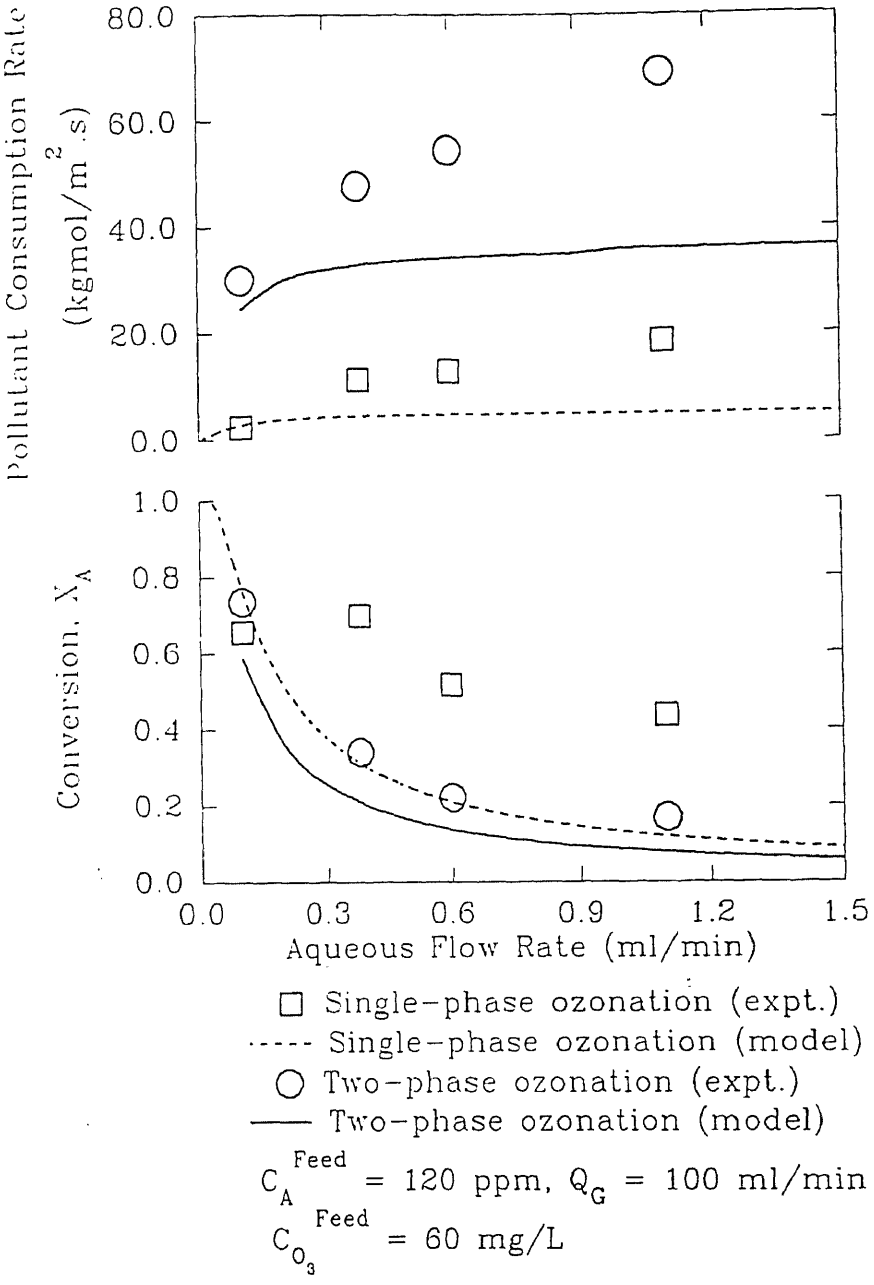

Figure 3.4.11. Comparison between single-phase and two-phase ozonation of nitrobenzene: pollutant consumption rate and conversion.

ozonator. At low aqueous flow rates, i.e. high residence times, however, the performances of both reactors are somewhat similar. The single-phase membrane ozonator had a far higher aqueous contact area (4.01 e-2 m^2) as compared to the two-phase membrane ozonator (3.88 e-3 m^2). At long residence times, this becomes less of an issue, as the pollutant molecule in the aqueous phase has adequate time to come into contact with an ozone molecule.

Comparison of the two reactors brings up a question: are the two reactors merely doing the same task in two different fashions or is there an added dimension to the utility of an inert FC medium in the case of two-phase membrane ozonator. The single phase-membrane ozonator is a simple device with very little associated complexity in terms of operation and the performance. It improves upon conventional contacting equipment by providing a larger interfacial area per unit volume of the reactor and thereby improving the volumetric mass transfer; it is however limited in its capacity to handle large pollutant concentrations as evinced by the low pollutant consumption rates. The two-phase membrane ozonator on the other hand can handle much higher feed concentrations as seen in sections 3.4.3 c and d, and is capable of high pollutant consumption rates. The single-phase membrane ozonator is extremely amenable to scaleup and simpler to operate, while the two-phase membrane ozonator is more versatile, in that it can handle volatile pollutants, like TCE and non-volatile pollutants like nitrobenzene. It can also handle high inlet concentrations of the aqueous pollutant. Therefore it seems logical that the two reactors are essentially complements of one another, at least for nonvolatile compounds like nitrobenzene and phenol. The two-phase membrane ozonator is capable

of handling high feed concentrations decreasing the pollutant concentration to a point where the single-phase membrane ozonator can effectively handle the treatment of the aqueous stream.

i) Cumulative durability of the ozonation module

The SILTEF #1 module was exposed to ozone for a total period of 135 hours. Though there seemed to be no visible deterioration of the silicone capillaries, the epoxies used in the construction of the module, adopted a yellowish tinge and displayed the onset of fine cracks, that led to the leakage of the FC membrane liquid. This leakage in the epoxy can be repaired by pouring in some fresh epoxy to seal the cracks.

CHAPTER 4

INTEGRATED ABSORPTION-OXIDATION MEMBRANE OZONATOR

4.1. Introduction

The removal of volatile organic compounds (VOCs) from gas streams vented to the atmosphere is necessary to avoid the depletion of the ozone layer and curb the photochemical formation of smog. VOCs appear in gas streams as a result of a variety of commercial, industrial and to an extent environmental processes. Since VOCs are made of low-boiling organic compounds, they are emanated wherever solvents are used in a commercial process, e.g. dry-cleaning operations, where the solvent used is perchloroethylene or painting operations where a solvent is used as a base for the paint. In industrial operations, solvents are frequently used as cleaning agents, reaction media, reaction intermediates, etc. VOCs are also found to be emanated by virtue of soil remediation operations.

There is no simple destructive method available, as yet, to handle a broad array of dilute VOCs in an effluent gas stream and flexible enough to be used in a variety of applications. Recently membrane-based processes have been studied to recover vapors from gaseous effluent streams (Baker, et al., 1996; Poddar et al., 1996a, 1996b). These processes entail the physical recovery of VOCs and are economically attractive especially if the concentrations of the VOCs in the gas stream is high and there are only few VOC species present in the gas stream allowing reuse of the recovered solvents. There are few processes available which either chemically or biologically destroy the VOCs from the

effluent gas stream. Chemical processes destroy the VOCs either catalytically or thermally at elevated temperatures; at low concentrations of VOC streams, secondary fuel is required to maintain the necessary oxidation temperatures. Biological processes are limited to dilute VOC streams and are not yet flexible enough to handle different species of VOCs simultaneously (Mukhopadhyay and Moretti, 1992).

The versatility of ozone as an oxidant and the hydrophobic nature of the fluorocarbon medium presents an interesting opportunity to study the removal of VOCs from effluent gas streams. If a gas stream containing VOCs were brought into contact with the fluorocarbon stream, then the fluorocarbon would absorb the organic compounds from the gas stream, in a manner similar to the extraction of hydrophobic organic compounds from wastewater. The organic compound extracted into the organic medium would then react with ozone, as it would in the two-phase membrane ozonator. The use of tubular membranes to contact the FC phase and the VOC containing gas stream seems logical given the prior experience with the two-phase membrane ozonator.

In this part of the study, the removal of VOCs, (trichloroethylene (TCE) and toluene) will be studied using a membrane ozonator. The integrated absorption-oxidation membrane ozonator used in this study will have one set of nonporous silicone capillary membranes to absorb the VOCs from the gas phase and a second set of nonporous silicone capillary membranes to absorb O_3 from a O_3/O_2 mixture in a membrane module. The shell space of this membrane module will have the FC phase, in a manner similar to that discussed in detail in Chapter 3. A set of microporous Teflon tubules are also provided to recirculate deionized water. This is to serve as a sink for any acidic products

of ozonation, viz. HCl or oxalic acid that have been reported in literature. The subsequent sections will discuss in greater detail the construction of such a membrane ozonator and examine its performance to treat toluene and TCE as model VOCs. The study will also experimentally examine the feasibility of such a device to handle high feed concentrations ($\sim$ 50,000 ppmv) of VOCs for TCE as the model VOC.

4.2. Experimental Procedure

4.2.1. Materials, Chemicals and Equipment

The following materials, chemicals and equipment were used in the experiments.

Ozone generator (Model T-408, Polymetrics, Colorado Springs, CO).

Ozone monitor (Model HC 400, PCI Technologies, West Caldwell, NJ).

High Performance Liquid Chromatograph, HPLC (Model 1090A, Hewlett Packard, Paramus, NJ) with a UV filter photometric detector.

HPLC integrator (Model 3390, Hewlett Packard, Paramus, NJ).

HPLC autosampler (Micromeritics, Alcott Chromatography, Norcross, GA).

HPLC column (type Hypersil ODS, length 10 cm, dia. 3 mm, Chrompack, Bridgewater, NJ).

Gas Chromatograph, GC (Model 3400, Varian Associates, Sugarland, TX) equipped with a flame ionization detector (FID), a thermal conductivity detector (TCD) and a 6 port gas sampling valve.

GC column, Carbopack C 80/100 column, type 0.3% Carbowax 20M (Alltech Associates, Deerfield, IL).

Diaphragm gas flow controllers with adjustable span (J&W Scientific, Baxter Diagnostics Inc., Edison, NJ).

Masterflex variable speed pump with controller and Easy-Load Head (Curtin Matheson Sci., Morris Plains, NJ).

Masterflex viton pump tubing, size 13 (Curtin Matheson Sci., Morris Plains, NJ).

Teflon tubules (Impra/IPE Inc., Tempe, AZ).

Silicone capillaries (Silastic, medical-grade, (Dow Corning, Midland, MI), Baxter Diagnostics, Edison, NJ).

FEP tubing and polypropylene barbed crosses (Cole Parmer, Chicago, IL).

Four Way Valve (cross-over), 1/8" NPT (Swagelock, R. S. Crum, Mountainside, NJ).

pH Meter and electrode (Model 140, Corning, Corning, NY).

Mass flow controller transducer (Model 8272, Matheson, East Rutherford, NJ).

Multichannel dyna-blender (Model 8284, Matheson, East Rutherford, NJ).

Toluene and nitrogen gas mixture (205 ppm) (Matheson, East Rutherford, NJ).

Trichloroethylene and nitrogen gas mixture (220 ppm) (Matheson, East Rutherford, NJ).

Oxygen extra dry, helium high purity, nitrogen extra dry, air zero, hydrogen zero (Matheson, East Rutherford, NJ).

Toluene and trichloroethylene (ACS grade, Fisher Scientific, Springfield, NJ).

FC 43, perfluorobutylamine, (3M, St. Paul, MN).

Acetonitrile (HPLC grade, Fisher Scientific, Springfield, NJ).

4.2.2. Fabrication of Membrane Reactor

The fabrication of the integrated membrane absorber-ozonator employed nonporous silicone capillaries (0.3 mm ID, 0.63 mm OD) and microporous Teflon tubules (0.99 mm ID and 2.0 mm OD). The two silicone capillary sets were of silastic medical grade. The porous Teflon tubules had a porosity of 50% and a pore size range of 12-19 μm. The

two sets of silicone capillaries and the set of Teflon tubules were counted, cut to length and laid out in the form of a mat. The ends of the silicone capillaries and Teflon tubules were bunched together and tied, keeping the bunched silicone ends separate from the bunched Teflon ends. The capillaries and tubules were simultaneously inserted in a transparent FEP shell (0.61 cm ID, 1.03 cm OD; Cole Parmer, Chicago, IL). This was achieved by tying the bunched ends together by means of a string, covering the bunched tubule and capillary ends by means of a piece of Teflon tape and the pulling the ends through the shell by means of a string tied around them. The disparate bunched ends were separated from one another and adjusted so that the shorter Teflon tubules and the longer silicone capillaries were centered with respect to the FEP shell. The bunched capillaries and the tubule ends were next drawn through a polypropylene T-fitting (with barbed ends) at each end of the FEP shell. The set of Teflon tubules were drawn into the T-end perpendicular to the axis of the module. The third end which now solely consisted of the two sets of silicone capillaries was connected to polypropylene crosses (with barbed ends) by means of a short length of FEP tubing. Each silicone set was drawn into the barbed end perpendicular to the axis of the module. In order to complete the construction of the module, the fiber ends were subsequently potted using epoxy as described below.

Each of the six fiber ends was potted in turn using two sets of epoxies (Beacon Chemical Co., Mount Vernon, NY). The external tube sheet was formed using the A2 epoxy with activator "A", using 8 drops of activator to 5 grams of epoxy. The A2-A epoxy, a viscous paste, was liberally applied by means of a spatula to seal the void space

between the silicone capillaries and barbed cross-connector. The same procedure was repeated for the Teflon tubules. The internal tube sheet was formed using the C4 epoxy with activator "D", using 1 part activator to 4 parts epoxy by weight. The C4-D epoxy mixture was degassed in a desiccator by a vacuum pump. The two T-fittings and the two crosses had small holes predrilled into the ends in order to pour in the epoxy into each fiber end side of the barbed cross-fitting taking each of the ends in turn. The hole itself was sealed up with the epoxy. The epoxies were allowed to cure for seven days, before the module was filled with water on the shell and the pressure in the shell was raised to 10 psig to check for leaks. Table 4.2.1 provides the geometrical specifications of the membrane module, henceforth identified as NEWCON #1. Figure 4.2.1(a) shows the arrangement of the epoxy layers in the capillary ends of the module while Figure 4.2.1(b) shows a photograph of the module. Figure 4.2.2 shows a schematic of the completed module.

Table 4.2.1. Details of integrated absorption-oxidation (NEWCON) membrane-based ozonator

Module No.	Active Length cm	First Fiber Set[a]		Second Fiber Set[b]		Third Fiber Set[c]	
		Total Nos.	ID/OD μm	Total Nos.	ID/OD μm	Total Nos.	ID/OD μm
NEWCON 1	20.3	25	304.8/ 609.6	25	304.8/ 609.6	5	990/ 2280

[a] Nonporous silicone tubules. [b] Nonporous silicone tubules. [c] Teflon tubules.

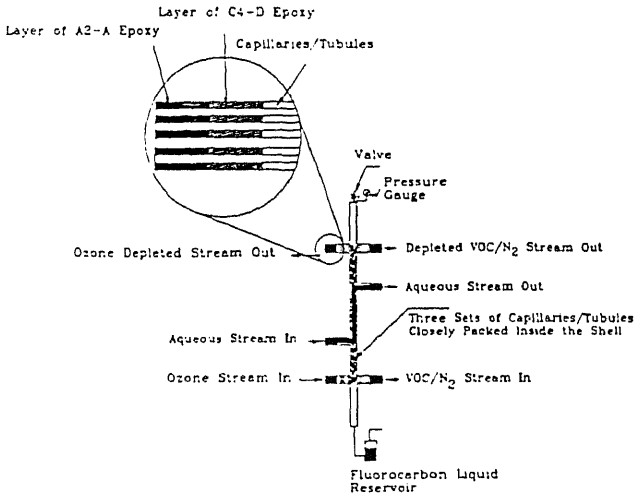

Figure 4.2.1(a). Schematic of integrated absorption-oxidation membrane ozonator module showing the fiber ends embedded in an epoxy layer.

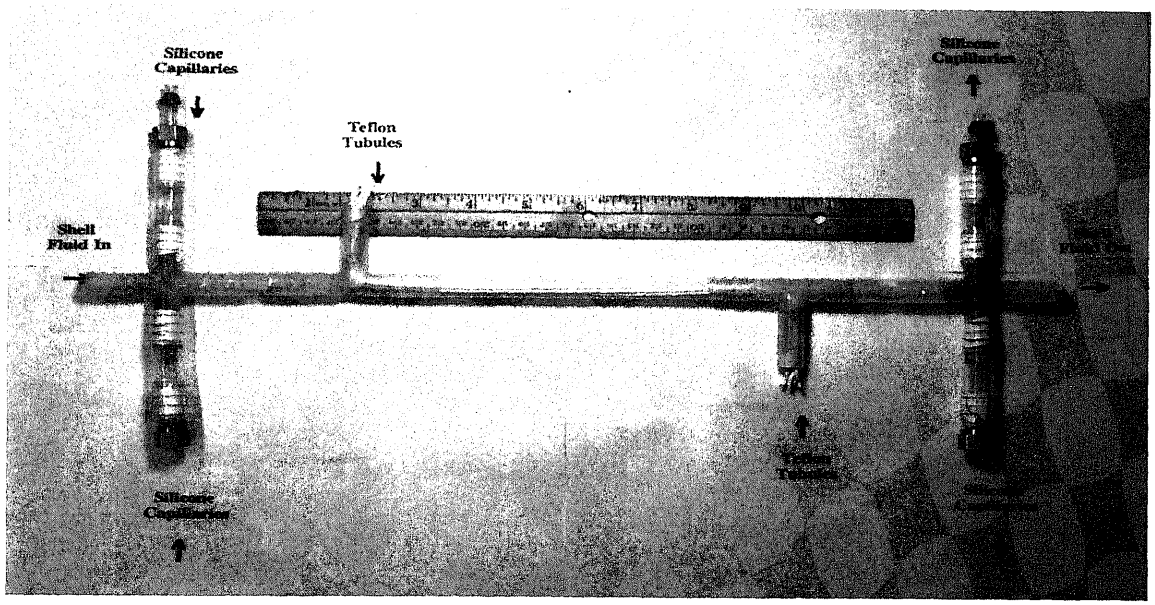

Figure 4.2.1(b). Photograph of the integrated absorption-oxidation membrane ozonator.

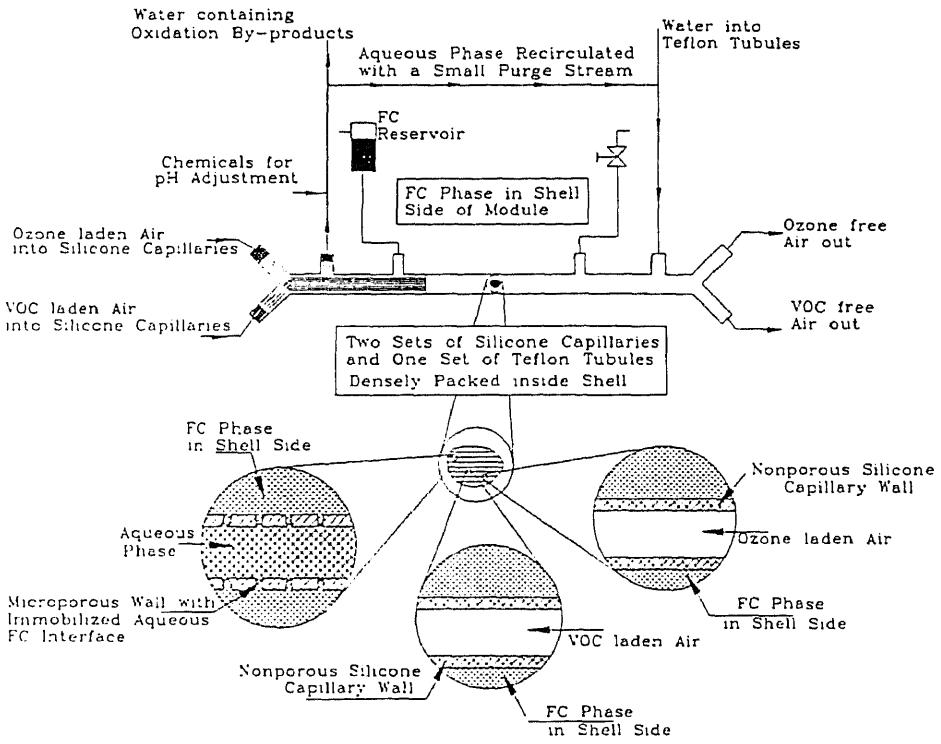

Figure 4.2.2. Schematic of the integrated absorption-oxidation membrane ozonator.

4.2.3. Analytical Techniques to Measure Organic Pollutants in Water

The aqueous feed was analyzed for pollutants using a HPLC equipped with a Hypersil ODS analytical glass column and a filter photometric UV detector. Table 2.2.2 indicates the HPLC conditions to detect and determine the concentration of pollutants in the aqueous phase. The HPLC was initially calibrated, by injecting samples of known composition of each of the pollutants and noting the area of the peaks recorded by the integrator. Aqueous samples of toluene and trichloroethylene were prepared by spiking deionized water with a pure liquid sample of the pollutant to give the necessary feed composition. Samples of lower concentrations of toluene and trichloroethylene were obtained by spiking deionized water with pure samples of the two compounds by means of Hamilton microliter syringe. Sample calibration curves for toluene and trichloroethylene are shown in Figures 3.2.3 and 3.2.4 respectively.

4.2.4. Source of VOC and Analytical Techniques to Measure the VOC Composition in the Gas Phase

A constant steady stream of VOC was supplied to the experimental setup in two ways. Lower concentrations (220 ppmv and lower) were obtained from a standard gas mixture (a mixture of the VOC in N_2) (Matheson, E. Rutherford, NJ). Higher concentrations were obtained by bubbling nitrogen through a pure liquid sample of the VOC. The concentration obtained in such a case would be determined by the vapor pressure of the VOC at the ambient temperature and pressure (the pressure was kept as close to atmospheric as possible) and contacting efficiency. The VOC bearing gas phase was analyzed for the pollutant using a Gas Chromatograph, (Varian 3400, Varian Associates, Sugarland TX), whose operating conditions are shown in Table 4.2.2.

Table 4.2.2. Operating conditions of the gas chromatograph to measure the concentration of a volatile organic compound in a gas phase.

Gas Chromatograph	Varian Model 3400
Detector	Flame Ionization Detector (FID)
Sampling Method	6 port gas sampling valve
Data Acquisition	Varian integrator 4290.

Column : 0.3% Carbowax 20M, Carbopack C, Mesh 80/100, 0.085" ID, 0.1625" OD, 10 feet length.

Property	Condition
Column Temperature	150 °C
Injector Temperature	220 °C
Detector Temperature	250 °C
Attenuation	6
Threshold	3.0

To obtain different VOC concentrations, a setup shown in Figure 4.2.3 was completed. The VOC feed stream was mixed with a makeup stream of nitrogen (extra dry) (Matheson, E. Rutherford, NJ) to get the necessary feed VOC concentration. The gas flow rates were controlled by a pair (one for the VOC feed and the other for the N_2 makeup) of Diaphragm Flow Controllers (J & W Scientific, Baxter, Edison, NJ). The

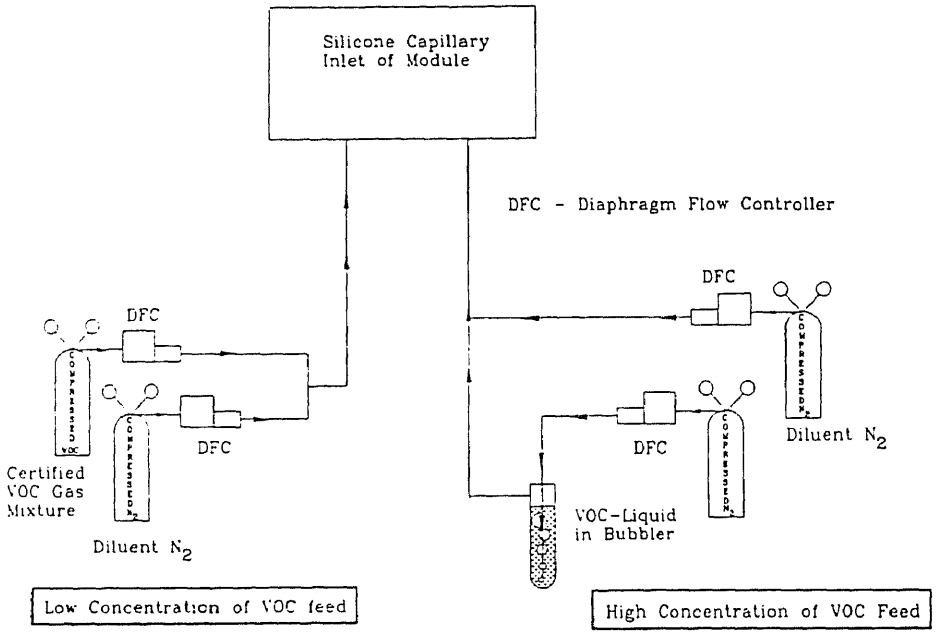

Figure 4.2.3. Schematic of the setup to generate different concentrations of VOC in a gas phase.

calibration of the GC for higher concentrations of VOCs was carried out with the diaphragm flow controllers in conjunction with a Matheson mass flow controller (Matheson, E. Rutherford, NJ) which was used to generate a diluent N_2 stream.

The gas chromatograph was calibrated upto a concentration of 220 ppmv (parts per million based on volume : volume ratio) using a certified gas mixture of (220 ppmv of TCE with N_2 as a diluent) in the low concentration range. Intermediate concentrations were obtained by blending this cylinder mixture with a second stream of pure N_2. The calibration curve of peak area versus gas phase concentration in ppmv is shown in Figure 4.2.4. The calibration curve for toluene is shown in Figure 4.2.5.

To generate high concentrations of trichloroethylene, a TCE vapor stream was obtained by bubbling pure N_2 through a pure sample of trichloroethylene. The flow of this N_2 stream was controlled by the diaphragm flow controller. This was then diluted by a makeup N_2 stream whose flow rate was controlled by a Matheson flow controller. The flow rate of the makeup N_2 was so adjusted that the peak areas thus obtained were equal to those resulting from the injection of the 220 ppmv certified gas mixture. This gave the concentration of the vapor stream; subsequently intermediate concentrations were obtained by blending this gas stream with the second stream of N_2. The calibration curve of peak area versus gas phase concentration for higher concentrations of trichloroethylene in N_2 is shown in Figure 4.2.6.

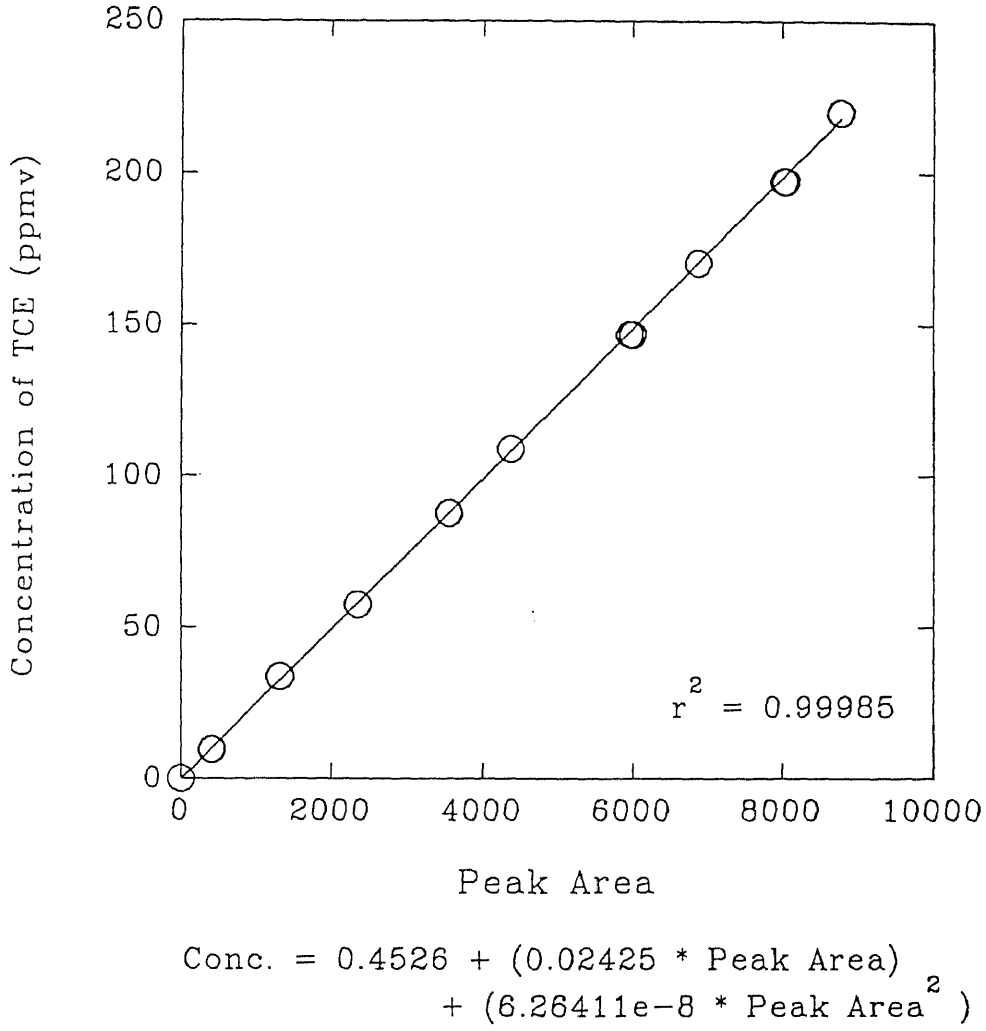

Figure 4.2.4. GC calibration curve for TCE for the low concentration range.

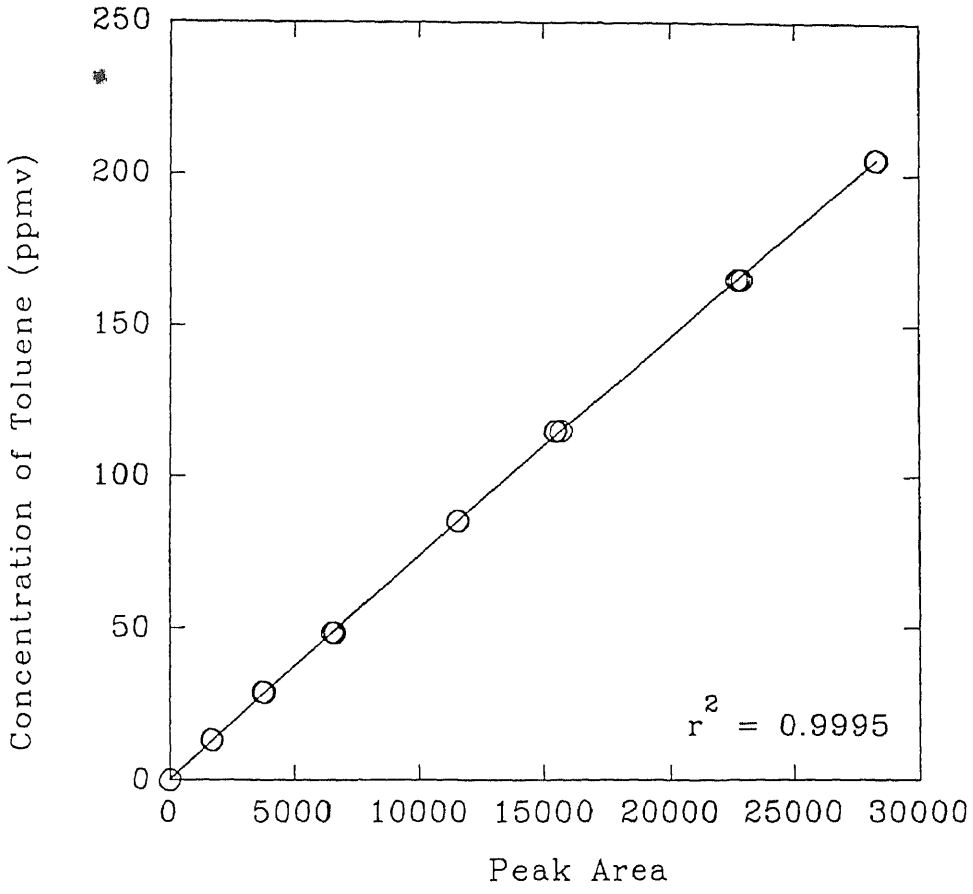

Figure 4.2.5. GC calibration curve for toluene for the low concentration range.

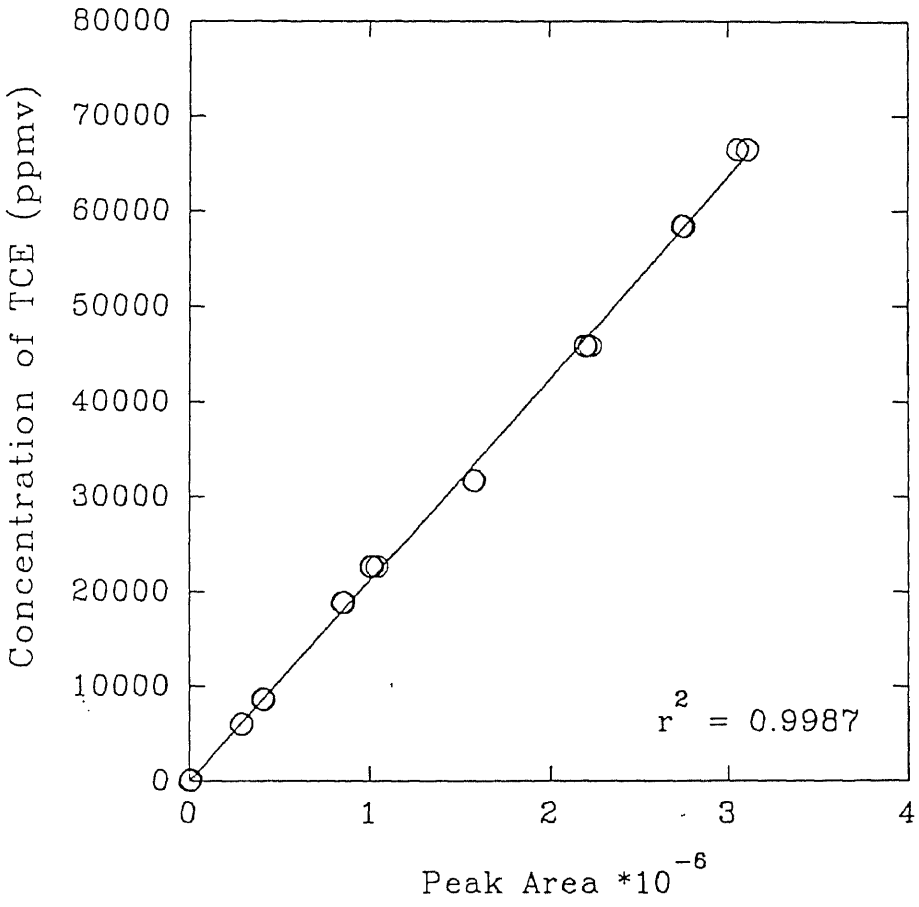

$$\text{Comp.} = 104.7 + (0.0298e{-}6 * \text{Peak Area}) - (1.3587e{-}22 * \text{Peak Area}^2)$$

Figure 4.2.6. GC calibration curve for TCE for the high concentration range.

4.2.5. Source of Ozone

Ozone was generated by feeding a pure oxygen stream to the ozone generator. The ozone generator was operated at a voltage setting of 90 volts; the pressure within the ozone generator was held at 9 psig (163.4 kPa) by a back pressure regulator. The flow rate of oxygen through the ozone generator was maintained at 0.6 standard liters per minute (SLPM). A small portion of the ozone/oxygen mixture (O_3/O_2) was diverted for experimental purposes. The major portion of this gas was vented after passing through two KI (2% concentration by weight) wash bottles linked in series to break down any ozone and a sodium thiosulfate bottle to trap any entrained iodine.

4.2.6. Study of Degradation of VOCs in the Novel Membrane Reactor

Ozonation studies were carried out in a reaction loop shown in Figure 4.2.7. The reactor-based setup consisted of four major sections all connected to the membrane reactor: 1) an ozonator to supply ozone, 2) a FC-liquid reservoir, 3) a VOC source and finally 4) an aqueous phase recirculation unit.

Since the operating gas flow rate of the ozonator was very high, a major portion of the gas stream was diverted to the fume hood after being bypassed through two KI wash bottles (to break down the ozone) and a thiosulfate wash bottle (to capture any entrained iodine). The other stream was sent to a set of the silicone capillaries. Gas side flow rate and pressure were kept as close to atmospheric as possible and were controlled by means of a Teflon needle valve (Cole Parmar, Chicago, Il) placed at the outlet of the module. The spent gas stream was passed through a KI wash and then through a soap

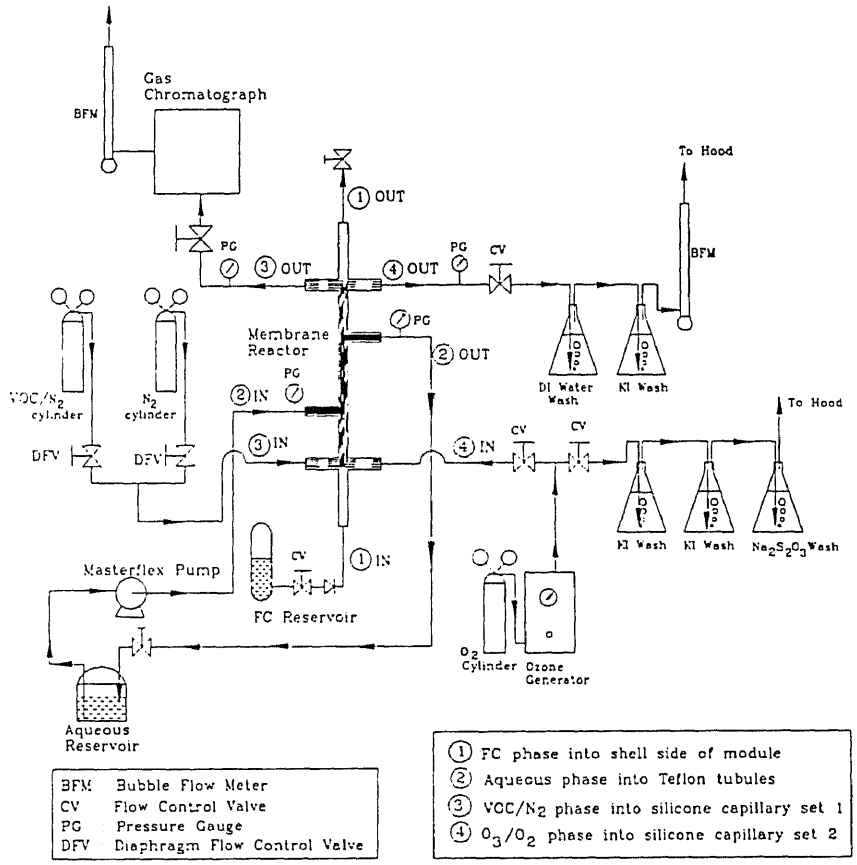

Figure 4.2.7. Schematic of the experimental loop to study the removal of VOCs from air using the integrated absorption-oxidation membrane ozonator.

bubble flow meter and finally to the exhaust hood. The VOC- laden stream was admitted into the second set of silicone capillaries, its concentration being adjusted by the diaphragm flow control valves. The spent VOC stream was then sent to the GC to sample the exit concentration. The pressure on the VOC side was also maintained as close to atmospheric as possible. The aqueous stream was recirculated through the Teflon tubules by a Masterflex Pump (Curtin Matheson Scientific, Morris Plains, NJ).

The fluorocarbon phase was admitted into the shell side of the module from a small aluminum storage vessel. Prior to the start of the experiment, this vessel was filled partially with the fluorocarbon phase, FC 43. The physical properties of the fluorocarbon fluid are summarized in Table 3.3. Experiments were conducted by first starting the flow of the aqueous phase through the Teflon tubules at a pressure of 1 ~ 2 psig (108.2 ~ 115.1 kPa) and a predetermined flow rate. The fluorocarbon phase was then admitted into the shell side of the module. Since the FC reservoir was kept at a higher position than the module, the fluorocarbon phase would flow into the module by gravity. However, on occasions it was necessary to gently begin the flow of the FC phase by pressurizing the FC reservoir with nitrogen. The O_3/O_2 gas phase was passed through the lumen of the first set of silicone capillaries, while the VOC phase was passed through the lumen of the second set of silicone capillaries. The aqueous phase flow rate was controlled by means of a needle valve and the pressure of the aqueous phase was kept slightly higher than that of the fluorocarbon phase maintained at atmospheric pressure. The aqueous phase was sampled periodically and a sample was injected into the HPLC to determine the concentration of the pollutant in the aqueous phase. The flow of O_3/O_2

phase was monitored by means of a bubble flow meter and the flow rate was adjusted by means of valve A, shown in Figure 4.2.7. Aqueous phase samples were injected into the HPLC to observe any degradation products. The pH of the aqueous phase before and after the experiment was measured (Corning, Model pH meter 140, Corning, NY).

4.3. Results and Discussion

4.3.1. Introduction

The physical characteristics of the integrated absorption-oxidation membrane ozonator that was constructed are summarized in Table 4.2.1. The experimental results are presented and discussed in the following order: 1) experimental performance of the membrane ozonator at high inlet concentrations of trichloroethylene (TCE); 2) experimental performance of the reactor at low inlet concentrations of trichloroethylene (TCE); 3) experimental performance of the membrane ozonator at low inlet concentrations of toluene.

4.3.2. Performance of the Reactor

The fluorocarbon used in all experiments was FC 43; its physical properties are summarized in Table 3.2.3. The conversion of VOC species A in the membrane ozonator is defined as follows:

$$\text{Conversion}\ ,\ X_A = \frac{C_A^{in} - C_A^{out}}{C_A^{in}} \qquad (4.3.1)$$

The major resistances to transport of ozone and the VOC species include the membrane resistances contributed by the silicone capillary walls and the FC contained liquid membrane.

a) Experiment with high concentrations of trichloroethylene

The performance of the integrated absorption-oxidation membrane ozonator is presented in Table 4.3.1. Each result shown in this represents the steady state performance recorded at the end of an 8 hour period.

Table 4.3.1. Performance of the integrated absorption-oxidation membrane ozonator at high TCE feed concentrations

Run No.	VOC Flow Rate ml/min	VOC Feed Conc. ppmv*	VOC Exit Conc. ppmv	Conv. X_A	O_3/O_2 Flow Rate ml/min	Aq. Flow Rate ml/min	Aq. TCE Conc. ppm	pH of Aq. Phase	
								Init.	Fin.
1	32	51,350	20,625	0.60	27	4.2	97	6.13	2.71
2	34	50,320	17,425	0.65	54	3.8	70	6.13	2.74
3	50	31,860	18,210	0.42	29	6.6	81	4.99	2.95

*For the VOC feed, nitrogen (extra dry) was bubbled through pure TCE and blended with a second stream of nitrogen (extra dry) to give the desired feed concentration. FC43 used as shell-side liquid.

It is seen from the above table that between runs 1 and 2 and 3, the TCE/N_2 flow rate was almost doubled (the residence time consequently, was almost halved) causing the TCE conversion to fall from a value of 0.6 to a value of 0.4. For a given flow rate of the VOC-containing gas, higher conversions would require larger surface areas. The substantial change in the pH of the aqueous phase over the duration of each run indicated that some of the TCE absorbed into the FC phase had been mineralized. Also it was found that at the end of the experiment, some TCE had broken through the

FC membrane and dissolved into the aqueous phase. Over runs 1 and 2, there is very marginal change in the observed TCE conversion, 0.6 to 0.65, despite increasing the flowrate of ozone by a factor of 2. Since TCE had broken into the aqueous phase, it is clear that the reactor was being operated in the ozone limited regime. Also it is seen that since the aqueous phase is recycled, its flowrate does not affect the performance of the reactor.

b) Experiments with low concentrations of trichloroethylene

Subsequent to the above experiments, low feed concentrations of TCE from a standard TCE/N_2 mixture gas cylinder of TCE concentration of 220 ppm was fed to the integrated absorption-oxidation membrane ozonator. These results are summarized in Figure 4.3.1. At VOC flow rates of 22 ml/min shown by Δ, conversions in excess of 0.9 were observed and these remained practically constant despite a four fold increase of O_3/O_2 gas flow rate from 20 ml/min to 80 ml/min. As the VOC flow rate was increased from 22 ml/min (Δ) to 34 ml/min ($\square$, $\blacksquare$) and then to 58 ml/min ($\bigcirc$), the observed conversion fell from 0.9 (Δ) to 0.6 ($\bigcirc$) and remained fairly unaffected by changes in O_3/O_2 gas flow rates as is evinced from Figure 4.3.1. The results shown by $\square$ were carried out first and after experiments at TCE/N_2 flow rates of 22 ml/min were carried, the run with a TCE/N_2 was carried out again and is shown as $\blacksquare$. This was done to ascertain the reproducibility of the performance of the reactor.

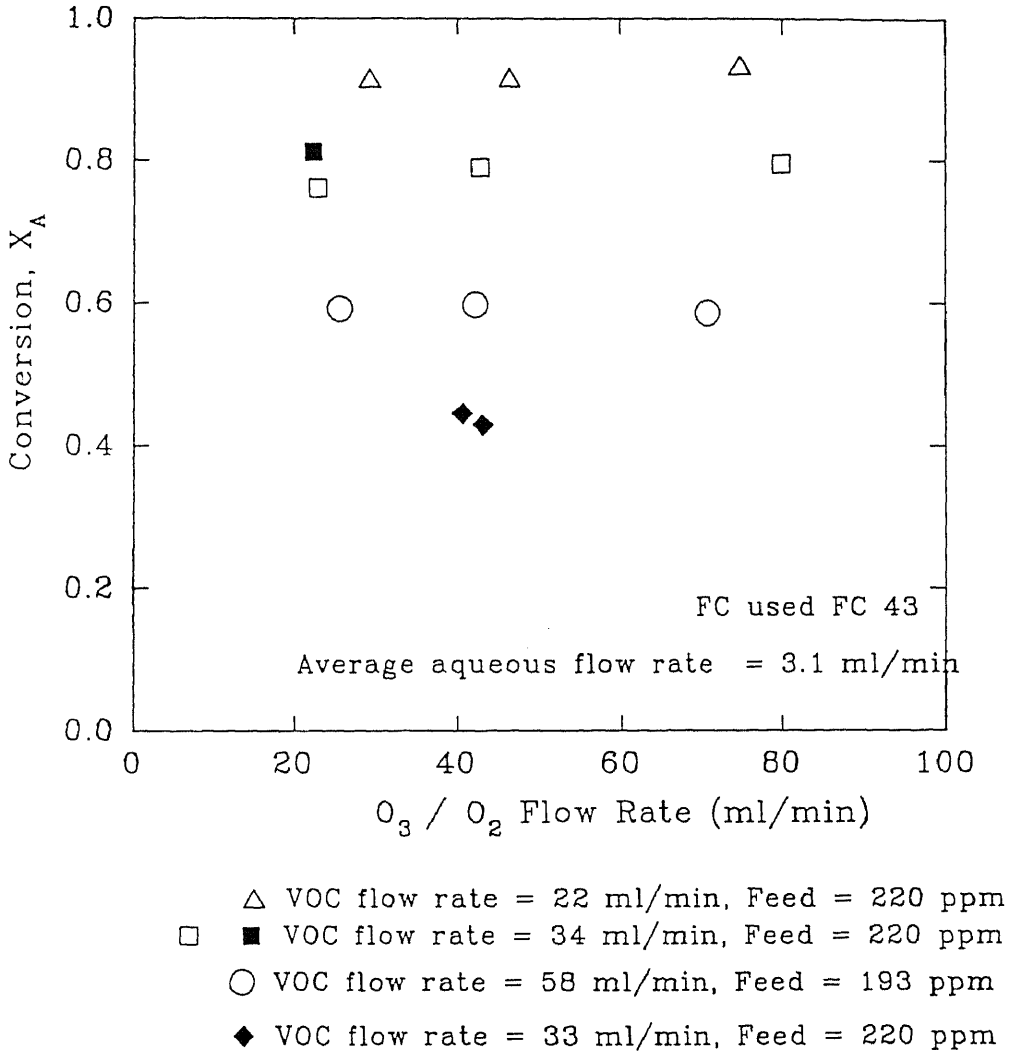

Figure 4.3.1. Degradation of TCE in the integrated absorption-oxidation membrane ozonator.

The results shown as ◆ are for a TCE/N_2 feed stream of 220 ppm at a flow rate of 33 ml/min. These results were obtained subsequent to experiments carried out with toluene as a VOC, after it was seen that the reactor performance had become considerably poorer. The reasons for this will be discussed in the next section where toluene is studied as a model VOC.

c) Experiments with low concentrations of toluene

The results with toluene as a model VOC are shown in Figure 4.3.2. The results shown with the symbol ○ are for a VOC flow of 11 ml/min and show conversions in the excess of 0.9. From Table 3.4.3, the second order rate constants found in literature for the ozonation of TCE in CCl_4 are higher than those for toluene resulting in lower observed toluene conversions at comparable VOC flow rates. For VOC flow rates of 25 ml/min shown as □, at O_3/O_2 gas flow rates of 40-80 ml/min, conversions of 0.85 were observed. As more experiments were carried out at lower O_3/O_2 flow rates, it was seen that the observed toluene conversion fell to 0.5, indicated by the cluster of symbols marked as □ for O_3/O_2 flowrates between 20 - 40 ml/min. The reasons for this was not clear at the outset since the results for TCE had not shown any such trends. Also since the reaction rate coefficient for the ozonation of toluene in CCl_4 is low, 0.166 M^{-1} s^{-1}, experiments were carried out in the absence of ozone to verify that indeed toluene is getting destroyed by ozone and not getting stripped out into the O_3/O_2 phase. These runs are shown as ■, the observed removal of toluene was far less than that observed for

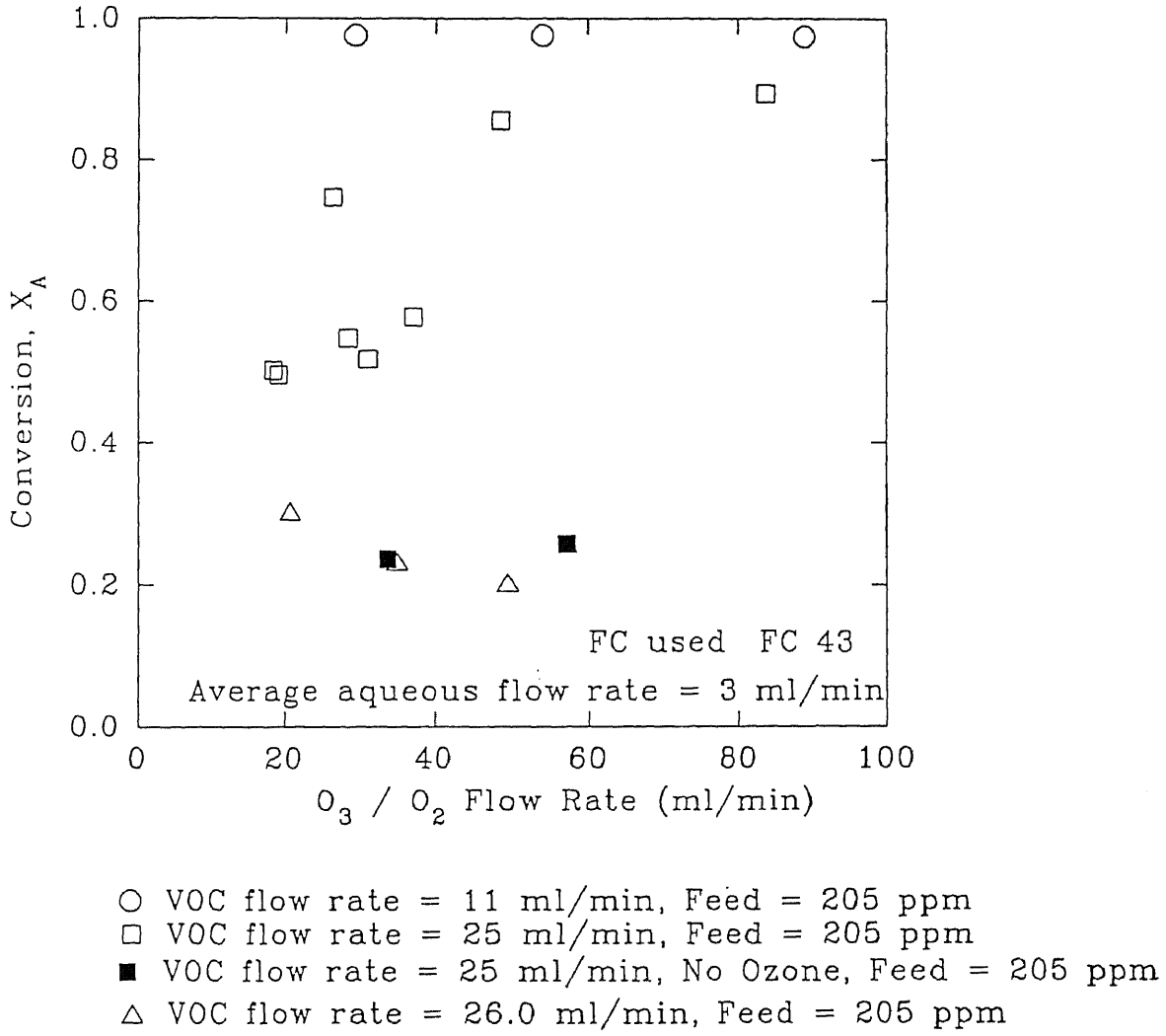

Figure 4.3.2. Degradation of toluene in the integrated absorption-oxidation membrane ozonator.

O_3/O_2. Subsequent to these runs were the runs marked with Δ, the observed conversion of toluene had dropped further and the run subsequent to this is run for TCE marked with ◆ (Figure 4.3.1). After the completion of these runs the permeability of ozone through the silicone capillaries was measured and was reported in Table 2.4.8. The value observed for NEWCON #1, 8.4 e-13 (kgmol m)/(m^2 s kPa) was not very different than that observed for SILCAP #5, 8.8 e-13 (kgmol m)/(m^2 s kPa). Therefore this indicated that the drop in performance was not due to the decrease in ozone permeability in the silicone capillaries. It is presently unknown how the permeability of the organic species, toluene and TCE is affected, but it may be postulated that the decrease in reactor performance is due to a decrease in the permeability of the organic species. Exposure to ozone does lead to some degree of hardening of the silicone polymer. The permeability of species through silicone polymer is given by the product of solubility (S) of the diffusing species in the polymer and the diffusivity (D) of the diffusing species in the polymer. VOC species like TCE and toluene are highly soluble in the silicone polymer matrix (e.g. 4.8 cm^3(STP)/ (cm^3-membrane cmHg) for TCE versus 2.5 e-3 cm^3(STP)/ (cm^3-membrane cmHg) for O_2 (LaPack et al., 1994)). Any "glassification" of the polymer is going to cause a sharp drop in the solubility of the diffusing species in the polymer matrix leading to a lower permeability of the diffusing species through the polymeric matrix. This effect is probably quite dramatic for the VOC species, since they are freely soluble in a rubbery matrix and nearly insoluble in glassy matrices and leads to the observed drop in membrane reactor performance. The drop in reactor performance can be ascribed to the fact that the resistance to permeation of the VOC through the

siliocne capillaries becomes large and controls the overall process. This drop in performance is therefore seen to be independent of the VOC used as can be observed by the drop in conversion for both TCE and toluene as model pollutants.

d) Cumulative durability of the ozonation module

Since in both the single-phase and two-phase membrane ozonators, silicone capillaries were used to supply ozone to the respective ozonators, the prolonged exposure did not seem to affect the reactor performance. In the case of the integrated absorption-oxidation membrane ozonators, however, the prolonged exposure to ozone did seem to be detrimental to the performance of the reactor. From the observations of the decline in reactor performance, which was not observed for the other two reactors, it can be inferred that due to hardening of the silicone capillaries, the permeability of the VOC molecules was diminished. This resulted in a drop in the experimentally observed conversion of the VOCs. As observed in the other two reactors, the epoxies did shown yellowing and the onset of small cracks, that were visible to the naked eye. The reactor was exposed to ozone for a total period of 90 hours before the onset of the observed drop in reactor performance. It was also observed that there was leakage of gas into the FC membrane phase at the module inlet and exit headers at about the same time. However it could not be verified whether this was due to the breakdown of the epoxy tubesheet or due to the breakage of silicone capillaries.

CHAPTER 5

CONCLUSIONS AND RECOMMENDATIONS FOR FURTHER WORK

The presence of organic pollutants in effluent gas and aqueous streams is of great concern. It is therefore imperative that these emissions are controlled or abated, efficiently and economically at ambient temperatures and pressures. The membrane reactors studied in this work can be used to treat either liquid or gaseous waste streams containing organic pollutants, with little modification.

a) The single-phase membrane ozonator, studied in Chapter 2, is a simple device that allows the membrane-mediated contact between a wastewater stream containing organic pollutants and an ozone-bearing gas stream. Since the two flowing streams are not dispersed in each other, the inherent limitations of packed beds and tray towers regarding the relative flow rates of the liquid and gas streams, viz. flooding and loading are absent in these membrane reactors. A single-phase membrane ozonator of ½" diameter and 1 foot length has been shown to handle aqueous feed solutions of phenol, acrylonitrile and nitrobenzene reducing a feed of concentration of 100 ppm to an outlet concentration of 40 ppm or less (~ 60 % conversion of the pollutant). The pollutant removal depends upon the residence time (flow rate) of the aqueous phase, the size and the number of the silicone capillaries used, the size of the module, etc. Extensive use of the single-phase membrane ozonator, however, is restricted by the size and durability of the membranes used and the durability of the potting material (epoxies) used to fabricate the module. The silicone capillaries used in the experiments had an O.D. of 0.025" (0.635 mm); this

placed an upper limit on the number of capillaries that could be packed within a module and consequently the available membrane area per unit reactor volume. The silicone capillaries were found to be stable for short exposures to ozone; upon longer exposure to ozone together with compounds like KI, they were found to become hard and less permeable to O_3.

The principal resistance to mass transfer in this process is the boundary layer resistance of the aqueous phase. The situation is compounded by problems of bypassing and channeling when the aqueous phase is passed on the shell side of the module. Therefore further studies based upon oxidation-resistant membrane materials, more durable potting materials and different module designs to mitigate the effect of the aqueous phase boundary layer resistance seem warranted. If the aqueous phase of the module were passed across the surface (cross-flow) of the tubular membrane, rather than parallel (parallel-flow) to the surface of the membrane, then this would enhance considerably the mixing in the aqueous phase and reduce the boundary layer resistance. Considerable increases in the mass transfer coefficients have been observed for the absorption of SO_2 into water by adopting the cross-flow configuration (Karoor and Sirkar, 1993). Studies with ozone-resistant microporous capillary membranes (e.g. of Teflon), would further aid in increasing the mass transfer coefficient of ozone by reducing the membrane resistance to passage of ozone. Heterogenous catalytic processes (CATAZONE) which use ozone in the presence of a TiO_2 catalyst (Masten and Davies, 1994) are potentially interesting avenues that need to be explored in conjunction with the single-phase membrane ozonator. This could be carried out by dispersing a small amount

of the powdered catalyst in a silicone polymer solution. The solution would then be deposited in the form of thin film on the surface of the porous membrane closest to the aqueous phase and cured in place. This would allow a thin layer of TiO_2 to be in intimate contact with ozone and the polluted aqueous phase and aid in enhancing the ozonation of the pollutant.

b) The two-phase membrane ozonator studied in Chapter 3 was found to ably degrade organic pollutants dissolved in wastewater. This ozonator worked by extracting the organic pollutant into an inert FC medium, within which ozone was independently supplied to degrade the pollutant. It was seen that the partition coefficient of the pollutant into the FC and the residence time of the aqueous phase in the reactor influenced the removal of the organic pollutant dissolved in the aqueous phase. It was also demonstrated that this type of membrane reactor could handle large feed concentrations ~ 1400 ppm for nitrobenzene as a model pollutant. The FC membrane phase was found to remain unaffected despite continued and prolonged exposure to ozone. Since this reactor used rather large tubular microporous Teflon membranes to admit the aqueous phase into the reactor, the amount of membrane area available for contact between the aqueous phase and FC phase was limited. Further studies of such a reactor should entail the use of finer Teflon tubules or hollow fibers. These would allow higher interfacial contact areas between the FC and aqueous phases and thereby increasing the ozonation efficiencies for destroying the pollutant.

The chemistry of ozonation of the organic compounds in the two-phase regime seems to be quite distinct from that either in the FC phase or in the aqueous phase alone.

However depending upon the concentration of the organic pollutant and the proximity of the FC-aqueous interface to the reaction region, it appeared to represent a reaction regime that approximated the situation in the FC phase alone. The relative proximity of the aqueous phase to the reaction zone affects the types of reaction products formed. Much of the understanding of the reaction chemistry has come about indirectly during the study of the utilization of ozone in the two-phase membrane ozonator. Further studies of such a reactor would have to look into the type of oxidation reactions for a given pollutant or type (olefin, aromatic, etc.) and the sort of reactions that would be required to degrade the pollutants to smaller, biodegradable products. Such a study would allow a better prediction of the reactor performance and ease the scale up of the device to handle larger liquid flows. The use of multiple pollutants simultaneously and the associated impact on the reactor performance and type of degradation products formed are also of interest. The use of a catalyst, viz. TiO_2 to mediate the photo-oxidation of trichloroethylene (TCE) and toluene in FC solvents has been studied (Sun et al., 1995). This could be achieved in the two-phase membrane reactor by immobilizing or depositing the catalyst on the membrane surface as outlined in (a) for the single-phase membrane reactor. In conjunction with the high concentrations of ozone in the FC phase, the catalyst would aid in degrading the pollutant efficiently. The amount of catalyst present in the ozonator would be a function of the membrane area available in the device.

c) The integrated absorption-oxidation membrane ozonator was found to be effective in handling the removal of VOCs like TCE and toluene from a VOC/N_2 gas stream. The reactor was similar to the two-phase membrane ozonator, but with an extra set of silicone

capillary membranes to convey the VOC/N_2 stream into the reactor. The drop in reactor performance over time, was most probably due to the reduction in the permeability of the VOCs in silicone rubber. This observation derives added credibility from the fact that an independent measurement of the permeability of ozone did not considerable change from that of the virgin polymer, so as to drastically affect the reactor performance. The use of stable materials is therefore an issue that affects the long term performance of the reactor. Also the extent of stripping of the FC phase into the gas phases, by observing the gas chromatogram of the pollutant exit stream, seems to be negligible. It is however unknown at this point if there are any components of the FC phase which pass through the Flame Ionization Detector (FID) unnoticed. If there is considerable loss of the FC phase then alternate FC compounds and their compatibility with the membrane materials also requires to be factored into future studies with this reactor. Further studies should also focus on developing a model for this type of reactor; this would facilitate the development of a concrete basis for comparing the economic performance of such a reactor with those of other VOC-destruction technologies.

In conclusion, this dissertation demonstrated the ozonation of organic pollutants found in aqueous and gaseous waste streams in a membrane device. This study underscored the utility of membrane-based contacting devices in increasing gas-liquid contacting efficiencies without the use of additional pumps, formation of dispersions, etc. It also demonstrated the ozonation of VOCs from gaseous waste streams at ambient pressures and temperatures, an avenue of VOC removal that was not possible with conventional gas-liquid contactors.

APPENDIX 1

EQUIVALENT RADIUS OF FREE SURFACE DEFINED BY HAPPEL'S MODEL

The flow of liquid in the shell side of a tubular membrane module is too complicated in nature to be described by a simple mathematical model. The liquid should ideally surround each tubular membrane as it flows through the shell but depending upon their distribution and packing density, some of the liquid may not come into contact with the membranes. The flow situation and the subsequent effects upon heat transfer from tube banks have been studied by a number of researchers (Happel, 1959; Sparrow and Loeffler, 1959; Sparrow et al., 1961 and Schmid, 1966). The "free surface" model described by Happel (1959), however is a model that can be easily incorporated to describe the concomitant behavior of mass transfer and the nonideality of the aqueous flow in the module shell.

The use of Happel's "free surface" model was used to describe hollow fiber-based reverse osmosis (Gill and Bansal, 1973) and the absorption of CO_2 and SO_2 into water in a parallel flow shell-and-tube type microporous hydrophobic hollow fiber device (Karoor and Sirkar, 1993). The model does not account for variation in the liquid distribution, like by-passing around the membrane bundle and therefore is representative of the upper limit of the experimentally realizable concentrations.

To determine the equivalent radius of the free surface, the relative volume of the absorbent liquid surrounding a single fiber in the free surface envelope is considered to be same as the relative volume of the total liquid surrounding all hollow fibers in the module. This can be expressed mathematically as follows:

$$\frac{\pi r_f^2 L - \pi r_o^2 L}{\pi r_o^2 L} = \frac{\pi r_s^2 L - N_{sil} \pi r_o^2 L}{N_{sil} \pi r_o^2 L} \qquad \text{(A.1.1)}$$

where r_o, r_s and r_f are the outer radius of the tubular membrane, the internal radius of the shell and the radius of the "free surface" respectively.

Upon rearrangement this gives:

$$\frac{r_f^2}{r_o^2} = \frac{r_s^2}{N_{sil} r_o^2} \qquad \text{(A.1.2)}$$

The void fraction in shell side of the module, ϵ, is defined as follows:

$$\epsilon = 1 - \frac{N_{sil} \pi r_o^2}{\pi r_s^2} \qquad \text{(A.1.3)}$$

where $N_{sil}\ \pi r_o^2$ is the cross-sectional area occupied by the tubular membranes in the module and πr_s^2 is the corresponding area for the shell. Rearranging equation A.1.3 gives:

$$\frac{1}{1-\epsilon} = \frac{r_s^2}{N_{sil} r_o^2} \qquad \text{(A.1.4)}$$

Comparing the result with equation A.1.2. leads to:

$$r_f = \left[\frac{1}{1-\epsilon} \right]^{\frac{1}{2}} r_o \qquad \text{(A.1.5)}$$

APPENDIX 2

THOMAS ALGORITHM TO SOLVE A TRIDIAGONAL SYSTEM OF EQUATIONS

This section outlines the Thomas algorithm for tridiagonal systems that is implemented in a Fortran program to solve the equations for the performance of the single-phase membrane ozonator (de Vahl Davis, 1986).

Consider a system of equations shown below

$$a_i x_{i-1} + b_i x_i + c_i x_{i+1} = d_i \tag{A.2.1}$$

where i = 1, ..., n.

The symbols a, b, c denote the subdiagonal, diagonal and supradiagonal coefficients respectively and d the right hand side of the equation. The following strategy is adopted to solve the set of equations, eliminate x_{i-2} from the $(i-1)^{th}$ equation which gives

$$\beta_{i-1} x_{i-1} + \gamma_{i-1} x_i = \delta_{i-1} \tag{A.2.2}$$

where the β_{i-1}, γ_{i-1}, δ_{i-1} are coefficients that have yet to be determined. Using equation (A.2.2), x_{i-1} is eliminated from the i^{th} equation as shown below

$$x_{i-1} = \frac{(\delta_{i-1} - \gamma_{i-1} x_i)}{\beta_{i-1}} \tag{A.2.3}$$

Inserting the result from (A.2.3) into (A.2.1) yields the following result

$$\left[b_i - \frac{a_i \gamma_{i-1}}{\beta_{i-1}} \right] x_i + c_i x_{i+1} = d_i - \frac{a_i \delta_{i-1}}{\beta_{i-1}} \tag{A.2.4}$$

Comparing the above result with equation (A.2.2) yields by analogy

$$\beta_i x_i + \gamma_i x_{i+1} = \delta_i \tag{A.2.5}$$

where

$$\beta_i = b_i - \frac{a_i \gamma_{i-1}}{\beta_{i-1}} \quad ; \quad \gamma_i = c_i \quad ; \quad \delta_i = d_i - \frac{a_i \delta_{i-1}}{\beta_{i-1}}$$

The above equations are then used to calculate values of β, γ and δ recursively, beginning with the first equation shown below

$$\beta_1 x_1 + \gamma_1 x_2 = \delta_1 \qquad \text{(A.2.6)}$$

and then progressively calculating the values of β, γ and δ as shown below

$$\beta_1 = b_1 ; \quad \gamma_1 = c_1 ; \quad \delta_1 = d_1$$

and for i = 2, 3, ..., n-1

$$\beta_i = b_i - \frac{a_i \gamma_{i-1}}{\beta_{i-1}} \quad ; \quad \gamma_i = c_i \quad ; \quad \delta_i = d_i - \frac{a_i \delta_{i-1}}{\beta_{i-1}}$$

and the n^{th} equation is

$$\beta_n x_n = \delta_n$$

$$\text{which yields} \quad x_n = \frac{\delta_n}{\beta_n}$$

Upon substitution of this result in the $(n-1)^{th}$ equation the result for x_{n-1} is obtained as follows

$$\beta_{n-1} x_{n-1} + \gamma_{n-1} x_n = \delta_{n-1} \qquad \text{(A.2.7)}$$

$$\text{or} \quad x_{n-1} = \frac{(\delta_{n-1} - c_{n-1} x_n)}{\beta_{n-1}}$$

or in general

$$x_i = \frac{(\delta_i - c_i x_{i+1})}{\beta_i} \quad ; \text{ i = n-1 , n-2, ..., 1}$$

The Thomas algorithm outlined above is implemented in a Fortran subroutine which is used to solve the set of equations derived in section 2.3.

APPENDIX 3

COMPUTER PROGRAM TO SIMULATE THE PERFORMANCE OF THE SINGLE-PHASE MEMBRANE OZONATOR

```
C     ***************** Copyright 1997 *********************
C     ***************** Purushottam V. Shanbhag ************
C     ************* Single Phase Modelling  *****************
C     *************** Finite Differences *********************
      PARAMETER (NR = 10, NB = 1000)

      REAL PLIP

C     *********** VARIABLES *********************
      INTEGER I,J, ITER

      REAL U(NR,NB), V(NR,NB), DAL, DBL, BA, DELX, DELETA, X
      REAL UNEW(NR,NB), VNEW(NR,NB)
      REAL ETA(NR),RF,RI,RO,R,L,DAM,DBM, FETA(NR),ALP,BETA
      REAL CAIL, CBOL, ATERM1(NR,NB), ATERM2(NR,NB)
      REAL BTERM1(NR,NB), ARHS(NR,NB), BRHS(NR,NB)
      REAL BTERM2(NR,NB), BTERM3(NR,NB), BCOEFF
      REAL ATERM3(NR,NB), ACOEFF, BUKKA,BINTER
      REAL AINTER, AUKKA,NFIBS,LAM,K2
      REAL BRHTP1, BRHTP2, BRHTP, KONS, EKKA
      REAL KG, QM, REM, TOL, REM1, MW, EX, GFP
      REAL UBACK(NR,NB), VBACK(NR,NB)
      REAL QTEMP, CAOUT, CBOUT, COFFA, UNIVR, TEMP
      REAL UEXIT,VEXIT, SUM, SUMVR, SUMOZONE, SCALE
      REAL GASFLOW,W(NB),CBGM, GASEXIT, WEXIT, INTFAREA
C     ***********  COMMON STATEMENTS ******************
      COMMON/CONS/RF,RI,RO,DAM,DBM,ALP,PHI
      COMMON/CONS2/BETA, NFIBS, PIE, LAM, K2
      COMMON/CONCS/CAIL,CBOL,DAL,DBL
      COMMON/GASCON/KG,QM,KONS,BA, SCALE, COFFA

C     ***** CONSTANT INITIALIZATION *************
C     ****** ALL CONSTANTS IN SI UNITS! ***********

MW= 123.11          ! MW - NITROBENZENE
QG = 100            !QG - Flowrate of Ozone in lumen of silicone capillaries
CAIL=110            !CAIL - Inlet Conc. of Pollutant, cc/min
GFP=2               !GFP - Gas Feed Pressure, psig
CBOG= 180           !CBOG - Feed Concentration, mg/lit (of O2)
```

```
K2=0.6                    !K2 - Second Order Constant
BA=2.5                    !BA - Stoichiometric Constant
QM=8.0 e- 13              !Permeability of Silicone to O2
H=9465.0                  !H - Henry's Law Coefficient for Ozone in Water
DA=0.8346e-9              !Diffusivity of Nitrobenzene in Water, SI
DB=2.01e-9                !Diffusivity of Ozone in Water, SI
DS=0.5                    !Shell ID, inches
DI=0.012                  ! ID of Silicone, inches
DO=0.025                  ! OD of Silicone, inches
L=8.0                     ! Length of Module, inches
NFIBS=97.0                !NFIBS - No. of Capillaries
RS = 2.54e-2 * DS *0.5    !Shell RADIUS
RI = 2.54e-2 * DI *0.5    !IR of the Silicone Capillary
RO = 2.54e-2 * DO *0.5    !OR of the Silicone Capillary
L = 2.54e-2 * L     !Length of Module
GASFLOW = QG *1.0E-6/60 ! CONVERSION M3/S
PI = 3.1416
UNIVR = 8.3144            ! KPA M3/(KGMOLE K)
TEMP = 298
C     ********** FREE SURFACE CALCULATION *************

      RF = (RS*RS/NFIBS)**0.5

C     ******** PARAMETER ESTIMATION ********************
        CAILPPM = CAIL
        CAIL = CAIL/(MW*1000)
        CBGM = CBOG
        CBOG = CBOG/(48*1000)        !GM MOLES/LIT OF O2
        CBOG = CBOG * 24.451         !LIT OF O3/LIT OF O2
        CBOG = CBOG* ((14.696+GFP)*101.325/14.696)
                        !PARTIAL P OF O3, KPA
        CBOL = CBOG/H               !CORRESPONDING AQUEOUS PH CONC.
        ALP = K2*CAIL*RF*RF/DAL
                        !DIMENSIONLESS CONSTANT
        LAM = RO/RF
        PHI = 2*(1-LAM*LAM)/(3+LAM**4.0-(4*LAM*LAM)+4*LOG(LAM))
                        !CONSTANT FOR FETA, HAPPEL FREE SURFACE

        KONS = ((RO/QM)*(LOG(RO/RI)))*(DBL/(RF*H))
                              !CONSTANT FOR GAS TRANSFER

        DELETA = (RF - RO)/(RF*FLOAT(NR-1))
                        !DELTA DIM.LESS RADIUS
        DELX = 1/FLOAT(NB)
```

```
                    !DELTA DIM.LESS LENGTH
      COFFA = (1/L)*(LOG(RO/RI))*(1/(2*PI*NFIBS))
      COFFA = COFFA *GASFLOW/ (UNIVR*TEMP*QM)

C     ********* FLOW LOOP ******************
      DO 599 QTEMP = 0.01,2.0,0.01
      Q=QTEMP
      Q = Q * 1E-6/60            !CONVERT TO M3/S

      VAVG = Q/(PI*RS*RS-PI*RO*RO*NFIBS)
                    !AVERAGE VELOCITY IN THE MODULE

      BETA = (RF*RF*VAVG)/(L*DAL)

C     **********  CONCENTRATION INITIALIZATION  *******
      DO 10 I=1,NR
      U(I,1)=1.0         !INITIAL CONCENTRATION OF POLLUTANT
      V(I,1)=1.0E-10     !INITIAL CONCENTRATION OF OZONE IN AQ. PHASE
10    CONTINUE


c     ************ INITIAL GUESSES! ******************

      DO 20 J = 2, NB
      DO 30 I = 1, NR
      U(I,J) = 0.1                !OVER REST OF THE MODULE

      V(I,J) = 1.0E-6       !OVER REST OF THE MODULE
      UBACK(I,J) = U(I,J)
      VBACK(I,J) = V(I,J)
30    CONTINUE
20    CONTINUE

      ITER = 1
      TOL = 1E-7

80    CONTINUE

      CALL SPEC_A (U, V, UBACK, VBACK, DELX, DELETA)
      CALL SPEC_B (U, V, W, UBACK, VBACK, DELX, DELETA)

      ITER = 2

      DO 145 J = 2, NB
```

```
      DO 155 I = 1, NR

      IF (U(I,J).LE.1.0E-10) THEN
        U(I,J) = 1.0E-10
        ELSE
        ENDIF
        UBACK(I,J) = U(I,J)
      IF (V(I,J).LE.1.0E-10) THEN
        V(I,J) = 1.0E-10
        ELSE
        ENDIF
        VBACK(I,J) = V(I,J)
155   CONTINUE
145   CONTINUE
90     CONTINUE

      CALL SPEC_A (U, V, UBACK, VBACK, DELX, DELETA)
      CALL SPEC_B (U, V, W, UBACK, VBACK, DELX, DELETA)

C     ************************************************************
C     *** CONVERGENCE TESTING!*********************************
C     ************************************************************
        PLIP = 0.0
      DO 60 J = 2, NB
      DO 70 I = 1, NR
      IF (U(I,J).LE.1.0E-4) THEN
        U(I,J) = 1.0E-4
      ELSE
        ENDIF
        IF (V(I,J).LE.1.0E-10) THEN
        V(I,J) = 1.0E-10
      ELSE
        ENDIF
      IF (ABS((U(I,J)-UBACK(I,J))/UBACK(I,J)).GT.TOL) THEN
        PLIP = 1.0
        UBACK(I,J) = U(I,J)
        VBACK(I,J) = V(I,J)
        ELSE
        PLIP = 0.0
        ENDIF

70    CONTINUE
60    CONTINUE
```

```
      IF (PLIP.EQ.1.0) THEN
      iter = iter+1
      GOTO 90
    ELSE
    ENDIF
C     ********** MATERIAL BALANCES **********
      SUM = 0.0
      SUMVR = 0.0
      SUMOZONE = 0.0
      UEXIT = 0.0
      VEXIT = 0.0
      J =NB

    ETA(1) = RO/RF
    FETA(1) = PHI *(ETA(1)**2-LAM**2 + 2*LOG( LAM/ETA(1) ))

      SUM = SUM + U(1,J)*FETA(1)
      SUMOZONE = SUMOZONE + V(1,J)*FETA(1)
      SUMVR = SUMVR + FETA(1)

    ETA(NR) = 1
    FETA(NR) = PHI *(ETA(NR)**2 - LAM**2 + 2*LOG (LAM/ETA(NR)))

      SUM = SUM + U(NR,J)*FETA(NR)
      SUMOZONE = SUMOZONE + V(NR,J)*FETA(NR)
      SUMVR = SUMVR + FETA(NR)

      DO 91 I = 2,NR-1
      ETA (I) = ETA(I-1) + DELETA
      FETA(I) = PHI * (ETA(I)**2 - LAM**2 + 2*LOG (LAM/ETA(I)))

      SUM = SUM + U(I,J)*FETA(I)
      SUMOZONE = SUMOZONE + V(I,J)*FETA(I)
      SUMVR = SUMVR + FETA(I)

91    CONTINUE
      WEXIT = W(NB)
      UEXIT = SUM/SUMVR
      VEXIT  = SUMOZONE/SUMVR
      CAOUT = CAIL*UEXIT*1000*MW
      CBOUT = CBOL*VEXIT
      GASEXIT = W(NB)*CBGM
      XCONV = (CAILPPM - CAOUT)/CAILPPM
      EKKA = ((CAILPPM-CAOUT)*Q/(1000*MW))/INTFAREA
```

```
C     ***************************************************
c     ***************** Print Outs! *********************
c     ***************************************************
      WRITE(24,*)CAOUT,EKKA,QTEMP,XCONV,GASEXIT
      CAOUT = 0.0
      CBOUT = 0.0
      DO 62 J = 1,NB
      DO 61 I = 1, NR
      UBACK(I,J) = 0.0
      U(I,J) =0.0
      VBACK(I,J) =0.0
      V(I,J) = 0.0
61    CONTINUE
62    CONTINUE
599   CONTINUE
      STOP
      END

C     ****** SUBROUTINE FOR SPECIES A .... POLLUTANT ************

      SUBROUTINE SPEC_A (U, V, UBACK, VBACK, DELX, DELETA)
       PARAMETER (NR = 10, NB = 1000)
        REAL CONS(NR,NB)
C     ********** VARIABLES *********************
      INTEGER I,J, ITER
      REAL UBACK(NR,NB), VBACK(NR,NB)
      REAL U(NR,NB), V(NR,NB), DAL, DBL, BA, DELX, DELETA, X
      REAL UNEW(NR,NB), VNEW(NR,NB)
      REAL ETA(NR),RF,RI,RO,R,L,DAM,DBM, FETA(NR),ALP,BETA
      REAL CAIL, CBOL, ATERM1(NR,NB), ATERM2(NR,NB)
      REAL BTERM1(NR,NB), ARHS(NR,NB), BRHS(NR,NB)
      REAL BTERM2(NR,NB), BTERM3(NR,NB), BCOEFF
      REAL ATERM3(NR,NB), ACOEFF, BUKKA,BINTER
      REAL AINTER, AUKKA,NFIBS,LAM,K2
      REAL BRHTP1, BRHTP2, BRHTP, KONS
        REAL COFFA, UNIVR, TEMP, W(NB)

      REAL KG, QM, REM, TOL, REM1, MW, EX, GFP
C     ***********  COMMON STATEMENTS ******************
      COMMON/CONS/RF,RI,RO,DAM,DBM,ALP,PHI
      COMMON/CONS2/BETA, NFIBS, PIE, LAM, K2
      COMMON/CONCS/CAIL,CBOL,DAL,DBL
      COMMON/GASCON/KG,QM,KONS,BA, SCALE, COFFA
```

```
C   ******* EQUATION FOR POLLUTANT IN AQUEOUS PHASE ************
    DO 100 J = 2,NB
C    *********** BOUNDARY CONDITION AT I = 1 **************
    ETA(1) = RO/RF

    FETA(1) = PHI *( ETA(1)**2-LAM**2 + 2*LOG( LAM/ETA(1) ))

CONS(1,J) = ((DELX*DELETA)/(2*ETA(1))-DELX)
 ATERM1(1,J) = 0.0                    !U(0,J)= 0.0

 ATERM3(1,J) = -((DELX*DELETA)/(2*ETA(1))+DELX)
 ATERM3(1,J) = CONS(1,J) + ATERM3(1,J)
 AINTER = ((ALP*CBOL/CAIL)*DELX*DELETA*DELETA*(V(1,J)-  V(1,J-1)))
 ACOEFF = BETA*FETA (1)*DELETA*DELETA +2*DELX
 AUKKA = (ALP*CBOL/CAIL)*DELX*DELETA*DELETA*V(1,J-1)
 ATERM2(1,J) = AUKKA + ACOEFF                              !U(I,J)

 ARHS(1,J) = U(1,J-1)* (BETA*FETA(1)*(DELETA*DELETA)-AINTER)
                                                  !U(I,J-1)

C    ***** BOUNDARY VALUE AT I = NR ***************
    ETA(NR) = 1
    FETA(NR) = PHI *  (ETA(NR)**2 - LAM**2 + 2*LOG (LAM/ETA(NR)))
    CONS(NR,J) = -((DELX*DELETA)/(2*ETA(NR))+DELX)      !U(I+1,J)
 ATERM3(NR,J) = 0.0            !U(NR-1,J)=U(NR+1,J)

 ATERM1(NR,J) = ((DELX*DELETA)/(2*ETA(NR))-DELX)         !U(I-1,J)
 ATERM1(NR,J) = ATERM1(NR,J) + CONS(NR,J)
 AINTER=((ALP*CBOL/CAIL)*DELX*DELETA*DELETA*(V(NR,J)- V(NR,J-1)))
 ACOEFF  = BETA*FETA(NR)*DELETA*DELETA +2*DELX
 AUKKA = (ALP*CBOL/CAIL)*DELX*DELETA*DELETA*V(NR,J-1)
 ATERM2(NR,J) = AUKKA + ACOEFF                             !U(I,J)
 ARHS(NR,J) = U(NR,J-1)* (BETA*FETA(NR)*(DELETA*DELETA)-AINTER)
                                                  !U(I,J-1)

C    ********** GRID POINTS INSIDE **************

    DO 200 I = 2, NR-1
    ETA (I) = ETA(I-1) + DELETA
    FETA(I) = PHI * (ETA(I)**2 - LAM**2 + 2*LOG (LAM/ETA(I)))


 ATERM3(I,J) = -((DELX*DELETA)/(2*ETA(I))+DELX)              !U(I+1,J)
 ATERM1(I,J) = ((DELX*DELETA)/(2*ETA(I))-DELX)        !U(I-1,J)
```

```
 AINTER = ((ALP*CBOL/CAIL)*DELX*DELETA*DELETA*(V(I,J)-  V(I,J-1)))

 ACOEFF = BETA*FETA (I)*DELETA*DELETA  +2*DELX
 AUKKA = (ALP*CBOL/CAIL)*DELX*DELETA*DELETA*V(I,J-1)
 ATERM2(I,J) = AUKKA + ACOEFF                          !U(I,J)
 ARHS(I,J) = U(I,J-1)* (BETA*FETA(I)*(DELETA*DELETA)-AINTER)
                                                       !U(I,J-1)

200   CONTINUE

      CALL THOMAS(ATERM1,ATERM2,ATERM3,ARHS,UNEW,J)

      DO 60 I = 1, NR
      UBACK(I,J) = U(I,J)
      U(I,J) = UNEW(I,J)
60    CONTINUE
100   CONTINUE

    RETURN
    END

C    ***************** SUBROUTINE FOR SPECIES B....OZONE *******
      SUBROUTINE SPEC_B (U, V, W, UBACK, VBACK, DELX, DELETA)

      PARAMETER (NR = 10, NB = 1000)

      REAL CONS1(NR,NB), CONS3(NR,NB)
C    ************ VARIABLES *********************
    INTEGER I,J, ITER

    REAL U(NR,NB), V(NR,NB), DAL, DBL, BA, DELX, DELETA, X
    REAL UNEW(NR,NB), VNEW(NR,NB), W(NB)
    REAL ETA(NR),RF,RI,RO,R,L,DAM,DBM, FETA(NR),ALP,BETA
    REAL CAIL, CBOL, ATERM1(NR,NB), ATERM2(NR,NB)
    REAL BTERM1(NR,NB), ARHS(NR,NB), BRHS(NR,NB)
    REAL BTERM2(NR,NB), BTERM3(NR,NB), BCOEFF
    REAL ATERM3(NR,NB), ACOEFF, BUKKA,BINTER
    REAL AINTER, AUKKA,NFIBS,LAM,K2
    REAL BRHTP1, BRHTP2, BRHTP, KONS, COFFA
    REAL KG, QM, REM, TOL, REM1, MW, EX, GFP
    REAL UBACK(NR,NB), VBACK(NR,NB), CK
C    ************  COMMON STATEMENTS ********************
    COMMON/CONS/RF,RI,RO,DAM,DBM,ALP,PHI
    COMMON/CONS2/BETA, NFIBS, PIE, LAM, K2
```

```
      COMMON/CONCS/CAIL,CBOL,DAL,DBL
      COMMON/GASCON/KG,QM,KONS,BA, SCALE, COFFA

C     ************************************************************
      CK = 1 + DELX/COFFA

      W(1) = 1          !INLET OZONE GAS CONCENTRATION

      DO 100 J = 2, NB

C     ********* GAS PHASE MODELLING **********************

 W(J) = (1/CK)*(W(J-1)+V(1,J-1)*(CK-1))

C     ****** BOUNDARY CONDITION AT I = 1 *****************

      ETA(1) = RO/RF
      FETA(1) = PHI * (ETA(1)**2 - LAM**2 + 2*LOG(LAM/ETA(1)))

c     ********** change it here **********

 BTERM1(1,J) = 0                !V(0,J)
      CONS1(1,J) = (DELX*DELETA)/(2*ETA(1))-DELX        !V(I-1,J)

 BINTER = (ALP*DELX*DELETA*DELETA*(DAL/DBL)*BA*(U(1,J)-U(1,J-1)))

 BRHS(1,J)=V(1,J-1)*(BETA*FETA(1)*(DELETA*DELETA)*
     & (DAL/DBL)-BINTER)

 BRHS(1,J) = BRHS(1,J) - W(J)*CONS1(1,J)*(2*DELETA/KONS)
                                  !V(1,J-1)
 BTERM3(1,J) = -2*DELX
 BCOEFF = BETA*FETA(1)*DELETA*DELETA*(DAL/DBL)+2*DELX
 BUKKA = ALP*DELX*DELETA*DELETA*(DAL/DBL)*BA*U(1,J-1)

 BTERM2(1,J) = BCOEFF+BUKKA                        !V(I,J)
 BTERM2(1,J) = BTERM2(1,J) - CONS1(1,J)*(2*DELETA/KONS)

C     ********** BOUNDARY CONDITION AT I = NR ****************
      ETA(NR) = 1
      FETA(NR) = PHI *  (ETA(NR) **2 - LAM**2 + 2*LOG (LAM/ETA(NR)))

 BTERM3(NR,J) = 0.0             !V(NR-1,J)=V(NR+1,J)
```

```
      CONS3(NR,J) = -((DELX*DELETA)/2*ETA(NR)  +DELX)     !V(I+1,J)
      BINTER = (ALP*DELX*DELETA*DELETA*(DAL/DBL)*BA*(U(NR,J)-U(NR,J-1)))

      BRHS(NR,J)=V(NR,J-1)*(BETA*FETA(NR)*(DELETA*DELETA)*
     &  (DAL/DBL)-BINTER)
                                        !V(I,J-1)

      BTERM1(NR,J) = (DELX*DELETA)/(2*ETA(NR))-DELX      !V(I-1,J)
      BTERM1(NR,J) = BTERM1(NR,J)+CONS3(NR,J)
      BCOEFF = BETA*FETA (NR)*DELETA*DELETA*(DAL/DBL)+2*DELX
      BUKKA = ALP*DELX*DELETA*DELETA*(DAL/DBL)*BA*U(NR,J-1)
      BTERM2(NR,J) = BCOEFF+BUKKA                        !V(I,J)

C     ******* INSIDE GRID POINTS FOR O3 IN AQUEOUS PHASE ************

          DO 200 I = 2, NR-1
          ETA (I) = ETA(I-1) + DELETA
          FETA(I) = PHI *  (ETA(I) **2 - LAM**2 + 2*LOG (LAM/ETA(I)))

      BINTER = (ALP*DELX*DELETA*DELETA*(DAL/DBL)*BA*(U(I,J)-U(I,J-1)))
      BRHS(I,J)=V(I,J-1)*(BETA*FETA(I)*(DELETA*DELETA)*
     &  (DAL/DBL)-BINTER)
                                        !V(I,J-1)
      BTERM1(I,J) = (DELX*DELETA)/(2*ETA(I))-DELX        !V(I-1,J)
      BTERM3(I,J) = -((DELX*DELETA)/2*ETA(I)  +DELX)     !V(I+1,J)
      BCOEFF = BETA*FETA (I)*DELETA*DELETA*(DAL/DBL)+2*DELX
      BUKKA = ALP*DELX*DELETA*DELETA*(DAL/DBL)*BA*U(I,J-1)
      BTERM2(I,J) = BCOEFF+BUKKA                         !V(I,J)

  200  CONTINUE
          CALL THOMAS (BTERM1,BTERM2,BTERM3,BRHS,VNEW,J)
            DO 60 I = 1, NR
            VBACK(I,J) = V(I,J)
            V(I,J) = VNEW(I,J)
   60     CONTINUE
  100  CONTINUE
          RETURN
          END

C ******************** THOMAS ALGORITHM ***************************
C     **** Algorithm from, Page 86, Numerical Methods in Engineering
c     **** and Science, Graham de Vahl Davis, Allen and Unwin (pub.),
c     **** TA 335.D38.1986
c     ***********************************************************
```

```
      SUBROUTINE THOMAS(A1,A2,A3,A4,X,J)

       PARAMETER (NR = 10, NB = 1000)
C     ********** VARIABLES *********************
      INTEGER I,J

      REAL X(NR,NB)
      REAL A1(NR,NB), A2(NR,NB), A4(NR,NB)
      REAL A3(NR,NB), BETA(NR), DELTA(NR), EPS

      BETA(1) = A2(1,J)
      DELTA(1) = A4(1,J)

      DO 100 I = 2, NR
      EPS = A1(I,J)/BETA(I-1)
      BETA(I) = A2(I,J) - EPS*A3(I-1,J)
      DELTA(I) = A4(I,J) - EPS*DELTA(I-1)
100   CONTINUE
      X(NR,J) =  DELTA(NR)/BETA(NR)
      DO 200 I = NR - 1, 1, -1
      X(I,J) = (DELTA(I)- A3(I,J)*X(I+1,J))/BETA(I)
200   CONTINUE
      RETURN
      END
```

APPENDIX 4

DETERMINATION OF R_T; AN ESTIMATE OF THE NO. OF MOLES OF OZONE DIFFUSING ACROSS THE SILICONE CAPILLARIES OVER THE WHOLE MODULE SILTEF #2

Module Characteristics of SILTEF #2

Effective module length : 20.8 cm.

Silicone capillaries : 48 nos.; ID / OD : 0.0305 mm / 0.0635 mm.

Teflon tubules : 6 nos.; ID / OD : 0.99 mm / 2.00 mm.

Effective membrane thickness when the Teflon tubules are not wetted out by the FC phase : 4800 μm.

Effective diffusivity of ozone in FC 43, $D_{O_3}^{FC}$, at 25°C calculated from the Wilke-Chang equation : 1.3702 e-5 cm²/s.

Permeability of ozone in silicone membranes, $Q_{sil}^{m} \approx$ 1.0 e-12 (kgmole.m)/(m².s.kPa).

From Trivedi (1992) ~60 mg O_3/L of air gave an equilibrium concentration of 78 mg ozone /L FC43.

Henry's Law Constant calculated for equlibrium of ozone between gas phase and FC43 as the fluorocarbon phase $\approx$ 1.905 e+3 (kPa)/(kgmol of ozone/ m³ of FC43).

Consider the permeation of ozone across the silicone capillaries through the fluorocarbon medium to the aqueous-organic interface. An assumption is made that the concentration of ozone at the aqueous-organic interface is zero and therefore the diffusional resistance in the aqueous phase boundary layer can be ignored. In the absence of any reaction, it is apparent from Figure 3.3.1 that ozone has to permeate across three distinct regions to

reach the aqueous-organic interfaces, the silicone capillary wall, the fluorocarbon phase and the microporous Teflon tubule wall wetted out by the FC phase.

The permeation flux of ozone across the silicone capillaries can be described as follows:

$$J = \frac{R_T}{A_{sil}} = \frac{Q^m_{sil}}{\delta_{sil}} (p_i^{sil} - p_o^{sil}) \qquad \text{(A.4.1)}$$

where A_{sil} is the logarithmic mean permeation area (equation 2.4.1) shown below :

$$A_{sil} = \pi \frac{(d_o^{sil} - d_i^{sil})}{\ln (d_o^{sil} / d_i^{sil})} N_{sil} L \qquad \text{(A.4.2)}$$

δ_{sil} is the wall thickness of the silicone capillaries and Q^m_{sil} is the permeability coefficient of ozone across the silicone capillary membrane.

The permeation of ozone across the FC liquid membrane can be written as follows:

$$\frac{R_T}{A_{lm}} = k_m (C_o^{sil} - C_o^{Tef}) = \frac{k_m}{H_{FC}} (p_o^{sil} - p_o^{Tef}) \qquad \text{(A.4.3)}$$

where H_{FC} is the Henry's Law constant for ozone between the gas phase and the FC phase. k_m is the mass transfer coefficient of ozone through the FC phase and is given by $D_{O_3}^{FC} / \delta_m$ where δ_m is the experimentally determined liquid membrane thickness. A_{lm} is the log mean transfer area and is calculated as follows :

$$A_{lm} = \pi L \frac{(d_o^{Tef} N_{Tef} - d_o^{sil} N_{sil})}{\ln (d_o^{Tef} N_{Tef} / d_o^{sil} N_{sil})} \qquad \text{(A.4.4)}$$

The permeation flux of ozone across microporous Teflon tubules may be written as follows:

$$\frac{R_T}{A_{Tef}} = k_{Tef}\,(C_o^{Tef} - 0) = \frac{k_{Tef}}{H_{FC}}\,(p_o^{Tef} - 0) \qquad \text{(A.4.5)}$$

where H_{FC} is the Henry's law constant for ozone between the gas phase and the FC phase and k_{Tef} can be written as follows :

$$k_{Tef} = \frac{D_{O_3}^{FC}\,\epsilon_s}{\tau_s\,\delta_{Tef}} \qquad \text{(A.4.6)}$$

where ϵ_s is the porosity of the Teflon tubule and has a value of 0.5 for the Teflon tubules. τ_s is the tortuosity of the pores in the Teflon tubules and is 1.5 for the Teflon tubules. A_{Tef} is defined as follows:

$$A_{Tef} = \pi\, N_{Tef}\, \frac{(d_o^{Tef} - d_i^{Tef})}{\ln(d_o^{Tef} / d_i^{Tef})}\, L \qquad \text{(A.4.7)}$$

At steady state the amount of ozone permeating per unit time across each of the regions is constant and equal to R_T. Therefore equations (A.4.1), (A.4.3) and (A.4.5) can be rearranged and rewritten as follows :

$$R_T \left\{ \frac{1}{\left[\frac{Q_{sil} A_{sil}}{\delta_{sil}}\right]} + \frac{1}{\left[\frac{k_m A_{lm}}{H_{FC}}\right]} + \frac{1}{\left[\frac{k_{Tef} A_{Tef}}{H_{FC}}\right]} \right\} = p_i^{sil} \qquad \text{(A.4.8)}$$

From equations A.4.2, A.4.4 and A.4.7, A_{sil}, A_{lm} and A_{Tef} are calculated to be 1.4115 e-2 m^2, 1.37 e-2 m^2 and 6.06 e-3 m^2 respectively. k_m is calculated to be 2.86 e-7 m/s and k_{Tef} is calculated to be 4.25 e-7 m/s. For a feed composition of 60.87 mg/L of O_2 (1.268 e-3 kgmol of O_3/m^3 of O_2), **R_T was calculated to be 2.5477 e-12 kgmol/sec.**

APPENDIX 5

COMPUTER PROGRAM TO SIMULATE THE PERFORMANCE OF THE TWO-PHASE MEMBRANE OZONATOR

```
C     ***************** Copyright 1997 **********************
C     ***************** Purushottam V. Shanbhag *************
C     ************************************************
C     ************* DATE : 31 OCTOBER 1996 **************
C     ************************************************
C     Program to solve degradation  of hazardous organics
c     from wastewater in the novel membrane reactor
c     using FC-phase as inert second phase;
c     Second order reaction rate is used to solve
c     concentration profile for pollutant and ozone
c     CAB = > PPM = mg/liter = gm/m**3
c     ********* mg/liter = gm/m**3=(1.0E-3/AMW) kgmole/m**3 **********
c     ****  P concentration of ozone in gas -phase in mg/liter *******
C     ****** SK2 second order rate constant sec-1 liter-mole-1 *******
C     ****** SK2 second order rate constant sec-1 (m**3/kgmole)-1 ****
c     ****** SK2 converted to SKF (sec-1) ***************************
C     ****** temp temperature of the system (K) **********************
C     ****** stoichiometric ratio SR *********************************

      CHARACTER COMP*20
      INTEGER IWORK(59810),DIV
      REAL BETA(10),DPHIDR(10),DIF(50),UKKA
      REAL XXINIT(101),YYINIT(4,101),XXF(101),YYF(4,101),CAI(50),
     2   ER(4),CA(9,101),DCADX(9,101), CB(9,101),DCBDX(9,101),
     4    WORK(59810),CAB0
      REAL CAB, CABULKIN, CAIN, CAPSE1, CABIN2, CABIN3, QFI
      REAL AKW, CAIGESS, CABI, HEN
      REAL P, GCONP, PARTIALP, UNIVR, DARS, AREAS, ZOKA
      REAL Q, GCONQ, PARTIALQ, CBIGESS, CBB0, PERM, DELSIL, RT
      REAL SLOPE, TEMPVAR2, TEMPVAR3, TEMPVAR4, PARTG, PGESS
      REAL CBIN, CBOUT, CBG, PARTIALG(1000), PINTER(1000), CBTEMP
      REAL PARTIAL2G(1000), PINTER2(1000), FLUXA,FLUXB
      REAL CASIN, CASOUT, CBSIN, CBSOUT, CASAVG, CBSAVG
      REAL PART2G, RT2, CABIN4, P2GESS, CBG2, FLUX2O3, CAB2
      REAL ACK1, ACK2, ETA, EKKA,CAI2GESS
      REAL W1(101), W2(101), W3(101), W4(101)
      EXTERNAL FCN1,FCN2,FCN3,B2PFD
      COMMON GAMA1,GAMA2,CA0,CB0,SR
      COMMON/VAR2/CAB0,CBB0
```

```
C     *** CHARACTERISTICS OF INDIVIDUAL POLLUTANT ******
C     FOR PHENOL (Molecular Weight : 94.0)
C     COMP='PHENOL'
C     DATA AMW,AMI,SKF,DA,DAW,DZONE/94.0,0.01,1.0,2.2E-9,0.9135e-9,
C     1     4.0E-9/
C     DATA SK2,SR/40.0,2.0/

C     FOR ACRYLONITRILE (Molecular Weight : 53.0)
c     COMP='ACRYLONITRILE'
c    DATA AMW,AMI,SKF,DA,DAW,DZONE/53.0,0.12,0.01,2.32E-9,1.1621E-9,
c     1     1.37E-9/
c     DATA SK2,SR/38.2,0.5/
c     DATA SK2,SR/155,1.0/

C     FOR NITROBENZENE (Molecular Weight : 123.0)
      COMP='NITROBENZENE'
  DATA AMW,AMI,SKF,DA,DAW,DZONE/123.0,1.9,5.0E-4,0.556E-9,0.8346E-9,
      1     1.37E-9/     !DZONE CALCULATED FOR FC43
      DATA SK2,SR/3.5,3.0/

C     FOR TCE (Molecular Weight : 131.4)
c     COMP='TCE'
c     DATA AMW,AMI,SKF,DA,DZONE/131.4,19.0,1.3245E-3,2.05E-9,4.0E-9/
c     DATA DAW/0.84E-9/
c     AMI = 10.0
c     DATA SK2,SR/40.0,3.0/

c     FOR TOLUENE (Molecular Weight : 92.0)
C     COMP='TOLUENE'
C   DATA AMW,AMI,SKF,DA,DAW,DZONE/92.0,45.0,1.38E-4,1.80E-9,0.86E-9,
C     1     4.0E-9/
C     ************ MODULE CHARACTERISTICS **********************
C     *************** SILTEF MODULE *************************
      DATA NMODUL,DFI,DFO,RLEN,NFIBF/6,990.0E-6,2280.0E-6,
      2     0.208,6/
      DATA TEFF/4800.0E-6/
      DATA DSI, DSO, NSIL/305E-6, 635E-6, 48/
C     ***********************************************************
      tau = 1.5
      EPS = 0.5
      DTFLM = (DFO-DFI)/(LOG(DFO/DFI))
      CONA = (TAU*(DFO-DFI))/EPS
      TEFF = ((DFI/DTFLM)*CONA) + (DFI/DFO)*TEFF
```

```
C     ************************************************************
C     ********** DEFINITION OF SOME CONSTANTS USED ************
C     ************************************************************
      DB=DZONE
      UNIVR = 8.3144 !KPA M3/(KGMOLES K)
      DIV = 375
      TEMP = 298.0
      hen = 1.906e3
C     ********** MARK1 ***************************
      PIE = 3.14159
      PERM = 8.0E-13
                        !(KGMOL.M/M2.SEC.KPA)
      UKKA = PIE*DFI*FLOAT(NFIBF)
      ZOKA = PIE*((DSO-DSI)/(LOG(DSO/DSI)))*FLOAT(NSIL)
      DELSIL = (DSO-DSI)/2.0
      RLEN = RLEN
      AREAF=RLEN*UKKA
      AREAS=RLEN*ZOKA
      ARF=PIE*DFI*DFI/4.0
      ARSIL = PIE*DSI*DSI/4.0
      DLEN = RLEN/FLOAT(DIV)
      DAREA = UKKA*DLEN
      DARS = ZOKA*DLEN
C     ********** INFLUENT GAS CONCENTRATION ********************
c     P=60.0*2.0
      P=60.0*3.0
      GCONP = (P/48.0)*1E-3 !(KG MOLE /M3)

      PARTIALP = GCONP*UNIVR*TEMP
                        !(PARTIAL PRESSURE OF O3 IN O2 AT INLET)

      CB0 = PARTIALP/HEN
C     ************************************************
      SKF=SK2*CB0       !CALCULATION OF K2 FROM (PSEUDO K1)/CB0
C     ********** GAS FLOWRATE = VG CC/MIN ************
C     VG = 30.0   ! USED FOR NITROBENZENE
      VG = 100.0  ! USED FOR NITROBENZENE
      VJOE = VG
      VG=VG*1.0E-6/60.0 !GAS FLOWRATE IN M**3/SEC
C     ************ MARK2 **********************
      RT = 2.5477E-12/FLOAT(DIV)    !WORKS FOR PERM=8E-13
C     ************ DEFINE ETA ************
      ETA = (PERM/DELSIL)*((UNIVR*TEMP*DARS)/(VG))
```

```
C     ** INFLUENT POLLUTANT (BULK) CONCENTRATION *********

      CAIN = 120.0
C     CAIN = 978.0
c     CAIN = 1400.0
      CABULKIN=CAIN/AMW*1E-3   ! CONVERSION TO KGM MOLE/M**3
      CA0=CABULKIN*AMI
C     ****************************************************************
      DO 500 I=1,20

      QFI = 0.1+(I-1)*0.1              FLOW RATE cc/min
      QF=QFI*1.0E-6/60.0               !FLOW RATE m**3/sec

C     FLOWRATES (PER FIBER) : M**3/SEC
      QFPF=QF/FLOAT(NFIBF)
                        ! SPECIFY INLET COMPOSITION
      CAPS2IN=CABULKIN
C     ################################################################
C     calculation of mass transfer coefficient in the feed side
C     cross sectional area of one feed fiber
C     velocity of feed solution solution
      VF=QFPF/ARF

C     calculation of the product of NRe & NSc
      RESC=(DFI*VF/DAW)
      GZNUM=PIE*DFI*RESC/(4.0*RLEN)
      J=1
      SUM=0.0
129   BETA(J)=4.0*FLOAT(J-1)+(8.0/3.0)
      DPHIDR(J)=1.01276/(BETA(J)**(1.0/3.0))
      PHI=-(BETA(J)**2)*(2.0*RLEN/DFI)/RESC
      ANUM=DPHIDR(J)*EXP(PHI)
      DENOM=8.0*ANUM/(BETA(J)**2)
      IF (DENOM.LT.1.0E-5) THEN
      SUM=SUM+DENOM
      SHNUM=0.5*(DFI/RLEN)*RESC*((1.0-SUM)/(1.0+SUM))
      AKW=(DAW/DFI)*SHNUM
      ELSE
      SUM=SUM+DENOM
      J=J+1
      GO TO 129
      END IF
C
C     ******* G - GAMMA - HATTA NO. ************
```

```
      G=TEFF*SQRT(SKF/DA)
      ANUM=(EXP(G)-EXP(-G))
      DENOM=(EXP(G)+EXP(-G))
      F1=ANUM/DENOM
      R2=G*DA*AMI/(TEFF*F1*AKW)
C     ********** SPECIFY INLET CONCENTRATIONS ***********
      CAPSE1 = CAIN/AMW*1E-3
      CAB = CAIN/AMW*1E-3 ! CONVERSION TO KGM MOLE/M**3
      CBG = GCONP
C     ************ BEGIN MODULE LOOP **********************
      DO 2000 L=1,DIV
      CAIGESS=AMI*CAB/(1.0+R2)
C     CAIGESS = INTERFACIAL CONCENTRATION IN THE FC PHASE
      CAPK = AMI*CAPSE1/(1+R2)
      IF (L.EQ.1) THEN
      PARTG = PARTIALP              !FOR DIV = 1
      ELSE
      PARTG = PARTIALG(L-1)
      ENDIF
      PGESS = PARTG - (RT/(DARS*PERM/DELSIL))
C     ****************************************************
      IL=1
      CBB0 = PGESS/HEN ! iN THIS CASE CONC. IN THE FC PHASE
      CAB0 = CAIGESS          !IN THIS CASE CONC. IN FC PHASE
      CABI = CAB0/AMI
      CAPSK = CAPK/AMI
      QLUX = G*DA*CAPSK*AMI/(TEFF*F1)
55    FLUXBL=AKW*(CAB-CABI)
      GAMA1=SK2*CB0*TEFF*TEFF/DA
      GAMA2=SR*SK2*CA0*TEFF*TEFF/DB
C     #  SOLVING BOUNDARY VALUE PROBLEM USING B2PFD    #
      JJ=1
      XA=0.0
      XB=1.0
      N=4
      NGMAX=101
      NGRID=51
      IP=2
      IR=0
      LDFIN=4
      LDINI=4
      TOL = 0.1
      PSTEP=0.0
      PRNT=.FALSE.
```

```
      LIN=.FALSE.
      II=1
      R1=CA0/CB0

      G1=TEFF*SQRT(SK2*CB0/DA)
      G2=TEFF*SQRT(SR*SK2*CA0/DB)
      IF (G2.GT.75)THEN
      G2 = 75
      ELSE
      ENDIF

      DO 21 J=1,NGRID
      XXINIT(J)=FLOAT(J-1)*(XB-XA)/FLOAT(NGRID-1)+XA

      A1=0.5*(EXP(G2)+EXP(-G2))

      A4=0.5*(EXP(G1)-EXP(-G1))

      A9=0.5*(EXP(G1)-EXP(-G1))       !SINH G1

      A10=0.5*(EXP(G1)+EXP(-G1))    !COSH G1

      A5=0.5*(EXP(G1*(1.0-XXINIT(J)))-EXP(-G1*(1.0-XXINIT(J))))

      A6=0.5*(EXP(G1*(1.0-XXINIT(J)))+EXP(-G1*(1.0-XXINIT(J))))

      A7=0.5*(EXP(G1*XXINIT(J))+EXP(-G1*XXINIT(J))) !COSH(G1_X)

      A8=0.5*(EXP(G1*XXINIT(J))-EXP(-G1*XXINIT(J)))   !SINH(G1_X)

      YYINIT(1,J)=A6/A10*(CAB0/CA0)
      YYINIT(2,J)=-G1*(A5/A10)*(CAB0/CA0)

      A2=0.5*(EXP(G2*XXINIT(J))+EXP(-G2*XXINIT(J)))

      A3=0.5*(EXP(G2*XXINIT(J))-EXP(-G2*XXINIT(J)))

      YYINIT(3,J)=A2/A1*(CBB0/CB0)

      YYINIT(4,J)=(A3/A1)*G2*(CBB0/CB0)

21    CONTINUE

      CALL B2PFD(FCN1,FCN2,FCN3,FCN1,FCN3,N,IP,IR,XA,XB,
```

```
     1  PSTEP,TOL,NGRID,XXINIT,YYINIT,LDINI,LIN,PRNT,
     2   NGMAX,NF,XXF,YYF,LDFIN,ER,
     3   WORK,IWORK)

      DO 900 J = 1,NF
      W1(J) = YYF(1,J)
      W2(J) = YYF(2,J)
      W3(J) = YYF(3,J)
      W4(J) = YYF(4,J)
900   CONTINUE

C     ************************************************************
C     *************IMSL ENDS**************************************
C     ************************************************************
      FLUXO3=YYF(4,NGRID)*DB*CB0/TEFF

      FLUXR=-YYF(2,1)*DA*CA0/TEFF
C     ************************************************************
      CAB0 = YYF(1,1)*CA0
      CABI = CAB0/AMI
      CBB0 = YYF(3,NGRID)*CB0
30    CONTINUE
C     ************** AQUEOUS PHASE BALANCE  *********************
      FLUXA=FLUXR
      CASIN = CAB
      CABIN2 = 0.0
      CABIN2=CAB-((DAREA*FLUXR)/QF)
      CAB = CABIN2
      CASOUT = CAB
      CABIN3=CAPSE1-((DAREA*QLUX)/QF)
      CAPSE1 = CABIN3
C     ******************* GAS PHASE BALANCE ********************
      CBB0 = YYF(3,NGRID)*CB0
      PINTER(L) = CBB0*HEN
      FLUXO3=YYF(4,NGRID)*DB*CB0/TEFF
      IF (L.EQ.1) THEN
      PARTIALG(L)=((2/ETA-1)*PARTIALP+2*PINTER(L))/(2/ETA+1)
      ELSE
      PARTIALG(L)=((2/ETA-1)*PARTIALG(L-1)+2*PINTER(L))/(2/ETA+1)
      ENDIF
C     ************************************************************
C     ******* To Examine Interfacial Fluxes and Concentrations ***********
C     *************** Restart Loop ***************************
C     ************************************************************
```

```
C     *** TO CALCULATE THE POL. INTERFACIAL CONCENTRATION **
      RK = 1.0
22    CAB2 = CASIN
      FLUXCAL = (QF*(CASIN - CASOUT))/DAREA
      CASAVG = (CASIN + CASOUT)/2.0
      CAI2GESS = CASAVG - (FLUXCAL/AKW)
C     ** TO CALCULATE THE OZONE INTERFACIAL CONC. AT SIL/FC **
      CBG2 = CBSIN
      PAVG = (PARTIALG(L-1)+PARTIALG(L))/2.0
      PART2G = PAVG
      CONS = (VG*DARS)/(UNIVR*TEMP)
      RT2 = (PARTIALG(L-1)-PARTIALG(L))*CONS
      IF (RT2.EQ.0.0) THEN
      RT2 = RT/10.0
      ELSE
      ENDIF
      P2GESS = PART2G - (RT2/(DARS*PERM/DELSIL))
      IL=1
      CBB0 = P2GESS/HEN ! iN THIS CASE CONC. IN THE FC PHASE
      CABI = CAI2GESS          !IN THIS CASE CONC. IN AQ. PHASE
      CAB0 = CABI*AMI
56    FLUXBL2=AKW*(CAB2-CABI)
      GAMA1=SK2*CB0*TEFF*TEFF/DA
      GAMA2=SR*SK2*CA0*TEFF*TEFF/DB

C
C     #  SOLVING BOUNDARY VALUE PROBLEM USING B2PFD    #
C     DO 30 JJ=1,20

      JJ=1
      XA=0.0
      XB=1.0
      N=4
      NGMAX=101
      NGRID=51
      IP=2
      IR=0
      LDFIN=4
      LDINI=4
      TOL=0.01
      PSTEP=0.0
      PRNT=.FALSE.
      LIN=.FALSE.
      II=1
```

```
      R1=CA0/CB0

      G1=TEFF*SQRT(SK2*CB0/DA)
      G2=TEFF*SQRT(SR*SK2*CA0/DB)

      DO 26 J=1,NGRID

      XXINIT(J)=FLOAT(J-1)*(XB-XA)/FLOAT(NGRID-1)+XA

      YYINIT(1,J) = W1(J)
      YYINIT(2,J) = W2(J)
      YYINIT(3,J) = W3(J)
      YYINIT(4,j) = W4(J)
26    CONTINUE

      CALL B2PFD(FCN1,FCN2,FCN3,FCN1,FCN3,N,IP,IR,XA,XB,
     1  PSTEP,TOL,NGRID,XXINIT,YYINIT,LDINI,LIN,PRNT,
     2   NGMAX,NF,XXF,YYF,LDFIN,ER,
     3   WORK,IWORK)

      DO 902 J = 1,NF
      W1(J) = YYF(1,J)
      W2(J) = YYF(2,J)
      W3(J) = YYF(3,J)
      W4(J) = YYF(4,J)
902   CONTINUE

C     ************************************************************
C     *************IMSL ENDS**************************************
C     ************************************************************

      FLUX2O3=YYF(4,NGRID)*DB*CB0/TEFF

      FLUXR2=-YYF(2,1)*DA*CA0/TEFF

C     ******************** FLAG3 *********************************

      CAB0 = YYF(1,1)*CA0
      CABI = CAB0/AMI
      CBB0 = YYF(3,NGRID)*CB0
      XR = CAB0
      FXR = FLUXBL2 - FLUXR2

101   CONTINUE
```

```
C     *** RECALCULATED AQUEOUS PHASE BALANCE ******
      CABIN4 = 0.0
      CABIN4=CAB2-((DAREA*FLUXR2)/QF)
      CAB2 = CABIN4
C     ****************** GAS PHASE BALANCE ******************
      CBB0 = YYF(3,NGRID)*CB0
      PINTER2(L) = CBB0*HEN

      IF (L.EQ.1) THEN
      PARTIAL2G(L)=((2/ETA-1)*PARTIALP+2*PINTER2(L))/(2/ETA+1)
      ELSE
     PARTIAL2G(L)=((2/ETA-1)*PARTIAL2G(L-1)+2*PINTER2(L))/(2/ETA+1)
      ENDIF
      CBG2=PARTIAL2G(L)/(UNIVR*TEMP)

      ACK1 = (CASOUT-CAB2)/CASOUT

      ACK2 = (PARTIAL2G(L)-PARTIALG(L))/PARTIAL2G(L)

      IF ((ABS(ACK1).GE.1E-4).OR.(ABS(ACK2).GE.1E-4)) THEN

      CASOUT = CAB2
      PARTIALG(L) = PARTIAL2G(L)

      RK =RK +1
      GOTO 22
      ELSE
      ENDIF

C     ****************** FLAG4 ************************


C     ***************************************************
C     ******* MOVING TO THE NEXT SEGMENT *****************

      CAB = CAB2
      CBG = CBG2

2000  CONTINUE

C     ****************** FLAG5 ********************************

      CAOUT = CAB*AMW*1000
      CAPSE = CAPSE1*AMW*1000
```

```
C     **** INTERFACIAL AREA = 3.88E-3 *************

C     ****** DEFINE EKKA AS POLLUTANT CONSUMPTION ****
C     ***** KGMOL/ (M2(AQ.-ORG INTERFACE) S) **************
      EKKA = ((CABULKIN - CAB)*QF)/3.88E-3
      WRITE (29,*) QFI, CAOUT, VF, PARTIAL2G(DIV),
     1     CAPSE
      WRITE (37,*) QFI, CAOUT, VF, EKKA
500   CONTINUE
      STOP
106   FORMAT(10X,I2,4X,F5.3,5X,F5.3,2X,E15.8,1X,E15.8,1X,F8.3)
111   FORMAT(2X,I3,4X,F7.4,2X,F7.5,3(2X,E15.8),2X,F6.4/)
115   FORMAT(9G)
      END
      SUBROUTINE FCN1(N,X,Y,P,YPRIME)
      REAL Y(N),YPRIME(N)
      COMMON GAMA1,GAMA2,CA0,CB0,SR
      COMMON/VAR2/CAB0,CBB0
      YPRIME(1)=Y(2)
      YPRIME(2)=GAMA1*Y(1)*Y(3)
      YPRIME(3)=Y(4)
      YPRIME(4)=GAMA2*Y(1)*Y(3)
      RETURN
      END
      SUBROUTINE FCN2(N,X,Y,P,PD)
      REAL Y(N),PD(N,N)
      COMMON GAMA1,GAMA2,CA0,CB0,SR
      COMMON/VAR2/CAB0,CBB0
      PD(1,1)=0.0
      PD(1,2)=1.0
      PD(1,3)=0.0
      PD(1,4)=0.0
      PD(2,1)=GAMA1*Y(3)
      PD(2,2)=0.0
      PD(2,3)=GAMA1*Y(1)
      PD(2,4)=0.0
      PD(3,1)=0.0
      PD(3,2)=0.0
      PD(3,3)=0.0
      PD(3,4)=1.0
      PD(4,1)=GAMA2*Y(3)
      PD(4,2)=0.0
      PD(4,3)=GAMA2*Y(1)
      PD(4,4)=0.0
```

```
RETURN
END
SUBROUTINE FCN3(N,YA,YB,P,F)
REAL YA(N),YB(N),F(N)
COMMON GAMA1,GAMA2,CA0,CB0,SR
COMMON/VAR2/CAB0,CBB0
F(1)=YA(1)-(CAB0/CA0)
F(2)=YA(4)
F(3) = YB(2)                !FLUX OF B INTO AQ.PH. ZERO
F(4) =YB(3) - (CBB0/CB0)
RETURN
END
```

APPENDIX 6

CONCENTRATION PROFILES OF POLLUTANTS AND OZONE ACROSS THE LIQUID MEMBRANE IN THE TWO-PHASE MEMBRANE OZONATOR

This section discusses the concentration profiles of pollutants and ozone across the liquid membrane in the two-phase membrane ozonator calculated by the model described in section 3.2. Figure A.6.1 shows the dimensionless concentration profiles across the liquid membrane for the three pollutants phenol, acrylonitrile and nitrobenzene in turn. The term C^{F}_{inlet} indicates the concentration of the species (organic and ozone) in the FC phase in equilibrium with the module inlet compositions (of organic and ozone) of the flowing phases. The inlet concentrations of the pollutants were as follows: phenol, 152 ppm; acrylonitrile, 158 ppm; nitrobenzene, (1) 120 ppm, (2) 1400ppm.

The effective membrane thickness (EMT), y_l is calculated from the aqueous-organic interface at the inner diameter of the Teflon tubules to the outer diameter of the silicone capillaries (Sengupta et al., 1988; Basu and Sirkar, 1991) and is based upon the total solute transport rate per unit permeator length. For a hydrophobic substrate this is given by:

$$y_l = \frac{d_i}{d_{lm}} \frac{\tau}{\epsilon} \frac{(d_o - d_i)}{2} + \frac{d_i}{d_o} \delta_m \qquad \text{(A.6.1)}$$

where τ, the tortuosity of the Teflon tubules, is equal to 1.5; ϵ, the membrane porosity, is equal to 0.5 for the Teflon tubules used in this work (Green, 1994). The Teflon tubules had a d_i of 990 μm and d_o of 2280 μm.

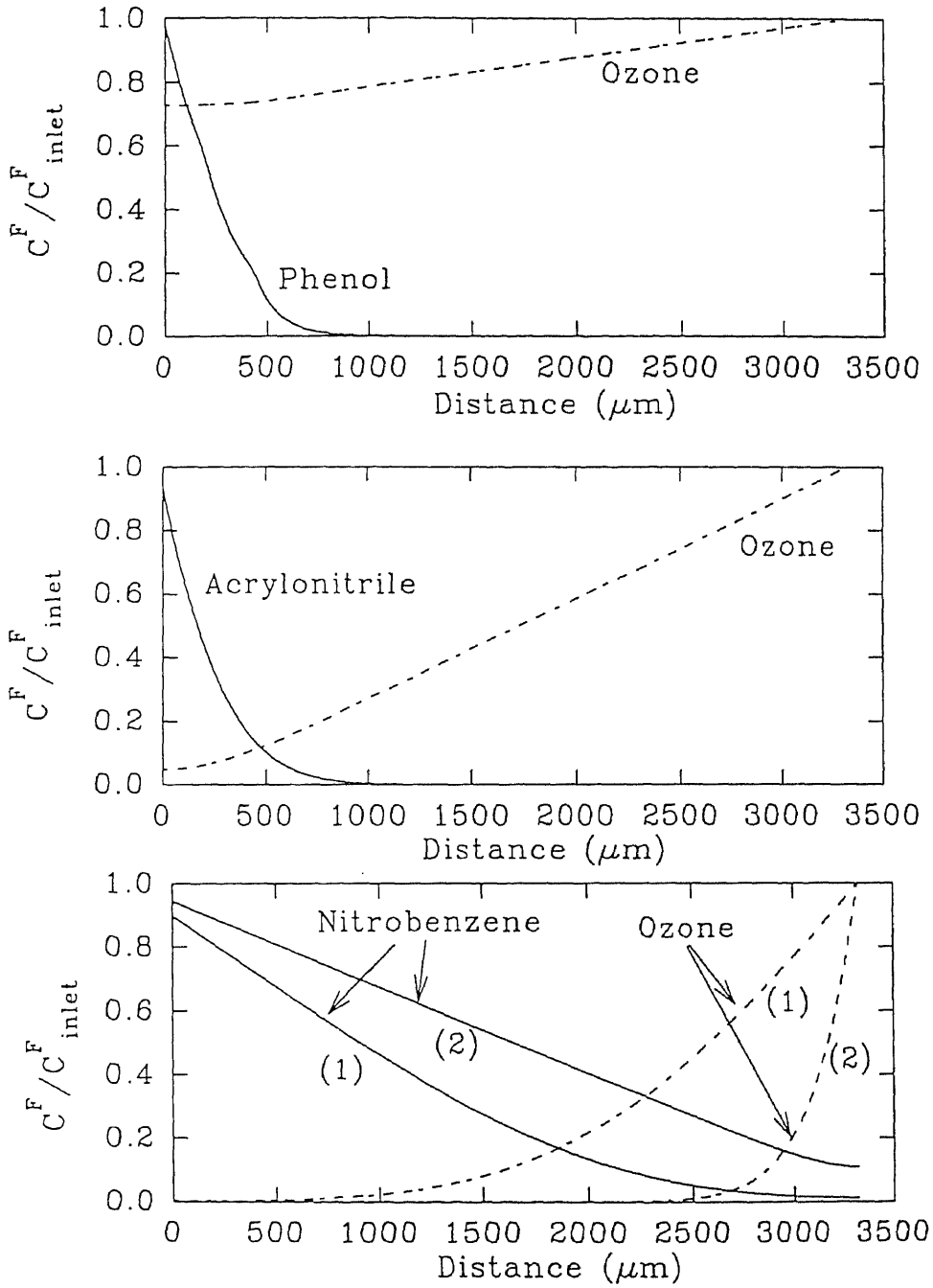

Figure A.6.1. Concentration profiles of organic pollutants and O_3 across the FC-phase in the two-phase membrane ozonator.

The term d_{lm} is defined as follows:

$$d_{lm} = \frac{d_o - d_i}{\ln (d_o / d_i)} \qquad \text{(A.6.2)}$$

The experimentally determined membrane thickness from the outer diameter of the Teflon tubules to the outer diameter of the silicone capillaries, δ_m (Section 3.2), was found to be 4800 μm. Past studies, for the permeation of permanent gases across water as a contained liquid membrane, have shown that this simple model for the EMT, y_l, compares fairly well with that calculated from a rigorous two dimensional model (Majumdar, et al., 1989). Also other studies employing hollow fiber membrane bundles in a shell surrounded by a liquid have modeled the system by considering two flat membranes separated by a liquid thickness equivalent to the EMT (Chen et al., 1992). This approach is essentially similar to the method followed above with one exception, this study accounts for the cylindrical nature of the tubular membranes used by including the d_{lm} term.

From Figure A.6.1 it is clear that the concentration profiles of ozone and phenol in the two-phase membrane ozonator reinforces the assumption of nearly constant ozone concentration in the FC phase, adopted in the pseudo-first order model. The concentration profile for acrylonitrile seems to be similar to phenol but the corresponding ozone concentration profile is steeper than that for phenol. The reasons for this are two-fold: firstly, the partition coefficient, m_A, of phenol is 10 times less than that of acrylonitrile (Figure 3.4.1). This means that there is 10 times as much acrylonitrile as there is phenol in the FC phase. Secondly the second order reaction rate of acrylonitrile, 90 m^3/(kgmol-s) is about 2.5 times that for phenol (Figure 3.4.3). Therefore even though

there is 10 times as much acrylonitrile in the FC phase, the concentration profiles of acrylonitrile and phenol look similar because of the higher reaction rate coefficient for acrylonitrile. The higher acrylonitrile concentration in the FC phase however results in greater consumption of O_3 which is indicated by the sharper slope of the O_3 concentration profile.

For nitrobenzene as a model pollutant, two sets of simulations were undertaken. One simulation was for a low feed concentration, 120 ppm, identified as line (1), while the second was for a feed composition of 1400 ppm, identified by line (2). Nitrobenzene has a m_A about 10 times that of acrylonitrile, therefore the concentration profiles of the pollutant are not as steep as that for acrylonitrile and phenol. The same reason is applicable for the steeper declines in O_3 concentration. From the graph it is very clear that at high nitrobenzene feed concentrations (2), most of the ozone is consumed very close to the FC-silicone interface.

These concentration profiles have far greater utility towards improving the ozonator design, rather than appearing at first glance to be a simple pedantic exercise. For pollutants with a low m_A, the ozone concentration does not change significantly across the FC phase, therefore increasing the mass transfer area of the aqueous side would allow better utilization of O_3 in the device. For pollutants with a higher m_A, O_3 becomes the limiting reactant, therefore increasing the number of silicone capillaries will allow the delivery of higher ozone doses, leading to improved pollutant destruction. It may be extrapolated that for pollutants with extremely high m_A like toluene and trichloroethylene (TCE), ozone becomes the limiting reactant in the present version of the two-phase membrane ozonator.

BIBLIOGRAPHY

Aleksandrov, Y. A., B. I. Tarunin and M. L. Perepletchikov, "Solubility of ozone in liquids", *Russian Journal of Phys. Chem.*, **1983**, *57*, 1445.

Atkinson, R., S. M. Aschmann, D. R. Fitz, A. M. Winer and J. N. Pitts, Jr., "Rate constants for the gas phase reactions of O_3 with selected organics at 296 K", *Int. J. Chem. Kinet.*, **1982**, *14*, 13.

Atkinson, R., D. L. Baulch, R. A. Cox, R. F. Hampson, Jr., J. A. Kerr and J. Troe, "Evaluated kinetic and photochemical data for atmospheric chemistry: supplement III", *J. Phys. Chem. Ref. Data*, **1989**, *18*, 881.

Atkinson, R., E. C. Tuazon, T. J. Wallington, S. M. Aschmann, J. Arey, A. M. Winer and J. N. Pitts, Jr., "Atmospheric chemistry of aniline, N, N-dimethylaniline, pyridine, 1, 3, 5-triazine and nitrobenzene", *Environ. Sci. and Tech.*, **1987**, *21*, 64.

Bailey, P. S., *Ozonation in Organic Chemistry; Volume II. Nonolefinic Compounds*, Academic Press, NY, **1982**.

Baker, R. W., N. Yoshioka, J. M. Mohr and A. J. Khan, "Separation of organic vapors from air", *J. Membr. Sci.*, **1987**, *31*, 259.

Baker, R. W., J. Kaschemekat and J. G. Wijmans, "Membrane systems for profitable VOC recovery", *CHEMTECH*, **1996**, *7*, 37.

Basu, R. and K. K. Sirkar, "Hollow fiber contained liquid membrane separation of citric acid", *AIChE J.*, **1991**, *37*, 383.

Bhattacharyya, D., C. E. Hamrin, Jr. and R. P. Northey, "Oxidation of hazardous organics in a two-phase fluorocarbon-water system", *Haz. Wast. Haz. Mat.*, **1986**, *3*, 405.

Bhattacharyya, D., T. F. Van Dierdonck, S. D. West and A. R. Freshour, "Two-phase ozonation of chlorinated organics", *J. Haz. Mat.*, **1995**, *41*, 73.

Bhaumik, S., S. Majumdar and K. K. Sirkar, "Hollow-fiber membrane-based rapid pressure swing absorption", *AIChE J.*, **1996**, *42*, 409.

Bhowmick, M. and M. J. Semmens, "Laboratory-scale testing of a continuous CLAS process", *J. AWWA*, **1994**, *6*, 86.

BIBLIOGRAPHY
(Continued)

Bohn, H., "Consider biofiltration for decontaminating gases", *Chem. Eng. Prog.*, **1992**, *4*, 34.

Bruining, W. J., G. E. H. Joosten, A. C. M. Beenackers and H. Hofmann, "Enhancement of gas-liquid mass transfer by a dispersed second liquid phase", *Chem. Eng. Sci.*, **1986**, *41*, 1873.

Caprio, V., A. Insola and G. Volpicelli, "Ozonation of aqueous solutions of nitrobenzene", *Ozone Sci. and Eng.*, **1984**, *6*, 115.

Castro, K. and A. K. Zander, "Membrane air-stripping: effects of pretreatment", *J. AWWA*, **1995**, *3*, 50.

Chang, C -Y and J. -N. Chen, "Ozonolysis of 2,4-dichlorophenol in a two-phase solvent/water system", *Water Sci. Tech.*, **1994**, *29*, 343.

Chen, S., H. Fan and Y. -K. Kao, "A membrane reactor with two dispersion-free interfaces for homogeneous catalysis", *Chem. Eng. J.*, **1992**, *49*, 35.

de Vahl Davis, G. *Numerical Methods in Engineering & Science*, Allen & Unwin Inc., MA, 1986.

Fleming, H. L. and C. S. Slater, "Pervaporation : definition and background", in *Membrane Handbook*, W. S. W. Ho and K. K. Sirkar (eds.), Van Nostrand Reinhold, NY, 1992.

Freshour, A. R., S. Mawhinney and D. Bhattacharyya, "Two-phase ozonation of hazardous organics in single and multicomponent systems", *Wat. Res.*, **1996**, *30*, 1949.

Gill, W. N. and B. Bansal, "Hollow fiber reverse osmosis sytems analysis and design", *AIChE J.*, **1973**, *19*, 823.

Glaze, W. H., J. -W. Kang and D. H. Chapin, "The chemistry of water treatment processes involving ozone, hydrogen peroxide and ultraviolet radiation", *Ozone Sci. and Eng.*, **1987**, *9*, 335.

Glaze, W. H. and J. -W. Kang, "Advanced oxidation processes for treating groundwater contaminated with TCE and PCE: laboratory studies", *J. AWWA.*, **1988**, *80*, 57.

BIBLIOGRAPHY
(Continued)

Glaze, W. H. and J. -W. Kang, "Advanced oxidation processes, description of a kinetic model for oxidation of hazardous materials in aqueous media with ozone and hydrogen peroxide in a semibatch reactor", *Ind. Eng. Chem. Res.*, **1989**, *28*, 1573.

Green, A., "Personal communication", 1994.

Hamrin Jr., C. E., D. Bhattacharyya and W. K. Glynn, "A membrane-organic phase oxidation process for the destruction of toxic organics in hazardous wastewaters", NTIS Report No. PB85-214575, VA, 1984.

Happel, J., "Viscous flow relative to arrays of cylinders", *AIChE J.*, **1959**, *5*, 174.

Heck, R. M. and R. J. Farrauto, *Catalytic Air Pollution Control, Commercial Technology*, Van Nostrand Reinhold, NY, 1995.

Ho, W. S. W. and N. N. Li, "Emulsion liquid membranes : definitions, theory", in *Membrane Handbook*, W. S. W. Ho and K. K. Sirkar (eds.), Van Nostrand Reinhold, NY, 1992.

Hoigne, J. and H. Bader, "Rate constants of reactions of ozone with organic and inorganic compounds in water - I, non-dissociating organic compounds", *Water Res.*, **1983a**, *17*, 173.

Hoigne, J. and H. Bader, "Rate constants of reactions of ozone with organic and inorganic compounds in water - II, dissociating organic compounds", *Water Res.*, **1983b**, *17*, 185.

Huang, C. -R. and J. W. Bozzelli, "Degradation of industrial organic water pollutants by reaction with ozone or hydrogen peroxide and ultraviolet radiation, phase II", Final Report, BICM-16, submitted to the Hazardous Substance Managment Research Center at the New Jersey Institute of Technology, Newark, NJ, 1988.

Hutter, J. C., G. F. Vandegrift, L. Nunez and D. H. Redfield, "Removal of VOCs from groundwater using membrane-assisted solvent extraction", *AIChE J.*, **1994**, *40*, 166.

Joshi, M. G. and R. L. Shambaugh, "The kinetics of ozone-phenol reaction in aqueous solutions", *Wat. Res.*, **1982**, *16*, 933.

BIBLIOGRAPHY
(Continued)

Junker, B. H., T. A. Hatton and D. I. C. Wang, "Oxygen transfer enhancement in aqueous/perfluorocarbon fermentation systems: I. experimental observations", *Biotechnol. Bioeng.*, **1990**, *35*, 578.

Karoor, S. and K. K. Sirkar, "Gas absorption studies in a microporous hollow fiber membrane modules", *Ind. Eng. Chem. Res.*, **1993**, *32*, 674.

Kent, J. A. (ed.), *Riegel's Handbook of Industrial Chemistry*, Chapman Hall, NY, 1992.

Keshavaraj, R. and R. W. Tock,"Changes in crosslink density of structural silicone sealants due to ozone and moisture", *Polym. -Plast. Technol. Eng.*, **1994**, *33*, 397.

Kim, J. S. and R. Datta, "Supported liquid-phase catalytic membrane reactor-separator for homogeneous catalysis", *AIChE J.*, **1991**, *37*, 1657.

Langlais, B., D. A. Reckhow and D. R. Brink, (eds.), *Ozone in Water Treatment, Applications and Engineering*, Lewis Publishers Inc., MI, 1991.

LaPack, M. A., J. C. Tou, V. L. McGuffin and C. G. Enke, "The correlation of membrane permselectivity with Hildebrand solubility parameters", *J. Membr. Sci.*, **1994**, *86*, 263.

Majumdar, S., L. B. Heit, A. Sengupta and K. K. Sirkar, "An experimental investigation of oxygen enrichment in a silicone capillary permeator with permeate recycle", *Ind. Eng. Chem. Res.*, **1987**, *26*, 1434.

Majumdar, S., A. K. Guha and K. K. Sirkar, "A new liquid membrane technique for gas separation", *AIChE J.*, **1988**, *34*, 1135.

Majumdar, S., A. K. Guha, Y. -T Lee and K. K. Sirkar, "A two-dimensional analysis of membrane thickness in a hollow-fiber-contained liquid membrane permeator", *J. Membr. Sci.*, **1989**, *43*, 259.

Majumdar, S., K. K. Sirkar and A. Sengupta, "New membrane processes under development : hollow-fiber contained liquid membrane" in *Membrane Handbook*, W. S. W. Ho and K. K. Sirkar (eds.), Van Nostrand Reinhold, NY, 1992.

Masten, S. J. and S. H. R. Davies, "Use of ozone and other strong oxidants for hazardous waste management", in *Environmental Oxidants*, J. O. Nriagu and M. S. Simmons (eds.), John Wiley & Sons, Inc., NY, 1994.

BIBLIOGRAPHY
(Continued)

Matson, S. L. and J. A. Quinn, "New membrane processes under development : membrane reactors" in *Membrane Handbook*, W. S. W. Ho and K. K. Sirkar (eds.), Van Nostrand Reinhold, NY, 1992.

Modell, M., G. G. Gaudet, M. Simson, G. T. Hong and K. Biemann, "Supercritical water testing reveals new process holds promise", *Solid Wastes Manag.*, **1982**, *25*, 26.

Mukhopadhyay, N. and E. C. Moretti, *Current and Potential Future Industrial Practices for Reducing and Controlling Volatile Organic Compounds*, Center for Waste Reduction Technologies, AIChE, NY, 1993.

Munshi, H. B., S. R. Rao and R. M. Iyer, "Rate constants of the reactions of ozone with nitriles, acrylates and terpenes in gas phase", *Atmosph. Environ.*, **1989**, *23*, 1971.

Nakagawa, T. W., L. J. Andrews and R. M. Keefer, "The kinetics of ozonization of polyalkylbenzenes", *J. Amer. Chem. Soc.*, **1960**, *82*, 269.

Ollis, D. F., J. B. Thompson and E. T. Wolynic, "Catalytic liquid membrane reactor: I. concept and preliminary experiments in acetaldehyde", *AIChE J.*, **1972**, *18*, 457.

Pate, C. T., R. Atkinson and J. N. Pitts, Jr., "The gas phase reaction of O_3 with a series of aromatic hydrocarbons", *J. Environ Sci. Health*, **1976**, *A-11*, 1.

Perry, R. H. and D. W. Green (eds.), "Perry's chemical engineers' handbook", McGraw-Hill, Inc., NY, 1984.

Poddar, T. K., S. Majumdar and K. K. Sirkar, "Membrane-based absorption of VOCs from a gas stream", *AIChE J.*, **1996a**, *42*, 3267.

Poddar, T. K., S. Majumdar and K. K. Sirkar, "Removal of VOCs from air by membrane-based absorption and stripping", *J. Membr. Sci.*, **1996b**, *120*, 221.

Prasad, R. and K. K. Sirkar, "New membrane processes under development : membrane-based solvent extraction" in *Membrane Handbook*, W. S. W. Ho and K. K. Sirkar (eds.), Van Nostrand Reinhold, NY, 1992.

Pryor, W. A., D. Giamalva and D. F. Church, "Kinetics of ozonation. 1. electron-deficient alkenes", *J. Am. Chem. Soc.*, **1983**, *105*, 6858.

BIBLIOGRAPHY
(Continued)

Pryor, W. A., D. H. Giamalva and D. F. Church, "Kinetics of ozonation. 2. amino acids and model compounds in water and comparisons to rates in nonpolar solvents", *J. Am. Chem. Soc.*, **1984**, *106*, 7094

Qi, Z. and E. L. Cussler, "Microporous hollow fibers for gas absorption. I. mass transfer in a liquid", *J. Membr. Sci.*, **1985**, *23*, 321.

Reed, B. W., R. Klaassen, A. E. Jansen, J. J. Akkerhuis, B. A. Bult and F. I. H. M. Oesterholt, "Removal of hydrocarbons from wastewater by membrane extraction", presented at the *Separation Processes for Environmental Applications-1* session, AIChE Spring National Meeting, April 17-21, 1994, Atlanta, GA.

Robb, W. L., Report No. 65-C-031; R&D Center, General Electric Co., NY, **1965**, *10.*

Rook, J. J., "Chlorination reactions of fulvic acid in natural waters", *Environ. Sci. and Tech.*, **1977**, *11*, 478.

Schmid, J., "Longitudinal laminar flow in an array of cylindrical cylinders", *Int. J. of Heat and Mass Transfer*, **1966**, *9*, 925.

Scott, J. P. and D. F. Ollis, "Integration of chemical and biological oxidation processes for water treatment: review and recommendations", *Environ. Prog.*, **1995**, *14*, 88.

Sengupta, A., R. Basu and K. K. Sirkar, "Separation of solutes from aqueous solutions by contained liquid membranes", *AIChE J.*, **1988**, *34*, 1698.

Shanbhag, P. V., "Kinetic studies of two-phase ozonation of organic pollutants in wastewater", M. E. Thesis, Stevens Institute of Technology, Hoboken, NJ, 1992.

Sharma, M. M., "Perspectives in gas-liquid reactions", *Chem. Eng. Sci.*, **1983**, *38*, 1.

Sirkar, K. K., "New membrane processes under development : other new membrane processes" in *Membrane Handbook*, W. S. W. Ho and K. K. Sirkar (eds.), Van Nostrand Reinhold, NY, 1992.

Sirkar, K. K., D. A. Vaccari and A. K. Guha, "A novel membrane reactor for the oxidative degradation of hazardous organic wastes", Final Report, BICM-27 & 34, submitted to the Hazardous Substance Managment Research Center at the New Jersey Institute of Technology, Newark, NJ, 1994.

BIBLIOGRAPHY
(Continued)

Sparrow, E. M. and A. L. Loeffler, "Longitudinal laminar flow between cylinders in regular array", *AIChE J.*, **1959**, *5*, 325.

Sparrow, E. M., A. L. Loeffler and H. A. Hubbard, "Heat transfer to longitudinal laminar flow between cylinders", *ASME J. of Heat Transfer*, **1961**, 415.

Stephanopoulos, G., *Chemical process control : an introduction to theory and practice*, Prentice-Hall, NJ, 1984.

Stich, F. A. and D. Bhattacharyya, "Ozonolysis of organic compounds in a two-phase fluorocarbon-water system", *Environ. Prog.*, **1987**, *6*, 224.

Sun, Y., G. M. Brown and B. A. Moyer, "TiO_2 mediated photooxidation of trichloroethylene and toluene dissolved in fluorocarbon solvents", *Chemosphere*, **1995**, *31*, 3575.

Tang, T. E. and S. -T. Hwang, "Mass transfer of dissolved gases through tubular membrane", *AIChE J.*, **1976**, *22*, 1000.

Trivedi, D. H., "Destruction of hazardous organics in wastewater using a novel membrane reactor", M. E. Thesis, Stevens Institute of Technology, Hoboken, NJ, 1992.

Ward, W. J. and W. L. Robb, "Carbon-dioxide -oxygen separation: facilitated transport of carbon dioxide across a liquid film", *Science*, **1967**, *156*, 1481.

Westerterp, K. R., W. P. M. Van Swaaij and A. A. C. M. Beenackers *Chemical Reactor Design and Operation*, John Wiley & Sons, NY, 1984.

Williamson, D. G. and R. J. Cvetanovic, "Rates of reactions of ozone with chlorinated and conjugated olefins", *J. Am. Chem Soc.*, **1968**, *90*, 4248.

Wojtowicz, J. A., "Ozone", in *Kirk-Othmer Encyclopedia of Chemical Technology*, J. I. Kroschwitz and M. Howe-Grant (eds.), Wiley-Interscience, NY, 1991, *17*, 953.

Yang, D., S. Majumdar, S. Kovenklioglu and K. K. Sirkar, "Hollow fiber contained liquid membrane pervaporation system for the removal of toxic volatile organics from wastewater", *J. Membr. Sci.*, **1995**, *103*, 195.

BIBLIOGRAPHY
(Continued)

Yun, C. H., R. Prasad and K. K. Sirkar, "Membrane solvent extraction removal of priority organic pollutants from aqueous waste stream", *Ind. Eng. Chem. Res.*, **1992**, *31*, 1709.

Zimmerman, E. J., "New waste disposal process", *Chem. Eng.*, **1958**, *65*, 117.

Zolandz, R. R. and G. K. Fleming, "Gas permeation : theory", in *Membrane Handbook*, W. S. W. Ho and K. K. Sirkar (eds.), Van Nostrand Reinhold, NY, 1992.